AD-762 281

WIDEBAND COMMAND AND CONTROL MODEM

Albert R. Martin, et al

Radiation, Incorporated

Prepared for:

Advanced Research Projects Agency

December 1972

AD-762 281

DISCLAIMER NOTICE

THIS DOCUMENT IS THE BEST
QUALITY AVAILABLE.

COPY FURNISHED CONTAINED
A SIGNIFICANT NUMBER OF
PAGES WHICH DO NOT
REPRODUCE LEGIBLY.

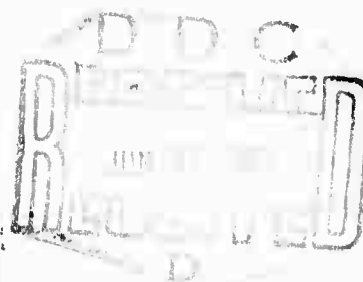RADC-TR-73-91
Final Technical Report
December 1972

WIDEBAND COMMAND AND CONTROL MODEM

Radiation, Incorporated

Sponsored by
Defense Advanced Research Projects Agency
ARPA Order No. 2154

Approved for public release;
distribution unlimited.

The views and conclusions contained in this document are those of the
authors and should not be interpreted as necessarily representing the
official policies, either expressed or implied, of the Defense
Advanced Research Projects Agency or the U. S. Government.

Rome Air Development Center
Air Force Systems Command
Griffiss Air Force Base, New York

RADIATION
DIVISION OF HARRIS-INTERTYPE CORPORATION

267

DOCUMENT CONTROL DATA - R & D

(Security classification of title, body of abstract and indexing annotation must be entered when the overall report is classified)

1. ORIGINATING ACTIVITY *(Corporate author)*	2a. REPORT SECURITY CLASSIFICATION
Radiation, A Division of Harris-Intertype Corporation	Unclassified
	2b. GROUP

3. REPORT TITLE

Wideband Command and Control Modem (Waveform and Modem Conceptual Design Study)

4. DESCRIPTIVE NOTES *(Type of report and inclusive dates)*

Final Technical Report   14 Jun 1972 to 14 Dec 1972

5. AUTHOR(S) *(First name, middle initial, last name)*

Albert R. Martin, Jay D. Knoner, Raymond F. Cobb

6. REPORT DATE	7a. TOTAL NO. OF PAGES	7b. NO. OF REFS
December 1972	~~260~~ 267	7

8a. CONTRACT OR GRANT NO	9a. ORIGINATOR'S REPORT NUMBER(S)
F30602-72-C-0498	
b. PROJECT NO	
2154	
c.	9b. OTHER REPORT NO(S) *(Any other numbers that may be assigned this report)*
d.	

10. DISTRIBUTION STATEMENT

Approved for Public Release.   Distribution Unlimited.

11. SUPPLEMENTARY NOTES	12. SPONSORING MILITARY ACTIVITY
Monitored by: RADC/DCRC Griffiss AFB NY 13441	Advanced Research Projects Agency Washington, DC 20301

13. ABSTRACT

This report contains the tradeoffs and resultant baseline design for a Wideband Command and Control Modem. The waveform design for this modem provides uplink command data from a master ground station to each of 25 vehicles and receives status data in return. In addition, wideband imagery information is received from up to five of the vehicles in the target area. The application of this modem to remote pilotless vehicle (RPV) missions requires jam-resistant communications, especially for the command uplink, and requires a modem design with extremely low recurring costs for the vehicle electronics.

The outstanding features of the baseline design are (1) implementation with surface wave and digital devices in order to realize the low recurring cost design requirement and (2) incorporation of operational flexibility into the modem such that application to a variety of RPV missions is practical. The surface wave matched filters and digital timing loop provide simple hardware realization of a novel spread spectrum waveform design using frequency-hopped chirp signals. Also, the use of convolutional coding provides optimum performance over a wide range of data rates and of the number of RPV's in a given mission.

14 KEY WORDS	LINK A		LINK B		LINK C	
	ROLE	WT	ROLE	WT	ROLE	WT
Remote Pilotless Vehicle Data Links						
Spread Spectrum Communications						
Binary Chirp Signals						
Surface Wave Device Chirp Matched Filters						
Digital Signal Processing						
Multiple Access Communications						
Waveform Design						
Time Division Multiple Access						
Modulation Techniques						
Modem						

WIDEBAND COMMAND AND CONTROL MODEM

Albert R. Martin
Jay D. Knoner
Raymond F. Cobb

i-t

PUBLICATION REVIEW

This technical report has been reviewed and is approved

RADC Project Engineer

i-c

TABLE OF CONTENTS

TABLE OF CONTENTS (Continued)

ABSTRACT

RPV SPREAD SPECTRUM SIGNAL DESIGN

This report presents the preliminary results of an ARPA-funded program for determining the command and control data links for RPV's. The initial study phase has resulted in a baseline design for the spread spectrum multiple access communications. The waveform design for this modem accommodates uplink command data from a master ground station to each of 25 RPV's and status data on the return downlink. In addition, wideband imagery information is multiplexed on the downlinks of five of the RPV's which are in the target area. Ranging for position location is also provided by the spread spectrum waveform.

The baseline design is given by the modulation, the multiple address or access, and the spread spectrum waveform for each of the links as summarized in the following table:

Link	Modulation	Spread Spectrum	Multiple User
Command	Up/Down Chirp	F-H/T-H Chirp	TDM
Status	DPSK	PN Direct Sequence	TDMA
Video	Offset DQPSK	PN (Option)	FDMA

Position location estimation is determined from the range measurements at the Master Ground Station and a single Slave Station.

The outstanding features of the design are: 1) implementation of the command demodulator in the RPV with surface wave device matched filtering and with digital logic timing circuitry, and 2) operational flexibility such that the performance improves as the data rate or the number of vehicles is reduced. The surface wave device implementation, made possible by a novel chirp signaling scheme, has the potential of very low recurring cost for the vehicle electronics. Convolutional coding is employed in order to get full performance advantage of repeated data and realize the operational flexibility advantage. These design features constitute the necessary ingredients of future RPV mission demands of the military.

SUMMARY

The advent of remote pilotless vehicles (RPV) poses challenging problems in command and control communications from which jam resistant spread spectrum signals are required and for which the RPV cost constraints are foremost. This report describes the results of a study and includes tradeoffs and a resultant baseline design of a modem which satisfies the communication data link requirements. An overview of the Report is provided by the subsequent summary paragraphs: Technical Problem, Study Methodology, Technical Results, and Conclusions.

Technical Problem

The performance requirements of the modem are predicated on the demands of pertinent RPV missions. Line-of-sight communications are appropriate for both a short-range 50-mile strike mission and a long-range 250-mile reconnaissance mission. Position location, as provided for 100-foot position location accuracy is necessary to support the strike mission. The data links to support the command and control functions include a 2-kb/s command link from the ground controller to each vehicle, a 2-kb/s status link from each vehicle to the ground controller, and a 20-Mb/s video link from five selected vehicles in the target zone to the ground controller. The number of vehicles is, of course, dependent on operational constraints during a given mission; however, for the waveform design, a maximum of 25 vehicles will be simultaneously controlled by the ground station with no more than five of these in a terminal phase with video transmission requirements. The modem design shall be modular such that if a fewer number of vehicles are actually used, improved performance (processing gain) is obtained. The jamming threat is most demanding for the RPV modem design – a minimum of 30 dB processing gain with spread spectrum techniques shall be provided for the command links and protection shall also be provided for the vehicle status and video links to the extent determined by the cost-effectiveness of the design approaches. These requirements are summarized by the pictorial description of Figure S-1.

In addition to these requirements, there are additional guidelines which are important to the selection of a waveform design. The RPV dynamics enter into the design of tracking loop bandwidths, etc.; a MACH 1 speed of approximately 1000 feet/second and an acceleration of 20 g's are assumed as nominal maximum values. The dynamic range of the status and command links is 48 dB which corresponds to the signal level differences between 1 and 250 nmi or equivalently between 1/5 and 50 nmi. The video dynamic range is considerably less since this mode is only activated in the designated target zone; a range of 20 dB between received video signals is assumed adequate. The strategies and requirements for reacquisition of the code tracking loops is determined from the mission profiles of typical RPV missions. Emphasis is given to a fast reacquisition strategy for short signal fades of the order of one second and reacquisition must be assured for longer signal outages (a nominal 30-second duration is assumed) and should be probabilistic for even longer durations.

Requirements for the study include the RF considerations for frequency assignments in the C-, X-, or Ku-bands. Consistent with the allocations possible in these bandwidths, the total RF bandwidth should be constrained to a nominal value of 500 MHz. Both uplinks and downlinks are adjacent channels in order that common antennas are usable for both transmit and receive.

iv
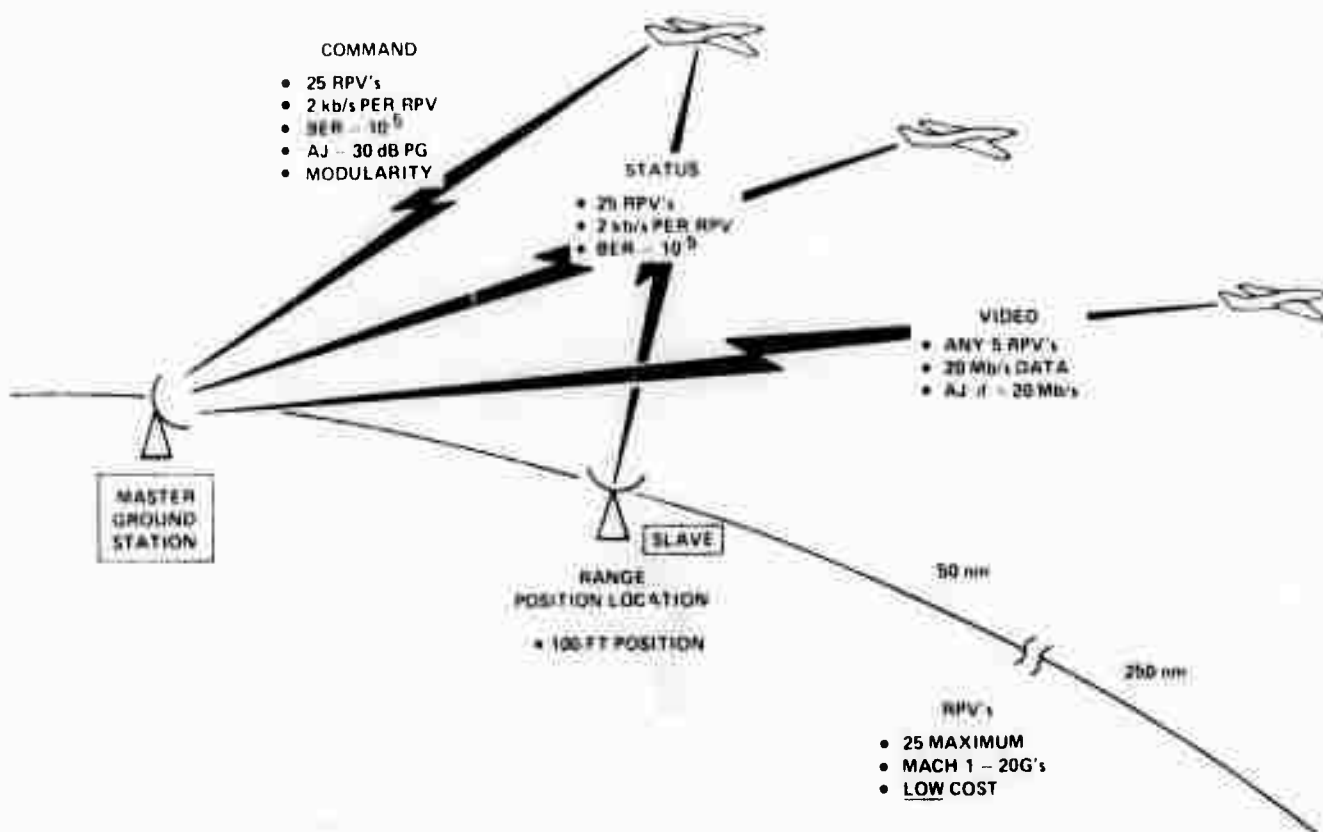
Figure S-1. Modem Requirements

v

Special emphasis is given the RF considerations which constrain or influence the waveform design of the modem; in particular, the effects of a limiting RF power amplifier, like a TWT, provide strong influence on the design of the IF Modem.

Requirements of the study also include a ranging capability for a position location accuracy of 100 feet for the 50 nmi strike mission. Since the required ranging accuracy for this 100 foot position is a strong function of the ground station separation and the RPV location, a system configuration has to be postulated. A baseline separation of 20 nmi is chosen as typical for this class of application. A ranging accuracy requirement of 20 feet results from a position location analysis based on a two-station system and a reasonable operational restriction to a 90 degree sector at the maximum range. This analysis assumes maximum likelihood processing of the range information in order to estimate position. Due to the relatively high update rate compared to the dynamics of the RPV, additional time smoothing would effect a further decrease in the position error. These considerations provide guidelines for the waveform design; viz., 1) the interstation distance which influences the signal format to require reception at a remote slave station, and 2) the ranging accuracy which determines entries in the range error budget, especially the time resolution of the signal.

The analysis and design tasks for the Modem Study emphasize the required low-cost system design, especially for the vehicle electronics. A guideline value of 1000:1 was assumed for the ratio of ground versus vehicle complexity. The study was required to investigate potential low-cost vehicle designs such as implementations with surface wave devices and with LSI-compatible solid state circuits. The study was based on applying today's state-of-the-art technologies such that breadboard experimental verification can be obtained within one year and such that operational cost estimates can be made on a recurring basis for the 1975-1980 time frame.

Study Methodology

The study organization and tasks were established to emphasize a practical modem design as the desired result of the study. Thus, both analytical support and hardware design tasks were equally considered during the tradeoffs and selection process. The study evolved from considering initially a broad range of approaches to a few likely candidate schemes, then to the selected baseline, and finally to a design plan and its implementation.

The design philosophy established during the early phase of the study was most important in the choice of the baseline design. The overwhelming singlemost consideration was the low recurring cost requirement of the RPV electronics which is basic to the RPV concept itself. This consideration manifested itself in two ways: 1) the command demodulator located in the RPV became the key subsystem (modulators are generally much simpler than demodulators, especially for spread spectrum signals), and 2) the operational flexibility became more important since a single modem design must serve a variety of missions and work in different modes.

The methodology for estimating the performance of the design approaches is worth mentioning. In general, analysis techniques included the use of computers to solve mathematical expressions and to simulate input signals to estimate a bit error rate performance for the case

of the video link). In addition, experimental results were used to verify the design choices in two cases: 1) the nonlinear effects of amplitude limiting on the phase modulated wideband video, and 2) the operation of the second order digital timing loop and acquisition strategy. These experimental results were obtained from existing laboratory breadboard equipments.

Technical Results

The baseline signal design resulting from the tradeoffs is the principal technical output of the study. These results are presented in the subsequent paragraphs with a brief rationale and description of the video, status, and command links.

Video

The basic approach for providing five video links each with information rates up to 20 Mb/s is frequency division multiple access. The trade-off analysis indicates this approach is decidedly simpler than those involving TDMA due to its large storage requirements, or CDMA, due to its large bandwidth requirements.

The modulation is chosen on the basis of a power-limited and bandwidth-constrained channel; in addition, operation with a saturated power amplifier or limiter is desired. Quadriphase modulation is the selected modulation since it provides good signal-to-noise performance with a bandwidth occupancy of about one-half that of the more conventional biphase. Furthermore, offset quadriphase is proposed since this technique is less susceptible than normal QPSK or biphase to spectrum "splatter" caused by hard limiting the signal after filtering.

The parameters chosen for the Offset QPSK FDMA baseline as justified from the analytical and empirical results are: 20 Mb/s, 10M symbols/s, 25-MHz channel separation, and 20 MHz transmit and receive filters. The 25-MHz channel separation results in only 125-MHz channel occupancy for all five video signals and provides efficient bandwidth utilization. Five local oscillator signals are generated in each vehicle by a simple comb generator approach in order to provide the capability of each vehicle being commanded to any one of the five available channels.

An additional noteworthy feature of the quadriphase baseline is the capability of providing processing gain for AJ protection if the basic 20-Mb/s rate can be reduced. That is, if the information rate for video is reduced for a given mission, the data can be spread by a quadriphase sequence generator such that the same nominal 20-MHz channel bandwidth is utilized. The 12.8-MHz sequence generator used for the status modulator is used for this purpose such that a constant channel bandwidth is employed and an amount of processing gain equal to the reduction in bit rate is obtainable.

Status

The multiplexing of status with the video for each of the vehicles is considered first. Multiplexing of these two signals which are in separate frequency bands is desired such

that a single RF channel and a single power amplifier will suffice. The selected approach combines these two signals at an IF frequency and uses a center frequency for the status channel which is sufficiently separated from the video channels to avoid crosstalk interference (the status frequency is selected 60 MHz above the highest video channel). Design considerations have accounted for the signal suppression and the intermodulation distortion due to both status and video in the limiter nonlinearity. Since the status signal level can be substantially less than the video level due to the large disparity in data rates, the potential problems due to the nonlinearity can be adequately controlled. Thus, a design is realized which has the hardware advantages of a single channel and the performance advantage of operating into the high power, saturated region of the power amplifier.

The format for the status waveform, in order to provide multiple access between each of the 25 vehicles as well as the return ranging to master and slave stations, is time division multiple access, TDMA, based on the trade-off results. Frequency division multiple access, FDMA, was rejected due to the excessive guard bands required to accommodate the near-far problem; i.e., simultaneous receptions of signals from close in and far away vehicles. Code division multiple access was also rejected due to the requirement for vehicle transmitter power control caused again by the near-far situation or by propagation anomalies, etc. The TDMA approach is relatively simple especially from the vehicle standpoint since the Master Station, being the central controller for all vehicles, can transmit a command word to each vehicle to appropriately time that vehicle's burst transmission and assure the desired time division multiple access operation. A frame rate of 50 per second is selected as the optimum update rate which allows sufficient guard times to accommodate a 20 nmi separation between master and slave stations.

Next, the spread spectrum signal structure for each TDMA burst transmission is chosen as direct sequence PN. The modulator for this scheme is simple and results in minimum RPV vehicle electronics consistent with the design philosophy of minimum RPV cost and complexity. The rate of the spread spectrum signal is based on the ranging requirement (resolution cell less than 100 η sec); hence, a modest AJ processing gain results. The signal design for the status link is thus a PN spread spectrum signal at a 12.8 Mc/s rate which is transmitted in bursts in a TDMA scheme. Despite the major difference in the system concept, the actual modem design for the status link is similar to the modem design of Ohio State University as monitored RADC. Differential PSK modulation is employed due to the few number of bits per burst (40) in the design. Other parameters selected are: 80 kb/s data rate, 50 updates per second, and guard times of ±125 μs to accommodate a master-slave baseline of 20 nmi.

Command

The waveform design for the command link is the most important of all the trade-offs since its result determines the vehicle complexity and, hence, the feasibility for RPV application. This baseline waveform is a linear FM signal, commonly called chirp, which represents a unique signaling scheme tailored to the RPV mission in that the vehicle demodulation is potentially very low cost, consisting of a surface wave device and digital logic timing circuitry. The individual considerations of multiple access and modulation support the baseline chirp waveform and are discussed subsequently.

The addressing of each of the 25 vehicles for the command link is sequential and constitutes a time division multiple address (TDM) format. This format was chosen primarily because the effective data rate is increased with TDM which lessens the degradation caused by oscillator instability or Doppler. Also, the shorter bit time better matches the integration time of the matched filter demodulator. In addition, the TDM format is generally compatible with the status link design for the vehicle address; this would not be the case for frequency division or code division multiplexing.

The modulation considerations for the command link provide heavy emphasis on the acquisition and reacquisition of the spread spectrum signals during temporary signal outages. These considerations strongly suggest that the choice of modulation of the spread spectrum waveform not require frequency or phase acquisition. The chirp baseline approach allows binary modulation with up or down slope chirped signals which are noncoherent orthogonal binary waveforms and do not require frequency control or phase-lock techniques for acquisition or demodulation. This choice of modulation, thus, provides significant acquisition advantage and more than offsets the potential 3 dB performance loss of noncoherent modulation. Other spread spectrum waveforms, like direct sequence PN, normally utilize coherent modulation techniques, or at least differentially coherent techniques, and thus have degraded acquisition performance.

Another significant consideration in the command link waveform design is the use of error correction coding techniques. The combination of rate one-half convolutional coding and maximum likelihood decoding has specific advantages against a selective jammer and was initially considered for this reason; however, further investigation revealed even more significant advantages. The decoder, configured to process repeated transmissions, provides optimum performance advantage as the information rate decreases or as the number of vehicles decreases; e.g., 7 dB advantage if the rate were changed from 2 kb/s to 400 b/s or the users dropped from 25 to 5 vehicles. Thus, significant modularity or operational flexibility advantage is provided at the expense of more logic circuitry in the vehicle – an added complexity which required substantial justification. It is felt that this feature of offering optional additional processing gain for selected vehicles provides an operator with an adaptive capability for matching the mode of the modem with the operating environment.

In summary, the waveform design for the command link consists of the chirped signal structure in a TDM address format. The following parameters apply to the transmitted signal:

- Frame time – 500 μs

- Subframe time – 250 μs (each coded bit is sent in a subframe)

- Bit time for chirp – 10 μs (corresponding to 25 users)

- Modulation–up and down chirp signals

- Chirp bandwidth – 12.8 MHz (for signal time bandwidth of 128)

- Number of orthogonal chirps – 128 frequency-hopped signals (corresponding to 128 different center frequencies spaced 100 kHz apart)

The receiver consists of a single matched filter which is matched to each of the transmitted waveforms and which produces a time-hopped signal output. The sequence generators, at both transmitter and receiver, are locked together such that the starting frequencies are randomly selected each bit time. In addition, the vehicle which is assigned the first bit in the subframe is randomly selected which provides time-hopping between the individual users to combat a dedicated jammer. The following parameters apply for the received signal.

- Matched filter time dispersion – 20 μs
            bandwidth – 25.6 MHz
            time bandwidth – 512

- Pulse output width – 78.25 η s

- Demodulation – up/down matched filters with envelope detectors

The tracking loop in the vehicle receiver tracks the time-hopped output of the matched filter in synchronism with its internal sequence generator and, thus, gates the signal at only the appropriate times. This tracking loop is at baseband since the matched filter and envelope detector provide output video pulses; in addition, the implementation is digital in order to provide hardware design with potential low recurring costs. Thus, the combination of matched filtering with a surface wave device implementation and a video tracking loop with digital implementation results in a significant technology development for the RPV modem.

Conclusions

The newly developed technologies in surface wave devices and in digital devices have significant potential application to RPV's where emphasis is on low recurring costs and small size. In fact, the success of future RPV programs is dependent on the technology developments and applications of such device techniques. Radiation has designed a spread spectrum demodulator which incorporates a surface wave matched filter and a video tracking loop having digital implementation. This technology development has resulted from the trade-off studies of the "Wideband Command and Control Modem," and together with other significant features, constitutes the selected modem baseline.

The continuance of this modem development into the hardware phase is the next logical step. Although limited breadboarding has been performed during the study for concept feasibility, the recommended hardware phase goes beyond this. It would demonstrate the design applications and limitations of the chirp spread spectrum waveform and the digital timing loop, for example. It would determine the design parameters and performance of the data links for different RPV missions. It would provide demonstration test data during actual fly-by tests such that meaningful results would be obtained under various environmental conditions. The hardware demonstration phase is strongly recommended to the government for follow-on to the study.

The realization of the advantages of the baseline modem design is dependent on the device packaging and this phase of the program is recognized as a subsequent requirement prior to application of the modem to RPV missions. The advantage of the baseline design is such that

x

overall improvements in performance and packaging are available as growth features commensurate with further developments in device technology. For example, as the chirp filter devices are produced with larger time bandwidth products, then greater processing gain performance is realizable. Also, as more LSI circuitry is used for the digital timing implementation, greater savings in cost and size would result.

SECTION 1.0

COMMAND AND CONTROL COMMUNICATIONS - RPV

1

1.0 COMMAND AND CONTROL COMMUNICATIONS - RPV

The approaching era of the RPV, remote pilotless vehicle, introduces a new and challenging problem in communications for command and control. This introductory section describes the requirements of a general class of RPV missions for both data link communications and for the vehicle position location. Subsequent sections discuss the Tradeoffs (Section 2.0), the Baseline Modem Description (Section 3.0), the Baseline Implementation (Section 4.0), an RF Configuration (Section 5.0), and a System Example (Section 6.0). In addition, supporting analyses are provided in the appendices.

1.1 General System Requirements

The RPV mission considered for this study consists of a multitude of vehicles, up to 25, which are controlled by a single ground station. Two classes of missions are accommodated: a short range strike mission having a range of 50 nmi and a long range, high altitude reconnaissance mission having a maximum range of 250 nmi. Line-of-sight communications prevail for both of these missions.

The cost-effective design for the RPV command and control necessitates low recurring vehicle costs. The large number of RPV's assigned to a given control station (say 100, in order to provide 25 in flight) and the predicted high attrition rate (compared to the life cycle costs of the Control Station) provides the rationale for the emphasis on low vehicle costs. A guideline established during the study was a ratio of at least 1000 : 1 between ground and vehicle costs; that is, a thousand dollars of ground equipment can be afforded before one additional dollar is designed into the vehicle. The recurring costs of the vehicle electronics are predicated on large quantities, like 1000, in order to properly stress the ground versus vehicle tradeoffs. Thus, vehicle cost estimates in this report are based on large quantity and are for the purpose of assessing tradeoffs relative to the ground and vehicle designs and are not meant to convey any meaning of nonrecurring development costs.

The RPV mission must be performed in a hostile jamming environment; thus, AJ requirements are imposed on the data link. The line-of-sight model for the ground-vehicle communications has the command uplink as the most vulnerable link requiring the most AJ protection. The specific requirement of 30 dB processing gain for this link is thus consistent with the mission. In addition, the vehicle-to-ground communications may require AJ techniques; however, no specific numerical requirements are provided other than providing maximum AJ consistent with cost-effective tradeoffs. Spread spectrum AJ communications impose further requirements for timing maintenance (viz., acquisition and reacquisition of synchronization); further discussions of these requirements are deferred to the specific command link requirements.

The vehicle dynamics impose constraints on the design of the communications data links such that guidelines are required. During the study, it was determined that the basic design should accommodate reasonably worst-case vehicle dynamics and upper limit values of MACH 1 (~1000 feet/second) and 20 g's were assumed. Improved performance would result when a specific mission does not demand such high dynamics.

2

One final general requirement imposed on the system design is that of flexibility and modularity. Performance and/or cost benefits should occur when fewer than the maximum of 25 vehicles are employed or when less than the maximum information rates are required for specific missions. The lack of any quantitative values for this requirement of modularity does not lessen its importance in the design tradeoffs.

1.2 Data Links

The Wideband Command and Control Modem includes the data link equipments for providing command information from ground to vehicle, for status information from each vehicle to the ground, and for imagery (or video) information from selected vehicles back to the ground control station. The video information is hereby considered an integral part of the command and control communications; in fact, it is this video information which provides the real-time control capability for the remoted pilot on the ground. Additional communications for the vehicle payload is not specifically considered as it can be accommodated by the command and status links. The data links include, in general, all the functions between the baseband user equipments and the antennas and thus, include baseband, IF, and RF designs. Specific requirements for these links are considered in the following paragraphs.

1.2.1 Command Uplink

The command data link is required to provide a nominal 2 kb/s information throughput from the master control station to each of the 25 vehicles for the purpose of flight, sensor, and perhaps, payload control commands. The quality of the data is specified by the bit error rate (BER) requirement of 10^{-5}. Since all commands originate from the common master station, the multiple command transmissions to each vehicle is defined as a multiple address problem in contrast to a multiple access situation. The interfaces for this link are the ground command formatter/encoder whose output is a data bit stream, and the command decoder located in the vehicle. RF considerations for each of the C, X, and Ku frequency bands are required.

The command data link is required to have a processing gain of 30 dB in order to provide protection against various types of jammer. Specific jammer threats include CW, Swept CW, pulsed, and Gaussian noise jammers; in addition, anti-spoof protection, as against a replica jammer, is desired. The design approach includes waveform design tradeoffs and performance estimates for each of these jammer types plus others which may pose a potential threat, including the intelligent jammer. Since the performance of a given waveform design against any one of these jamming threats is specified in terms of jammer-to-signal power ratio (J/S) for a given BER, this parameter is emphasized throughout this report.

The reacquisition time, following loss of timing synchronization, is an important performance parameter of a spread spectrum system especially one having the dynamics of an RPV mission. Two classes of signal outage which require reacquisition are considered: one, a short duration outage in the order of seconds due to changes in the vehicle attitude, signal

3

reflections, etc., and secondly, a longer duration outage in the order of a minute due to line-of-sight obstructions such as mountains, etc. The design considerations must include these signal outages and minimize the time for reacquisition.

The command demodulator which is located in the RPV is required to have a design consistent with low recurring cost. The demodulator of a spread spectrum link is generally somewhat complicated and expensive; hence, with this AJ requirement, double emphasis is required to simplify the vehicle electronics. Specific technologies which are required by the Statement of Work for considerations are surface wave device and digital device (i.e., reducible to LSI) technologies.

The flexibility requirements discussed in the general system requirements apply especially to this command link. The vehicle design, in order to emphasize the low recurring costs, must be able to accommodate missions having fewer than the full complement of 25 vehicles or less than the maximum data rate of 2 kb/s.

1.2.2   Status/Video Downlink

The data link requirements for the vehicle-to-ground communications include both status (or telemetry) data and imagery (or video) data. The status data required is given as 2 kb/s from each of the 25 vehicles with a BER of 10^{-5}. The video data requirement is given as a maximum of 20 Mb/s from any of five of the vehicles and with a BER of 10^{-3}. The five vehicles requiring video transmission would be in the target area, such as in the terminal phase of a strike mission.

In addition to the specific requirements provided in the Statement of Work, additional guidelines and imposed requirements are given in the following paragraphs.

For the status data link, the multiple access requirements constitute the primary design considerations and the familiar near-far problem of multiple access communications is paramount in these considerations. A minimum range assumed during the early study phase thus establishes a dynamic range requirement: 1) for the long range reconnaissance mission, a minimum range of one mile is taken such that the signal strength change between the 1 and 250 mile ranges is 48 dB; 2) for the strike mission, this dynamic range design would allow 1/5 mile minimum range for the 50-mile range case. A few dB additional margin is prudently included in the design guidelines to allow for antenna gain variations, variations in the propagation media, etc.

For the video link, the dynamic range requirements can be relaxed somewhat since imagery is used only in the target area and not at the minimum ranges as is the status data. This dynamic range requirement for the video varied between 10 and 20 dB during the study period with the final choice favoring the maximum value.

The protection of the video link against a potential jamming threat is one of the design considerations and although no specific requirements are stated, the resultant design

4

must be compatible with such options. One such consideration is providing spread spectrum AJ protection, especially if the data rate for the video data were reduced by later developments in source encoding techniques. A design imposition is thus suggested which provides a spread spectrum option with a resultant processing gain capability consistent with the reduction of video bit rates below the 20 Mb/s. For example, a reduced bit rate of 1 Mb/s video would allow a 13 dB spread spectrum option. A second consideration for protecting the video link is to provide security or privacy to the data itself. This consideration is primarily aimed at "hiding" the line sync signal of the video data to prevent it from being jammed or spoofed. Thus, a design for the video data link modem which provides an option for protecting the sync information is included as an added design guideline.

The interface of the status and video data links are the data formatter and imagery sensor outputs in the RPV, and the corresponding status and video processors and displays at the master ground station. The RF considerations, excluding the antennas, cover each of the C, X, and Ku frequency bands, and together with the command uplink, constitutes an overall frequency plan. Although frequency allocation determination is not a specific task of the study, it must be realized that a modem design which utilizes excessive bandwidth will be more difficult to accommodate in an operational system. A design guideline established during the study was to restrict the total bandwidth requirements of the modem, including uplink, downlink, and transmit/receive guard band to a maximum of 500 MHz. This permits common microwave components, such as the antennas, for each of the links and is consistent with such potential frequency allocations.

1.3   Position Location and Ranging

The spatial location of each of the RPV's is required to an accuracy commensurate with its required mission. For the short range strike mission, a position location accuracy of less than 100 feet is a stated requirement. For the long range reconnaissance mission, somewhat reduced accuracy is allowed.

The waveforms used for the data links are also useful to provide ranging measures from which position location can be determined. Since the command and status links provide continuous signaling to each of the 25 vehicles, these waveforms are required to provide the ranging. The wideband spread spectrum signals provide an inherent high resolution for accurate ranging; the ranging accuracy requirement is determined by the 100 foot position accuracy and the geometry of the data link terminals.

Position location is determined from ranging information by lateration techniques or rho-rho measurements. Thus, one or more slave stations are required, in addition to the master control station, in order to provide multiple range measurements and, hence, position location. The separation between slave and master stations, as well as the number of slave stations, is required to be consistent with the position location accuracy requirement. It is

5

assumed that the sole purpose of the slave stations is to receive the status waveform at that location for range mensuration. Thus, the slave stations do not need to demodulate the status data or the video data; however, in an operational system, this might be desirable to provide a backup communications capability.

SECTION 2.0

WAVEFORM DESIGN TRADEOFFS

2.0 WAVEFORM DESIGN TRADEOFFS

The trade-offs portion of the Modem Study is the most important single task and constitutes the majority of the study efforts. These efforts include both analysis and design support in order to estimate and optimize performance while at the same time evaluating the hardware impact of the different implementation approaches. The blend of performance advantages and hardware implementation reductions is predicated on the design philosophy established for the study.

The design philosophy becomes evident when the basic mission of RPV systems is examined. The success of an RPV modem design is measured by the extent to which the cost of the vehicle electronics can be reduced. The pertinent cost is the large quantity recurring dollar value of the vehicle portion of the modem which includes the command demodulator, the status modulator, and the video modulator. A demodulator is generally more complicated than a modulator, especially for spread spectrum modem; hence, the command demodulator is identified as the key element. The design philosopy, thus established, is to emphasize the command demodulator design in order to minimize its recurring costs!

This trade-offs section starts off with a brief summary description of the selected baseline design in Paragraph 2.1, then proceeds to develop the rationale for this selection. Paragraphs 2.2, 2.3, and 2.4 discuss the salient tradoffs for the three separate links: status, command, and video, respectively. Paragraph 2.5 concludes the section with the considerations of the RF design.

2.1 Baseline Waveform Design Summary

The results of the trade-offs study are presented briefly in this section, then followed by the arguments and analyses which justify this baseline selection. The reader is thus given the results first, such that he can proceed to a subsequent paragraph of interest to determine the rationale for the selection of that particular approach.

The baseline description of the waveform design includes the signal structure for each of the three links; command, status, and video. The command link from ground to each vehicle is a time-division multiple addressed format employing noncoherent orthogonal chirp signals for binary modulation and using frequency-hopped and time-hopped chirp signals for spread spectrum AJ. In addition, error-correction coding is used for improved performance and flexibility. The status downlink has a time-division multiple access format which utilizes differentially coherent phase shift keyed modulated signals and direct sequence pn spread spectrum. The video downlink is a frequency division multiple access format which employs differential, offset quadriphase modulated signals with an option for pn spread spectrum for potential lower data rate modes. In addition, the video and status signals of each vehicle are combined by frequency division multiplexing in order to require only a single RF channel and power amplifier. Figure 2.1 displays the baseline selection for the waveform design in compact summary form.

	MODULATION	SPREAD SPECTRUM	MULTIPLE
COMMAND:	UP/DOWN CHIRP (WITH CODING)	F-H/T-H	TDMA
STATUS	DPSK	PN DIRECT SEQUENCE	TDMA
VIDEO	DQPSK OFFSET	(PN OPTION)	FDMA
V/S MUX			FDM

86482-53

Figure 2.1. Baseline

9

Two outstanding features of this waveform design are considered sufficiently important to highlight in this summary:

First, the chirp signal structure for AJ is a novel spread spectrum technique which can be implemented using surface wave devices for the matched filters and using digital devices for the timing loop. This design approach is considered a significant state-of-the-art development for spread spectrum communications. These devices offer the promise that recurring costs for large quantity buys can be made compatible with the demands of low cost RPV's.

Second, the operational flexibility of the design which employs rate one-half convolutional coding with the binary modulated chirp signals constitutes an important user feature. This design provides improved AJ performance when the number of vehicles for a given mission are less than the maximum value of 25. Also, the design inherently allows full performance capability of the modem as the data rate is reduced below the 2 kb/s maximum command rate. Thus, the operational flexibility permits a custom configuration of data rates and number of vehicles in order to optimize system effectiveness.

The remaining highlight of this Baseline Summary is an estimate for the recurring costs of the vehicle electronics for the wideband command and control functions. This estimate is based on a large quantity (~1000) buy and does not include developmental costs to initially design the surface wave and digital device circuits. The costs, necessarily order-of-magnitude estimates, are displayed in Table 2.1. The costs of the chirp demodulator and the RF elements, which are the principal contributors, are backed up with cost data provided in Paragraphs 2.3 and 2.5, respectively. The total cost of $4,300 is given without the power amplifier, since its choice is based on developments in solid-state microwave power amplifiers at the pertinent C-, X-, or Ku-band frequency and by the potential interrelationship with the antenna, such as an array design. Projected development of IMPATT solid-state power amplifiers in the 1975-80 time frame provides a $1,600 estimate for a 10 watt power amplifier. Current costs of a TWT, including power supply, for this power level, is approximately $5,000.

Table 2.1. Vehicle Modem Costs

Unit	Cost
Chirp Demodulator	$1,734
RF (excluding P.A.)	1,263
Video/Status Modulators	800
Miscellaneous	500
Total (without P.A.)	$4,300

2.2 Status

The status signal designs must be capable of multiple access, relaying the ranging information to the ground stations, and transferring the 2 kb/s status data to the ground. Implementation of this signal is complicated primarily by the number of simultaneous RPV transmissions and by the widely varying ranges between the ground stations and the RPV's in that the received signal strengths are a function of range. Three multiple access techniques (CDMA, FDMA, and TDMA) were considered for the status waveforms and will now be described. Because a TDMA format was selected, it will be discussed in greater detail than the other two.

Because of the unbalanced receive signal levels, the CDMA system is subjected to significant self-jamming problems unless RPV transmitted power control is used. This power control would be required to vary the transmitted power over a range equivalent to the dynamic range of the possible distances between the ground stations and the RPV's. An assumption was made that the RPV's must be controlled and monitored from 1 to 250 miles which corresponds to a received signal dynamic range of 48 dB. This transmitter control introduces two additional problems. First of all, an indication of range must be available at the vehicle to control the transmitter. Two approaches were investigated: transmission of a range coordination word to the RPV on the command link which would be used to control the gain of the power amplifier. Because this approach did not adapt to transmission medium anomalies or antenna pattern nulls or lobes, the second approach, which used the receiver agc signal to control the transmitter, was selected. However, the second problem, that of transmitter efficiency and cost, was found to be the more significant in a low-cost RPV modem design. In the frequency bands of interest, low-cost medium power (~10 W) power amplifiers currently available, are generally TWTA's. Linear or unsaturated TWTA's are expensive to build and are less efficient than the more common saturated amplifiers. In addition, the TWTA self-noise limits the achievable output dynamic range. Also, the CDMA signal requires 25 parallel receiver channels at the ground station because of the simultaneous and continuous nature of the status signals. For these reasons, a CDMA status signal waveform was rejected.

FDMA was quickly eliminated because the multiple access antijam and ranging requirements result in an extremely wide bandwidth. This fact may be illustrated as follows:

a. The position location accuracy requirement dictates a ranging accuracy of 5 to 10 feet.

b. This, in turn, implies that the chip rate must be in the neighborhood of 10 Megachips/second.

c. The RF bandwidth of this signal is at least 10-20 MHz.

d. With a dynamic range requirement of 48 dB, nominal guard band must be allowed which is comparable to the signal bandwidth.

e. Thus, FDMA frequency allocations would require for the 25 vehicles in the order of 500-1000 MHz which is considered impractical.

11

2.2.1 TDMA Considerations

Time-Division-Multiplex-Access (TDMA) is the selected approach for the RPV status communication links. In general, it was determined that a viable TDMA system required a solution to the network timing problem, a reduction of the guard times to increase channel efficiency, and a technique to maintain the ground station code tracking loop synchronization between data transmission bursts. The TDMA signal design development and a preliminary signaling format are discussed in the following paragraphs.
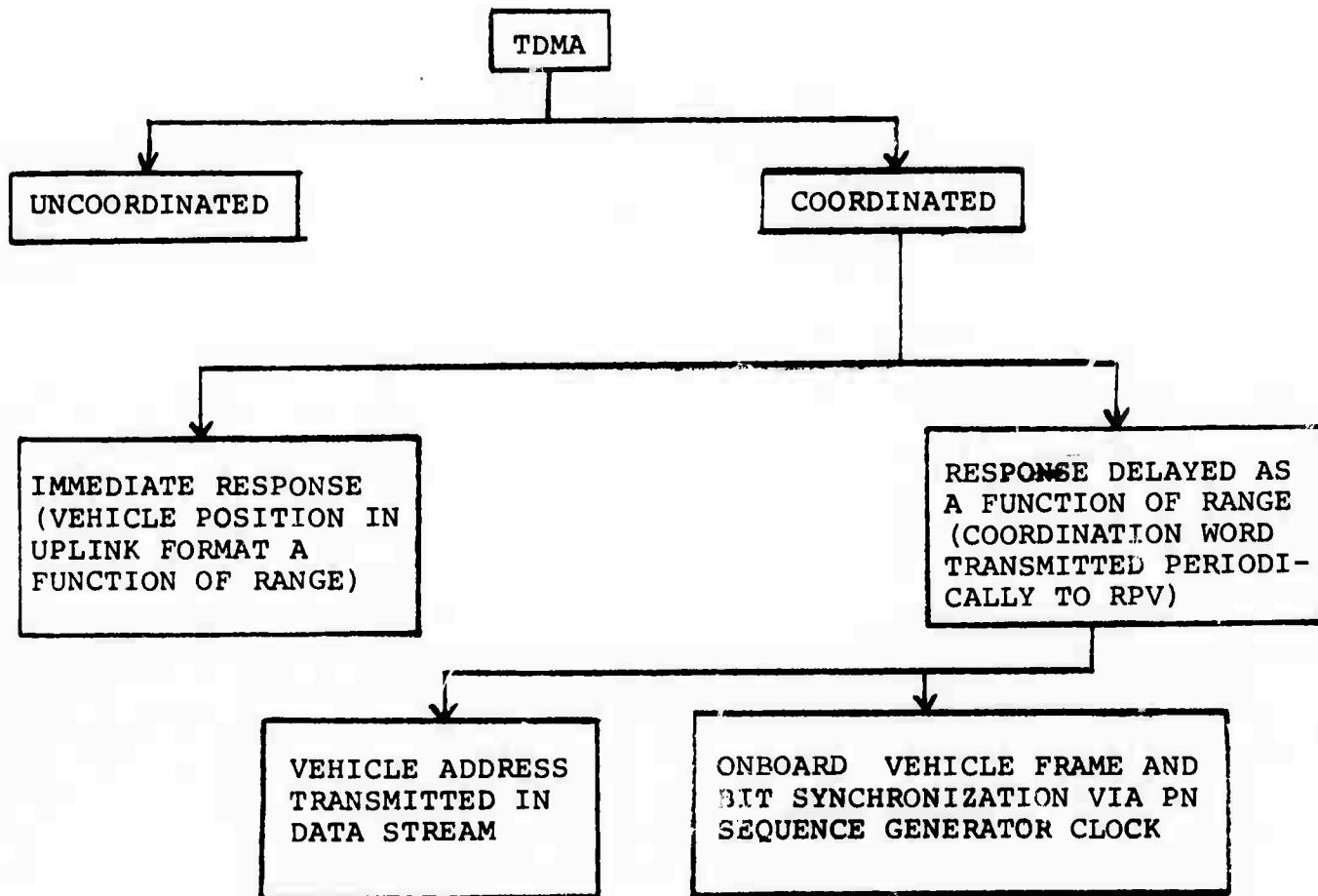
Signal Design Development

The evolution of the TDMA signaling format was based on the examination of several applications of TDMA as illustrated in Table 2.2.1. Within the general description of TDMA, the box titles correspond to system approaches which were examined during this study. As these are defined and the characteristic impact to the system operation evaluated, the evolution of the preferred system will become evident.

The first major division is between uncoordinated and coordinated TDMA. An uncoordinated TDMA system is defined as a system which does not utilize the range information available at the ground station to reduce the required guard times and increase channel efficiency. That is, after a vehicle is interrogated by the ground station, it waits for the entire vehicle response before interrogating the next vehicle. Conversely, a coordinated system uses the known vehicle position and corresponding path length delays to reduce the guard times by ordering the interrogation sequence or transmitting a favorable transmission time to the vehicle. Two system concepts were evolved which satisfied our definition of coordinated TDMA. These concepts were designated as the immediate response and commanded delay with an RPV code tracking loop system. For the immediate response system, the vehicle interrogation sequence is ordered as a function of vehicle position to obtain nonoverlapping signals at the ground station and reduce the 3 ms minimum required for the noncoordinated system. The primary drawbacks to this approach are the dependency of the channel utilization efficiency on the relative position of the vehicles and the requirement for the vehicle code tracking loop and viewer to be continuously looking for a command.

The second coordinated system investigated used the delayed response with the uplink command data combined into a continuous 50 kb/s data stream and spread by a single PN sequence. This enables the vehicle to track the uplink code and simplifies the vehicle equipments. Because the commands are continuously received by all vehicles, a technique for frame and message identification and synchronization is required. Two applicable techniques are identified in the last two boxes of Table 2.2.1. Transmitting the appropriate vehicle addresses in the data stream is a viable approach, however, it does require additional overhead bits (which results in decreased processing gain) and an address and/or sync pattern correlator onboard the

12

Table 2.2.1.   TDMA Tradeoffs

```
                        ┌──────────┐
                        │   TDMA   │
                        └────┬─────┘
            ┌────────────────┼──────────────────┐
            ▼                                    ▼
  ┌──────────────────┐              ┌──────────────────┐
  │  UNCOORDINATED   │              │   COORDINATED    │
  └──────────────────┘              └────────┬─────────┘
                           ┌─────────────────┴──────────────────┐
                           ▼                                     ▼
            ┌──────────────────────────┐      ┌──────────────────────────┐
            │ IMMEDIATE RESPONSE       │      │ RESPONSE DELAYED AS       │
            │ (VEHICLE POSITION IN     │      │ A FUNCTION OF RANGE       │
            │ UPLINK FORMAT A          │      │ (COORDINATION WORD        │
            │ FUNCTION OF RANGE)       │      │ TRANSMITTED PERIODI-      │
            │                          │      │ CALLY TO RPV)             │
            └──────────────────────────┘      └────────────┬─────────────┘
                       ┌────────────────────────┬──────────┘
                       ▼                        ▼
          ┌──────────────────────┐  ┌──────────────────────────────┐
          │ VEHICLE ADDRESS      │  │ ONBOARD  VEHICLE FRAME AND    │
          │ TRANSMITTED IN       │  │ BIT SYNCHRONIZATION VIA PN    │
          │ DATA STREAM          │  │ SEQUENCE GENERATOR CLOCK      │
          └──────────────────────┘  └──────────────────────────────┘
```

13

vehicle. The other technique is easily implemented with a series of counters that divide the PN sequence generator clock by the appropriate factors to provide bit, message, and frame timing. Because the vehicle clock must be exactly synchronized to the uplink sequence frequency and phase, it provides an ideal source for all vehicle data timing.

The system concepts presented above will be discussed in detail below with emphasis on the guard time considerations for each TDMA system approach.

An additional consideration for these TDMA concepts is the update rate. For the purposes of this investigation, the update rate has been defined as the number of message bursts received from each RPV each second. Thus, 50 updates per second correspond to 50 messages each 40 bits long-spaced uniformly in the received format. The update rate becomes important from an implementation standpoint when ranging/position location accuracy and short-term reacquisition of the code tracking loops are considered. If the update rate is too low, the vehicle dynamics and oscillator instabilities may result in significant initial phase errors at the beginning of each message burst and excessive code pull-in time. Also, a low update rate affects the ranging/position location accuracy of vehicle motion between sampling points (message bursts). As an example, if we specified a system at 10 updates/second, there would be 0.1 second between message bursts (range samples). Because the vehicle is assumed capable of 20 g maneuvers and 1,000 feet/second maximum velocity, the range difference (ΔR) between samples may be

$$\Delta R = vt + \frac{1}{2} at^2$$

$$= 103.2 \text{ feet.}$$

As the range accuracy must be 10 feet or better, this ΔR is clearly unacceptable and, even if sophisticated trajectory prediction programs were used at the ground station, the position location accuracy would probably not be met. A more detailed discussion of position location determination and range accuracy requirements is included in Paragraph 3.3 of this report.

The update rate also affects some of the operational characteristics of the system in that the degree of real time or near real-time vehicular control is affected by this rate. If the update rate is too low, the response time of the vehicle (caused by waiting for a proper status time slot, interpreting the received data at the master station, formulating an appropriate command and incorporating it into the correct time slot in the command format) may be unacceptably slow.

On the other hand, excessively high update rates will be shown in the following paragraphs to cause high transmitted data rates, and low channel utilization efficiency because of guard time requirements. Our selected update rate of 50 updates/second appears to be a reasonable compromise between high data rates and the problems resulting from low update rates.

14

As the TDMA system investigation progressed, the noncoordinated and immediate response approaches were found to be inadequate and were not considered further. A summary of the investigation and performance of the timed response coordinated TDMA system will now be presented.

The coordinated TDMA with timed response is a system that utilizes the vehicle ranging information to reduce the guard time in the status downlink. This is accomplished by commanding appropriate delays to the vehicles before they respond.

The minimum guard time is to be considered for two different reasons. They are the 1-250 nmi range requirements already discussed and the master and slave station configuration needed for determining vehicle position. Figure 2.2.1-1 illustrates the worst-case approach and indicates that a guard time of 12 μsec/nmi is required in this worst-case approach. When this amount of guard time is incorporated into the status downlink, the responses will not overlap (interfere) at the slave station. There will be no overlap at the master station either since the delayed return approach was incorporated specifically for this reason.

Figure 2.2.1-2 summarizes the different aspects of the guard time problem associated with the slave station. The left ordinate axis (upper half) gives the transmission time allocated each vehicle per frame, the right ordinate axis is the required bit rate that is needed so that each vehicle will have a throughput of 2000 b/s. The bottom left ordinate is the efficiency of the system, i.e., the amount of time the channel is being used to transmit information. The abscissa is updates per second which means the number of frames per second or the number of different times a vehicle is addressed per second. For example, if the update rate is 50 updates per second, the vehicle transmits 40 bits each time for 50 different times in one second thus yielding the 2000 b/s throughput. The number on each curve (i.e., 10, 20, 30 and 40 have units of nautical miles and refer to the distance between the master and slave ground stations. Consider another example, the case that requires 100 updates per second. From the figure, one sees that a bit rate of 80 kb/s is sufficient for the 10 nmi baseline. However, if a 20 nmi baseline is needed, the bit rate jumps to 180 kb/s with the change from 66 percent to 35 percent in efficiency. And for the 30 nmi baseline, it is impossible to achieve the 2 kb/s per vehicle throughput at 100 updates per second.

15
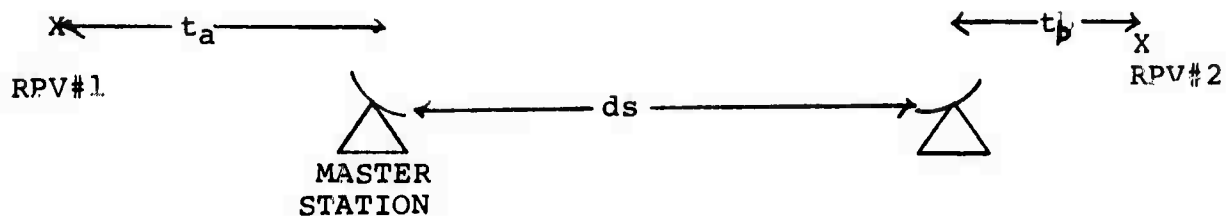
$$ts = ds/c \sim 6\,\mu\,sec/nmi$$

SAY VEHICLE #1 TRANSMITS FIRST FOR td SECONDS
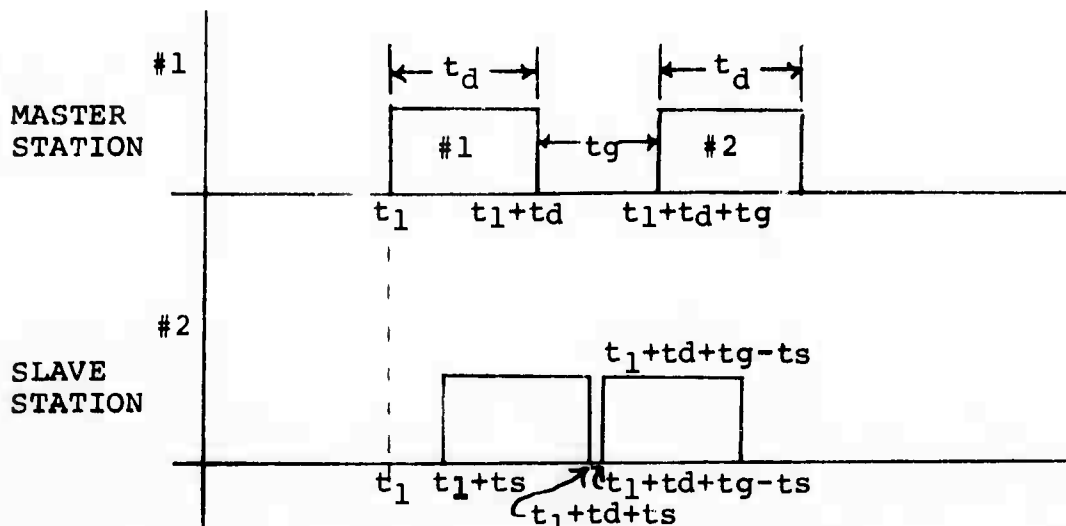
FOR NON OVERLAP, $t1+td+tg-ts \geq t1+ts+td$

or $tg \geq 2ts$

Figure 2.2.1-1.   Guard Time Considerations (Coordinated Returns)
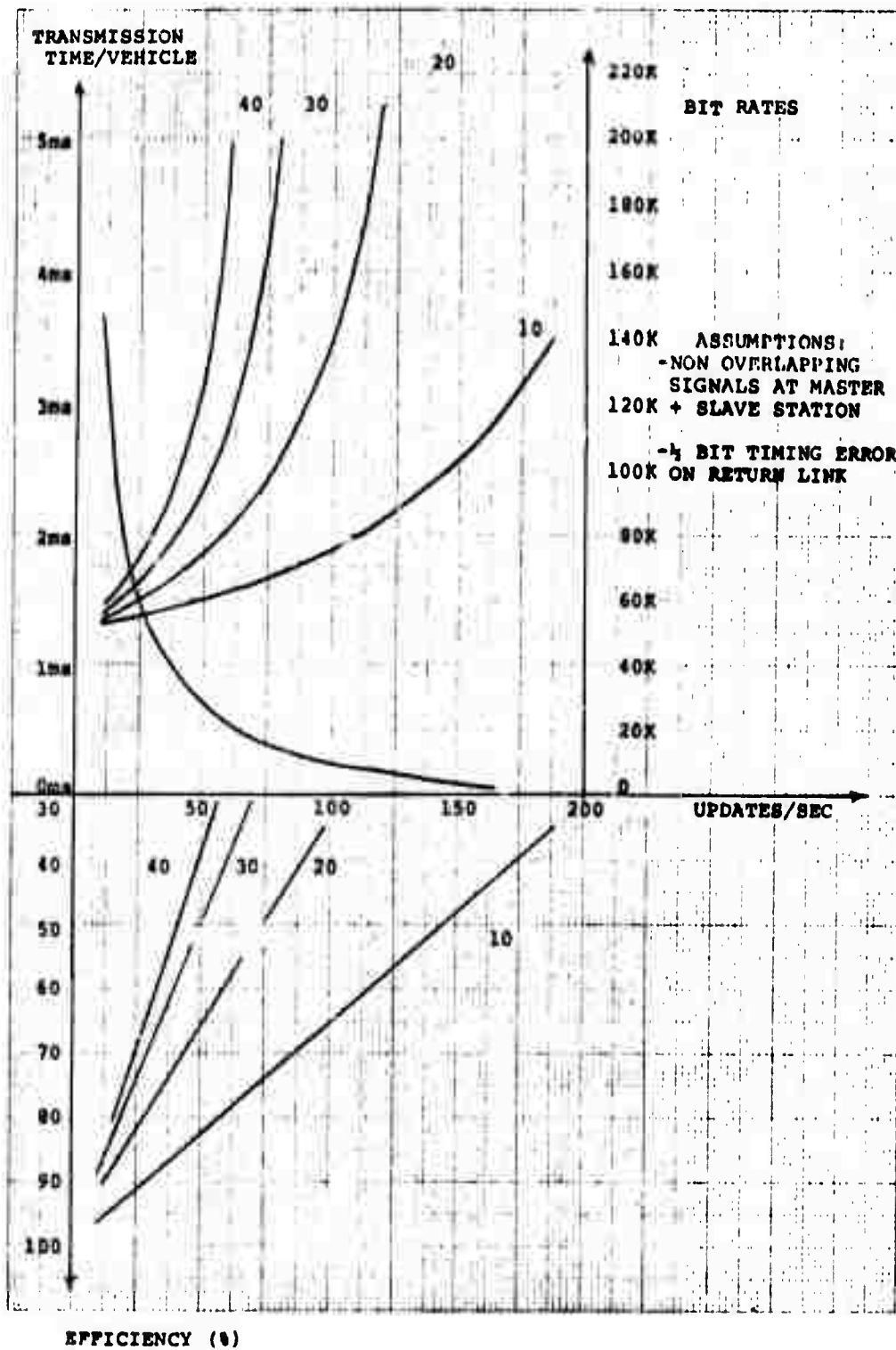
16

Figure 2.2.1-2. TDMA Transmission Rate Tradeoffs

17

Signal Design Format

The tradeoff results are summarized in Table 2.2.1-2 which provides the format of the TDMA signal. With the 50 updates per second, each of the 25 vehicles has a response time of 0.8 millisecond. The information bits are transmitted at an 80 kb/s rate in the 0.5 millisecond burst time such that 40 bits are transmitted each burst for the nominal 2 kb/s throughput rate. This format provides adequate preamble and guard times for reception of data by the master and slave stations.

18

Table 2.2.1-2. Preliminary Downlink TDMA Signaling Format

- 50 updates/second

- 40 bits/message

- 25 vehicles at 2 kb/s throughput/vehicle

- Coordinated returns

- Uplink PN code phase (derived from a continuously tracking delay locked loop) is used to directly spread the downlink data

- Nonoverlapping returns at both the master and slave stations (assuming a 20 nmi baseline)

- 80 kb/s transmitted data rate

- 62.5 percent overall downlink channel efficiency

- 0.8 ms (or 64 bit periods) available for each vehicle response

The 0.8 ms is allocated as shown below:

Downlink Time Allocation
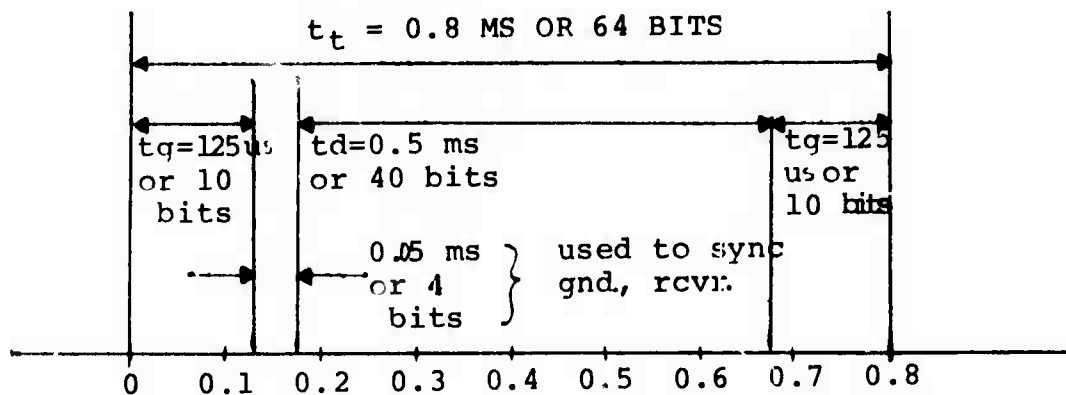
where:
- t_t = Total available time for an RPV response
- t_g = Guard time required to avoid overlapping signals at the slave station
- t_d = Time to transmit the required 40 bits/response

2.2.2   Status Modulation

The tradeoffs and baseline selection for the modulation of the TDMA burst signal are discussed next. This modulation includes both data modulation and spread spectrum/ranging modulation.

A logical first choice for the spread spectrum/ranging signal on the status downlink is the same as that used for the command uplink. As will be discussed subsequently in Paragraph 2.3, this baseline is a chirped signal providing spread spectrum signalling for both AJ and ranging. If this chirp signalling is a viable candidate for the status link, it must be shown that its modulator is as simple or more so as other signalling schemes since the design philosophy is to minimize the vehicle electronics. This is not true for a chirp signal – its modulator is more complicated than other schemes. (It was selected for the uplink based on the demodulator simplicity in the vehicle not the ground modulator.)

A second consideration suggests the use of a direct sequence PN spread spectrum signal which provides both AJ and ranging. This signal is easily generated with a simple switch, or balanced mixer, generally used as the modulator. The rate of this PN sequence is determined by the required AJ processing gain or the ranging accuracy. Since there is no specific requirement on the AJ, let us consider the ranging requirement established by the 100-foot position location specification. The expression for the RMS timing jitter of an SDDLL for each bit time, assuming square law detection is given[1] by:

$$\sigma_\epsilon = \frac{\Delta}{2} \left\{ \frac{1.215}{E_b/N_o} + \left[\frac{2.952}{\left(E_b/N_o\right)^2} \right]^{1/2} \right\}$$

where Δ is the chip time of the PN sequence expressed in time or equivalent distance and E_b/N_o is the familiar signal energy per bit to noise power density. For averaging over several bit times this jitter is reduced by the square root of the number of independent samples. For the burst time of 40 bits, then

$$\sigma_t = \frac{1}{\sqrt{40}} \sigma_\epsilon$$

and a few values are calculated in the following table for the case of $E_b/N_o = 10$ dB.

Table 2.2.2

Chip Rate $1/\Delta$	σ_t
50 Mc/s	0.6 ft.
20 Mc/s	1.5 ft.

[1] Huff, R. I., "TDMA Space Communication Systems"; RADC TR-255; Nov. 1971.

20

Table 2.2.2 (Continued)

Chip Rate $1/\Delta$	σ_t
10 Mc/s	3 ft.
5 Mc/s	6 ft.

For the desired position location, total ranging error should be held to approximately 20 feet (see Paragraph 6.2) for which the jitter contribution should be no greater than 10-20 percent in order to have relatively little impact on the error budget (see Paragraph 3.3). Thus, a chip rate of about 10 Mc/s is adequate for this ranging requirement; a value of 12.8 Mc/s is selected for the baseline in order to provide a 2^n number. The higher value of say 50 Mc/s is not required for ranging accuracy and would constitute an overdesign (excessive channel bandwidth and frequency allocation problems). The spread spectrum rate of 12.8 MHz provides substantial AJ protection, especially in light of the more vulnerable video link, and is the recommended amount of processing gain considered cost-effective for this link.

The remaining tradeoffs for the status link involves the modulation technique for the information. The candidate schemes, together with the direct sequence PN spreading, are biphase or quadriphase, either coherent or differentially coherent. Quadriphase is rejected since it complicates the vehicle modulator unnecessarily. Differentially coherent biphase, or DPSK, is favored over fully coherent PSK for TDMA formats in which there are a relatively few number of bits per burst as is the case here. Thus, the tenths of dB performance degradation associated with DPSK is justified in order to avoid the difficulties of the fully coherent phase-lock loop approach. The baseline selection for the status link includes DPSK modulation of the data at the burst rate of 80 kb/s and with a PN spread rate of 12.8 Mc/s. It is noted that this signal design is very similar to that of the TDMA program of Ohio State University* despite the different TDMA system concepts. This OSU development provides excellent background information, both analytical and experimental, to substantiate the performance estimates of this status link.

2.3 Command

The command uplink tradeoffs are most important, as previously discussed, because of the spread spectrum AJ requirements and the design emphasis for low recurring vehicle demodulator costs. Thus, somewhat greater detail is given to the tradeoffs, especially hardware implementation considerations, in this section compared to the other links. The general considerations for the waveform design are provided in Paragraph 2 3.1 whereby two candidate schemes, PN and chirp, survive. Paragraph 2.3.2 provides hardware design considerations for cost comparisons between these two candidates as well as ROM cost estimates for the demodulator. The baseline selection is then summarized in Paragraph 2.3.3.

---

*Op. cit.

21

2.3.1   Waveform Design Tradeoffs

The considerations in this paragraph include the multiple address requirements for commanding up to 25 vehicles simultaneously, the spread spectrum requirements for providing AJ processing gain, and the modulation requirements to support the 2 kb/s data throughput rate for each vehicle. The additional requirements of operational flexibility and modularity are also considered.

Multiple Address

The multiple address requirements are considered with code division, frequency division, and time division formats. The term multiple address is used in this section to distinguish it from multiple access since they differ in at least two important aspects. All transmissions emanate from a single terminal; thus, the signal strength for each vehicle's transmission is the same as others at that location. In other words, there is no near-far problem. Also, for the same reason, the phase of the signal is the same for each vehicle's address since it comes from a common transmitter.

The absence of the near-far problem might suggest the use of CDMA or FDMA techniques since one of the main problems with these multiple access schemes is the near-far condition. However, it is not logical to seriously consider either CDMA or FDMA for the command link if they are not also appropriate choices for the status link. That is, there is no CDMA code word already assigned to each vehicle by the status link. Nor is there a frequency assignment, generated from a frequency synthesizer, already assigned to a given vehicle as a result of the status link.

A TDMA technique is a logical choice for the command link, however, because the information rate is increased as a result of the time-division multiplexing and because any given vehicle can track the signal transmitted to the vehicles. The increase of information rate from the nominal value of 2 kb/s for each vehicle to 25 x 2 kb/s = 50 kb/s is advantageous since the effects of vehicle dynamics (i.e., Doppler and accelerations) are lessened at the higher bit rates. In fact, as will be pointed out later, the signal design on the uplink completely avoids the requirements for AFC and thus avoids this design complication. The other primary advantage is that the code tracking loop, or timing loop, in each vehicle is allowed the use of the total transmitter power for tracking as opposed to its normal proportionate share. Thus, each vehicle has a signal-to-noise advantage for the tracking loop which allows synchronization to be maintained in many cases when the signal strength drops well below the level required to provide adequate vehicle commands.

A TDMA format is chosen for the baseline of the command link.

Spread Spectrum

The waveform of the spread spectrum signal for the TDMA'ed command link is next considered. Time hopping (T-H), frequency hopping (F-H), PN, and other spread spectrum

22

techniques are possible approaches and have been evaluated during the study phase. Two candidate schemes evolved from these tradeoffs with others having been rejected. One is a direct sequence PN waveform and the other is an F-H, T-H chirp waveform which will be briefly described.

The waveform design for direct sequence PN spread spectrum signalling is commonly known and need not be described in detail here. One approach for reducing the complexity of the demodulator for these PN signals, however, is worth noting. The use of phase coded surface wave filters would provide a matched filter demodulation for "short" PN codes; however, these are not appropriate for a jamming environment because of their ease of spoofing. The use of suitable phase coded SWD's could potentially overcome this problem since the PN code of the filter could be changed in synchronism with the transmitter every frame time. This potential application of switchable SWD's explains the extensive research in these techniques although the development stage of these R&D devices is not far enough along for consideration in this RPV Program. Thus, the conventional and more complicated active correlators, or code tracking delay lock loops, are the considered implementation approach for the PN waveform approach.

The chirp wideband signal used for AJ applications with emphasis on the simplified demodulator design is a novel approach devised during the study which requires some explanation.* A chirp signal is a wideband signalling scheme like that of a PN signal and would suffer from the same disadvantage of the "short" code PN (i.e., potential vulnerability to spoofing) if other precautions were not taken. One desirable technique is to frequency-hop the center frequency of the chirp signals among many possible orthogonal frequencies. These signals are orthogonal if the center frequencies are separated by the bit rate and it has been shown that the amount of frequency hopping should equal the bandwidth of the chirp signal for time-bandwidth product optimization. Thus, the channel bandwidth with frequency hopping is twice the chirp signal bandwidth.

A second desirable technique for improving the AJ performance is to time-hop the TDMA chirp signals between the various vehicle users. The normal matched filter output for a chirped signal is a compressed pulse which is a well-known result, especially in radar applications. With chirped signals which are F-H'ed the compressed output pulse hops in different output time slots in accordance with the selected center frequency of that F-H'ed chirp. (Thus, the matched filter can be considered as converting F-H'ed input signals to T-H'ed output pulses.) Now with time-hopping between users, the compressed pulse output for a given vehicle address appears in not only one of N time slots per bit time but in one of 25 x N time slots. Further clarification of this signal design will be provided by the block diagrams and waveforms provided in the subsequent Section 3.0.

The primary rationale for considering the chirp signals is that a surface wave filter demodulator applies. The SWD matched filter for a single chirp waveform is well known and

---

* A patent disclosure has been submitted to RADC on this chirp spread spectrum signalling with surface wave device matched filters.

23

excellent measured results have been obtained for time bandwidth values exceeding 1000.* Thus, the state-of-the-art in these chirp SWD's will support this signal design approach. The same SWD matched filter for a single chirp will "match" the F-H'ed chirp signal if its time-bandwidth is increased to accommodate the extremeties of the frequencies of the highest and lowest F-H'ed signals. Thus, a single SWD matched filter will suffice for receiving the chirp signals even though they are frequency-hopped.

The SWD matched filter, followed by an envelope detector, provides sin x/x compressed pulses in accordance with the F-H chirped signals transmitted. A timing loop is then required to extract the basic clock such that the transmitter and receivers are synchronized, each having a "long" sequence generator. The compressed pulse from the matched filter is gated, assuming a synchronized condition, such that extroneous pulses in other time slots are rejected. (The sequence generator at transmitter and receiver determine which frequency/time slot will be effective each bit time.) The point of this discussion is that the timing loop to track the compressed output pulse is a baseband loop. This offers a considerable simplification in the tracking loop, especially if a digital design is developed and if the potential for LSI packaging exists. Further discussion of hardware design tradeoffs will be provided in the subsequent Paragraph 2.3.2.

Modulation and Coding

This paragraph addresses the trade-off results dealing with the transmission of the information at the 50 kb/s burst rate, or 2 kb/s throughput, with the required bit error rate. Two primary considerations are the type of modulation and the application of error correcting coding techniques.

The modulation tradeoffs show that a specific performance versus implementation trode results from coherent versus noncoherent signalling schemes. For the assumed parameters, it was determined that noncoherent modulation, though suffering a potential 3 dB performance loss, has the advantage that no phase tracking or AFC is necessary as it would be for coherent or differentially coherent modulation schemes. Because of the design philosophy of emphasizing the vehicle electronics, the noncoherent modulation approach is recommended. This opproach has decided advantages for reacquisition, when the synchronization between clocks is temporarily lost, since the odded dimensions of frequency and/or phase reacquisition is not required. The chirp signal format is easily suited for noncoherent modulation by using an up-down scheme: an up chirp for a "1" and a down chirp for a "0." Dual SWD matched filters followed by envelope detectors provide the essential demodulation for the data.

The opplicotion of error-correction coding for the command link is manifold and its inclusion in the baseline is recommended despite the violation of the rule: "keep the vehicle electronics minimum." Initially, rate 1/2 convolution coding was considered to improve the BER performance against a selective jammer (one who also chirps with the same slope). However, more significant advantages were reclized in the way of flexibility once the coding was considered.

---

* See, for example, the symposium proceedings of the Ultrasenics Symposium; Boston, Mass.; October 1972.

Without getting into the details in this section, it is sufficient to say that full performance can be realized from the command demodulator/decoder for different operating conditions which include fewer than 25 vehicles and less than 2 kb/s data rate for each vehicle. This is further discussed in Section 3.0.

2.3.2   Implementation

Since we have established two approaches – the chirped/match filter and direct PN spreading – which give the required processing gain on the command link, it is worthwhile to consider how each of these approaches would be implemented in order to obtain a clear idea of their relative complexity and cost. The result of this comparison will heavily influence the final choice for the command link modem. In particular, the complexity of the command demodulator, which is located in the vehicle, is of primary interest; because this unit will be built in high quantities and its recurring cost must, therefore, be minimized.

Figure 2.3.2 shows block diagrams of the candidate approaches. The chirp demodulator is shown at the top of the figure, and the demodulator for the direct-sequence spreading is shown at the bottom. While the latter is apparently significantly more complex, this is not necessarily true if the baseband delay lock loop, shown as one block on the figure, is, in fact, extremely complex. In fact, the loop contains a synthesizer which consists of a stable oscillator and some logic, a PN generator, and additional logic for keeping track of the format counts (the details appear in Paragraph 4.1). This is roughly equivalent to, although slightly less complex than, the baseband circuitry for the direct-sequence demodulator; which also requires a synthesizer and PN generator, plus biphase modulators and drivers and a more powerful local oscillator source.

The IF bandwidths are about the same for the two approaches, but the chirp approach requires more gain because of the high insertion loss of the dispersive delay lines (chirp matched filters). Implementation difficulties are about equivalent, however; because while the chirp demodulator requires higher total gain, the gain distribution is very difficult in the direct-sequence machine because the spectrum collapse occurs at IF. This means that we must minimize gain before spreading to avoid saturating the amplifier and mixers on broadband noise, and must, therefore, put a lot of gain at one frequency after despreading. This is difficult to manage in a small volume, without special shielding which increases the price. The gain can be distributed more evenly about the chirp filters, since the spectrum does not collapse until the signal is at baseband.

The key advantage to the chirp approach, however, is that the chirp delay lock loop accomplishes not only the basic sequence timing function, but also demodulates the data and supplies timing for the data detector. This is not the case for direct spreading. The demodulator, in that case, must first establish sequence timing for despreading; then, a carrier-tracking loop recovers a coherent carrier reference for data demodulation, then a third loop, contained in the data detector, establishes bit timing for optimum bit decisions. Thus, in addition to the delay lock loop, two additional loops are needed for data recovery. Additional analog circuitry is needed for the doubling process, including filters and amplifiers, while the chirp technique allows much of the processing to be done at baseband logic levels where large-scale integration can be used to reduce size and cost.

While the preceding can give some indication of why Radiation believes that the chirp approach is more economical, a more detailed analysis is needed to really pin down the

26
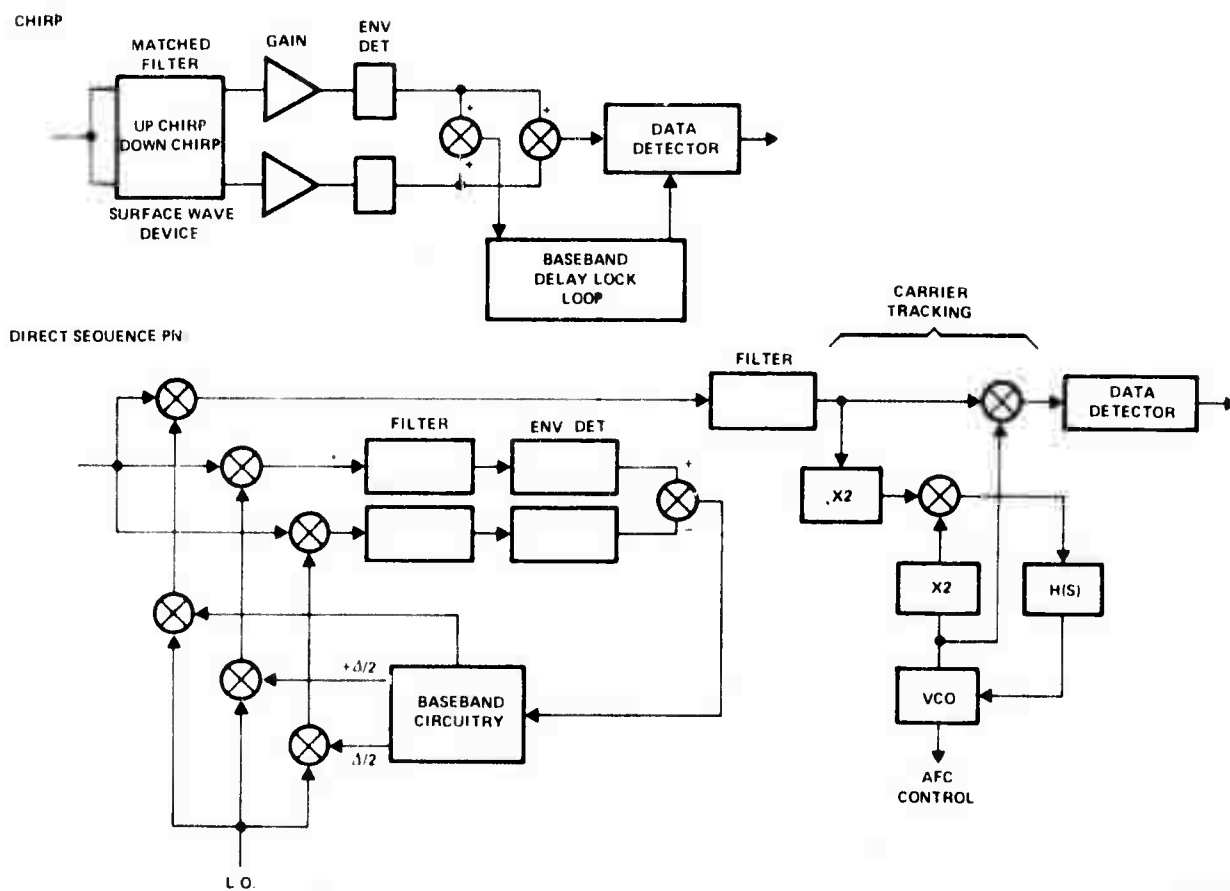
Figure 2.3.2. Two Possible Command Demodulators

27

differences. The following paragraphs will discuss in detail the two most expensive items - the IF amplifiers and the crystal oscillators - to obtain an optimum choice for these for each approach. Then, these numbers, together with the estimates, are combined with the costs of other materials for each approach; and the final large-quantity recurring costs for each approach are compared.

2.3.2.1   IF Amplifier Tradeoff

The tradeoff considers the cost per stage for a given typical stage gain and noise figure versus IF bandwidth and center frequency. The cost and gain per stage is based on 50-ohm cascadable hybrid microcircuits which lend themselves to automated mass production techniques. In large quantities, discrete component amplifiers are several times more expensive than hybrid microcircuits because of the nondiminishing labor cost, thence, are not considered. At the present time, maximum economies are achieved by use of the following techniques: (0 to 50 MHz) monolithic, (50 MHz to 500 MHz) thick film, (400 MHz to 1 GHz) thin film.

The cost for a given gain-bandwidth product climbs rapidly with increasing center frequency beyond 500 MHz. This accelerating increased cost with center frequency is caused by the meticulous and costly fabrication and processing techniques required to produce transistors which give satisfactory power gain with low feedback at these frequencies. Future production techniques may lower these curves to a more modest growth rate; however, over the past year, significant cost decreases have resulted from greater competition in the market rather than breakthroughs in design techniques. Thus, from a purely economic point of view, the IF center frequency should be chosen very low, even though this means a multioctave rather than a narrow band IF amplifier. However, there is another cost to be considered; the cost of image rejection filtering which is increased with lowered IF center frequency. This cost must be balanced against the cost of the basic IF amplifier to reach a least-cost combination.

Assume a -50 dBm minimum signal level is available from the first mixer preamplifier. A first IF with a gain of 42 to 50 dB is required to place the signal in the -8 to 0 dBm range for low-noise second mixing and low-gain parallel second IF's.

28

Tables 2.3.2.1a and 2.3.2.1b compare the cost of cascaded-stage IF amplifiers to meet the above gain objective. The first table shows bandpasses chosen to minimize cost with little regard for image rejection difficulties. The second table has bandpasses chosen to provide a more easily managed image problem. The final amplifiers chosen should lie between these two extremes.

It is assumed that most of the automatic gain control will be accomplished in the first IF. This will guarantee linearity in the high level second mixer and simplify the parallel second IF's. To accommodate an operating range from 1 to 250 nmi requires roughly 48 dB (inverse square loss) + 2 dB (fading) = 50 dB agc range. Through the use of soft limiting in the IF, the control range might be cut by 6 dB to 44 dB agc range. A good approach would be to modify the stage modules through the addition of PIN or Schottky diode gain control elements to provide a variable gain building block. The cost of this modification in large quantity buys is about +10% of the basic module cost.

2.3.2.2 Crystal-Controlled Frequency Source Tradeoff

Crystal-controlled frequency sources can be classified into four categories as a function of the method used to stabilize the output frequency. These categories are: uncompensated, temperature compensated, thermostat oven controlled, and proportional oven controlled. They have been listed in order of increasing stability.

Uncompensated crystal oscillators are used to provide frequency accuracies up to 2 parts in 10^5 over $-40°$ C to $+70°$ C and 1 part in 10^5 over a $0°$ C to $+65°$ C temperature range. The baseline system requires stabilities in the range of 1 part in 10^7. Hence, it is doubtful whether the temperature stability necessary to guarantee this accuracy for an uncompensated crystal oscillator could be maintained in the vehicle.

Referring to Table 2.3.2.2 on frequency sources, entries for the uncompensated oscillator have been deleted, since the accuracies are not considered sufficient for this application. The first column, the temperature compensated crystal oscillator, is an excellent choice for providing stabilities of 10^{-6} between $0°$ C to $65°$ C; but becomes more expensive than an oven controlled unit for the greater temperature ranges, $-40°$ C to $+70°$ C, and higher accuracies, 10^{-6} to 10^{-7}. Its three most attractive advantages are no oven power required, excellent short term stability, and that the oscillator is not placed in a maximum temperature aging environment dictated by an oven temperature set at the maximum transient temperature encountered in the vehicle. If the thermal environment in the vehicle has good short term stability, the temperature compensated oscillator can provide short term stabilities of 10^{-8} over several minutes and 10^{-9}/second which is excellent for our application. However, the rapidly increasing price above that of an oven controlled oscillator when accuracies of 10^{-6} or greater over the extended temperature range, $-40°$ C to $70°$ C are required, makes this a marginal choice. If we can tolerate $\pm 5 \times 10^{-6}$ ($-40°$ C to $70°$ C), $\pm 10^{-6}$ ($0°$ to $65°$ C), $\pm 10^{-8}$ 5 minutes, and $\pm 10^{-9}$/second, then the temperature compensated oscillator becomes economical in 1000 unit purchases.

29

Table 2.3.2.1a. Bandpass Chosen to Minimize Cost,
Image Rejection Secondary

BANDWIDTH	CENTER FREQ.	BAND EDGES MHz	# STAGES	COST PER STAGE	TOTAL COST	TOTAL GAIN
400 MHz	346 MHz	200 - 600	4	$45	$180	48 dB
200 MHz	283 MHz	200 - 400	3	$32	$ 96	42 dB
100 MHz	141 MHz	100 - 200	3	$20	$ 60	48 dB
50 MHz	71 MHz	50 - 100	3	$11	$ 33	54 dB

Table 2.3.2.1b. Bandpass Chosen for Easily
Managed Image Rejection

400 MHz	671 MHz	500 - 900	4	$105	$420	48 dB
200 MHz	592 MHz	500 - 700	3	$50	$150	42 dB
100 MHz	548 MHz	500 - 600	3	$38	$114	48 dB
50 MHz	524 MHz	500 - 550	3	$32	$96	54 dB

Table 2.3.2.2. Frequency Sources, Crystal Controlled (20 to 50 MHz)

Temperature Compensated	Oven, Thermostat Controlled	Oven, Proportional Control
+ low power (no oven)	+ high long term accuracy	+ high long term accuracy
+ wide temp. range without const. hi. temp aging	+ moderate cost for acc. $\pm 10^{-6}$ to $\pm 10^{-8}$ range	+ very high intermediate & short term stability
+ low cost for 24 hr stabilities below 10^{-6}	+ good very short term stability, $\pm 10^{-9}$/ms.	- moderately high cost
+ excellent short term stability	- poor short term stab. during temp cycle, typically $\pm 1/2$ accuracy	- oven power required
- high cost for 24 hr stability above 10^{-7}	- oven power required	
- max. sta. 10^{-7}		
$110, 100 quantity $\pm 10^{-6}$ over 0⁰ to 65°C $\pm 3 \times 10^{-7}$/mo, $\pm 10^{-8}$/hr, 10^{-9}/sec T = const.	$90, 100 quantity $\pm 10^{-7}$ over 0° to 50°C $\pm 5 \times 10^{-7}$ over temp. cycle. $\pm 10^{-9}$/ms.	$140, 100 quantity $\pm 10^{-7}$ over 0° to 50° $\pm 10^{-8}$/min. $\pm 10^{-9}$/sec.
$175, 100 price $\pm 10^{-6}$ over -40°C to 70°C $\pm 3 \times 10^{-7}$/mo, 10^{-8}/hr, 10^{-9}/sec T = const.	$135, 100 lot $\pm 10^{-7}$ over 0° to 50°C $\pm 5 \times 10^{-8}$ over temp. cycle $\pm 10^{-9}$/ms.	$190, 100 lot $\pm 10^{-8}$ over 0° to 50°C $\pm 5 \times 10^{-8}$/min $\pm 10^{-9}$/sec.
$240, 100 price $\pm 10^{-7}$ over 0°C to 65°C $\pm 10^{-7}$/mo, 10^{-8}/hr, 10^{-9}/sec T = const.		

31

The thermostat oven controlled crystal oscillator can be easily built to provide a $\pm 10^{-7}$ accuracy over $0°$ C to $50°$ C. The cost increases about 40 percent to provide the same accuracy over $-40°$ C to $+70°$ C with a drastic increase, about 10X, in oven power. Its main disadvantage is the cyclic frequency drift with oven cycle of approximately $\pm 5 \times 10^{-8}$ and, when the temperature range is extended, the high oven power and high temperature aging. Thus, we must choose the minimum temperature range acceptable if this oscillator is to be used, to minimize oven power, aging, and cost. The short term frequency stability, short with respect to the thermal cycle, is excellent, $10^{-9}/ms$. However, the stability over a minute can be relatively poor and could hamper reacquisition. Because of this last factor and the complications involved with extending the temperature range, the thermostat oven controlled crystal oscillator does not look attractive unless we can justify a restricted temperature range, say $0°$ C to $50°$ C on the vehicle.

The proportional oven controlled crystal oscillator is the most highly accurate and stable of all the crystal oscillators. The cost of the proportional controller over the thermostat controller is \$40 to \$50 in 100 quantities. The only gain over the thermostat oven is the elimination of the cyclic frequency shift over the thermostat temperature cycle. The cost for a 10^{-7} stability oscillator over $0°$ C to $50°$ C is attractive. However, when the temperature range is extended to $-40°$ C to $+70°$ C, the cost and oven power requirements are increased by factors of 2X and 8X, respectively. Again, we are faced with the problem of minimizing the expected temperature range in the vehicle to yield reasonable oscillator cost.

In conclusion, from a cost standpoint, the best approach might be as follows. Assume that the heat from the operating electronics holds the vehicle ambient above $0°$ C and that the temperature is essentially constant during the 2 or 3 minutes required for reacquisition. An oscillator with the following specifications will be adequate:

$\pm 10^{-6}$ stability over $0°$ C to $65°$ C

$\pm 3 \times 10^{-6}/month$, $\pm 10^{-8}/hour$, $\pm 10^{-9}/second$ (Temperature Constant)

Then the use of a temperature compensated oscillator with 1000 quantity cost of approximately \$85 will suffice.

2.3.3   Total Material Costs

The materials costs of the various approaches are detailed in Table 2.3.3, including the cost of translation to a C-band RF link frequency. Note that the chirp demodulator using the digital timing loop (see Paragraph 4.1) is the least expensive, while the chirp technique employing analog circuitry has the second lowest materials cost. While these two similar approaches differ by only \$20 in materials cost, the digital approach is more easily assembled and tested than the analog, which further reduces the total cost of a tested unit. The other approaches are not economically competitive with the chirp approach. The "CDMA coherent PSK" approach, which is also provided for this tradeoff discussion, has

Table 2.3.3. Vehicle Receiver Materials Costs

REQ'D	COMPONENT OR SUBSYSTEM	CDMA COHERENT PSK n	CDMA COHERENT PSK	TDMA COHERENT PSK n	TDMA COHERENT PSK	CDMA UNCOHERENT DPSK n	CDMA UNCOHERENT DPSK	TDMA UNCOHERENT DPSK n	TDMA UNCOHERENT DPSK	CHIRP TD-FDMA ANALOG n	CHIRP TD-FDMA ANALOG	CHIRP TD-FDMA DIGITAL n	CHIRP TD-FDMA DIGITAL
1	Temp. Compensated Osc., Xtal. 10-6 over temp, 10-8/3 min.		85		85		85		85		85		85
1	Delay Counter & Decoder Gate Logic												30
2	Freq. Multiplier to 2 GHz, -12 dbm. Thin Film		90		90		90		90		90		90
1	1st. Mixer, "C" Band		15		15		15		15		15		15
1	1st. IF, 50 dB Gain, 50 dB Fast AGC Thin Film		65		85		65		85		55		65
1	A.G.C. Filter, Gate & Hold Circuit		20		20		20		20		20		20
n	Balanced Mixers		70		70		35		35		16		15
n	2nd IF with DPSK decoding surface wave device B.D. 2 M.F.					4	280	4	180				
n	2nd IF Amp with Xtal or RC Filter (CDMA, TDMA, resp.)	8	225	8	225								
1	2nd IF with Up & Down Chirp SWD, B.P. Filt. & Matched Filt.									2	180	2	180
1	Programmable Hybrid Frequency Shifter		80	3	80		80		80		80		80
1	Dual Low Frequency L.O. Divider		35		35						100		100
1	P.R.N. Shift Register Generator		150		250		150		250				
1	State Decoder, Preset, Data Ctrs., 8 Coincidence Gates												
n	Envelope Detectors	2	45	2	85	2	45	2	85	2	40	2	40
n	Summing Amplifiers	1	20	1	20	2	20	2	20	2	20	1	20
n	Comparators		8		8	1	16	1	16	1	8		8
n	Hold or int./dump	1	16	1	35		8		8	2	32	3	24
1	Signal Squarer		10		20	2	32	2	45				
1	Monolythic Dual Coupled or L.C. B.P. Filter & Amp.												
1	Coherent Bit Detection Controller	1	20	2	20								
1	Command Decom. & Buffer		22		42		16		26		16		16
n	Threshold Gates		16		26		7		7		7		7
1	Acquisition & Search Control Logic		14		14		45		45		45		45
1	Phase & Frequency Control Loop Filter & Amp		45		45		30		30		30		30
1	Delay Line for D.L.L.		30		30		20		20		20		
	Total Cost		$1081		$1300		$1061		$1144		$887		$867

33

materials cost roughly 10 percent higher than the chirp approach and also requires more alignment.

The result of the tradeoffs discussed here is that, for a technically acceptable command system, the chirp approach has the lowest materials cost and assembly test costs. The chirp approach has, therefore, been selected for the baseline command system. The estimated total cost of this approach is taken as X2 the recurring materials cost, since the assembly and production line requirements are consistent with such a factor. Thus, a total estimated large quantity recurring cost of the chirp approach is taken as 2 x $867 = $1,734.

2.3.4   Command Link Baseline

The selection of the baseline approach for the command uplink was between the chirp and the PN spread spectrum waveforms as indicated in the previous paragraphs. The PN approach is attractive in that it is the conventional approach and there is less new design involved for the waveform implementation. The chirp approach is attractive, on the other hand, because of its design involving SWD's and digital devices which promise lower recurring dollar costs for the RPV electronics. The chirp approach for this application represents a new technology development and for this reason involves more design time for detailed hardware design and later implementation.

An evaluation of the technical risk was one of the influences in the baseline selection between these two choices. This evaluation consisted of two considerations: 1) the availability and performance of chirped surface wave devices, and 2) the feasibility of the digital implementation of the phase-lock loop timing circuitry. On separate programs internal to Radiation, positive evaluations resulted from both these considerations. It was determined that the specifications for the chirped SWD for the baseline design were not state-of-the-art and such devices were available from several different vendors. Also, a breadboard circuitry was constructed for a laboratory demonstration of the feasibility of the digital timing loop and this closed loop demonstration was successfully completed.

The choice for the baseline became obvious. The potential advantages of the chirp approach, especially with SWD implementation, are very attractive and with assurances that the technical risk is minimal, this approach is favored. Thus, the command uplink baseline consists of a time-division multiple addressed format with frequency hopping and time hopping for further spread spectrum AJ advantages. The design description of this command link in Paragraph 3.2 provides elaboration and clarification for this baseline selection.

34

2.4　Video Tradeoffs

The video data in the system consists of five video sources, each 20 Mb/s, which are sent from five RPV's and are received at the master ground station. The design trade-off considerations which will be discussed are multiplexing approaches for the five video channels and then modulation approaches.

2.4.1　Multiple-Access Tradeoffs

Frequency division multiple access is the selected multiplex approach for the video data with both code division and time division being rejected. The trade-off considerations in this selection are described in the following paragraphs.

A time division multiplex approach has two possible implementations. First, the video data can be time division multiplexed resulting in a 100 Mb/s plus overhead bit rate and second, both status and video data can be time multiplexed together resulting in a bit rate even higher than 100 Mb/s plus overhead. This second approach exists since twenty-five 2 kb/s status channels must also be sent from the RPV to the ground. In examining the first TDM approach, a basic cost implementation problem developed. Consequently, this consideration also eliminated the combined video/status TDM approach.

Assuming a high update rate (50 updates/second), in order to minimize storage requirements on each airborne vehicle, results in a transmitted video rate of 102.5 Mb/s. This represents an efficient TDM approach since the optimum bit rate is 100 Mb/s for the five 20 Mb/s video channels. However, the major implementation consideration is the cost of the buffer memory, which was estimated at over $1200 per vehicle for a 4K bit high speed memory. By increasing the update rate, the memory capacity can be reduced with the penalty being an increase in overhead data. Also, increasing the update rate doesn't impact the high speed requirement of the memory. In the future, the buffer cost may decrease to the point where Video TDMA is cost competitive with other multiplex techniques, however, with present technology, this approach was eliminated.

A code division multiplex approach spectrum spreads the five video channels in a given bandwidth where the bandwidth is dependent on the spreading factor. Different code sequences are used for each video signal to allow all signals to occupy the same bandwidth. Consequently, four of the video signals will increase the noise density in a given video receiver. To minimize this interference, sufficient processing gain must be provided to take into account the graceful degradation between codes as well as dynamic range variations between the various drones and the master ground station. Providing processing gains of 10 dB for the graceful degradation factor and 10 dB for dynamic range results in a spreading factor of one hundred. Clearly, one hundred times 20 Mb/s or 2 Gb/s is an excessive amount of bandwidth. For this reason, code division multiplex was eliminated from further consideration.

35

The disadvantages in the time and code division multiplex approaches are elimi-
nated or less severe for the frequency division multiplex approach. In this approach, the five
video channels are frequency multiplexed together with sufficient frequency space between
channels to keep crosstalk at an acceptable level for the expected system dynamic ranges. The
resulting bandwidth of the composite video signal is 138 MHz (3 dB points) which is much less
than the bandwidth requirement of a code division approach. The buffer storage is eliminated
which results in a significant cost savings relative to the time division approach. The above
basic considerations resulted in the conclusion which selected the frequency division multiplex
approach as the most cost-effective for the drone based on current and near-future projected
technology.

2.4.2   Modulation Approaches

The wideband video data rate is the system parameter which impacts the RPV power
amplifier requirement rather than the status data rate. The maximum status burst rate of 80 kHz
requires a receiver bandwidth or receiver noise power which is 24 dB less than a 20 Mb/s data
rate. The BER of 10^{-3} for the video data compared to 10^{-5} for the status data reduces this
difference to 21 dB, still a substantial power ratio. Therefore, in order to keep RPV cost down,
an efficient modulation approach must be selected in order to minimize the RPV power amplifier
requirement. This points to some type of coherent modulation such as coherent PSK, QPSK,
offset PSK or differentially coherent PSK.

The performance of moderate-rate PSK modems can normally be made quite close
to the ideal PSK error rate curve when sufficient care is taken in the design, and when the band-
width limitations are not severe. For our case, however, where five 20-megabit channels must
be grouped within a relatively narrow frequency band, some tradeoffs must be made which will
affect modem performance. These tradeoffs, together with their effects on the modem perform-
ance, are discussed next.

Biphase is normally preferred over quadriphase because it is simpler to implement
and is less sensitive to filtering effects and modem phase errors. However, quadriphase modu-
lation is more conservative of bandwidth and has, as we shall see, better characteristics in a
channel which contains limiting.

To see why the bandwidth efficiency is important, refer to Figure 2.4.2-1.
Figure 2.4.2-1a shows the spectra of two 20-megabit biphase signals. There is a great deal
of overlap of the signals, such that to separate them at all would require 20-MHz wide filters.
This, in turn, would result in significant degradation of the system bit error rate performance,
and hence provide a nonoptimum system. If we widen the spacing so that there is 50 MHz
instead of 25 between channels, the filter bandwidths would now equal twice the bit rate,
easing the performance degradation. However, the occupied bandwidth would now be 240 MHz
instead of the 120 MHz originally intended. Doubling the spectral occupancy in turn would
cause the command and status channels to be moved higher in frequency so that the diplexers
could provide adequate isolation. The system band occupancy would go from 500 MHz to more
than 700 MHz.

36
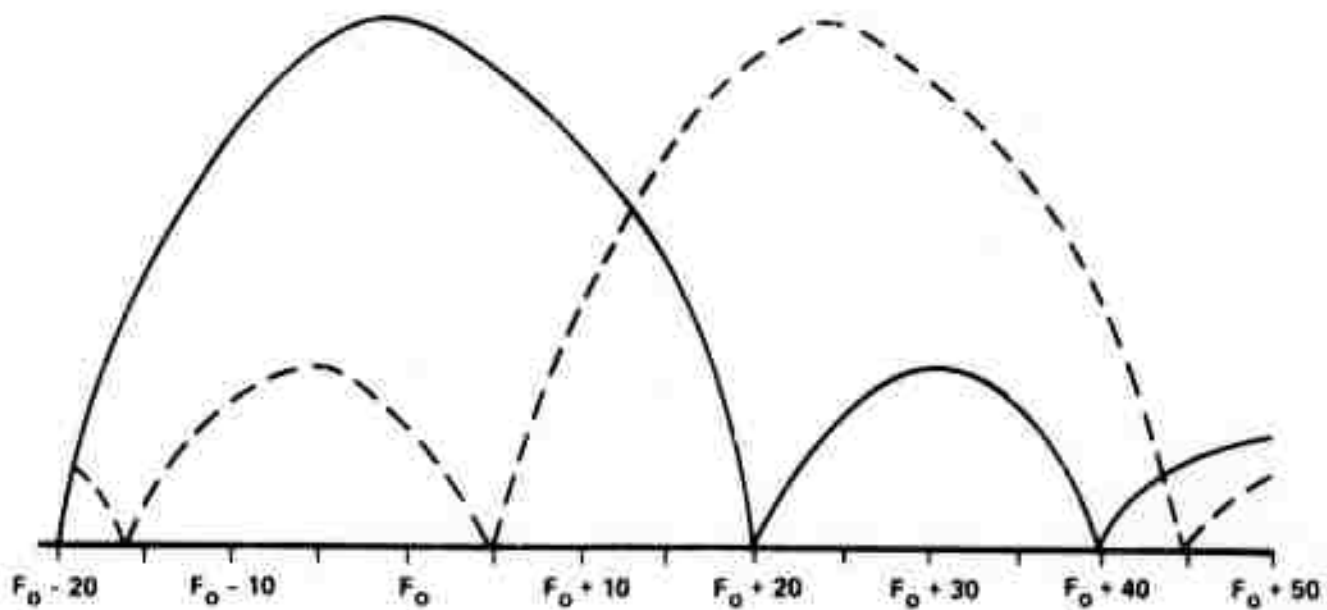
A. THE OVERLAP IS SEVERE FOR BIPHASE
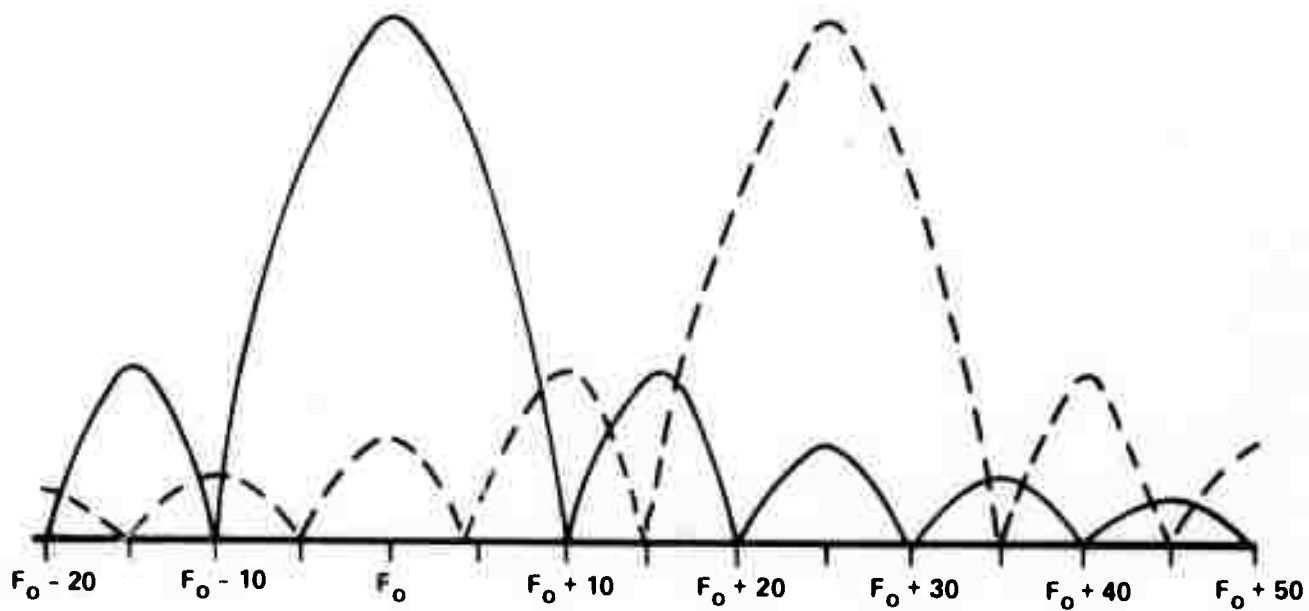
B. QUADRIPHASE RESULTS IN LESS SPECTRUM OVERLAP

86474-13

Figure 2.4.2-1. Adjacent - Channel Interference is Reduced
By Using Quadriphase Modulation

37

On the other hand, with quadriphase modulation the spectral occupancy is halved, thus permitting the video channels to be located 25 MHz apart. In this case, the IF bandwidth must be equal to the bit rate, that is 20 MHz, for adequate isolation of the channels. However, because quadriphase is more sensitive to phase nonlinearities in filtering, the degradation is still rather high - about 1 dB. It seems at first as though it would be easier to use biphase spaced at 25 MHz, together with the severe filtering, to get adequate isolation with no more degradation than that resulting from filtering the quadriphase. This is not true, however.

Look again at Figure 2.4.2-1. Note that a bandpass filter around the desired signal at frequency F_o, while eliminating the main lobe of the interference signal centered at $F_o + 25$, would still allow a considerable amount of side lobe energy to enter over the range of $F_o - 10$ to $F_o + 10$. This energy is enough to cause very severe performance degradation especially when adjacent video channels have significantly different received signal levels due to dynamic range considerations. The only way to eliminate this adjacent channel interference is to filter the interfering signal at the transmitter to keep its side lobes from ever radiating in the passband of the desired signal. This filtering could be done after the power amplifier, but it requires a 20-MHz wide filter at 5 GHz which, although realizable, will be lossy. This represents a direct loss in radiated power. Furthermore, the side lobe energy which, if filtered out, is also lost, represents a further reduction in radiated power.

It is preferable to place the filter preceding the power amplifier so that the insertion loss is sustained at low power levels, and so that the side lobe energy which is lost can be put back into the main lobe to help the system performance. Now consider what biphase modulation really is. It is double-sideband suppressed-carrier amplitude modulation, modulated by a signal which has only the levels +1 and -1. When this signal is filtered, the amplitude modulation is no longer rectangular but is made smooth. If this signal is passed through a limiting amplifier, the amplitude modulation is "squared up" once again, thus completely restoring the side lobes. Hence, it is not possible to filter a biphase signal ahead of a limiting amplifier.

To demonstrate the validity of the previous statement, a breadboard biphase modulator was assembled. The output was filtered and then passed through an amplifier. The results are shown in Figure 2.4.2-2. Photograph A shows the filtered spectrum when the amplifier output is at its 1 dB compression point. The remaining photographs show the output spectrum as the amplifier is driven further and further into saturation. Note that when the amplifier is 12 dB into limiting, the biphase spectrum is completely restored. This means that biphase modulation is totally unsuited to our requirement, because it must be used with transmitter filtering which results in significant transmitter output power loss. The other alternative of using a linear amplifier is not attractive, since this would draw more dc power and would be more difficult to realize for low cost.

Quadriphase looks like the better candidate, but we have not yet determined that it can be filtered and limited. Some of the phase shifts are now 90 degrees instead of 180 degrees, so the envelope does not go through zero as often, so limiting should have less effect. Figure 2.4.2-3 shows the results of tests run at Radiation. Here we see that, as we might expect, the limiting does restore some of the side lobe energy but not all of it. Thus, while filtering will be more helpful here, it is still not totally reliable.
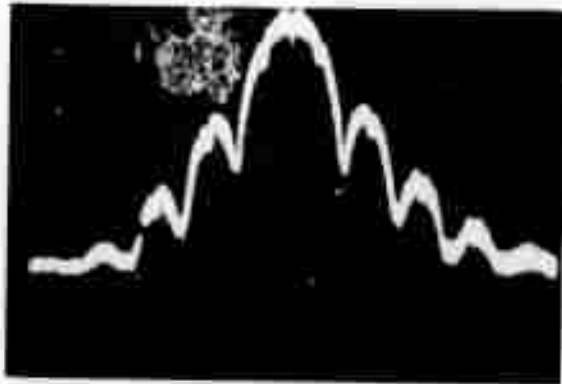
38

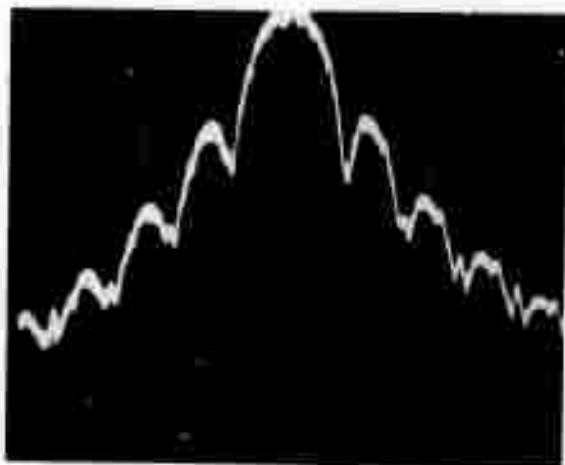A. LINEAR AMPLIFIER

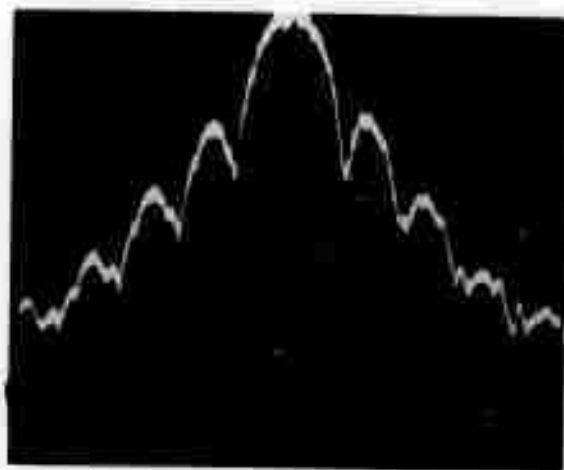B. AMPLIFIER 1/2 dB INTO LIMITING
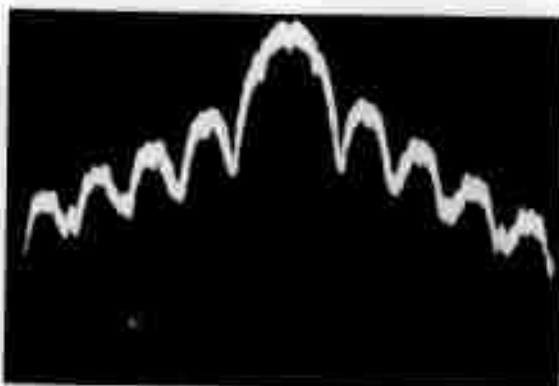
C. AMPLIFIER 6 dB INTO LIMITING

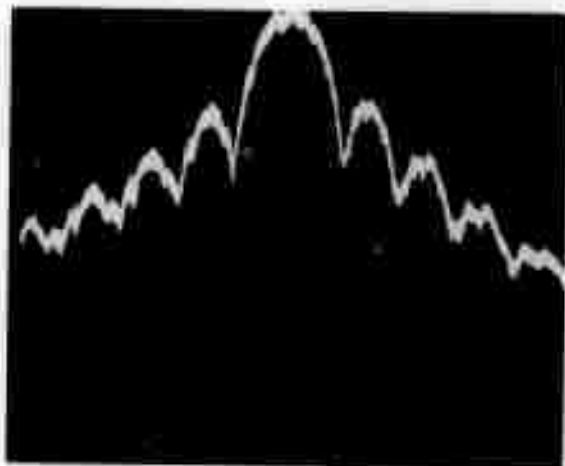D. AMPLIFIER 12 dB INTO LIMITING

86474-14

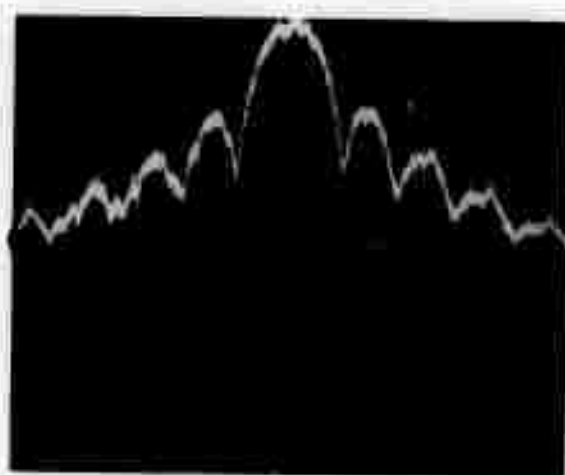Figure 2.4.2-2.   Hard Limiting Restores Virtually all of the Side Lobe Energy
of a Biphase Signal

39

A. LINEAR AMPLIFIER

B. AMPLIFIER 1/2 dB INTO LIMITING
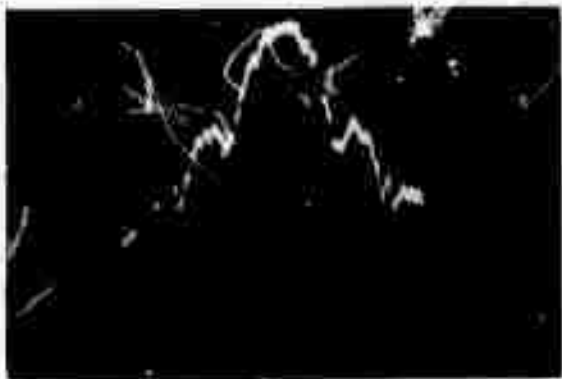
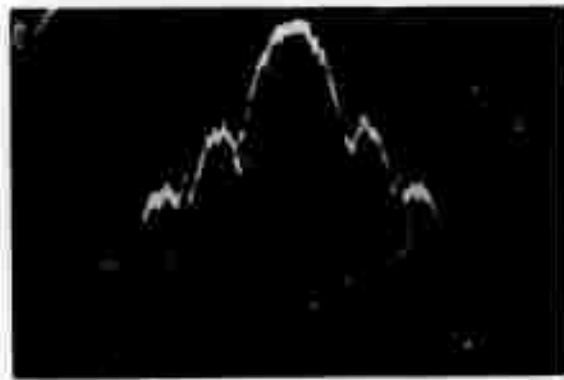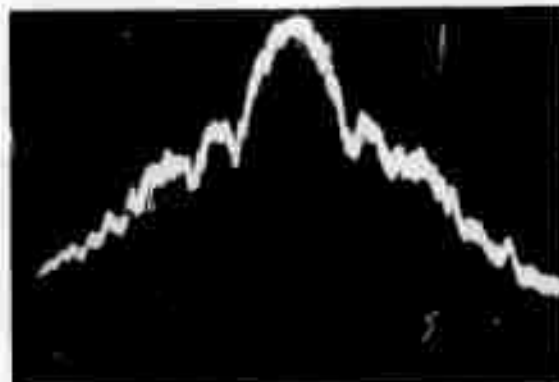C. AMPLIFIER 6 dB INTO LIMITING

D. AMPLIFIER 12 dB INTO LIMITING

86474–15

Figure 2.4.2-3. Hard Limiting Restores much of the Side Lobe Energy of a Quadriphase Signal

11

A. LINEAR AMPLIFIER

B. AMPLIFIER 1/2 dB INTO LIMITING

C. AMPLIFIER 6 dB INTO LIMITING

D. AMPLIFIER 12 dB INTO LIMITING

86474--16

Figure 2.4.2-4. Hard Limiting Has the Least Effect on the Offset-Keyed
Quadriphase Signal

2.5   RF Tradeoffs

This section identifies those tradeoffs associated with the RF hardware design and summarizes the results of these tradeoffs. The design approach taken was to achieve the RF performance requirements as dictated by system analysis of the candidate waveforms with emphasis on a cost effective design for the vehicle electronics. A factor of 1000:1 for the ground versus vehicle complexity was used as a guideline. Other design guidelines included frequency assignments in C-, X- or Ku-band plus maximum use of solid state and hybrid microwave integrated circuit (HMIC) technology for the 1975-1980 time frame with performance consistent with military environmental requirements.

Relative priorities for the RPV RF design were next considered to enable tradeoffs to be evaluated consistent with design objectives. These priorities are ordered as follows:

- Cost

- Size and Weight

- Transmitter Power

- Bandwidth

- Availability

- Power Drain

- Noise Performance

Cost, size and weight considerations are obviously given the highest priority for the RPV. Transmitter power and bandwidth are rated next since these parameters are critical to the RF hardware performance. Availability is a tradeoff between maintainability and reliability such that nonrecurring vehicle costs are optimized. Power drain, although it may have higher priority for the digital hardware, has a low priority for the RF hardware since RF hardware power requirement is typically a small percentage of total RPV power. Noise performance is given little priority since potential jamming signals can contribute significantly more noise than the receiver noise contributions.

In general, there are several approaches which will result in a cost effective design for the RPV.

- Increased Receive/Transmit Channel Separation

- Average Noise Performance

- Moderate Transmit Power

- Fixed Frequency Operation

- Temperature Controlled Environment

- CW Transmission

- RF Bandwidths less than 10 percent of RF Carrier

- HMIC Fabrication

Since minimum cost is of prime importance in the design approach, the factors which contribute to cost are identified and discussed for each of the RPV RF modules.

2.5.1   Diplexer

The diplexer design is without a doubt the most complex and crucial module of the RPV RF modules. The design parameters related to this module are functions of the receiver and transmitter as well as other system parameters identified below:

- Receiver and Transmitter Bandwidths

- Receive/Transmit Frequency Separation

- Transmitter Noise Characteristics

- Transmitter Power

- Spectral Spillover

- Transmitter Harmonic Rejection

- Receiver Noise Performance

- Receiver Overload

- Receiver Image Rejection

- Receiver Local Oscillator Reradiation

- Receiver Spurious Responses

- Insertion Loss

- Phase Linearity

44

The transmitted signal is greater than 100 dB *above* th desired received signal and constitutes a self-jamming threat. It must be suppressed to prevent any receiver overloading in spurious responses. Frequency discrimination of the **spectral** spillover and broadband noise must also be provided.

Since the requirement is for simultaneous transmission and reception of RF signals, receiver desensitizing techniques or T/R devices are not possible. Limiting devices are also not applicable as they deteriorate the receiver performance too drastically. A practical solution is to provide diplexing filters in the transmit and receive channels.

The transmitter filter must pass the transmitted energy while suppressing the transmitter generated spectral spillover and broadband noise in the receive and image frequency bands to a level below the receiver thermal noise to avoid transmitter degradation of receiver sensitivity. Additionally, this filter must suppress the harmonics of the transmitted signal consistent with EMI requirements. The latter requirement will result in an additional low pass filter since the bandpass filter will have harmonic responses.

The receiver filter is required to suppress the transmit signal to a level determined by the overload characteristics of the receiver components and any inband spurious signal created by the mixer and/or amplifier. Additionally, it suppresses the local oscillator signal and limits the reradiation to a level consistent with the EMI requirements and provides frequency discrimination of unwanted signals. Obviously increased R/T channel separation will minimize the requirements of both receive and transmit filters.

Insertion loss is also a serious consideration especially in the transmit path. For this reason the diplexer should be fabricated in waveguide to take advantage of the higher unloaded Q.

2.5.2   Power Amplifier

Trade-off considerations for the Transmitter Power amplifier can be identified by considering system performance requirement and design approaches such as:

- Power Output

- Modulation Characteristics

- Dual Transmitters

- Spectral Spillover

- Bandwidth

- Size and Weight

45

- Cooling

- Efficiency

The power output level and modulation characteristics are requirements defined by system analysis of the candidate waveforms. For the candidates under consideration these parameters are to first order approximation similar. The RPV will require nominal output power in the 1 to 10 watt range and bandwidths of 25 to 200 MHz. These requirements can be met using a TWT power amplifier or a solid state amplifier. Transmitter output power from a TWT power amplifier versus cost is shown in Figure 2.5.2-1 for C- and Ku-band units. The costs indicated include the power supply which represents approximately 60 percent of the total cost. Figure 2.5.2-2 compares cost performance of 1-10 watt TWT power amplifiers at C- and Ku-band with solid state power amplifiers using IMPATT diodes at the same power supply costs. Below 5 watts the solid state approach is approximately 50 percent the cost of the TWT approach. It is interesting to note that the solid state cost is not a function of frequency as in the case of the TWT. The limiting factor for the solid state approach is the low efficiency and limited power dissipation of the devices. The solid state approach is also consistent with minimum size and weight design goals.

Another trade-off area associated with the transmitter is the requirement for simultaneous transmission of the status and video information. The candidate waveforms under investigation require the status and video signals to be frequency division multiplexed. Combining of these signals may occur either before or after the power amplifier. Post power amplifier combining requires two power amplifiers with each signal losing 3 dB in the combining process. Therefore, the total power amplifier requirement will be two times greater than the single power amplifier approach. The precombining approach combines signals prior to the power amplifier. Whenever two or more signals are applied to the input of an amplifying device, the nonlinearities of the transfer characteristic will produce sum and difference components in the output. As the power amplifier is backed out of saturation, the intermodulation products in the output are attenuated relative to the desired signals. However, this means that a much higher power amplifier capability will have to be selected (for a given output power requirement per signal) in order for the intermodulation products to be kept at an acceptable level. Since power amplifier cost is directly related to the power requirements this approach is rejected as not being cost effective. The selected approach is to allow saturated power amplifier operation and define carrier frequencies such that intermodulation products fall into bands which will not significantly interfere with the desired signals. Since the video and status carrier frequencies are relatively close at RF, any sum or difference intermodulation products will fall outside the desired frequency band and be relatively easy to filter at the transmitter. Therefore, intermodulation products in a lower frequency spectrum such as the receiver IF are more likely to cause interference. Additional discussion of this problem is provided in Paragraph 2.5.4.

2.5.3   Receiver

During receiver design a tradeoff of noise performance versus cost is identified. This tradeoff is plotted in Figure 2.5.3 for two approaches. The low noise approach below
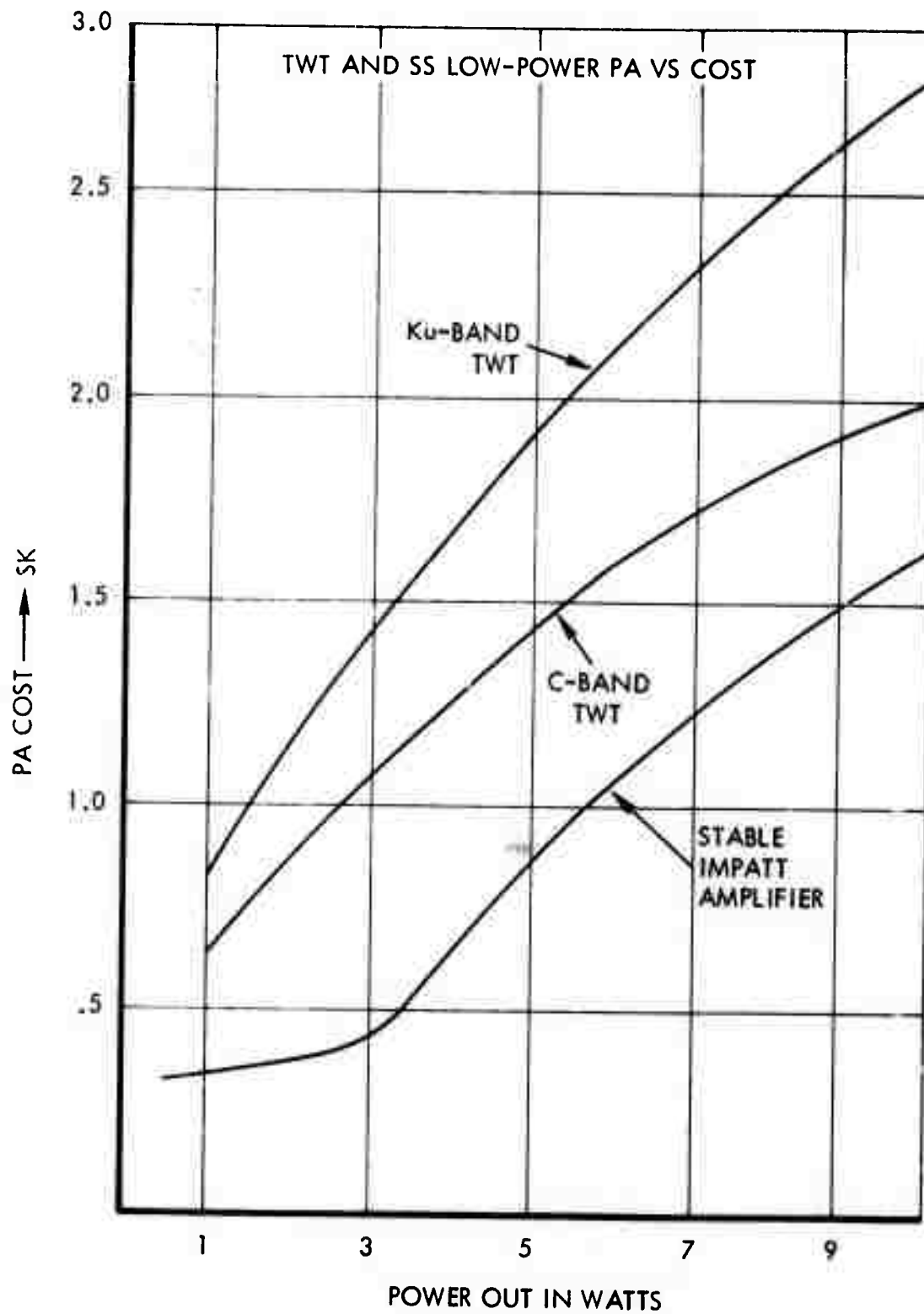
46

OUTPUT PA COST VS WATTS

TWT OUTPUT POWER VS COST
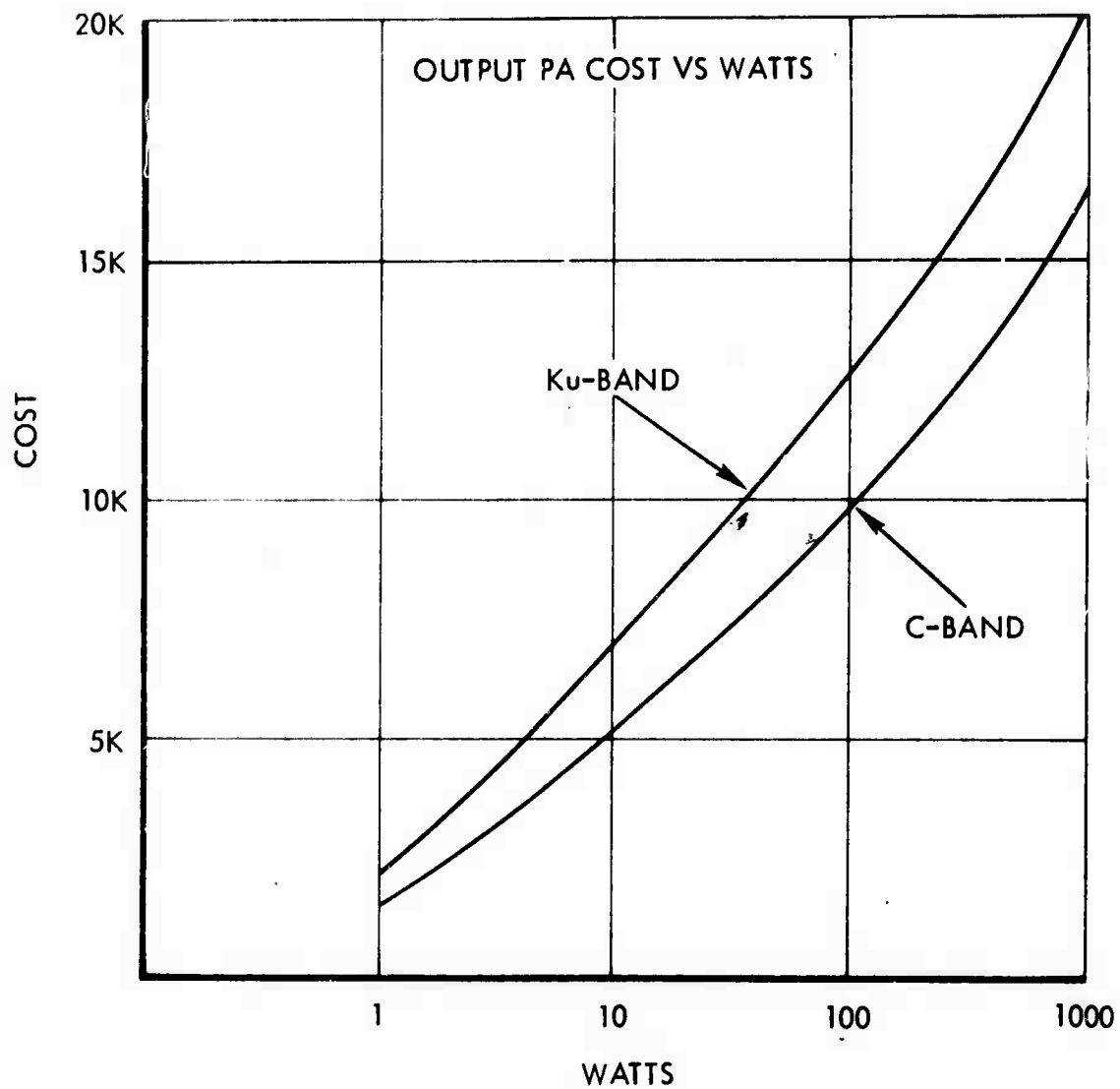
SOURCE
W.J.
QUANTITY: 1000
TUBE W/PS

87037-9

Figure 2.5.2-1

47

Figure 2.5.2-2.   Power Amplifier Costs

QUANTITY: 1000
NO POWER SUPPLY

87037-10

48

NOISE PERFORMANCE VS COST
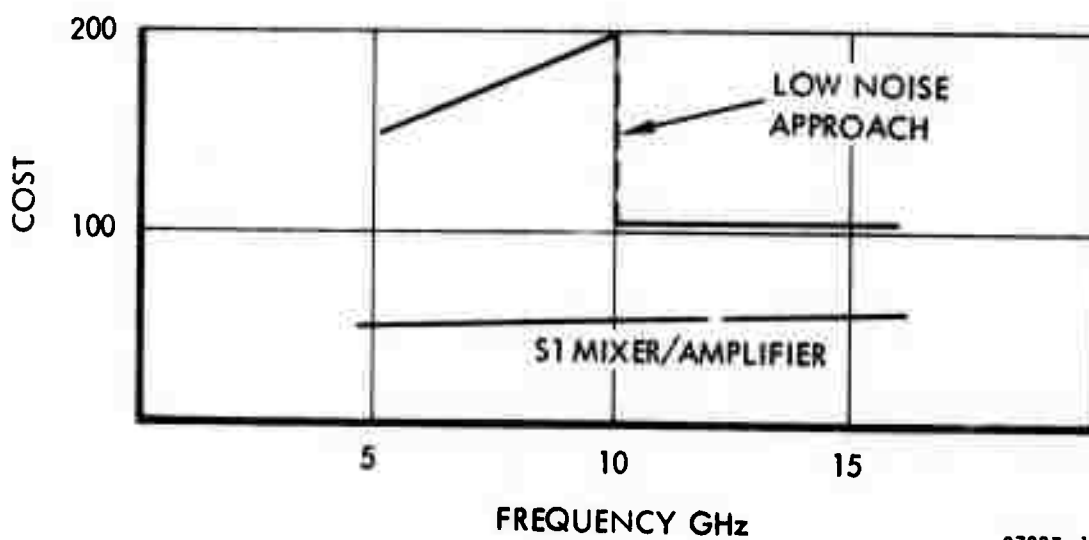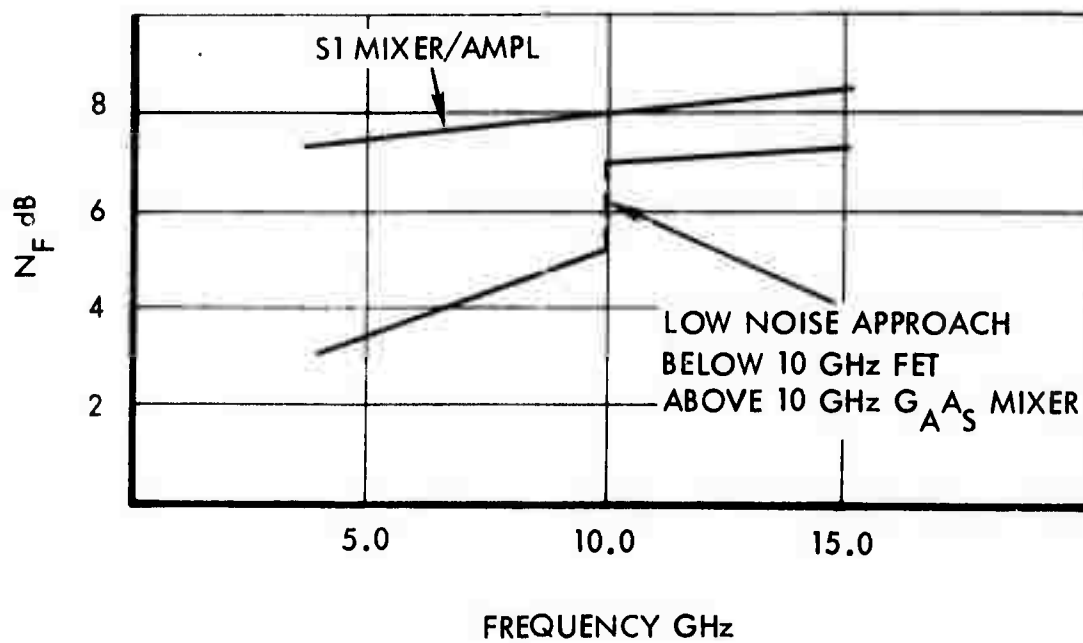
Figure 2.5.3

10 GHz is an FET RF preamplifier followed by a balanced mixer with GaAs diodes and the GaAs mixer alone above 10 GHz. The other approach is a conventional mixer/IF amplifier using inexpensive silicon diodes. The low cost approach is desired for the RPV receiver while recognizing this selection can impact the ground transmitter sizing. As shown by the command link power budget in Paragraph 6.1.1, an RPV receiver noise figure of 10 dB will not significantly impact the ground transmitter design relative to the cost weighting factor applied to ground equipments. Therefore the low cost, 10 dB RPV receiver is the selection.

2.5.4   Video/Status Multiplexer

The video/status multiplexer combines the video and status signals in the RPV prior to the power amplifier. At the master ground station five video signals from five RPV's plus a status signal must be frequency demultiplexed. The required frequency spacing between signals and IF selections involves a tradeoff of a large number of variables such as: filter characteristics, signal spectrum, relative signal levels, and allowable signal degradation. Each of these factors, in turn, impact filter parameter considerations such as: type, number of poles and ripple. The following material will emphasize overall considerations which resulted in selection of the composite signal frequency format rather than filter parameter tradeoffs.

The selected video signal modulation approach has a first null in its frequency spectrum ±10 MHz from center frequency. In order to minimize frequency spacing between video signals, filtering of each individual video signal is needed at both the transmitter and receiver. System analysis of co-channel interference impact on BER, allowing a nominal 15 dB dynamic range between video signals, resulted in a requirement for approximately 25 MHz video channel separation. This assumes a cost effective filter implementation (such as a four-pole 0.1 dB Chebychev filter with 20 MHz bandwidth) at both the transmitter and receiver.

Next, the frequency spacing between the status and upper video channels needs to be determined. The transmitter filtering and power amplifier operation are important since this determines the co-channel interference levels at the receiver. System implementation provides filtering prior to the power amplifier for both signals. This filtering is retained even after limiting in the power amplifier due to an offset-keyed QPSK implementation for the video signal and because of the power level of the status signal. The offset-keyed QPSK power spectrum considerations were covered in Paragraph 2.4.2. The status power level is approximately 12 dB less than the video power level at the power amplifier input and 18 dB less at the power amplifier output due to the small signal suppression effect. Therefore, the low level status signal will effectively see a linear power amplifier transfer function and thereby retain its pre-power amplifier power spectrum.

At the receiver the composite video/status is fed into a power divider. One output is filtered using a bandpass wide enough to pass the five video signals with rolloff characteristics which provide status signal suppression. The second power divider output is filtered using a bandpass wide enough to pass the status signal with rolloff characteristics which suppress all video signals. The required frequency separation of status and video signals is

50

determined by both the above filter characteristics and system dynamic range. Dynamic range impacts implementation since either the video or status signal can be significantly larger in power than the other at the ground receiver. Two worst cases are 1) status at minimum range, video at maximum range, and 2) status at maximum range, video at minimum range. In the first case, the video to status signal power density ratio is -30 dB. This number assumes a 4 dB larger E_b/N_o requirement for status data than video data. Also, 22 dB of spectrum spreading of the status data and a 48 dB dynamic range between the status and video signals are assumed. If the upper video channel carrier is 50 MHz away from status carrier, the status data within the video data bandwidth will not be any greater than -25 dB relative to the video signal assuming a 4 pole status filter at the transmitters. For the second case the video to status signal power density ratio is +30 dB. The assumptions are the same as the first case with the exception of dynamic range which is assumed to be 12 dB rather than 48 dB. Since video data will typically be transmitted from the target area, a 12 dB video data dynamic range is a more realistic system requirement than 48 dB. If the upper video channel carrier is 50 MHz away from the status carrier, the video data within the status data bandwidth will not be any greater than -15 dB relative to the status data assuming a video channel spectrum as shown in Figure 2.4.2-4. Therefore, this second dynamic range case represents the limiting model in establishing the status/video frequency separation. In fact -15 dB is marginal. An additional 10 MHz or 60 MHz total frequency separation would be more desirable.

Next the intermodulation products need to be considered. A four-pole, 25 MHz bandwidth filter around the received status data will provide adequate filtering to prevent any significant intermodulation products from occurring within the status channel due to video signals. A more difficult situation exists with the received video filter since the bandwidth of this filter is approximately 122 MHz. It can be shown that several second harmonic combinations due to status/video products will cause intermodulation products which can fall within a given video data channel. It is, therefore, necessary for the video filter (bandpass filter for the five video signals) to have a rapid rolloff in order to provide sufficient filtering on the status signal. If the video filter provides 30 dB of attenuation at the status channel frequency, the level of the undesired status signal at the video filter output will always be less than the video signals. By proper mixer design, the potential intermodulation products can be kept 20 dB below the video data level. By providing a bandpass, 5 pole 0.1 dB Chebychev filter around the five video signals, approximately 30 dB of attenuation is provided 64 MHz away from the highest frequency video channel. Since this filter represents a realistic design, a nominal 64 MHz separation between the highest frequency video channel and the status channel is needed, this bandwidth will also satisfy the co-channel interference requirement which was stated previously as 60 MHz. For implementation consideration, all frequencies are made a multiple of 12.8 MHz which is a reference signal available in the system. The resulting system frequency spectrum is shown in Figure 2.5.4.

It is desirable to keep the status/video multiplex/demultiplex units output IF as close to a standard 70 MHz as possible. Again, for ease in generating the various reference frequencies, an IF which is a multiple of 12.8 MHz was selected. Two possible choices are the fifth or sixth harmonic of 12.8 MHz. These frequencies are 64.0 MHz or 76.8 MHz. Due to data bandwidth considerations, the 76.8 MHz IF was selected.
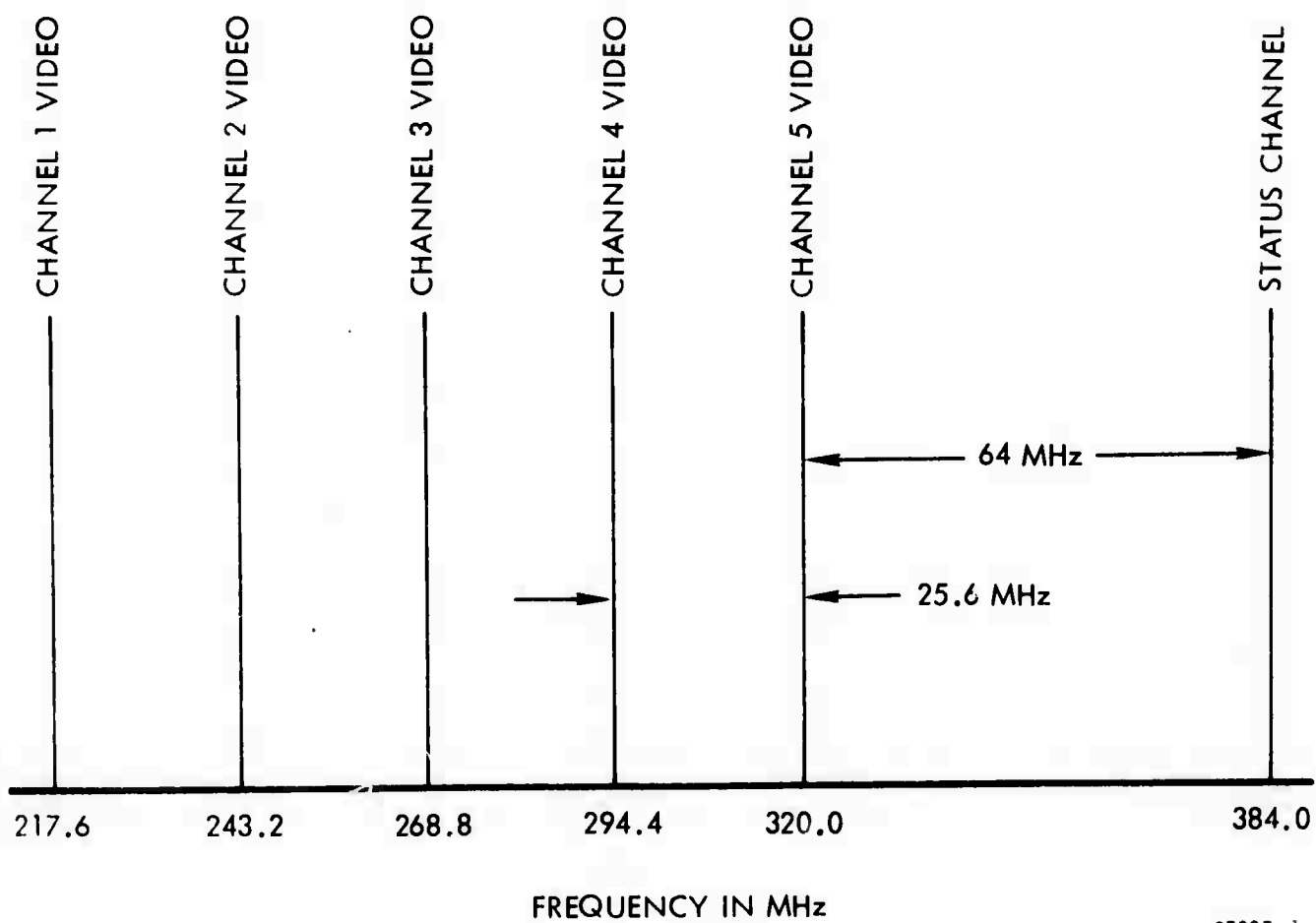
51

Figure 2.5.4.   Receive Signal Spectrum

52

2.5.5   Frequency Generator

Several tradeoffs were investigated to determine the approach for generating RF and IF carrier signals in the RPV. Microwave sources to upconvert the IF signals to RF and several frequency sources to accomplish the frequency division multiplexing of the video channels are required. A cost effective approach to this problem is to minimize the number of independent signals required by deriving the signals from a common reference frequency. In the case when the frequency assignment is allocated independently of the designer, an impact in hardware costs could result. The approach selected was to define modem frequencies to be a multiple of a basis system reference frequency.
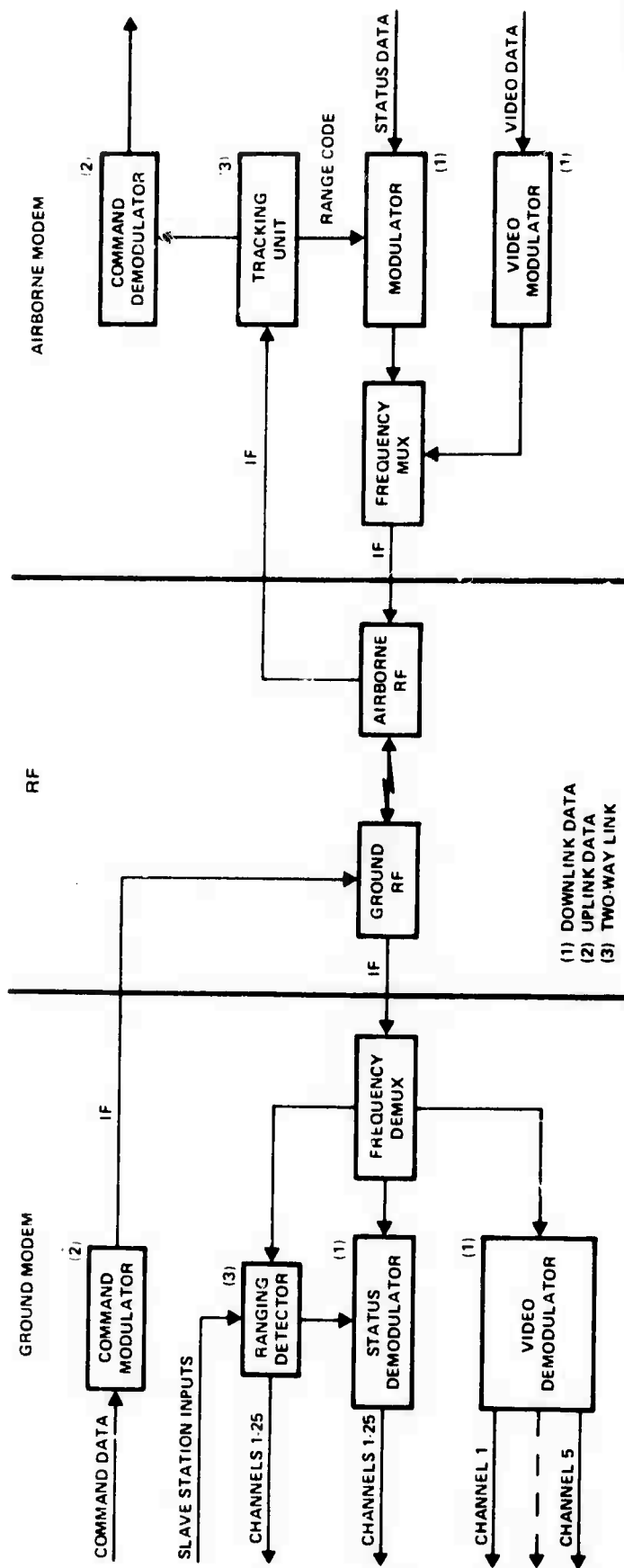
2.5.6   Baseline Cost Summary

The tradeoffs and design approaches discussed have resulted in the baseline design described in Section 5.0. This design has been detailed and priced out for the 1975-1980 time frame considering the current parts cost, inflation and technology predictions, large recurring quantities, and fabrication difficulty factors. Table 2.5.6 identifies the module cost breakdown for the RPV RF circuitry.

Table 2.5.6.   Cost Summary of RPV RF Baseline Design at C-Band

Diplexer	150
Receiver	174
Frequency Generator	172
Status/Video Multiplexer	392
Transmitter Upconverter	375
Power Amplifier	1600
Total Cost (dollars)	2863

53

SECTION 3.0

BASELINE MODEM DESCRIPTION

The proposed system provides AJ security by using a "nonlinear" sequence generator. Since security is of concern in the ultimate system, an approach which makes code breaking very difficult is justified rather than a sequence generated by a "linear" feedback register type approach. At this time, an alternate approach could supply a "linear" sequence generator with the demonstration equipment. At some future time, an encryption unit could be added to provide the necessary degree of security. One problem in this approach is assuring system stability for various data sequences out of the encryption unit, for example, long con-secutive data runs. An analysis of this problem is very difficult and actual experimental data to verify operation is recommended.

Additional detail in describing the Wideband Command and Control Modem in terms of the three links of Figure 3.0 will be given in the following paragraphs.

Figure 3.0. System Functional Block Diagram

3.1 Status/Video (Downlink)

Status and video data are received by the master ground modem from the airborne modems. Figure 3.1 shows the data flow from air-to-ground (downlink) from a maximum of twenty-five airborne modems. Multiple access to the airborne modems is obtained using time division for the status data and frequency division for the video data. A maximum of twenty-five users are accommodated in the time division multiple access format (status data) and a maximum of five users are accommodated in the frequency division multiple access format (video data). For airborne modems which are sending both status and video data, frequency division multiplexing is used to combine these signals at the airborne modem.

3.1.1 Link Characteristics

Figure 3.1.1-1 shows the status and video functions in the airborne and ground modem. The airborne equipment is shown above and the ground equipment below the dashed line. The status data from each drone is buffered into its assigned time slot with time of transmission being controlled by a time word received by the airborne modem from the master ground modem. This time word controls the airborne time of transmission to compensate for equipment and propagation delays. Consequently, the master ground modem is able to control the time of reception of each airborne transmission to prevent overlapping of signals at the ground receiver. After buffering and timing of the status data, in the airborne modem, this data is spread using a 12.8 MHz PN code. The spread data is then Differentially Phased Shift Keyed (DPSK) onto a subcarrier. For airborne modems which are sending both status and video data, the video data is frequency multiplexed with the DPSK status data. The relative levels of the two signals are controlled to permit operation during power amplifier limiting and to account for the different data rates between status and video data. The video data is offset quadriphase modulated which results in RF spectrum savings plus smaller side lobe levels when operating with a limiting power amplifier, relative to biphase PSK modulation.

The ground modem frequency demultiplexes the status and video signal from a given RPV plus four additional video signals each radiated by different users. Each video signal goes to one of five video data receivers. The status signal is mixed with a PN sequence from the range tracking receiver which collapses the spread data spectrum back to its original burst spectrum (80 kb/s). An automatic frequency control loop is used to remove Doppler and receiver local oscillator errors prior to status data detection thereby minimizing signal degradation due to frequency offsets. The output multiplexed data from up to twenty-five RPVs can be time demultiplexed into twenty-five 2 kb/s output data channels.

The status data time slots are assigned to each airborne modem prior to an operation. A total of twenty-five time slots are provided in the signal design to accommodate a maximum of twenty-five airborne users. Frame length is determined by the length of each time slot plus the total number of time slots. In establishing signal format two important trade-offs are communication efficiency and data update rate. Communication efficiency is determined by the relative data and guard times required for each time slot. Update rate determines storage

57
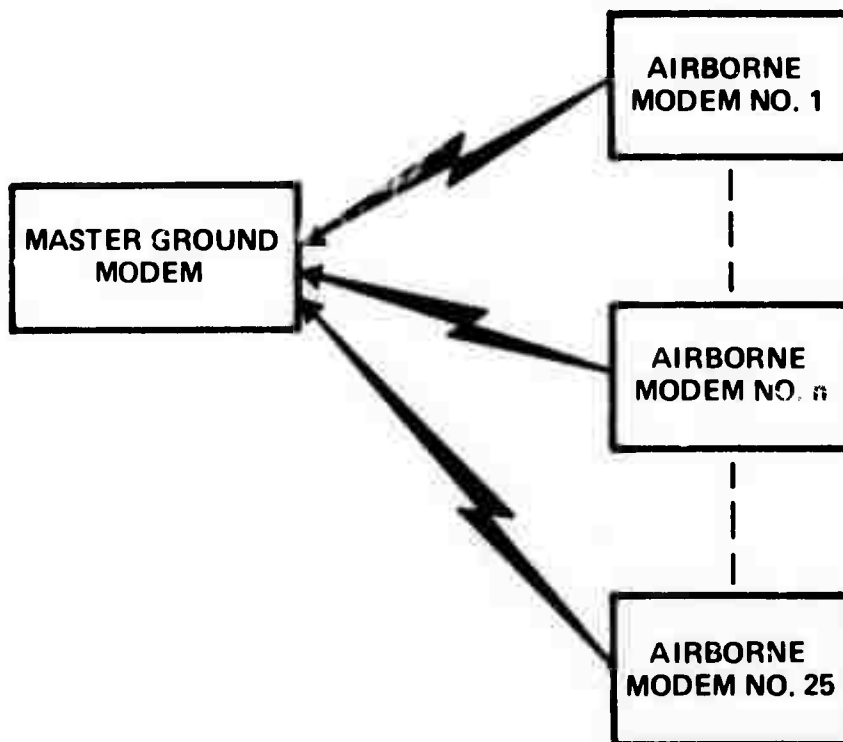
STATUS IS TIME DIVISION MULTIPLE ACCESS

VIDEO IS FREQUENCY DIVISION MULTIPLE ACCESS

STATUS/VIDEO IS FREQUENCY DIVISION MULTIPLEXED

(SIGNAL DESIGN FOR 25 OPERATIONAL RPV'S)

86482-20 A
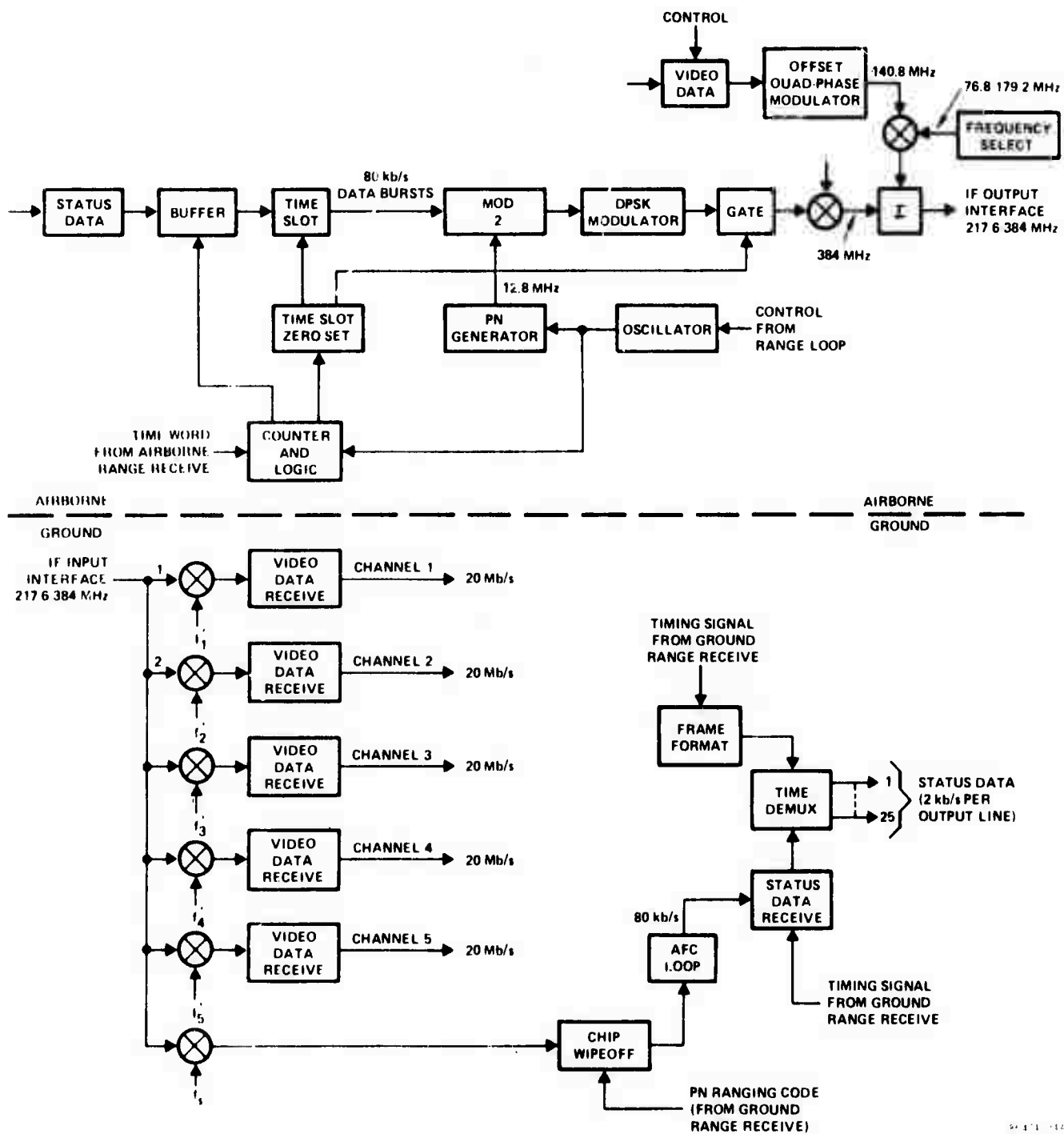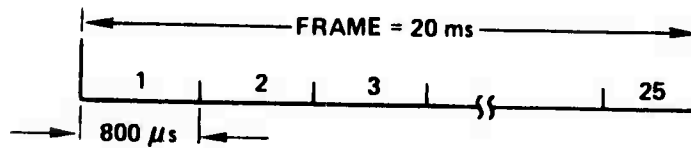
Figure 3.1. Status/Video (Downlink)

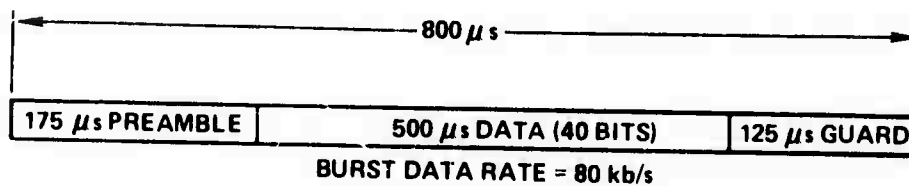Figure 3.1.1-1. Status/Video Functional Block Diagram

59

requirements and potential range smoothing (range data occurs at the same time multiplex rate as status data). Improved communication efficiency results from longer time slots whereas increased data updates requires shorter time slots. The parameters selected during the modem study plus associated waveforms are shown in Figure 3.1.1-2. Part (A) of this figure shows the frame format. The frame length is 20 milliseconds and is subdivided into twenty-five time slots each 800 microseconds in duration. An expanded view of a time slot is shown in Figure 3.1.1-2(B). Each time slot consists of preamble, data and guard time. The preamble lasts 175 microseconds and permits excellent bit synchronization prior to data detection. Data is sent for 500 microseconds at a burst rate of 80 kb/s. The guard time of 125 microseconds minimizes the overlap of signals from different RPVs at the slave ground station. Since the slave ground modem is geographically separated from the master ground modem and since system timing is referenced to the master ground modem, overlap of signals may occur at the slave ground receiver unless guard time is provided. A slave ground modem is used to obtain a range measurement independent from the master ground modem range measurement. Figure 3.1.1-2(C) shows the frequency spectrum at the input of the master ground modem. The six frequency multiplexed signals consist of five video signals and one status signal. (The status signal consists of twenty-five time division multiplexed signals.) The video signal bandwidth at the first null is ±10 MHz and results from the 10 Mb/s modulation data rate of each of the two orthogonal DPSK video channels. The status signal bandwidth is 12.8 MHz due to the pseudonoise spreading of this data. A frequency spacing of 64 MHz is provided between the status channel and adjacent video channel. This spacing minimizes potential interference which would otherwise exist due to differences in received signal level of the status and video data caused primarily by dynamic range considerations. As shown the total received spectrum is 189.2 MHz with the information within this spectrum consisting of status data from twenty-five airborne users, video data from five airborne users and ranging to twenty-five airborne users (ranging is contained in the pseudonoise code used to spread the status data).
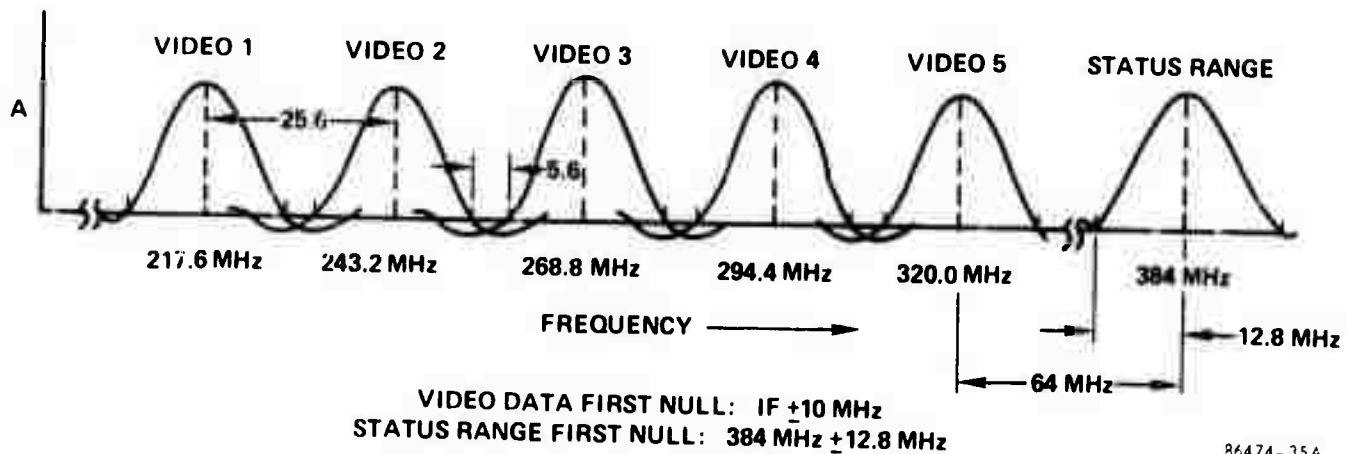
A. STATUS FRAME FORMAT

FRAME = 20 ms

1 | 2 | 3 | ... | 25

800 μs

(TOTAL OF 25 TIME SLOTS PER FRAME)

B. TYPICAL STATUS TIME SLOT

800 μs

| 175 μs PREAMBLE | 500 μs DATA (40 BITS) | 125 μs GUARD |

BURST DATA RATE = 80 kb/s

C. VIDEO/STATUS-RANGE SPECTRUM

VIDEO 1   VIDEO 2   VIDEO 3   VIDEO 4   VIDEO 5   STATUS RANGE

A

25.6

5.6

217.6 MHz   243.2 MHz   268.8 MHz   294.4 MHz   320.0 MHz   384 MHz

FREQUENCY ⟶

12.8 MHz

64 MHz

VIDEO DATA FIRST NULL: IF ±10 MHz
STATUS RANGE FIRST NULL: 384 MHz ±12.8 MHz

86474-35A

Figure 3.1.1-2. Status/Video Signal Parameters

61

3.1.2   Performance/Features

The downlink data consists of time division multiplexed status data and frequency division multiplexed video data. The status data consists of PN spread DPSK modulated data and the video data consists of two orthogonal PSK data channels.

The status data is recovered by regenerating the PN code, reproducing the DPSK waveform which collapses the status data spectrum to its prespread bandwidth and detecting this data in matched filters. The theoretical E_b/N_o requirement for the status link is that of matched filter processing of DPSK data. The sensitivity of the matched filter to frequency offset is high so frequency control to 3 kHz is required. Chip timing jitter and bandlimiting with 3 dB points at the spectral nulls of the PN spectrum were considered separately. A summary of the performance numbers for the status link is given below.

Status Link

Required BER	10^{-5}
Theoretical E_b/N_o	10.3 dB
Effect of Frequency Offset (3 kHz)	0.6
Effect of Timing Jitter (.1 x Chip time)	0.9
Effect of Bandlimiting	0.5
Required E_b/N_o	12.3
Processing Gain	$\dfrac{12.8 \text{ MHz}}{80 \quad \text{kHz}} \longrightarrow 22 \text{ dB}$

The bit error rate probability (BER) requirement of 10^{-5} corresponds to a theoretical energy per bit to noise density rates (E_b/N_o) of 10.3 dB for differential coherent PSK modulation. As shown, implementation loss is budgeted at 2 dB which results in a required E_b/N_o of 12.3 dB. The processing gain of 22 dB is computed as the ratio of the spread bandwidth to the data burst bandwidth.

The video link consists of QPSK data that has orthogonal binary streams offset in time by the bit period. Using this technique allows phase transitions of only 90 degrees at a time and greatly reduces the amplitude modulation caused by bandlimiting the transmitted signal.

Some excellent papers have been written describing implementation losses in biphase and quadriphase systems, however, each paper usually describes only one effect – such as bandwidth limiting or phase error – leaving the system designer to puzzle out how the effects

62

combine to produce his overall performance curves. That they cannot add directly is apparent when we consider that the effect of a static phase offset, for example, will certainly be less pronounced for a heavily filtered, "rounded" signal than it will be for a relatively lightly filtered signal having "square corners." Likewise, if two filters degrade the system performance by 1 dB and 0.5 dB, respectively, we would not expect that the filters cascaded would produce 1.5 dB performance loss. Some designers dodge the difficulty by root-sum-square (RSS) adding each individual effect; however, RSS addition is a statistical tool to estimate the composite of independent random functions, and implementation losses are not independent random functions.

Radiation has resolved this difficulty by formulating a computer program which computes the transient response of the communication system, from input to output, including all filters, reflections, and phase errors. The output waveform can then be analyzed to determine the true implementation loss. As expected, when we simulate only one of the effects through the program, our results agree very closely with those presented in the literature. And, as expected, when we combine effects, the composite loss is not the algebraic sum nor the RSS sum of the individual losses, but rather the true system loss.

Briefly, the computer program simply calculates the instantaneous phase of phase-shift keyed signal at the output of a system which includes filters described by their poles and zeros, reflections described by their magnitudes and phases, a phase detector which may have a faulty phase reference, and an "aperture filter" or finite-memory integrator which performs the final signal conditioning prior to the bit decision. By reading the system output at the bit-decision points, and comparing the actual values to the ideal, a determination can be made of the actual bit error probabilities.

The video link E_b/N_o requirement is based on coherent detection of QPSK data. The effects of hardware degradation such as timing and phase reference errors, bandlimiting, and crosstalk were analyzed by Radiation developed computer programs to give the net effects shown below. A loss from differential encoding because of higher error rates per bad decision is included.

*Video Link

Required BER	10^{-3}
Theoretical E_b/N_o	6.8 dB
Computer calculated loss	1.5
Differential Encoding	0.5
Required E_b/N_o	8.8
Processing Gain	Optional

*Frequency offset reduced to 5 percent.

The required BER of 10^{-3} corresponds to a theoretical E_b/N_o of 6.8 dB for coherent PSK with a budgeted implementation loss of 2 dB, the required E_b/N_o is 8.8 dB.

The video signal data rate is 20 Mb/s in the proposed system. Any significant spectrum spreading of this signal will result in excessive use of bandwidth as well as increasing acquisition times. Spectrum spreading could result in bandwidths greater than 100 MHz per video signal and resulting chip timing accuracy requirements greater than 10 nanoseconds in order to collapse this spectrum at the receiver. A different approach to achieve video processing gain would be source encoding to remove redundancy in the video data which would result in an information rate less than 20 Mb/s. In the proposed system, an implementation feature provided as an option spreads the video signal using the PN ranging code. If the video information rate were reduced as the result of source encoding to 2 Mb/s, a processing goin of 11.1 dB would result. This processing gain is obtained by modulating both channels in the proposed offset quadriphase modulation approach by the 12.8 MHz PN code. For further reductions in the video information rate, additional increases in processing gain may be realized. This potential feature in the proposed system does not complicate the acquisition problem since only one PN code needs to be acquired at the ground receiver. If video data processing is not performed to reduce potential video data redundancy, a degree of security may still be obtained by mixing with the PN code. This will prevent a low level jamming signal from disrupting low data rate portions of a video data sequence such as TV line synchronization. This security would be provided by feeding the video signal into a buffer register and then combining the register output with the pseudonoise ranging code. The buffer register is used to synchronize the video data with the pseudonoise code. This feature will effectively spread low data rate sequences in the video data to a bandwidth equal to the 12.8 MHz PN code.

3.2   Command (Uplink)

Command data is sent on the uplink by the master ground modem to the various airborne modems. Figure 3.2 shows the data flow from ground to air to a maximum of 25 airborne modems. Multiple access to the airborne modems is obtained using time division multiplexing.

3.2.1   Link Characteristics

Figure 3.2.1-1 is used to describe the command functions in the airborne and ground modem. The airborne modem equipment is shown below and the ground modem equipment above the dashed line. A buffer in the ground modem combines command data with a time word for each airborne user. This data is time division multiplex formatted and either upsweeps or downsweeps (chirps) the transmitter frequency in a given time interval. Each chirp signal for a given user is pseudo randomly hopped in both time and frequency. The time hopping selects one of twenty-five time slots and the frequency hopping selects one of 128 initial frequencies per chirp signal.
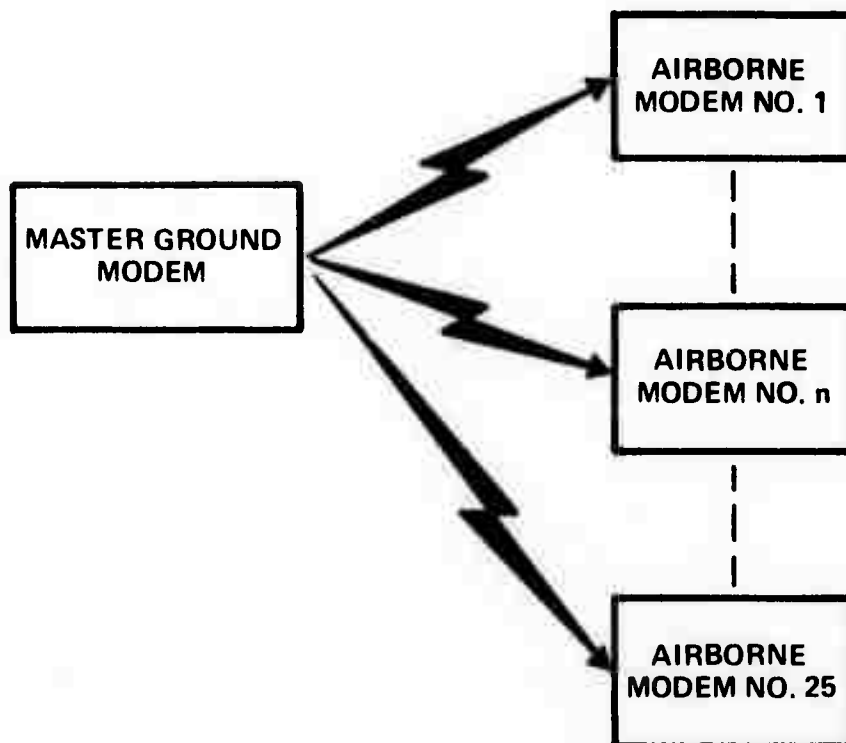
MULTIPLE ACCESS BY TIME DIVISION

(SIGNAL DESIGN FOR 25 OPERATIONAL RPV'S)
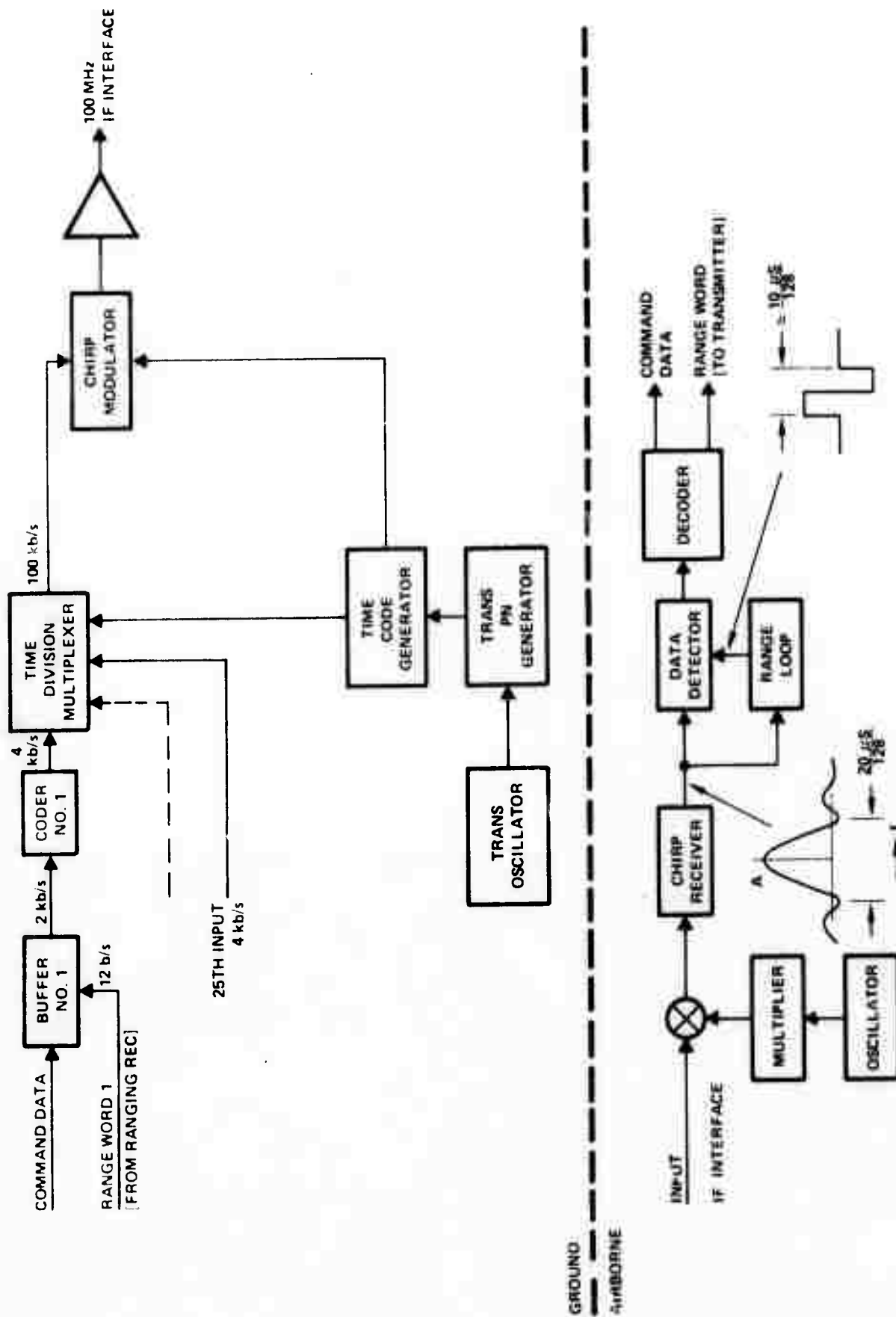
86482-23

Figure 3.2. Command (Uplink)

65

Figure 3.2.1-1. Command Functional Block Diagram

The chirp receiver for the airborne user consists of a filter which is matched to each swept transmitted waveform. Each airborne receiver output is a time hopped signal which is a function of the transmitter frequency hopping sequence only. Since the receiver is matched to all transmitted chirp signals, one output video pulse per time slot results. In contrast, the data for a given user is a function of both the frequency and time hopping sequences at the transmitter. In order to properly gate the receiver outputs, the airborne receiver PN sequence generator is locked to the ground transmitter PN sequence generator. When the airborne receiver range loop is locked, the two sequence generators are offset by an amount of time approximately equal to the propagation delay between transmitter and receiver. The chirp receiver output pulses (10/128 microseconds in width) will then be appropriately gated for data detection and range loop tracking.

The range loop error detector integrates all video pulses from the match filter which permit loop reacquisition and digital implementation features to be uniquely applied for a flexible and cast-effective RPV application. The use of a video tracking loop rather than a more conventional active correlator approach provides an important flexibility feature. This flexibility allows different strategies to be considered for acquisition:

1. A narrow gate which is swept through the total time uncertainty at a rate dependent on the smoothing requirement;

2. A widened gate which covers several chirp durations and which may be swept at a slower rate or may cover the entire time uncertainty with no sweeping at all;

3. Parallel processing whereby several narrow gates, each individually processed, cover the time uncertainty.

With a digital implementation, any of the above strategies can be easily provided in the system. The proposed system's reacquisition strategy is to widen the gate in distinct increments to a maximum width. This initial reacquisition step will reacquire the signal in the vast majority of all operational situations. If reacquisition should not occur, the wide gate will be swept to cover the maximum time uncertainty until lock does occur. Since the time uncertainty increases with time of loop unlack, the sweep width is programmed to increase with time. It is noted that an active correlator generally has only the narrow sweep strategy corresponding to 1. unless provisions for substantially increasing analog hardware are made.

The matched filter requirements for this chirp receiver can be implemented with surface wave device technology which constitutes one of its outstanding features. The potential low recurring costs of these surface wave chirped filters is especially attractive to the RPV missions due to the spread spectrum requirements and implementation constraints. In fact, this approach is an attractive alternative to the use of switchable tapped surface wave devices which are currently being researched for such low cost spread spectrum applications. The important performance parameter of a chirped matched filter is its time-bandwidth product $\beta\tau$. The

67

requirements are to match all possible transmitted signals (a single gated filter accomplishes this) and thus must have a bandwidth equal to the sum of the signal bandwidth plus the amount of frequency-hopping used, and a chirped slope equal to that of the signal. For the proposed modem parameters, the matched filter has 2 x 12.8 MHz bandwidth and 2 x 10 μsec dispersion delay or a total βT of 512. People knowledgeable with chirped surface wave technology recognize that these numbers are conservative and well within today's state-of-the-art. It is felt that the parameters proposed are entirely adequate for the feasibility demonstration although it is recognized that improved performance is now available and that with recent advances in chirp SWD technology, even greater improvements will be available in the near future.

As stated previously, the command link data consists of both command data and time words. The mission-oriented command data is used to control RPV mission functions whereas the time word is used to control internal timing of the airborne modem. The time word determines the airborne modem transmission time of its status data in order for this data to arrive at the ground within one microsecond of the start of a given ground time slot. It is desirable to minimize the time word since this represents overhead data. The time word size is determined by assuming a maximum range of 250 nmi, least significant bit having a nominal value of one microsecond and a one second update interval. Since 250 nmi corresponds approximately to 1500 μsec delay, a 12-bit word is required to transmit the timing information. In the airborne modem, bit changes between time words are detected. If an error does occur in a time word, it will be detected as an unrealistic value relative to the previous time word. The drone will ignore an incorrect time word and wait for the next input before making a time of transmission correction.

The ground modem command output consists of a continuous stream of up or down chirp signals resulting in a 100 kb/s data rate. Each airborne user is potentially able to receive the 100 kb/s data. The frame format, time slot waveforms, chirp frequency-time relationships, and chirp receiver output are shown in Figure 3.2.1-2. Figure 3.2.1-2 (A) shows the time slot/ frame format. Each time slot contains a chirp waveform which represents a data "one" or "zero." Characteristics of the transmitted chirp waveform are shown in Figures 3.2.1-2 (B) and 3.2.1-2 (C). A data bit is determined by the slope of the frequency versus time sweep. As shown, a total of 128 initial frequency values can be selected for a given data bit. After the initial frequency value is selected, each waveform is swept 12.8 MHz. At the chirp matched filter receiver, each ten microsecond time slot is subdivided into 128 divisions (Figure 3.2.1-2 (D)). The received chirp waveform is time compressed into one of these subdivisions. The initial frequency of the transmitted chirp waveform determines in which of the 128 subdivisions the received chirp signal will occur.

Each airborne user is assigned time slots in a frame. On a frame-to-frame basis, these time slots are hopped in a pseudo-random sequence. This same pseudo-random sequence also controls the selection of the initial frequency value of the chirp signal. For the case of a 4 kb/s data link per airborne user, a total of two bits per frame will be data detected. If an omni-directional ground antenna is used, a maximum of 50 signals per frame can be integrated by the range tracking loop. This feature provides additional energy to aid in the reacquisition of the range loop.
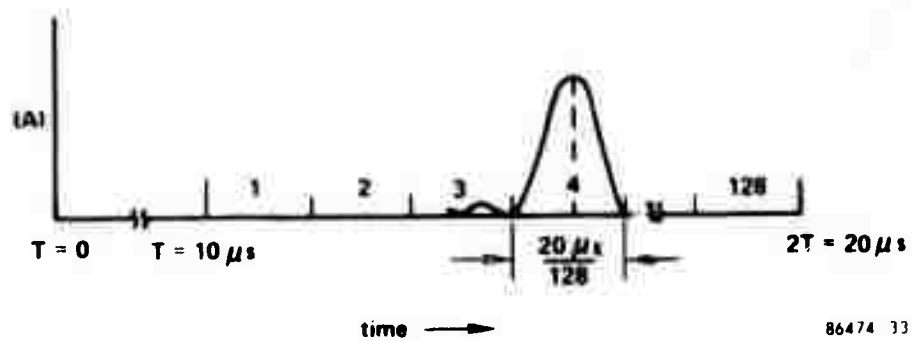
A. FRAME TIME

[TOTAL OF FIFTY TIME SLOTS PER FRAME]
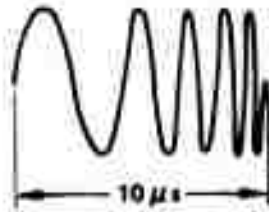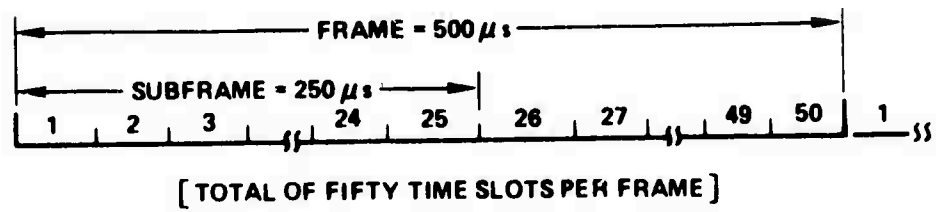
B. TIME SLOT WAVEFORM [AMPLITUDE VS TIME]

C. BINARY "1" CHIRP WAVEFORM
[BINARY "0" HAS OPPOSITE FREQUENCY SLOPE]

$$\frac{n}{T} = \frac{128}{10 \mu s} = 12.8 \text{ MHz}$$

$$\frac{1}{T} = 100 \text{ kHz}$$
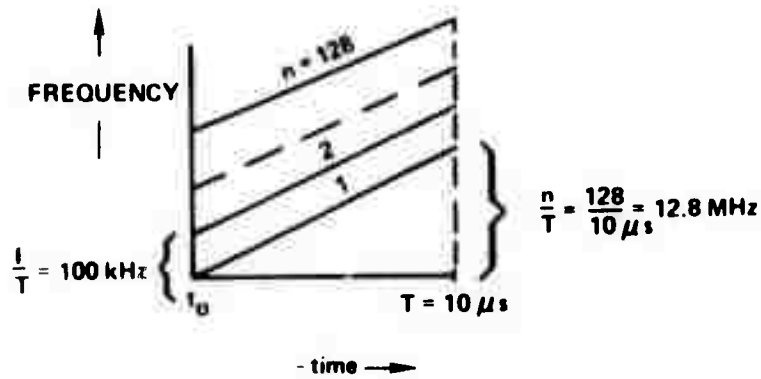
D. CHIRP RECEIVER OUTPUT

86474 33

Figure 3.2.1-2.   Command Data Waveforms

69

3.2.2   Performance Features

The command link data consists of time-division multiplexed chirp signals whose starting frequency has been pseudo-randomly selected. At the chirp receiver output in the airborne vehicle the data pulses will be gated into the data detector and range loop when the range loop is locked. Data pulses within a given airborne vehicle's time slot will be decoded by that vehicle.

To establish the chirp signal and receiver filter parameters, the following nomenclature is assumed.

Assume a linearly swept signal of the form

$$s(t) = A \cos\left(\omega_s t + \frac{r}{2} t^2\right) \qquad \begin{array}{l} 0 < t < T_s \\ \text{otherwise} \end{array}$$

$$= 0$$

where,

ω_s is the initial frequency of the chirp

r is the chirp rate $= \dfrac{2\pi\Delta f_s}{T_s}$

Δf_s is the range of the sweep

T_s is the time duration of the sweep

A is the peak amplitude of the signal $= \sqrt{2S}$

The receiver filter to be matched to this waveform will be assumed to have an impulse response of

$$m(t) = b(t) \cos\left[\omega_m t - \frac{r}{2} t^2 + \phi_e(t)\right]$$

where ω_m is the initial frequency of the impulse response

$\phi_e(t)$ is the phase error form ideal matching

T_m is the duration of the impulse response

and $b(t)$ is the envelope function of time and is only nonzero $0 < t < T_m$.

70

The output of the matched filter to a signal input can be written as

$$r(\tau) = \int_{-\infty}^{\infty} s(\tau - t) \, m(t) \, dt$$

The envelope value of the matched filter output is shown in Appendix A to be

$$\frac{A \sin \left[\left(\omega_m - \omega_s - r\tau \right) T_s / 2 \right]}{\omega_m - \omega_s - r\tau}$$

which has power

$$\frac{A^2 T_s^2}{8} = \frac{S T_s^2}{4}$$

At the time of peak signal from either the up-chirp or down-chirp filter, a comparison of the outputs is made and the bit decision is made corresponding to the largest envelope. Letting s be the signal envelope and r the envelope of noise alone, the envelope of signal plus noise is represented by a Ricean distribution

$$P(r_1) = \frac{r_1}{N} e^{-\frac{r_1^2 + s^2}{2N}} I_0 \left(\frac{r_1 s}{N} \right)$$

where r_1 is the envelope

N is the mean square noise

and I_0 is the modified Bessel function of the first kind and zero order.

The probability density function of the envelope r_2 out of the filter without a signal is Rayleigh distributed.

$$P(r_2) = \frac{r_2}{N} e^{-\frac{r_2^2}{2N}}$$

An error occurs if $r_2 > r_1$. Its probability can be written

$$P_e = \int_0^{\infty} P(r_1) \int_{r_1}^{\infty} P(r_2) \, dr_2 \, dr_1$$

71

This is shown in Appendix A to equal

$$P_e = \frac{1}{2} e^{-\frac{s^2}{4N}} = \frac{1}{2} e^{-\frac{1}{2}(S/N)}$$

Where S/N is the signal-to-noise power out of the matched filter. This curve is plotted in Figure 3.2.2-1. The improvement due to error correction coding is also shown in this figure. The required E_b/N_o for the command link is based on hard decisions from envelope detection of each bit processed by the chirp filter when these decisions are corrected by a rate 1/2 constraint length 3 convolution decoder. As shown in Figure 3.2.2-1, the theoretical E_b/N_o for a 10^{-5} BER is 12.4 dB. By budgeting losses, the required E_b/N_o for the command link is determined as shown below.

Command Link

Required BER	10^{-5}
Theoretical E_b/N_o	12.4 dB (Envelope Detection)
Loss from Frequency Offset (20 kHz)	0.6 dB
Timing Jitter (.1/Chirp Range)	0.2 dB
Band Limiting Loss	0.2 dB
Required E_b/N_o	13.4 dB

Frequency offset of the received chirp signal results in a time displacement of the chirp receiver output relative to the data sample time. Frequency offsets can be caused by Doppler and modem local oscillator errors and these offsets determine the magnitude of the timing error whereas the timing error direction is determined by the data. An up-chirp will cause a time offset in one direction and a down-chirp will cause a time offset in the opposite direction. For long consecutive data sequences the range loop will position itself to compensate for the time offset. But for alternate data 1's and 0's the range loop will seek a position midway between the total time displacement. Since the data sampling signal is obtained from the range loop, the sampling signal may be offset from the peak of a data pulse with a resulting degradation in signal-to-noise occurring.

The frequency offset is dependent on the RF frequency. At Ku-band the maximum Doppler is 15 kHz and at C-band the maximum Doppler is 5 kHz. An oscillator which has a 10^{-6} accuracy (5 kHz frequency error) is acceptable for C-band and a 10^{-7} accuracy oscillator
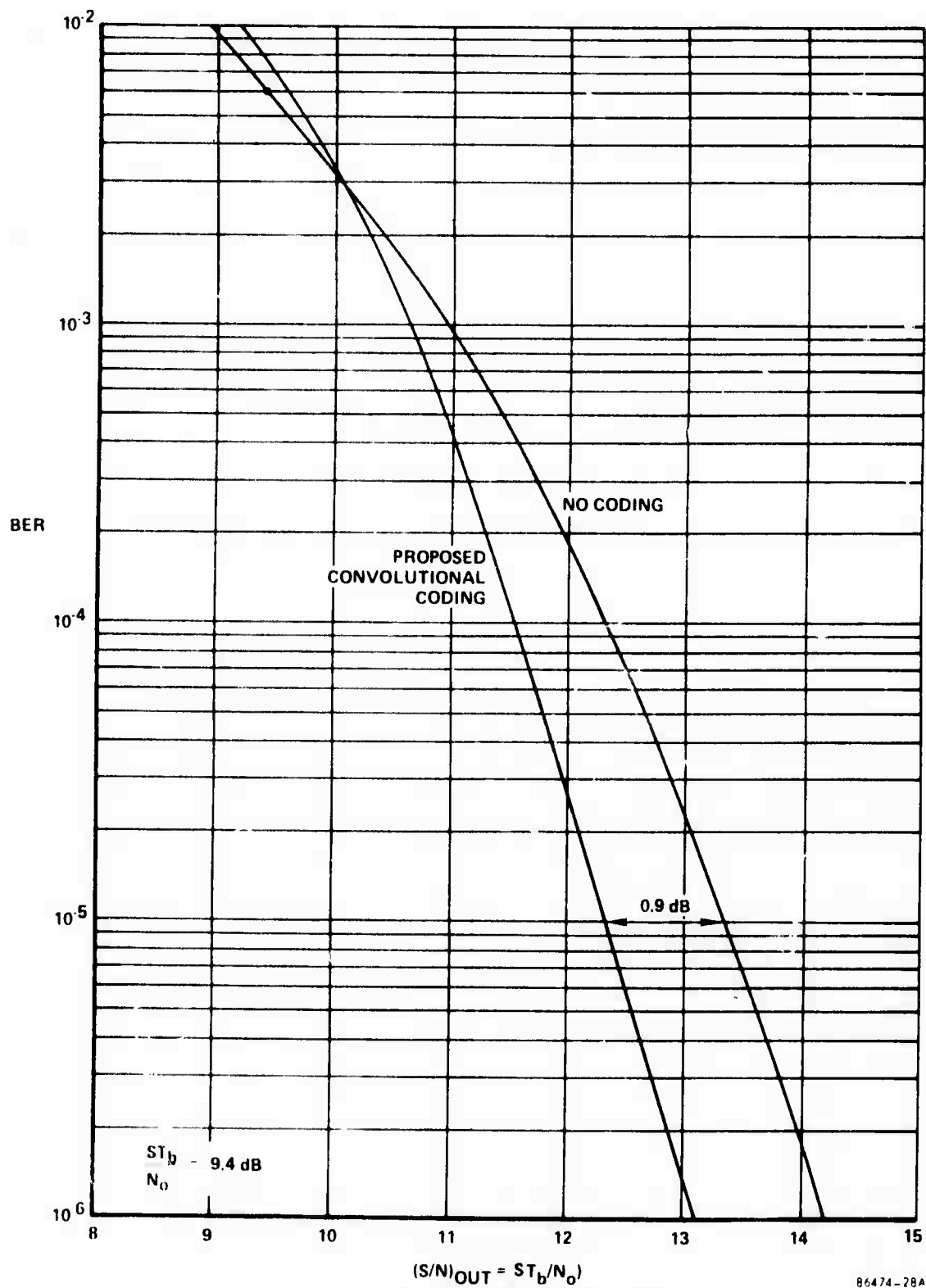
Figure 3.2.2-1. Up/Down-Chirp BER

73

(1.5 kHz frequency error) is acceptable for Ku-band. A smaller frequency error is required at Ku-band in order to keep the sum of Doppler and frequency error less than a nominal 20 kHz value. In the proposed system a 10^{-7} accuracy oscillator is used and, as shown above, 0.6 dB is budgeted for frequency offset errors.

Timing jitter errors are determined by the range loop signal-to-noise ratio. The band limiting reduces the amplitude of the peak primarily from phase shifts. A budgeted value of 0.2 dB is provided for this effect. Therefore, to meet a 10^{-5} BER requirement, an E_b/N_o of 13.4 dB is required.

The above E_b/N_o assumes a convolutional code. Coding on the command link is used for several reasons. First, the integration time is halved for the rate 1/2 convolution code proposed - the basic bit time is 10 μsec in the coded case and 20 μsec in the uncoded case. This shorter integration time decreases the degradation due to Doppler and oscillator drift. Also, the surface wave matched filters are simplified in requiring the shorter integration time. Another advantage, and perhaps the foremost one in using the coder/decoder, is that varying degrees of modularity are accommodated. By modularity we mean that a given vehicle can be assigned more than one time slot in the basic TDM command format or a given vehicle uses its assigned time slot at a reduced information rate while maintaining a constant bit rate. Two examples which illustrate the modularity feature are given in Figure 3.2.2-2. The first example shows a user assigned to time slots one through four. The same data is sent in all four time slots resulting in a bit rate of 16 kb/s for that user while the information rate remains at 2 kb/s. The 8/1 ratio which represents data redundancy will be discussed later regarding A/J protection. The second example in Figure 3.2.2-2 shows a user assigned to a single time slot, number twenty-four. As this time slot appears in subsequent frames, the same data will be repeated four times. The resulting bit rate for this user is 4 kb/s and the information rate is 500 b/s. Again, as in the first example, the data redundancy is 8/1. Figure 3.2.2-3 shows the efficiency which the decoder is able to use the extra energy represented by the redundant data transmission. The $M = 1$ curve represents a 2/1 data redundancy case. As shown, an input decoder error rate of 10^{-2} is corrected to a 5×10^{-5} error rate. When the modularity is increased to $M = 4$, the data redundancy is now 8/1. For a 10^{-1} input decoder error rate, the output decoder error rate is now 10^{-5}. Increasing the modularity from one to four resulted in a 50/1 increase in error correction capability. Table 3.2.2 shows for a constant decoder output error rate, the decoder input bit error rate as a function of modularity. As modularity increases, the system is able to tolerate significant input error rates with the system tradeoff being either fewer users or reduced information rate per user.

COMMAND LINK PERFORMANCE/FEATURES

MODULARITY 4 EXAMPLE
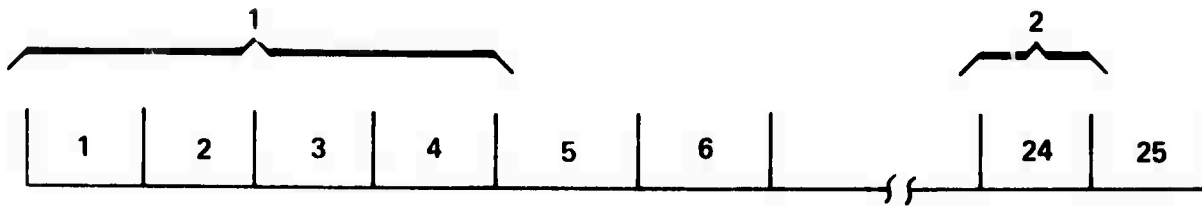
SYSTEM TIME SLOTS

EXAMPLE 1

ASSUME: USER ASSIGNED TIME SLOTS NUMBER ONE, TWO, THREE, FOUR

THEREFORE, BIT RATE = 16 kb/s PER USER

INFORMATION RATE = 2 kb/s PER USER

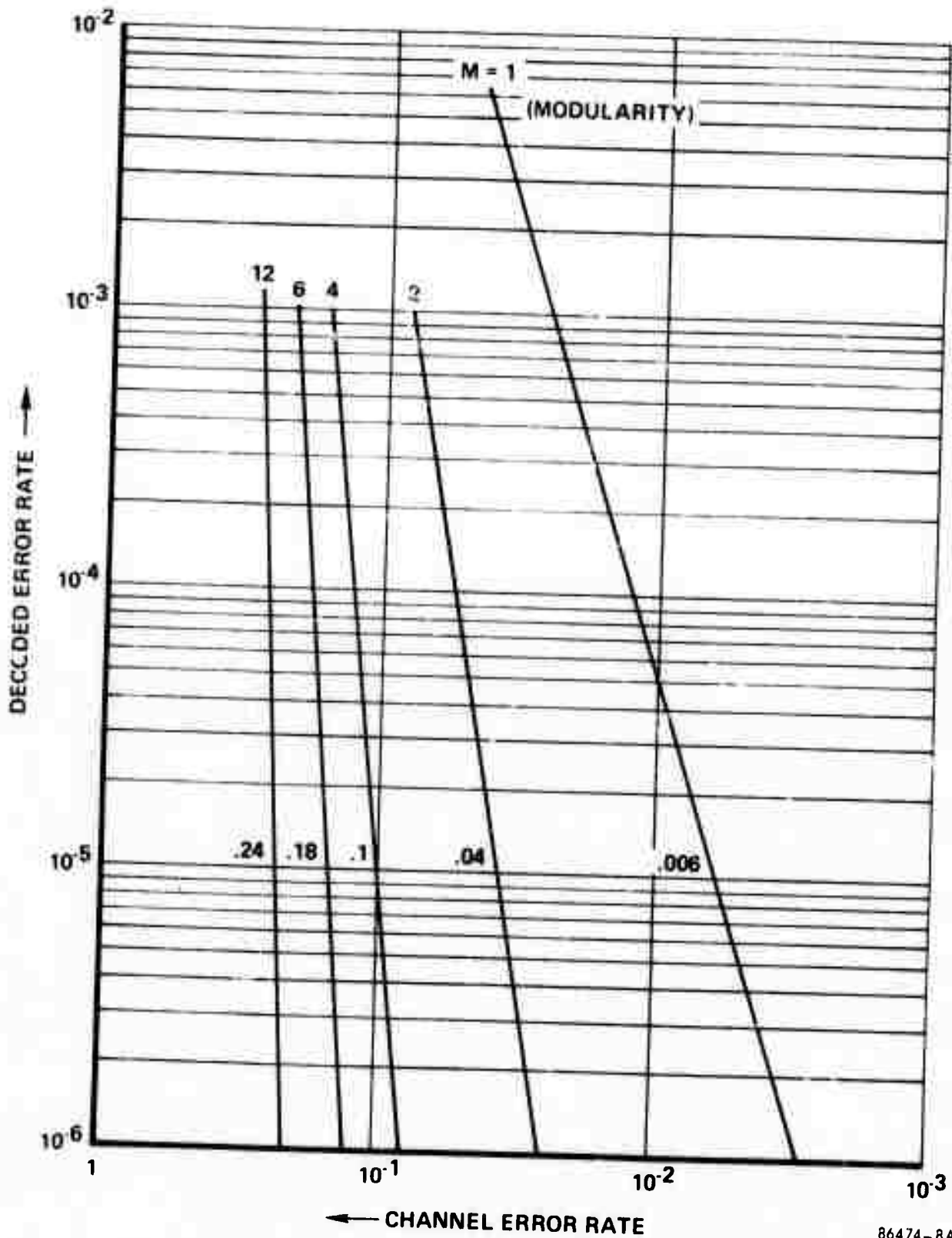$$\frac{\text{BIT RATE}}{\text{INFORMATION RATE}} = \frac{8}{1}$$

EXAMPLE 2

ASSUME: USER ASSIGNED TIME SLOT NUMBER TWENTY-FOUR

THEREFORE, BIT RATE = 4 kb/s PER USER

INFORMATION RATE = 500 b/s PER USER

$$\frac{\text{BIT RATE}}{\text{INFORMATION RATE}} = \frac{8}{1}$$

86482-26A

Figure 3.2.2-2

Figure 3.2.2-3. Coding Performance

86474-8A

76

Table 3.2.2. Modularity - Error Correction

Modularity*	Decoder Input BER	Decoder Output BER
1	0.006	10^{-5}
2	0.04	10^{-5}
4	0.1	10^{-5}
6	0.18	10^{-5}
12	0.24	10^{-5}

*Assumes constant bit rate as modularity changes.

Command link performance will now be defined for operation in various jamming environments. First, an equation will be given defining link BER performance for four types of jammers. Then, the performance improvement due to coding and modularity for a command link operating in a jamming environment will be defined.

White-Noise Jammer

This is a nonintelligent jammer which is assumed to transmit broadband white, Gaussian noise. The jammer transmitter is continuous and it is competing against a given command channel which is operating in a time-division mode. Appendix B derives an expression showing for operation against this jammer the resulting bit error probability for a given command channel is

$$BER = \frac{1}{2} e^{-\frac{1}{2}(S/N)_{out}} = \frac{1}{2} e^{-\frac{1}{2}\frac{S T_s}{N_o}}$$

where: S   = signal power

T$_s$ = signal duration (10 microseconds)

N$_o$ = jammer noise density.

77

If N_o is made from a power limited jammer, the power must be spread over $2\Delta f$ so

$$N_o = \frac{P_J}{2\Delta f}$$

where
P_J = jammer power

Δf = chirp frequency sweep (12.8 MHz)

also note

$$S = MP_s$$

where
P_s = average signal power per channel

M = number of time slots sharing the average power (25)

Therefore,

$$BER = \frac{1}{2} e^{-\frac{P_s}{P_J} M \Delta f\, T_s}$$

This last equation defines the command link performance when operating in a white-Gaussian jamming environment.

CW Jammer

This is a nonintelligent jammer which is assumed to transmit a continuous wave (CW). Again, this jammer is competing against a given command channel which is operating in a time-division mode. Appendix A derives an expression showing for operation against this jammer, the resulting amplitude response for a given command channel is

$$\left| R(\omega, \tau) \right| = \frac{1}{2} \sqrt{\frac{\pi}{r}} \left[\left(C(L_2) - C(L_1) \right)^2 + \left(S(L_2) - S(L_1) \right)^2 \right]^{\frac{1}{2}}$$

where L_2 and L_1 are functions of frequency and time.

where

$$C(L_2) - C(L_1) = \int_{L_1}^{L_2} \cos \frac{\pi}{2} X^2 \, dX$$

$$S(L_2) - S(L_1) = \int_{L_1}^{L_2} \sin \frac{\pi}{2} X^2 \, dX$$

where L_1 is the greater of $\dfrac{\omega - \omega_m}{\sqrt{\pi r}}$ or $\sqrt{\dfrac{r}{\pi}} \left(\dfrac{\omega - \omega_m}{r} + \tau - T_s \right)$

and L_2 is the lesser of $\sqrt{\dfrac{r}{\pi}} \left(\dfrac{\omega - \omega_m}{r} + T_m \right)$ or $\sqrt{\dfrac{r}{\pi}} \left(\dfrac{\omega - \omega_m}{r} + \tau \right)$

also

r is the chirp rate $\dfrac{2\pi \, \Delta f_s}{T_s}$

ω_m is the initial frequency of the impulse response

The largest value the Fresnel integral expression can achieve is 1.896 which occurs only when $L_2 = 1.20$ and $L_1 = 1.20$ or only at one r for a given frequency. Nominally, it will be 1.414 and this will be taken as the output for a unity amplitude sine wave. The output envelope for a sine wave of amplitude B is in this case.

$$J_e = B \times .707 \left(\frac{T_s}{2\Delta f} \right)^{\frac{1}{2}}$$

79

The signal envelope has been shown to be

$$S_e = \frac{A\, T_s}{2}$$

    A   is peak amplitude of the signal

    T_s is time duration of the sweep

An error will occur if the envelope of signal plus jammer at a random phase ϕ is less than the jammer alone.

    The BER expression is

$$BER = Pr\left((S_e + J_e \cos\phi)^2 + (J_e \sin\phi)^2 < J_e^{\ 2} \right)$$

and this is shown in Appendix B to equal

$$BER = \frac{1}{\pi}\, \cos^{-1}\, \frac{P_s\, M\Delta f\, T_s}{P_J\, 4}$$

P_s = average signal power per channel

P_J = jammer power

    This last equation defines a given command channel BER performance when operating against a CW jammer.

Chirp Replica Jammer

    This is an intelligent jammer which sends a constant train of chirp signals with the proper slope, each lasting for time T_J. The time overlap of the jamming signal and desired signal at the receiver is a random variable, therefore, in the following analysis, the jamming signal duration will be optimized for maximum bit error rate. Appendix B shows the matched filter response to this jamming signal is

80

$$r_J = J_e \frac{\sin r\, \tau'\, T_J/2}{r\, \tau'}$$

where τ' is the delay from output peak.

This will cause an error if the wrong up- or down-chirp filter is excited during a bit sample time and its amplitude is greater than the signal amplitude. This latter requirement is met if

$$r_J > \frac{A\, T_s}{2}$$

Assume the jammer can adjust T_J for maximum bit error rate. Appendix B derives a value for T_J of

$$T_J = \frac{A}{T_c} \frac{T_s}{.788467}$$

which is the optimum jammer sweep time for a given jammer-to-signal ratio. The worst-case bit error probability is shown in Appendix B to be

$$BER = \alpha = \frac{.231}{M\Delta f T_s} \frac{P_J}{P_s}$$

This last equation defines the command link performance when operating in a chirp-replica jamming environment.

Time-Position Jammer

This is an intelligent jammer which is again sending a constant train of chirp signals with the proper slope. This jammer differs from the chirp-replica jammer since this model assumes the chirp jamming signal and the desired chirp signal exactly overlap at the receiver. Therefore, the time position jammer must determine bit timing and simultaneously send chirps during this time to jam several of the time slots. The jammer would require power equal to the signal power for each of the time slots to be jammed. If the appropriate time slot was jammed, an error would occur with probably .5. The total power required would be that needed for each time slot jammed.

81

$$BER = \frac{.5}{M\Delta f T_s} \frac{P_J}{P_s}$$

This is believed to be the worst-case system in that the jammer is using just enough power to produce a given error rate.

The bit error rate equations for the four jamming models are plotted in Figure 3.2.2-4 as a function of P_J /P_s. These error rates are referenced to the decoder input. The two intelligent jammers are shown to degrade command link performance significantly. The nonintelligent noise and CW jammers will approach the time-position chirp jammer limit if the CW or noise is pulsed since the average power will remain constant but whenever the jammer is pulsed on the bit error, probability will approach 0.5. As shown, both the CW and noise jammers have a threshold value. As the P_J /P_s ratio approaches this threshold value, the performance of all command link channels degrades rapidly. Below this threshold value, the channels' performances are satisfactory. This is in contrast to the intelligent jammers which cause an increasing degradation in performance as the P_J /P_s ratio is increased. This is due to the intelligent jammers generating a frequency spectrum which is able to take advantage of the processing gain of the receiver-matched filter. To combat the intelligent jammer, coding and modularity are used in the system. It will be shown that coding and modularity greatly increase system performance when operating against intelligent jammers and slightly increase performance for the nonintelligent jammers.

The noise jammer curve in Figure 3.2.2-4 will be used to illustrate the improvement due to coding. Coding improvement will then be related to modularity and the resulting system performance improvement against all four jammers will be shown.

The noise jammer curve in Figure 3.2.2-4 resulted from plotting the following equation

$$BER = \frac{1}{2} e^{-\frac{1}{2} \frac{P_s \left[2 M\Delta f T_s \right]}{P_J}}$$

where $2 M\Delta f T_s$ represents the time-bandwidth product the jammer is spreading his energy relative to the time-bandwidth product of the data for a given channel. To transmit unspread command data, a time-bandwidth product of one is assumed, where the data bandwidth is the reciprocal of a data bit period. The spread time-bandwidth product of the system is $(25.6 \text{ MHz}) (0.25 \times 10^{-3} \text{ seconds})$ which is equal to the system spread time-bandwidth product $(2 M\Delta f T_s)$. The above BER equation is similar to the equation used in plotting the no-coding curve in Figure 3.2.2-1. In Figure 3.2.2-1 the equation used is:
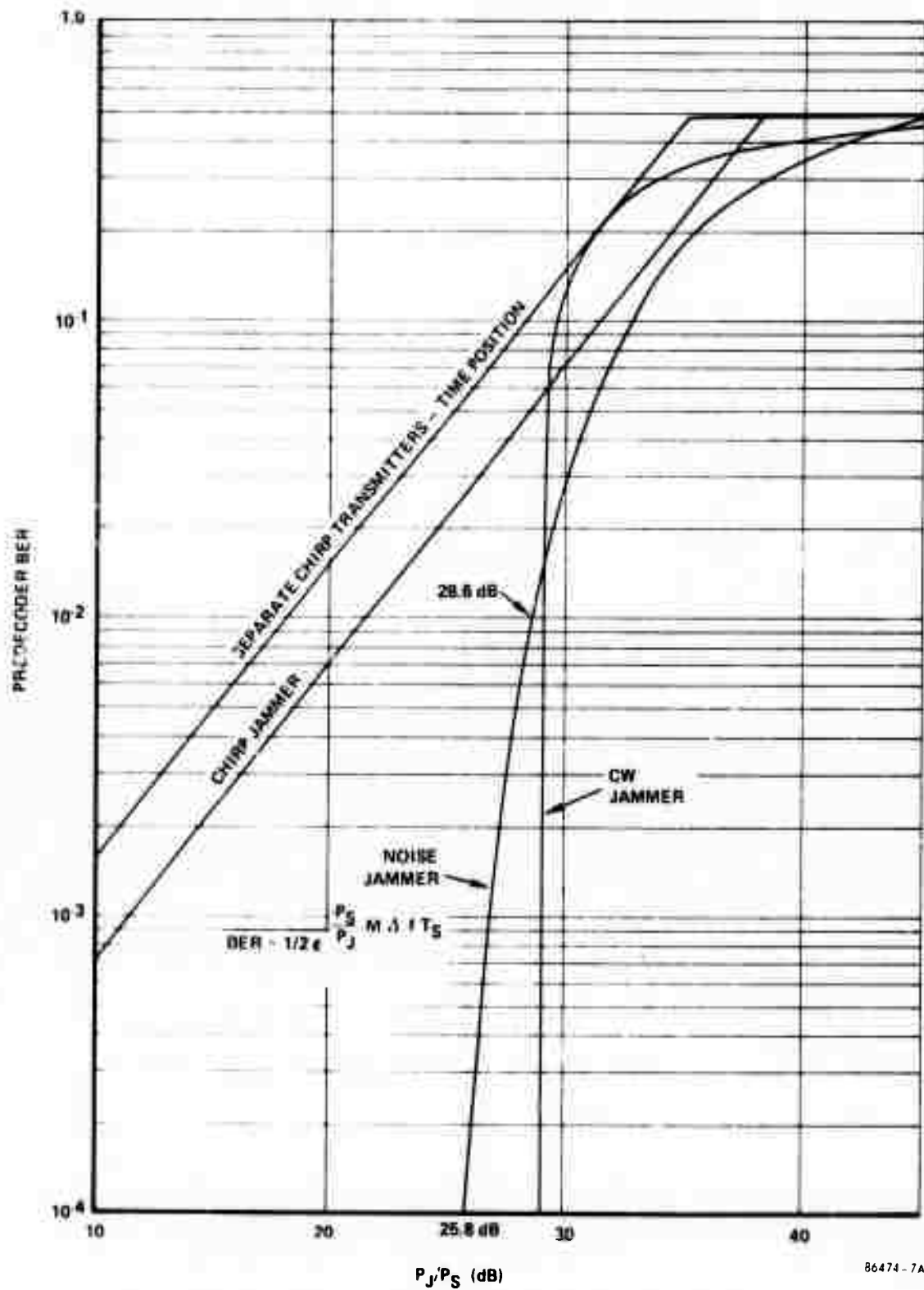
82

Figure 3.2.2-4. Bit Error Rate Versus Jammer Power

83

$$BER = \frac{1}{2} e^{-\frac{1}{2} \cdot \frac{S}{N}}$$

For equal BER, it is necessary for $S/N = \frac{P_s}{P_J} (2M\Delta f\, T_s)$. This is the case as

shown by selecting a BER from the curves in Figures 3.2.2-1 and 3.2.2-4 and comparing the values. For a 10^{-4} BER, the S/N in Figure 3.2.2-1 is approximately 12.3 dB and P_J/P_s in

Figure 3.2.2-4 is approximately 25.8 dB. The factor $\frac{P_s}{P_J} (2M\Delta f\, T_s)$ is 12.3 dB, therefore, as

expected, the command channel performance against this noise jammer is the same as when operating in a receiver limited noise condition. The difference between the shape of the curves in the two figures is due to the labeling of the abscissas. In Figure 3.2.2-1, S/N is plotted and in Figure 3.2.2-4 the effective reciprocal of S/N or P_J/P_s is plotted.

Next, the command channel performance improvement due to coding and modularity will be examined. Shown previously in Figure 3.2.2-3 were curves showing the error correction capability using the proposed convolutional coding. The M = 1 curve in this figure is for a 4 kb/s data rate and 2 kb/s information rate over the command link. The performance improvement defined by this curve was obtained from Figure 3.2.2-1 as will be shown in the following example.

In Figure 3.2.2-1 it can be seen from the coding curve that for a 10^{-5} bit error probability, the ST_b/N_o or energy per bit to noise density (E_b/N_o) ratio is approximately 12.3 dB. Therefore, for an E_b/N_o of 12.3 dB in the bandwidth preceding the decoder, the decoder output error rate is 10^{-5}. The error rate at the input to the decoder may be determined by moving vertically from the 12.3 dB point of the coding curve to the 12.3 dB point of the no-coding curve. An additional 3 dB must be subtracted from this number since the actual data signal-to-noise ratio at the decoder input is 3 dB less than E_b/N_o due to the 2/1 ratio between data and information rate. The resulting bit error rate at the decoder input is 6×10^{-3} which corresponds to the (12.3-3) dB point of the no-coding curve. Therefore, for a modularity of one, an input decoder error rate of 6×10^{-3} will be corrected to 10^{-5} at the decoder output which checks with Figure 3.2.2-3. Next, the M = 1 curve in Figure 3.2.2-3 is combined with each of the four curves in Figure 3.2.2-4 with the results shown in Figure 3.2.2-5. To illustrate the coding improvement, select the chirp jammer curve in Figure 3.2.2-4 as an example. For a 20 dB P_J/P_s ratio, the decoder input error rate is 7×10^{-3}. From Figure 3.2.2-3 this input error rate results in an output decoder error rate of approximately 2×10^{-5}. As shown in Figure 3.2.2-5, for a P_J/P_s of 20 dB, the resulting decoder output error rate for the chirp jammer is approximately 2×10^{-5}. As shown, the largest performance increase due to coding occurs for the intelligent jammers. As should be expected, much smaller error correction improvement is shown for the noise and CW jammers. The reason for this smaller performance improvement is due to the nonintelligent jammers spreading their energy over the entire system spectrum whereas the intelligent jammers concentrate their energy. Therefore, by repeating data, a high probability exists for some of the data to not be
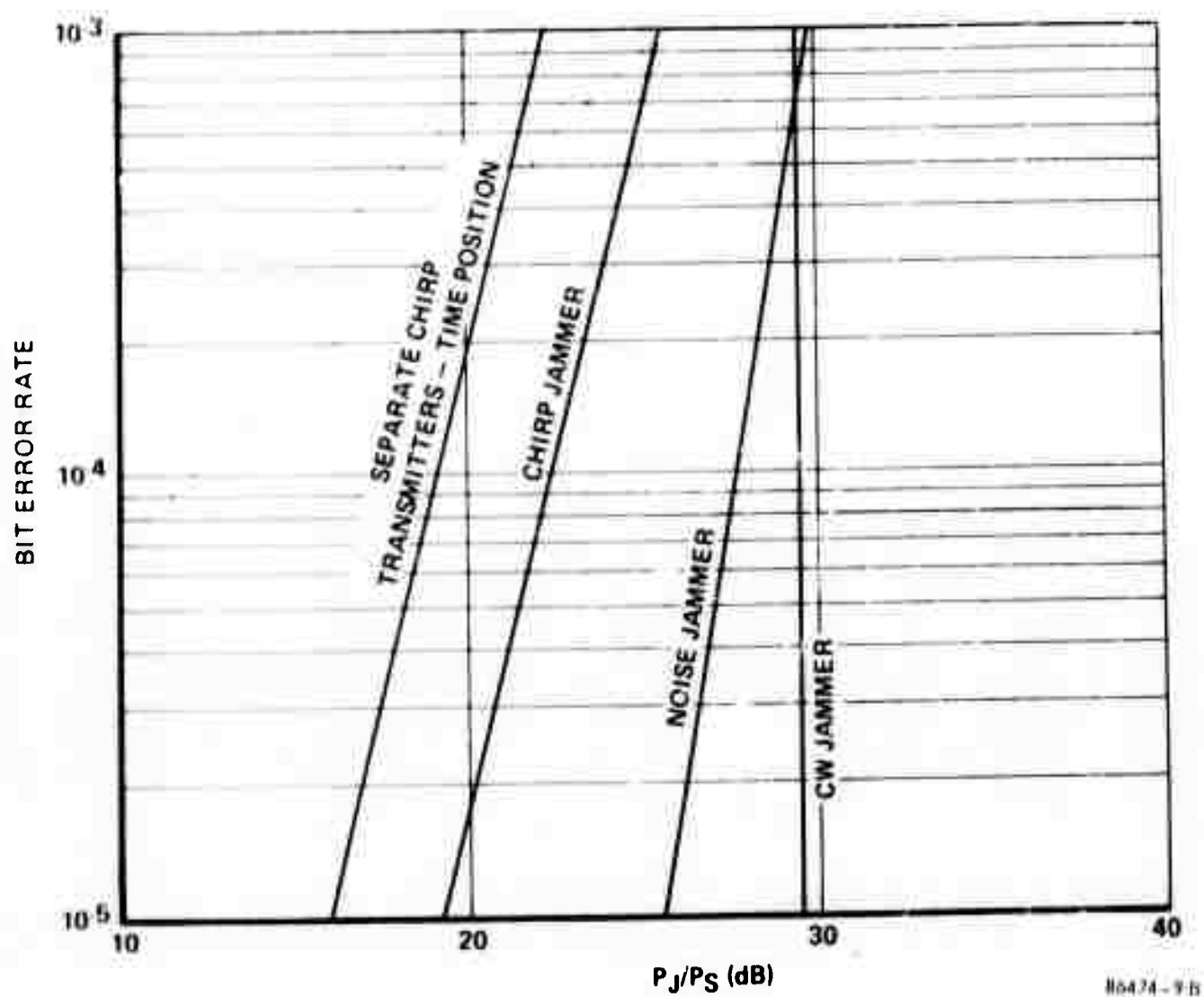
84

Figure 3.2.2-5. Decoder Output Error Versus Jammer Power – Modularity 1

85

jammed when operating against an intelligent jammer. Figure 3.2.2-6 shows the performance of the system when operating in a jamming environment for a modularity of two. Again, the largest performance improvement occurs against the intelligent jammers. As shown, the channel performance is now becoming independent of the jamming model. In the proposed system, the modularity can be increased to twelve with the resulting improvement shown earlier in Table 3.2.2 for a constant output BER.
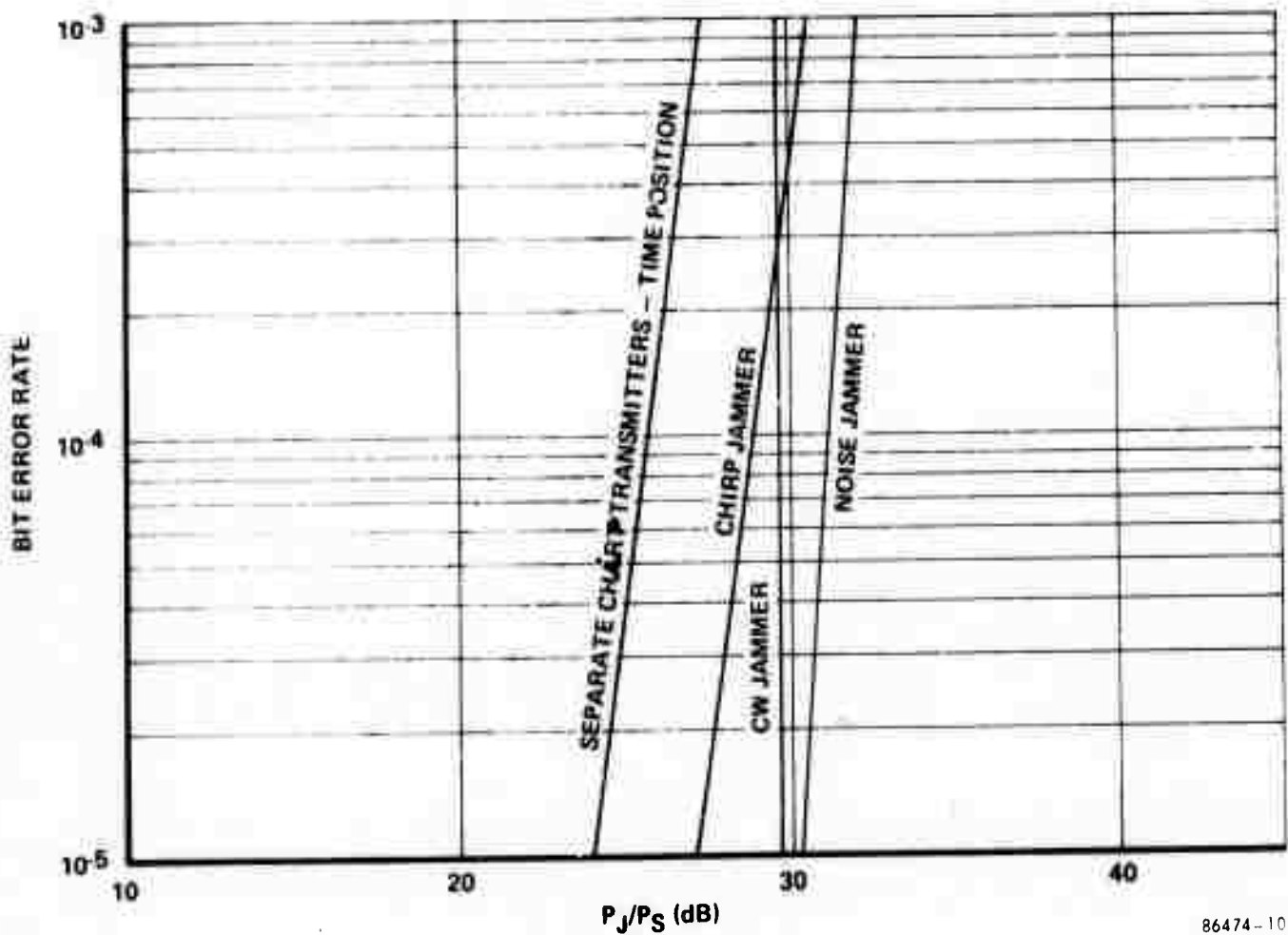
Figure 3.2.2-6. Decoder Output Error Versus Jammer Power - Modularity 2

3.3 Ranging (Two-Way Link)

The modem ranging capability allows range to be measured between the ground and each airborne user. As shown in Figure 3.3, the ranging requires waveforms on both the uplink and downlink. The uplink range waveform is a chirp signal and the downlink range waveform is pseudonoise code.

The range loop for tracking the uplink waveform can essentially operate in a continuous mode whereas the range loop for tracking the downlink waveform must operate in a time division multiplex mode. Each waveform in the downlink time division multiplex format can differ from other waveforms in frequency and phase since each waveform can be received from a different airborne modem.

3.3.1 Link Characteristics

Figure 3.3.1-1 functionally shows the ranging portions of the modem.

Both the vehicle and the ground based modems must be able to accurately track the phase of the received waveforms in order to demodulate the included data stream as well as provide an accurate ranging signal. The performance and operational characteristics of the tracking loops are therefore critical to the RPV mission success. In general, two distinctly different loop implementations are proposed because the selected uplink and downlink modulation formats are unique.

The ground station transmitter is continuously transmitting chirp waveforms which contain command data for twenty-five users. In the airborne vehicle the chirp receiver is matched to ground transmitted waveforms with a resulting 78 nanosecond output pulse possible every 10 microseconds. These output pulses are used to derive a range tracking loop error signal in the airborne vehicle to position the range gate. When the range loop is locked this gate signal will be delayed relative to the start of a ground time slot by the link propagation delay plus bias delays. Since the same source deriving the gate signal is also used to derive the pn range code, the result is a transfer of the propagation and bias delays to the pn range code. The same pn sequence used at the ground transmitter is programmed into the airborne vehicle pn sequence generator.

The airborne ranging code is used to spectrum spread the downlink status data. After spectrum spreading of the TDM status data, modulation and frequency translation to RF, the pn ranging code is transmitted in the system TDM format in order to time sequence it with other user ranging codes. The TDM approach is made relatively simple especially from the vehicle standpoint since the Master Station, being the central controller for all vehicles, transmits a command word to each vehicle to appropriately time that vehicle's burst transmission and assure the desired time division multiple access operation. (A twelve-bit word transmitted once per second will provide the required resolution and unambiguous range for this command word.)

At the ground receiver the received airborne pn ranging code is phase tracked which allows narrow band filtering of this signal. The phase of the received pn range code is then

88
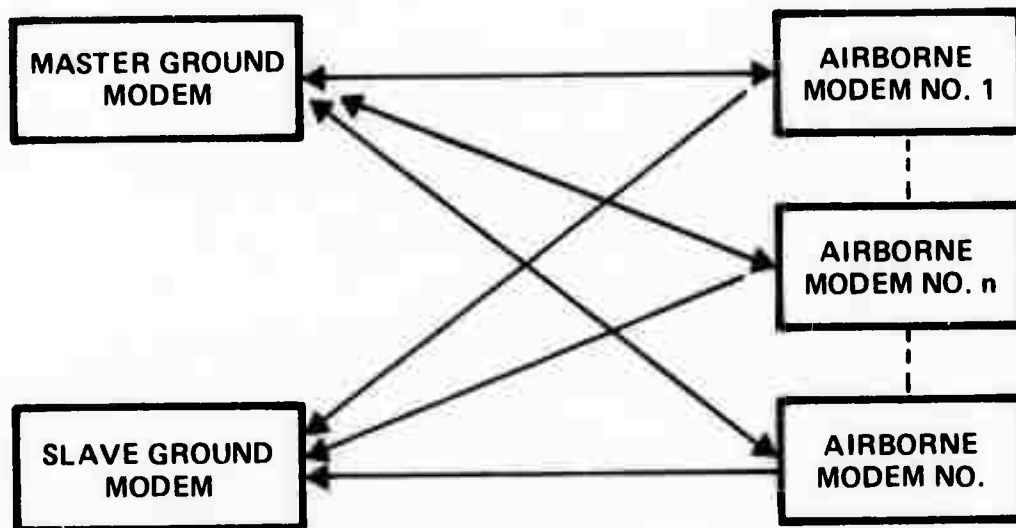
MULTIPLE ACCESS BY TIME DIVISION

(SIGNAL DESIGN FOR 25 OPERATIONAL RPV'S)

86482-29A

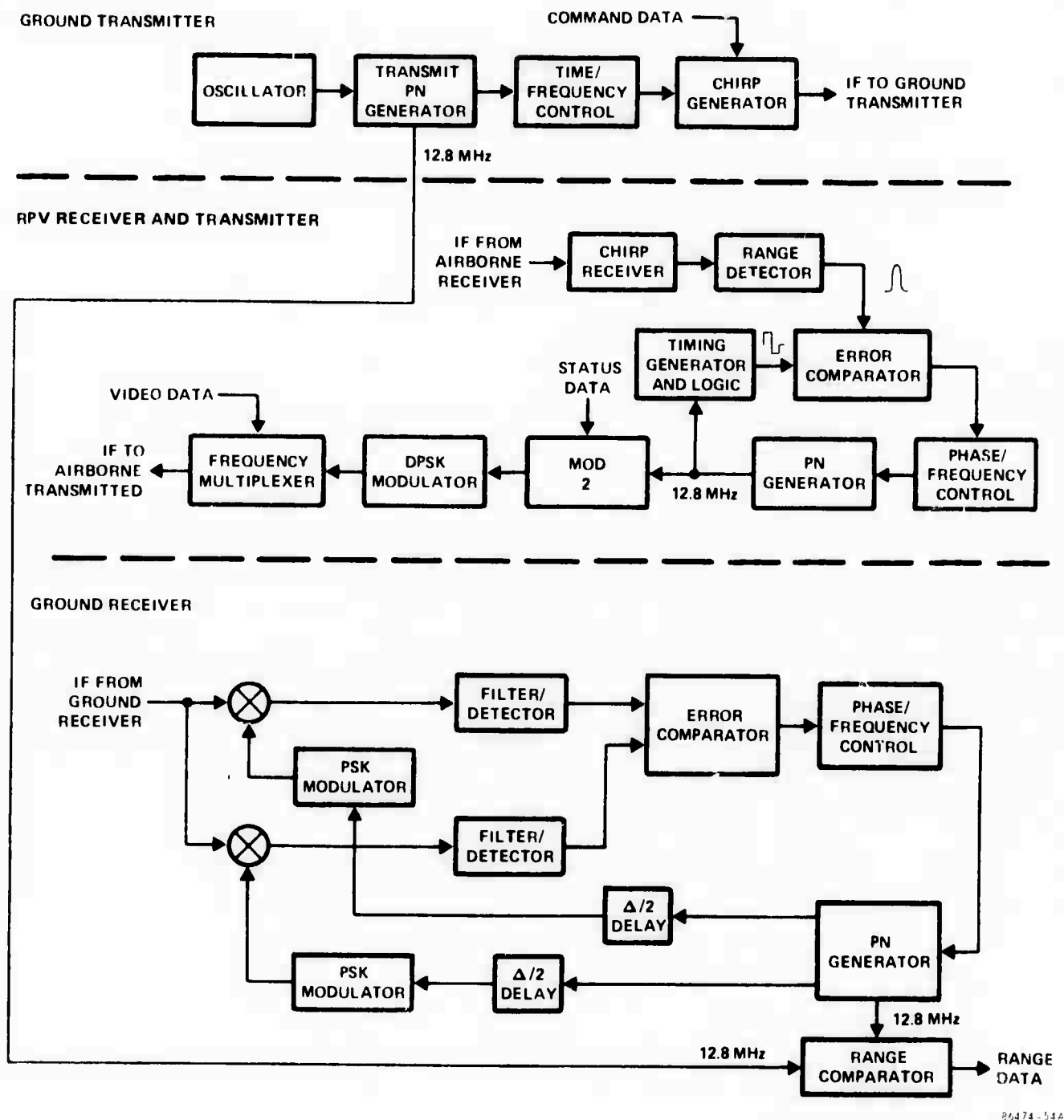Figure 3.3.   Range (Two-Way Link)

Figure 3.3.1-1. Range Data Functional Block Diagram

90

compared with the transmit pn code generator. The resulting phase difference between codes corresponds to the two-way range between ground and airborne vehicle.

The modem design for the downlink although different in system concept is similar to the modem design of Ohio State University.* Differential PSK modulation is employed, like that of OSU, due to the few number of bits per burst (40) in the design. Other parameters are: 80 kb/s data rate, 50 updates per second, and guard times of ± 125 μsec to accommodate a master-slave baseline of 20 nm. The 50 update/second value was chosen as a result of the trade-off study and is a compromise between the desire of a high update value for more "real-time" command and control, the buffer storage times, and the limitations of high data rate and low TDMA efficiency as the burst time is reduced.

The TDMA burst format and discussions involving accuracy, interference and acquisition are best explained by reference to Figure 3.3.1-2. At the Master Station each burst transmission is timed such that it arrives at the nominal "t_o" starting time. This "t_o" has a resolution of one chip due to the transmitted range command and the counting circuitry employed in the vehicle. If the Master Station's loop is locked, it knows precisely which chip will initiate transmission of preamble and data such that recovery of the data is assured. The accuracy of the transmission burst, and thus the accuracy of "t_o" and the assumed range of the command word, however, is not critical and a nominal value of 1.0 μsec is chosen. (As seen from the figure a tolerance of ± 125 μsec or ± 20 nm is allowable with the "no-transmit" guard time before crosstalk with adjacent time slots would occur at the slave station.)

Next, consider the case where the Master Station is not locked to a given vehicle such that acquisition over a given uncertainty is required. The vehicle continues transmitting using the last range command, and the chip time as well as the burst time are in error. The burst time can be in error by the same ± 125 μsec, or 20 nm, before crosstalk occurs and by as much as 675 μsec before the signal is out of the window. Thus, search and acquisition of the sequence generators can be accommodated over all time uncertainties of interest without concern for changing the windows or for the accuracy of the range command word. A preamble of 125 μsec in the burst is used to send the unmodulated sequence generator in order to provide ample time for the sampled data delay lock loop (SDDLL) to reduce its error prior to the time for demodulation.

The ground receiver must be capable of decoding up to twenty-five unique TDMA ranging signals. Therefore, certain portions of the ground receiver will be duplicated. These duplicated portions will be identified in Section 4.0.

---

* See for example, Huff, R. J., et al. "Additional Experimental Results Relevant to TDMA - System Synchronization;" RADC Report TR 72-134 March 1972.
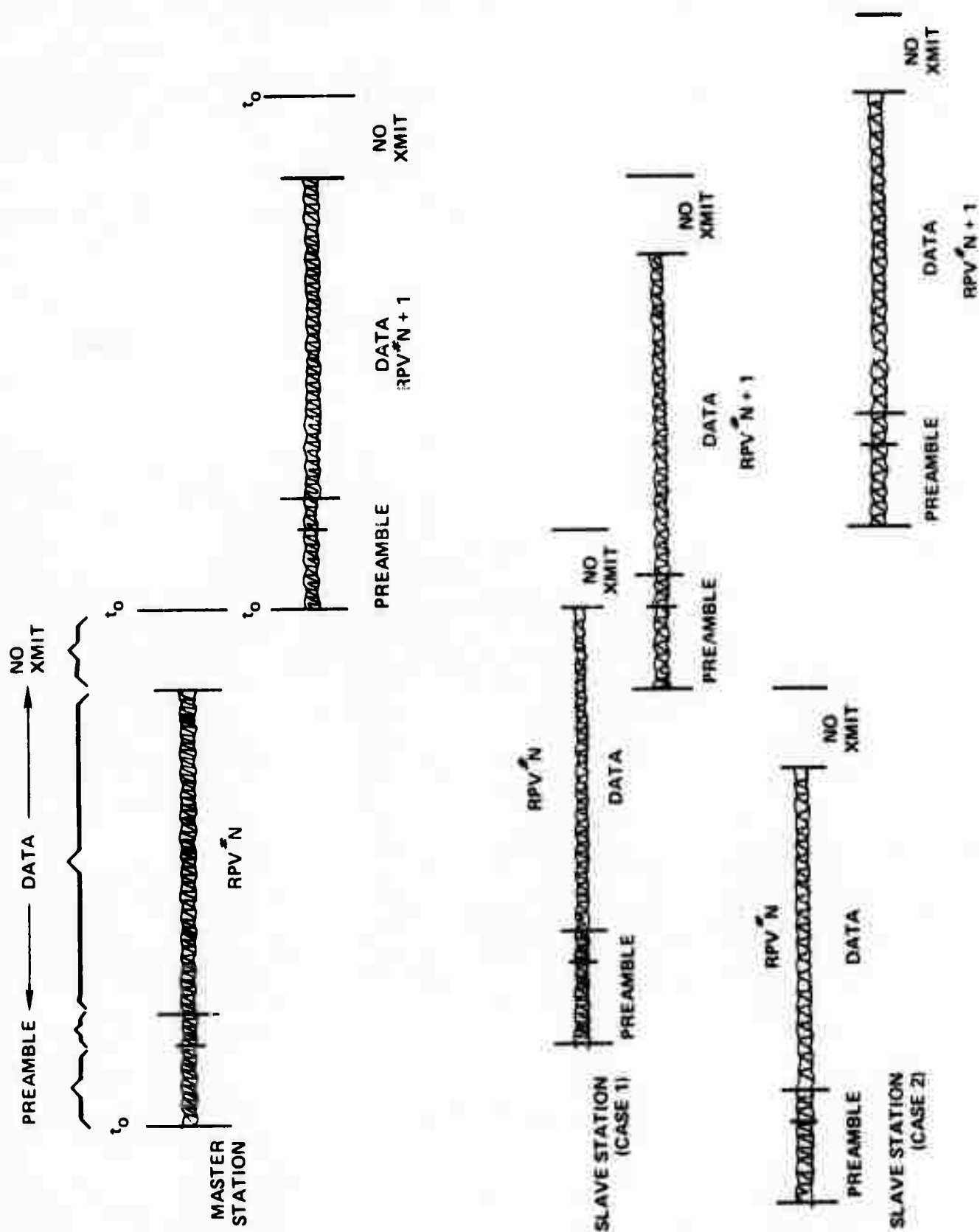
Figure 3.3.1-2. Range Signal Time Format

3.3.2   Performance/Features

The uplink tracking loop can essentially operate in a continuous mode. Thus, a tracking pulse, or phase error indication is available to the vehicle modem receiver every 10 μsec. During each 10 μsec time slot a pulse will be output from either the up-chirp or the down-chirp matched filter in one of the 128 time slots. The specific time slot is determined (functionally) by reading the state of the last seven stages of the PN sequence generator. At the expected pulse arrival time a gate will be opened which will be exactly aligned with the actual pulse arrival time if the phase and frequency of the vehicle PN generator is correct. Figure 3.3.2-1A illustrates a representative vehicle timing *diagram* where the vehicle gates are correctly aligned with the received pulse. Figure 3.3.2-1B illustrates a misaligned tracking loop and the output phase error values which will be used to develop a feedback error message to realign the vehicle clock.

The candidate loop model for uplink tracking, shown in Figure 3.3.2-2, is modeled after Tegnelia[1] although subsequent analysis and simulation will probably indicate that the simple implementation (using binary phase error quantization) as proposed by Cessna[2,3] provides satisfactory performance.

The operation of this loop is summarized here. The accumulator performs the operation

$$A(M) = \sum_{m=1}^{M} E(tm)$$

where $E(t_n)$ are the error samples shown in Figure 3.3.2-1 and $A(M)$ are the accumulated errors (added algebraically) at the end of M samples. At the end of M samples, the PN generator clock is changed an amount $\pm\Lambda$, depending on the sign of $A(M)$. In addition, a second accumulator sums algebraically the sign of $A(M)$ over all time which results in an average phase change per sample, or a frequency predictor. Thus, we have characteristics of a second order digital loop which is capable of tracking both phase shifts due to vehicular position changes and frequency offsets due to doppler and oscillator drift. Tegnelia has analysed the performance of this loop and his results are as follows.

---

[1] "A simple Second-Order Digital Phase-Locked Loop," C. R. Tegnelia, 1972 International Telemetry Conference Proceedings, Volume III, page 108.

[2] "Steady State and Transient Analysis of a Class of Digital Phase-Locked Loops Employing Coarse Amplitude Quantization and Sequential Loop Filters," J. R. Cessna, University of Iowa, Ph.D., 1970.

[3] "Digital Phase-Locked Loops with Sequential Loop Filters: A Case For Coarse Quantization," J. R. Cessna, 1972 International Telemetry Conference Proceedings, page 136.
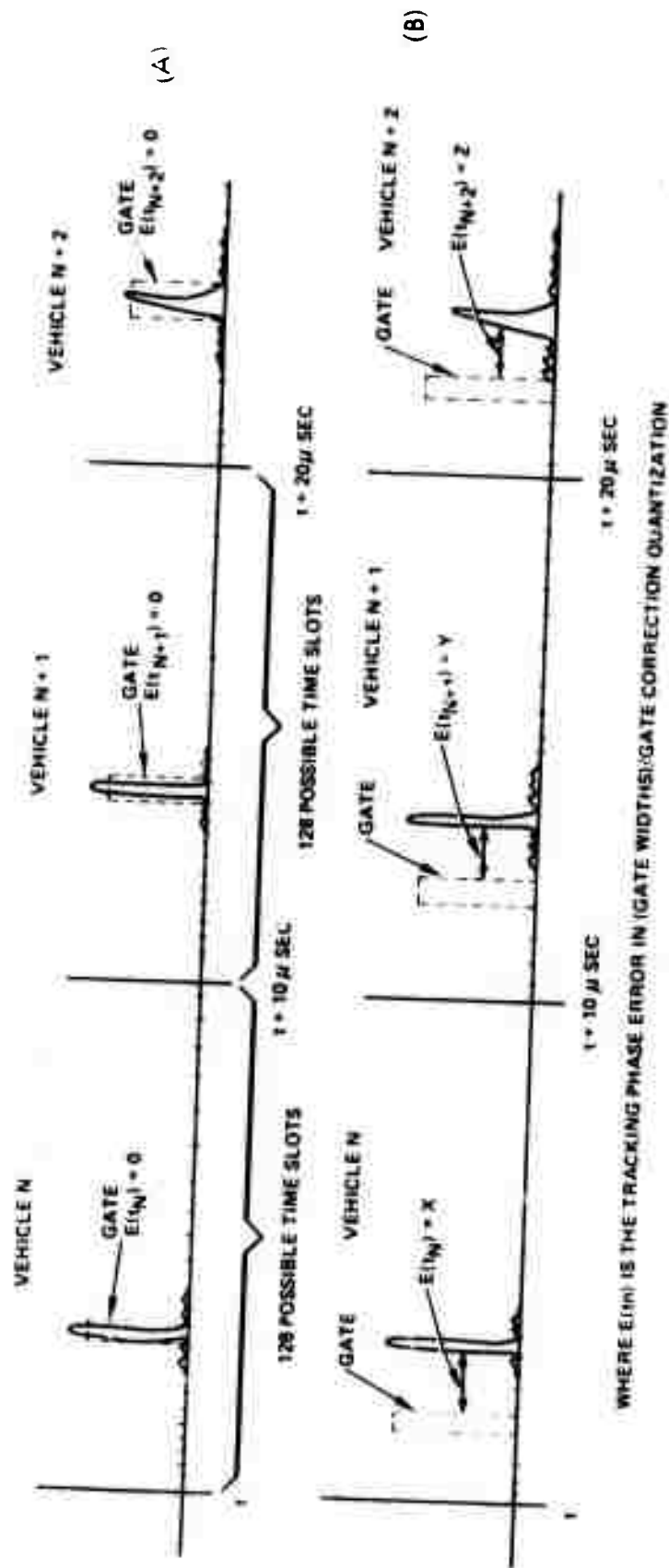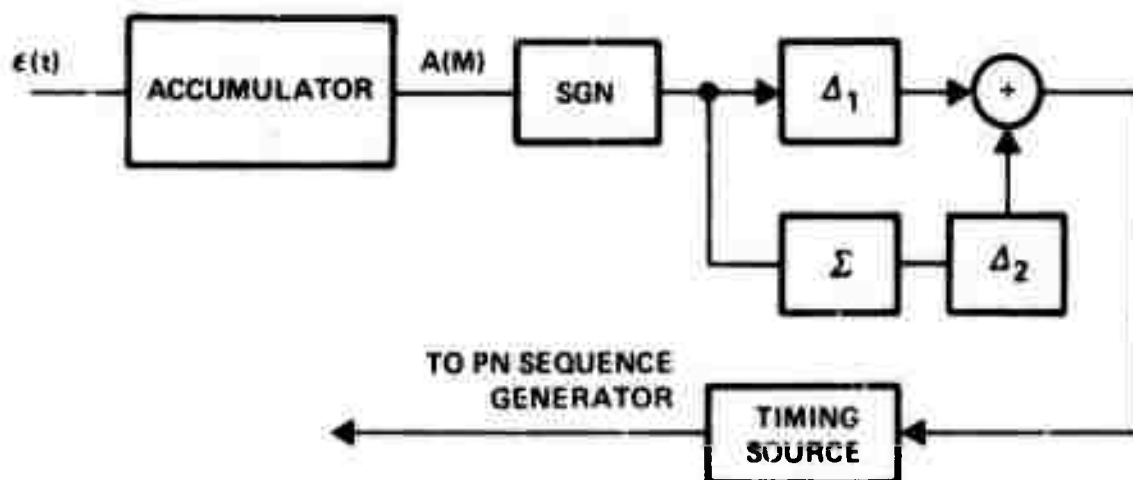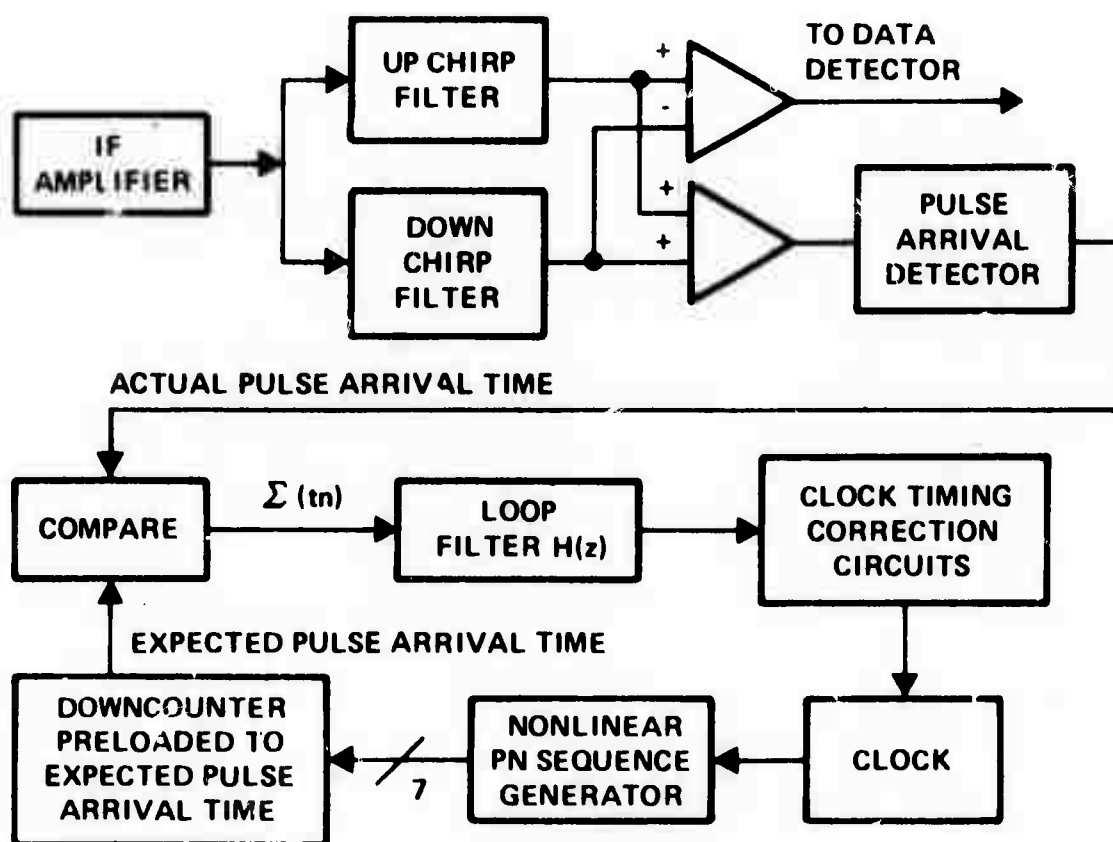
Figure 3.3.2-1. Example of Tracking Loop Phase Errors

94

FUNCTIONAL BLOCK DIAGRAM

DETAILED BLOCK DIAGRAM

86474-57

Figure 3.3.2-2. Uplink Tracking Functional Loop Model

95

The linear equivalent bandwidth of the loop is,

$$W_L = \frac{\Delta_2}{2\,MT_o\,\Delta_1} + \frac{2}{\pi}^{1/2} \rho^{1/2} \frac{\Delta_1}{MT_o\,\alpha} \quad \text{Hz}$$

where: T_o = the intersample period

α = the error slope at the zero crossing, or $\Delta_c/2$

Δ_c = the PN sequence chip width

$\Delta_1 = \mu\Delta_2 = \dfrac{\mu\Delta_c}{16}$ the quantized phase correction

$\Delta_2 = \dfrac{\Delta_c}{16}$ = the quantized integrated phase (frequency) correction

ΔF = the relative frequency offset of the two oscillators ($\sim 10^{-6}$)

The signal-to-noise ratio (ρ) out of the accumulator is given by:

$$\rho = M\,(S/N)_{\text{Chirp Filter Output}}$$

and the total phase error variance is given by:

$$\sigma_\phi^2 = \sigma_L^2 + \sigma_q^2 + \frac{\phi_d^2}{12} \quad (\text{rad})^2$$

where:

$$\sigma_L^2 = \frac{\Delta_2\,\pi^3\,\alpha^2}{4\Delta_1\,\rho} + \frac{\alpha\,\Delta_1\,\pi^{5/2}}{\sqrt{2\rho}} \quad (\text{rad})^2$$

$$\sigma_q^2 = \left[1 + (2\mu + 1)^2\right]\,\pi^2\,\Delta_2^2 \quad (\text{rad})^2$$

and $$\phi_d^2 = (2\pi\Delta F\,M)^2 \quad (\text{rad})^2$$

...after substituting, and observing that σ_q^2 is negligible for any reasonable M and ... the expression for $\sigma\theta^2$ becomes:

$$\sigma_\theta^2 = \left[\frac{\pi}{42\,M} - \frac{1}{128\sqrt{2}M} - \frac{1 - 2_- - 1^2}{2048} \right] \Delta_c^2$$

The original expression for $\sigma\theta^2$ was divided by $4\pi^2$ to obtain a normalized error relative to a chip width. Furthermore, if the chirp filter output S/N is used, the expression becomes:

$$\sigma_\theta^2 = \left[\frac{\pi}{42\,M\,(S/N)} - \frac{1}{128\sqrt{2M\,(S/N)}} - \frac{1 - 2_- - 1^2}{2048} \right] \Delta_c^2$$

Similarly, the expression for the equivalent bandwidth becomes:

$$W_L = \frac{1}{MT_o\mu} + \left(\frac{2}{\pi}\right) \frac{M(S/N)^{1/2}}{4\,MT_o} \quad \text{Hz}$$

The minimum phase correction Δ_2 was chosen to be 1/16 of the PN chip period Δ_c. This limited μ to a fairly small value to prevent the quantization error term σ_q^2 from dominating total phase error variance expression. Thus, the loop performance is now defined in terms of μ, M, T_o (the sampling period – 20 μsec), and the signal-to-noise ratio out of the chirp filter (S/N). Figure 3.3.2-3 illustrates the predicted phase error variance and loop bandwidth as a function of M and (S/N) with $\mu = 1$, 2 and $T_o = 20$ μsec.

As anticipated, with the reasonably high (S/N) required for the specified bit error performance, for most values of M the rms tracking error quickly approaches the loop correction quantization error limit. This limit is:

$$\frac{\sigma_\phi}{\Lambda_c} \doteq 0.07 \text{ for } \mu = 1$$

and

$$\frac{\sigma_\phi}{\Lambda_c} \doteq 0.11 \text{ for } \mu = 2.$$

The reacquisition of the phase of the received sequence at the vehicle in the event of a dropout due to a burst interference signal or antenna pattern null must include the ability to overcome phase changes due to vehicle motion or oscillator instabilities.
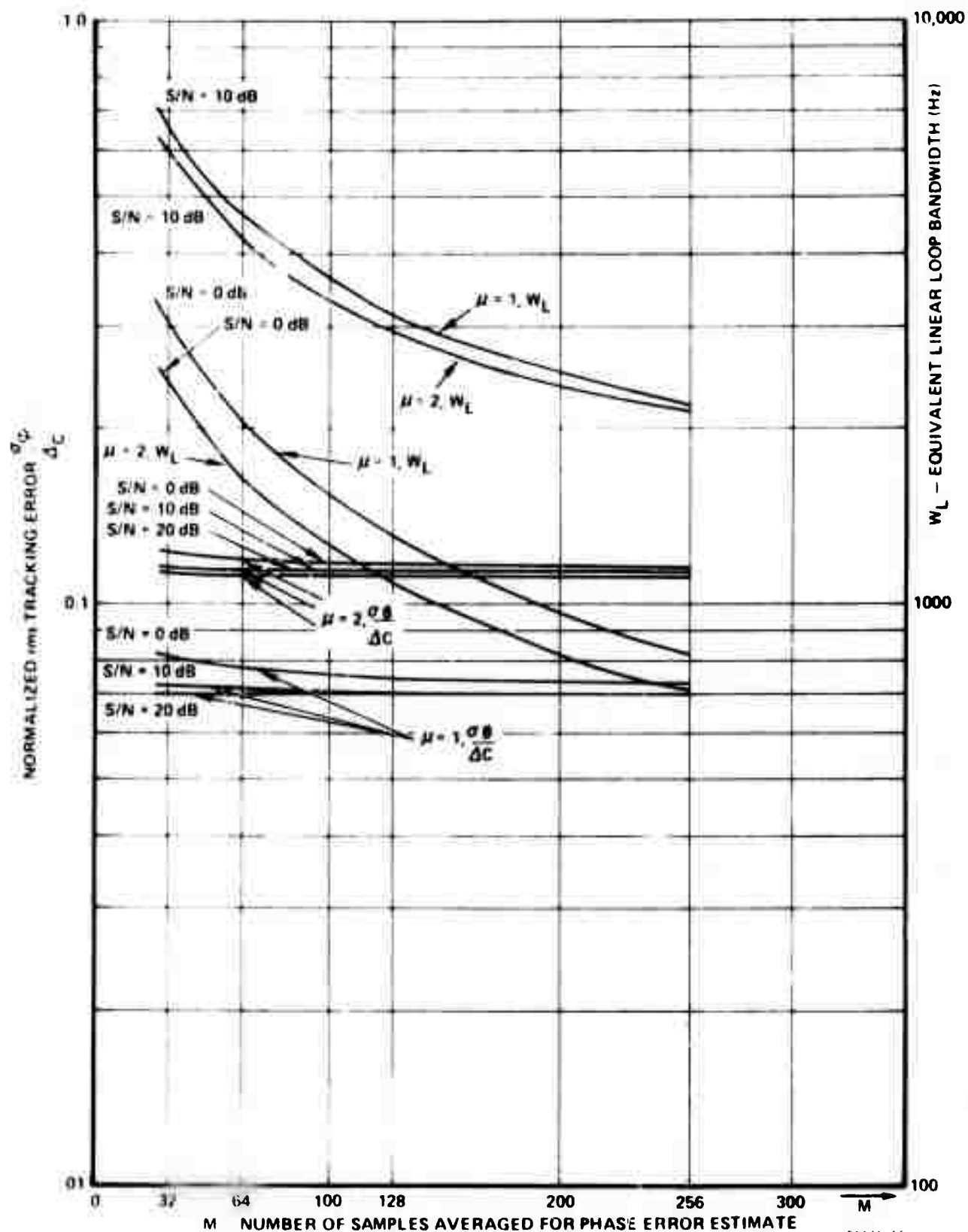
Figure 3.3.2-3. Prediction Phase Error

98

The reacquisition technique proposed here will employ two modes. The first will gradually open the tracking gate to accommodate position and oscillator uncertainties. This will be accomplished by counting 4,000 missed pulses and then widening the pulse present acceptance gate by one chip width. This is a worst-case design, and is based on the received phase uncertainty due to a Mach 1 velocity. This velocity uncertainty results in a 1,000-foot maximum position uncertainty per second, or a 1-microsecond phase uncertainty. Because the on-time tracking gate is approximately 80 ns wide, the adaptive gate must be widened ±1 gate width for every 80 feet of position uncertainty. Thus, the gate will be widened every 80 μsec, or each 4,000 pulses counted by the long-term confidence counter. The second reacquisition mode will occur when the confidence counter described above reaches a minimum level. At this time the clock which controls the PN sequence generator will be swept to encompass the increasing received signal phase uncertainty. The two modes are illustrated in Figure 3.3.2-4. The position uncertainty shown in Figure 3.3.2-4 represents the product of the velocity uncertainty and time since loss of signal. Thus, for the worst-case 1,000 foot/second velocity uncertainty discussed above, the modem will initiate the sweep mode 720 msec after loss of signal. However, because we are tracking velocity with the second order tracking loop, it is much more reasonable to assume that we know velocity to within 10 percent. This reduced velocity uncertainty results in a 7.2 second mode, one phase which appears compatible with vehicle dynamics, antenna nulls, etc.

The maximum width of the adaptive window was limited because the in-lock indication should not be overly vulnerable to a randomly pulsed jammer during reacquisition. The maximum proposed gate width (16 time slots out of 128) provides a fast acquisition mode without excessive jammer vulnerability. Since the short-term confidence counter must reach a count of 128 before true lock indication is noted, the probability of a jammer causing a false lock indication is low. As the gate is widened, and the received pulse intercepted, the gate widening process is inhibited because the 50 kHz downcount clock into the long-term confidence counter is inhibited each time a pulse is received within the adaptive window. This has the effect of widening the gate only the required amount to admit the pulse into the tracking loop circuitry and derive valid error signals to bring the loop back into lock. When the adaptive gate has reached its maximum value and lock has not been achieved, the clock which derives the PN sequence generator is swept and the adaptive gate remains at the maximum width. Thus, as the phase of the vehicle sequence is varied with respect to the received sequence phase, the two will become aligned and the lock-on process is then the same as above.

This implementation provides a strategy for search via the adaptive window for fast reacquisition after momentary signal dropouts in conjunction with a swept search to overcome large phase uncertainties in the event of a significant signal loss.

For each of the 25 reporting vehicles, the downlink TDMA format is similar to the situation investigated by Ohio State University. If we examine the signal from a single vehicle, the data is received in bursts (40 bits plus preamble) with a quiet period during the transmission bursts from each of the other 24 vehicles. This format has been discussed earlier and in summary, the data burst is 500 μsec long, the preamble is 175 μsec long and the time between bursts is 19.2 milliseconds resulting in a 50 data burst per second rate. The sampled

99
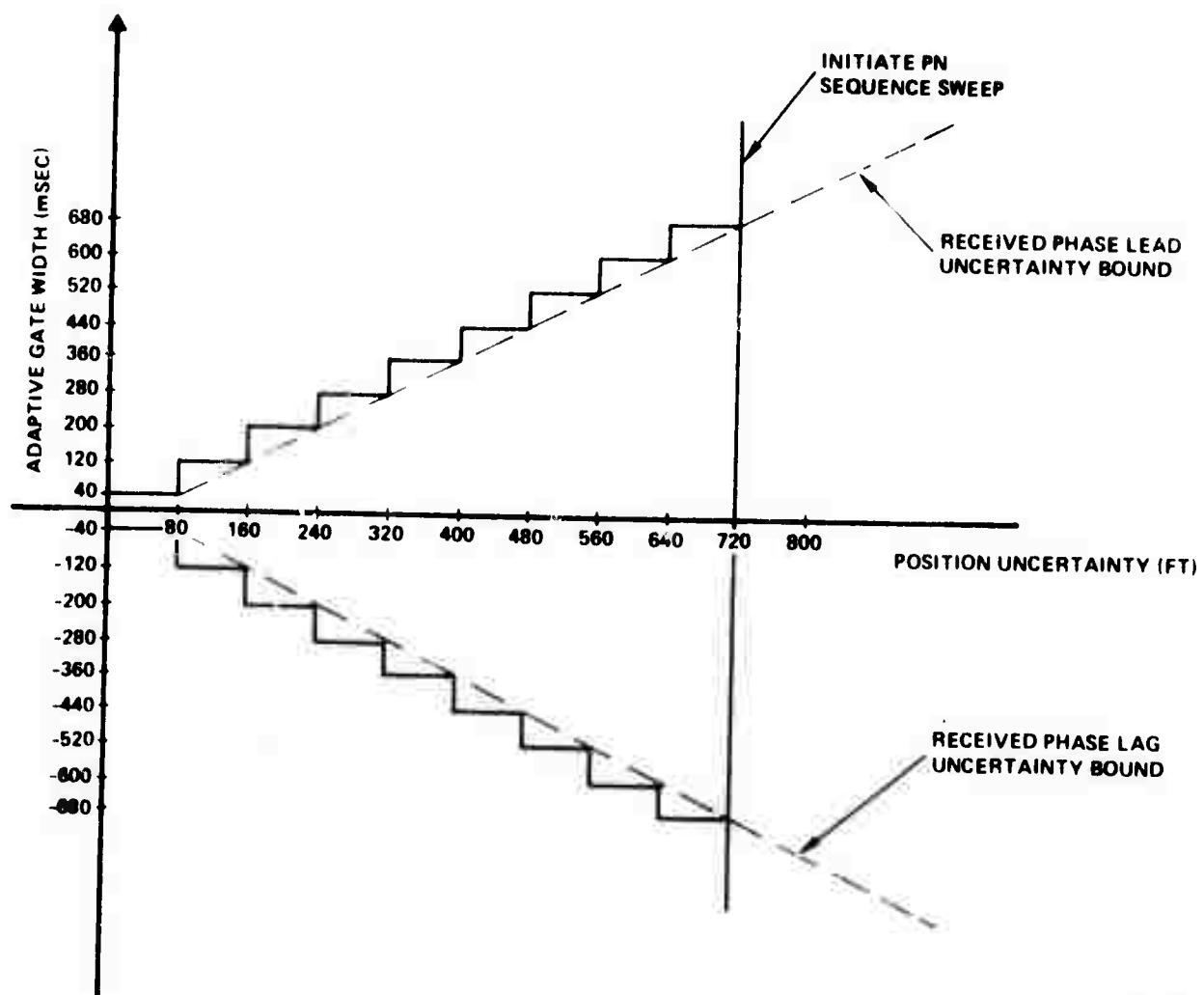
Figure 3.3.2-4. Range Loop Acquisition Modes

100

data delay locked loops described by Huff ore designed to trock this communicotion signals formot and will be used to track the received PN sequence at the ground stotions. A functional block diagram of the proposed loop is shown in Figure 3.3.2-5. The ground sequence is odvonced and retorded by $\Delta_c/2$, mixed with the received signal, bondposs filtered, and enveloped detected. A trocking error is obtained by sompling the difference of the envelope detector outputs ond used to correct the phose of the clock which drives the PN sequence generotor. In its present form, the Huff loop is o first order loop ond has o peok tracking error given by

$$\epsilon_{max} = \left(\frac{\dot{R}}{C} + \frac{\Delta F}{F} \right) \left[1 + \frac{A}{2} \left(\frac{N-1}{N} \right) \right] \frac{N \, KM\Delta_c}{A}$$

ond on rms tracking error given by

$$\frac{\sigma \phi}{\Lambda_c} \doteq 0.55 \left[\frac{A}{2-A} \right]^{1/2} \left(\frac{NE_b}{N_o} \right)^{-1/2} ; \, 0 \le A \le 2$$

where

$\dot{R}$ is the vehicle velocity (1000 feet/second)

C is the velocity of light (= 1 foot/ns)

$\Delta F/F$ is the oscillotor instability (10^{-6})

A is the gain of the loop (assumed equol to 1)

N is the number error voltage overoged by the loop filter

$KM\Delta_c$ is the interpulse period

ond

E_b/N_o is the energy per pulse (dota bit) to noise spectrol density rotio.

Huff hos shown thot the loop gain (A) can be mointoined very close to 1 for widely varying signol-to-noise rotio and will be assumed equol to 1 in the following discussion. Becouse of the 175 μsec preamble on the downlink dato streom, many error somples will be obtained during a single reception and it will not be necessory to overoge over more than one burst to obtain a valid tracking error estimate. Although the frequency offset results from o long term overage of the tracking errors, the number of phase error somples (N) in the obove equotion is equal to 1 because the phase error is obtoined from a single tronsmission. Finolly, the required E_b/N_o is opproximately 13 dB. Therefore, with no frequency compensotion $\epsilon_{max} = 40$ ns and $T_\phi/\Delta_c = 0.123$. This trocking performonce is unsotisfoctory and the proposed system will include a second order (frequency) correction which eliminotes rhe velocity trocking error ond results in a peok trocking error which is less thon 20 ns (1/4 of o chip period) and a corresponding decreose in the rms trocking error. In the proposed system formot 16-bit

101
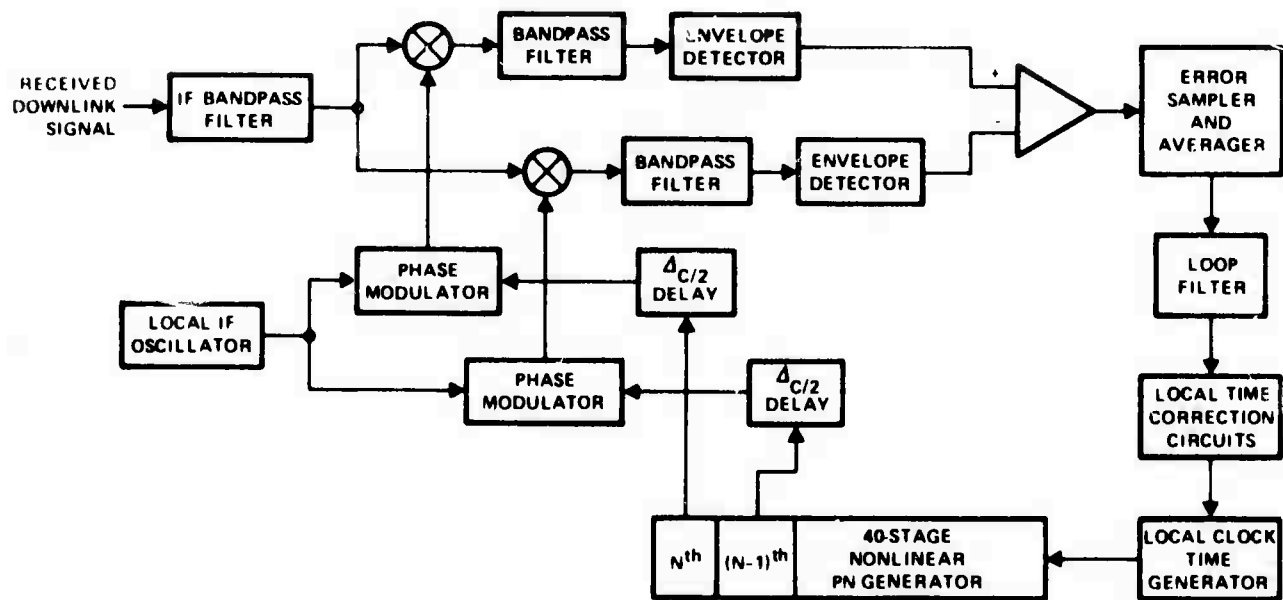
Figure 3.3.2-5.   Downlink Receiver Sample Data Relay Lock Code Tracking Loop

Table 3.3.2-1. Airborne Vehicle Range Error Caused by Frequency Offsets

Doppler Plus Local Oscillator Error (kHz)	Signal Loss/Pulse (dB)	Range Error (Ft.)
0	0	0
5	0	3.9
10	0.1	7.8
15	0.26	11.7
20	0.4	15.6
30	0.9	23.4
40	1.5	31.2
50	2.5	39.0

Table 3.3.2-2. Range Error Budget

	Range RMS Error (Feet)	
	Random	Bias
Quantizing	5	
Thermal Noise	1	
Receiver Variations	7	
Multipath	3	
Transmitter Trigger	12	
Timing Chains	10	
Signal Dynamics	9	
Doppler (Note 1)		1 (12)
Oscillator		4
Range Zero Set		2
Totals	20 (rss)	5 (rss)
Total (1 second smoothing) (Note 2)	3 (rss)	5 (rss)

Note: 1. 12 feet denotes offset caused by Doppler and 1 foot denotes residual error after computer correction.

2. Assuming ranging smoothing of 1 second [50 range measurements] reduces the random errors by $[50]^{1/2}$.

3.4   Modem Flexibility

An important feature in evaluating a system is its ability to adapt to changing
requirements without requiring redesign. Even a minimum amount of redesign is usually con-
sidered undesirable once units are operational since field modifications can result in both
scheduling and compatibility problems. Also, a low-cost RPV modem must benefit from present
and future technological savings. The proposed vehicle modem implementation consists basically
of two chirped matched filters and a digitally implemented code tracking loop. After demon-
strating concept feasibility with discrete digital building blocks, this approach can be easily
adapted to LSI technology and the achievable processing gain and antijam capability will
improve as the surface wave devices improve as a result of current and future research. Thus,
the operational modem design could be implemented (functionally) with two surface wave
matched filters and an LSI chip.

Modem flexibility will be discussed in the following paragraphs relative to
operational and growth considerations.

3.4.1   Operational

An important consideration in a multiple access system is the network control
approach. In the proposed system, the status, command, and range data are time division multi-
plexed and the video data is frequency division multiplexed. Both types of signals are main-
tained under tight control by the ground master station. In transferring TDM data, a predeter-
mined RPV is assigned full use of the data spectrum during a given time interval, thereby,
eliminating multiple access problems such as power sharing, link graceful degradation and user
identification. The status/range data transmission from the RPV is under complete ground
control since the ground maintains frequency and time lock with each user. Likewise, the
ground master station completely controls which RPV receives command data. System flexibility
is maintained by being able to program various pseudo-random sequences for each RPV plus
assigning additional time slots to a given RPV if mission requirements should dictate. Again,
the ground will control these changes by a manual programming of each user prior to a mission.
The command link will permit mission oriented programming to be accomplished automatically
over the link for the more sophisticated users.

The video data is frequency division multiplexed. The system design provides
sufficient spectrum for each video signal to allow operation at the required bit-error-rate under
varying system conditions. Since the video transmissions typically occur in the target region,
a limited dynamic range is expected and the channel crosstalk is held to a negligible value.
Additionally, with only five video signals simultaneously present, rather than twenty-five, the
spectrum required is relatively small.

The modularity of the system is a flexibility feature provided by the coder/decoder.
Modularity can be used to either increase or decrease the data rate to a given user or to vary the
processing gain to a given user. The degree of modularity for a typically RPV is programmed in

106

prior to a mission, however, for the more sophisticated users, the modularity could be controlled over the command link.

The data, range and timing acquisition/reacquisition are dependent procecures. Typically, loop lock will be established prior to takeoff. At this time, the range loop will be locked and zero set by measuring a known range and adjusting the phase of the user clock to compensate for equipment phase delays. Equipment stability will allow the range zero set to be valid for the duration of the mission, thereby this procedure is required only once regardless if the user should subsequentially lose range lock or not. Once the range loops at the RPV and ground receiver are locked, data detection occurs since the data and range code rates are synchronous. The range loop thereby derives the sampling signal which samples the data demodulator output. Once airborne range lock is achieved, the time word will be detected by the data demodulator and used by the RPV as the reference for controlling transmission time of data back to the ground.

The proposed system is designed to minimize the probability of losing lock. Typically, the jamming threat at the RPV receiver will be more severe than the jamming threat at the ground receiver. Therefore, the airborne ranging loop is more likely to unlock than the ground ranging loop. The range loop in the RPV is designed to integrate all pulses out of the chirp receiver, rather than only integrating data pulses addressed to it. This takes advantage of the ground antenna pattern by allowing RPV signal reception and thereby integration by the range loop during any given time slot. Therefore, a significant jamming threat is required to break range lock and consequently prevent data reception. If unlock should occur, then reacquisition must be initiated as rapidly as possible to minimize the data loss. Since the ground transmitter is fixed (not controlled by a range loop error voltage) the reacquisition can occur sequentially where the RPV first locks, then the ground stations lock. Initially, the range gate will be approximately doubled in size and will be positioned in time where the last valid ranging pulses were received. If reacquisition does not occur, then range loop processing gain will be exchanged for progressively wider range gates. If reacquisition has not occurred when the range gate is at its maximum designed opening, then the time gate will be time-sequenced through the unknown time interval until lock is re-established. When range lock is achieved in the RPV, the last valid time word received will be used to control the transmission of the status/range data. Since the ground should approximately know the value of this range word, the ground receiver only needs to search around this range word uncertainty plus or minus the range ambiguity which occurs during loss of lock. Once a valid lock is achieved at the ground receiver, a new timing word will be sent to the airborne user. A feature in the proposed system which will greatly increase loop acquisition is allowing the range loop to track all pulses transmitted by the ground. This is in contrast to requiring the range loop to wait until the next time slot assigned to the RPV before reacquisition can be initiated. Once the ground range loop is locked, the ground data demodulator will also be operating due to the synchronous relationship between status data and range code rates.

The ground receiver will continue to receive valid status data during most RPV range loop unlock periods. When an RPV range loop unlocks, this loop will be opened. Status data will continue to be combined with the ranging code and the ground receiver will continue tracking the "open loop" RPV range signal and demodulating status data. Since initial

107

reacquisition is implemented in the airborne vehicle by opening the range gate, the ground receiver will remain locked during this search period. This phase of the search procedure is expected to result in RPV range loop reacquisition for most operational conditions which caused the range loop to unlock. Should range reacquisition not occur by the time the range gate is at its maximum width, it then becomes necessary to sweep the opened time gate. During sweep, the dynamics on the range code are expected to be sufficiently large to cause the ground receiver to unlock.

3.4.2   Growth

Several growth features of the proposed system are its ability to adapt to variable information rates; provide additional system processing gain for command data; provide processing gain for video data; ability to operate as a time-frequency system; and adapt to various ground baselines.

Reduced information rates on the link are desirable for cases where transmit power has decreased and/or the jamming threat has increased. By reducing the information rate, the link operation can be maintained. The waveform design is able to reduce the information rate of 2 kb/s by selectable factors of 2, 3, 4, 6 or 12 for any combination of airborne vehicles. This is accomplished by maintaining a constant bit rate between ground and RPV while increasing the transmission redundancy by 2, 3, 4, 6 or 12. The interface between the demodulator and decoder takes advantage of this by providing increased processing gain whenever the link is transmitting redundant data. The link thereby maintains the required performance under degraded operating conditions. The system could also operate at an information rate greater than 2 kb/s by exchanging number of users for increased information rates. Time slots assigned to other users can be reassigned as a function of mission requirements. A given user could receive information rates of 2 kb/s, 4 kb/s, 6 kb/s, 8 kb/s, 12 kb/s and 24 kb/s. The upper limit of 24 kb/s exists since the chirp receiver is gated to prevent signals in adjacent time slots from being received to minimize potential interference problems.

The digital implementation of the airborne user equipment, in combination with the chirp receiver concept, allows relatively easy implementation of a parallel time search. Several range gates can be synthesized each one time offset from the other. By examining each range gate error output simultaneously, more rapid reacquisition can be provided.

The video signal can be provided with a degree of security coding. This will prevent a low jamming signal from disrupting low data rate portions of a video data sequence such as TV line synchronization. This security would be provided by feeding the video signal into a buffer register and then combining the register output with the pseudonoise ranging code. The buffer register is used to allow the video data rate to be made synchronous with the pseudonoise code rate. This feature will effectively spread low data rate sequences in the video data to a bandwidth corresponding to the 12.8 MHz ranging code.

The feature of trading video data rate for processing gain, as previously described, can be extended to higher values of processing gain. The reduced video rate of 2 Mb/s, as proposed in the option, is selected as a reasonable value of video bandwidth reduction resulting from

108

slow frame TV. If greater reductions are possible, then greater values of processing gain are achievable. The vehicle modem electronics, if this spreading option is incorporated, is independent of the extent of video bit rate reduction. The ground video demodulators would be selected for the particular video bit rate used for that mission.

The range link between ground and RPV locks the RPV clock to the ground clock. If the airborne modem could zero set its clock then each RPV could be an accurate source of timing. This accurate timing could complement other systems on the RPV for situations where one way air-to-air communications are desirable. Also certain missions may limit the transmission time of the ground transmitter to prevent enemy "homing" on this signal. If accurate timing is available each RPV will be able to continue transmitting status/ranging in its assigned time slots. Ranging could continue on a one-way basis rather than a round trip basis with range accuracy determined by the stability of the airborne modem oscillator. At predetermined intervals the ground would transmit data which would be used by all airborne modems to correct their clocks and frequency sources. The proposed modem provides the capability of accurately setting clocks in each RPV since timing information is contained in the uplink range word. In the proposed system this range word has a least significant bit of approximately one microsecond which corresponds to approximately one thousand feet. This resolution can be improved by increasing the proposed range word size.

The status/range time slot format has 125 microseconds guard time between the end of data and start of the next time slot. This number was based on a twenty-mile baseline between master and slave ground stations in order to provide the slave with 425 microseconds of noninterfering ranging signal. The master station receives 175 microseconds of preamble in order to assure a good lock for data demodulation and 500 microseconds of data. These numbers can be easily adjusted. Therefore, the proposed system format can be adapted to be compatible with various ground network station geometries.

SECTION 4.0

BASELINE IMPLEMENTATION

Figure 4.1.1-1. The Command Modulator Simplified

112

often as possible to provide the best demodulator operation. In addition, further processing gain must be implemented to derive the necessary antijam protection for the command link. How this is done is described below.

The 12.8 MHz oscillator drives a pseudo-random noise (PN) sequence generator which produces a PN sequence at the 12.8 MHz rate. The sequence drives an 8 bit serial-to-parallel converter which is clocked at an 800 kHz rate to form a random 8-bit word once every 10 microseconds. The 800 kHz clock is obtained by dividing the 12.8 MHz reference rate by 16. Only 7 bits of the 8-bit word are required, so that the most significant bit of the random word always remains "hidden."

The output of the serial/parallel converter is a random number between 0 and 127, so that there are 128 possible numbers. Once every 10 microseconds, the new number is loaded into a count-down generator which begins to count from the number loaded in down toward zero at a 12.8 MHz rate, or one count every 10/128 microsecond. For example, if the number 50 is loaded in, the counter will count from 50 down to zero in 500/128 micro-seconds. When the count reaches zero, a pulse appears at the counter output, which goes to a pair of AND gates, one of which is enabled. Suppose line "A" in Figure 4.1.1-1 is high. The pulse then propagates through that AND gate and onto the surface wave dispersive delay lines marked "1A" and "0A" in the figure. Device 1A then begins to put out a signal whose frequency increases linearly with time, i.e., an "up-chirp," while the 0A device produces a decreasing frequency, or "down-chirp." The former line represents a data "1," while the latter represents a "0."

The signal at the output of each device is a frequency ramp which is increasing (or decreasing) at the rate of 12.8 MHz per 10 microseconds. The duration of the sweep is 20 microseconds, so that a total of 25.6 MHz is swept each time a device receives an impulse. Figure 4.1.1-2 shows graphically the operation of the dispersive delay lines. The energizing pulse appears at some time, τ, which is determined by the pseudo-random number into the count-down circuit. When this pulse reaches a line, say an up-chirp line in this case, the output signal starts at 12.8 MHz below its nominal center frequency, f_o, and increases linearly with time until, at time τ plus 20 microseconds, it has reached f_o plus 12.8 MHz.

Next consider the data pulse which was discussed previously. This data pulse lasts for 10 microseconds, and is clocked by the same 12.8 MHz reference as the pulse-generating system so that the data pulse always lasts from time 10 to time 20 microseconds after the zero reference of the time scale in Figure 4.1.1-2. (The zero reference is the time at which the delay line would receive its impulse if the random number which determines the start time were 0.) When the data bit occurs, a gate (actually an RF switch) is actuated at the output of the delay line so that its output is gated to the transmitter for that 10 microsecond interval. This is shown at the bottom of Figure 4.1.1-2.

The transmitted output is therefore a swept frequency which always starts at the same time (gated by the data bit), but which starts at one of 128 pseudo-randomly selected frequencies. Looking at the dotted impulse at the top of the figure, we see that a different
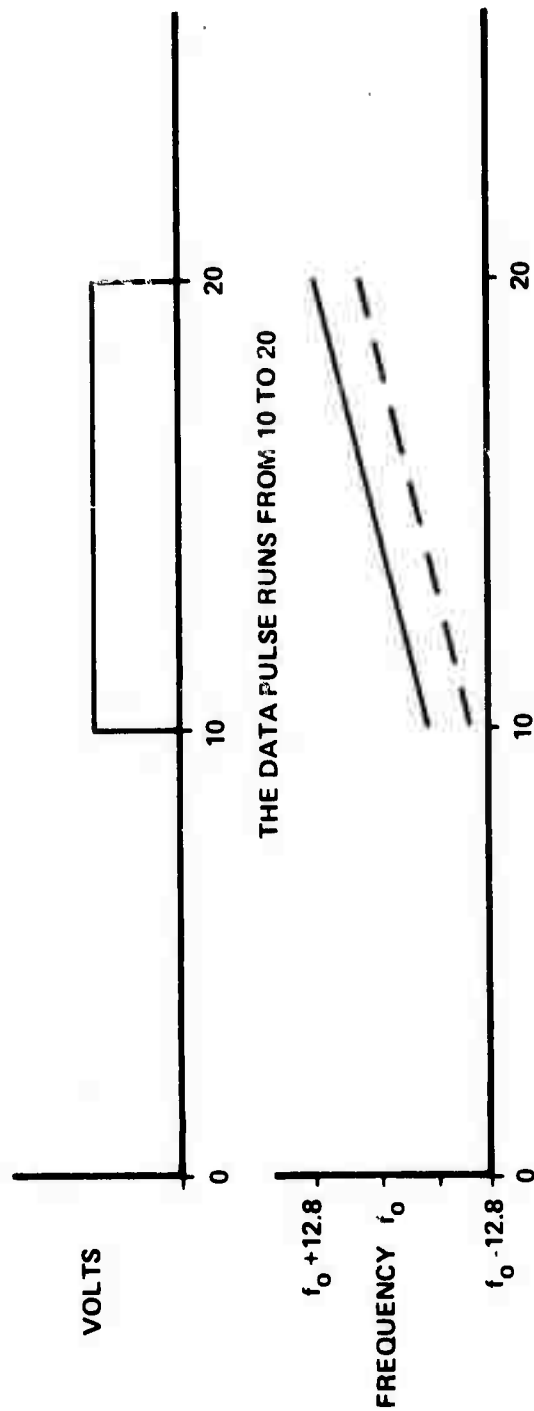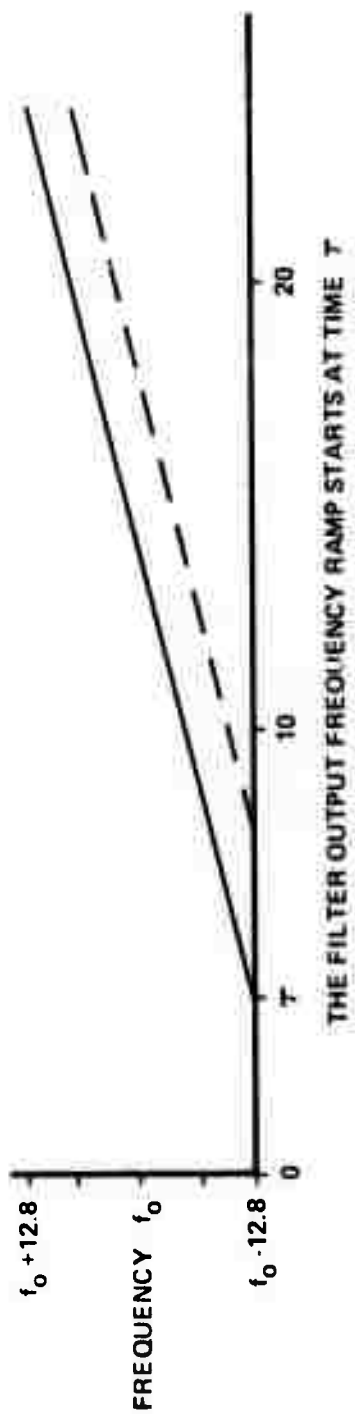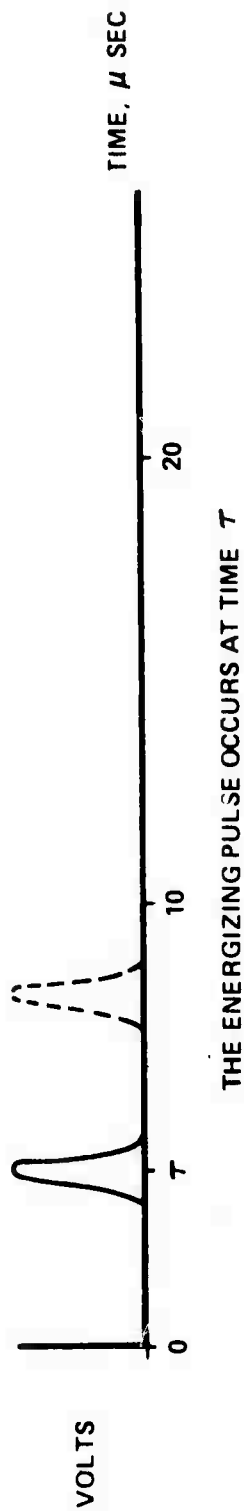
Figure 4.1.1-2.   How the Data Ramp is Generated

114

random number, resulting in a different impulse arrival time, will result in a different set of frequencies being sent (the dotted line at the bottom of the figure) over the data time interval.

How does the system differentiate between a data "1" and a "0"? Referring again to Figure 4.1.1-1, each pulse out of the counter energizes two delay lines of opposite sense. If a data "1" is to be sent, the output of the up-chirp filter is gated to the transmitter; while for a "0," the output of the down-chirp filter is gated through.

Why are there four delay lines instead of just two? This is because each frequency sweep lasts for 20 microseconds, but the 100 kilobit data must be sent at the rate of one bit every 10 microseconds. Therefore, only alternate bits are sent by each pair of lines; and we have an "A" pair and a "B" pair alternately transmitting a bit every 20 microseconds. This alternating is controlled by the formatter, which is discussed below.

The formatter acts as a sort of master of ceremonies to control and keep track of the vehicle data. The data format, as described in Section 3.0, is a 500 microsecond-long frame in which each vehicle receives two 10 microsecond-long data bits (when all twenty-five vehicles are in use). In addition to supplying the alternating "A" and "B" enable signals, the formatter determines which vehicle will be the first in each 250 microsecond interval to receive data, clocks the data for the rest of the vehicles through in sequence, and changes the format as required when less than 25 vehicles are in use. How this is done is shown in Figure 4.1.1-3, which is a somewhat more detailed block diagram of the command modulator. The formatter functions are shown broken out separately on the figure to provide a more meaningful presentation.

An important function of the formatter is to determine which vehicle receives the first data bit in each subframe. The vehicle number is determined in a pseudo-random fashion to increase the difficulty of concentrating the jamming on a single vehicle. The number of the initial vehicle is determined by the same PN generator which determines the chirp frequency. The output of this generator goes through a delay which compensates for the residual delay through the chirp lines (the reason for this will be discussed in Paragraph 4.1.2) to a modulo 25 counter. Whenever the input bit is a "1," the counter counts up one interval; and when the bit is a "0," the counter does not count. When the count reaches 24, the next input "1" resets it to zero and the count starts over, so that at any given instant the counter is set at one of twenty-five pseudo-randomly determined numbers between 0 and 24. The counter counts at an 800 kHz rate, so that the number changes every 1.25 microseconds if the input is all "1's." A five-digit number is required to describe the state of the counter, but the least significant bit is left off to be supplied further downstream.

The output of the counter, a four-digit binary number between 0 and 13, is then loaded into another modulo 25 counter. The least significant bit into the counter, which requires a five-bit number, is supplied by the LSB control. The LSB control generates alternate "1's" and "0's" so that the counter input alternates between even and odd numbers. This is done so that the delay lines will always be pulsed alternately from the end of one frame to the beginning of the next, and there will not be a requirement to send two odd-numbered (i.e., "A") or even-numbered ("B") bits in adjacent time slots.

115

Figure 4.1.1-3. The Command Modulator Showing Formatter Function.

After the second modulo 25 counter is loaded with the number of the first vehicle in the frame, the master format unit delivers the order to begin counting up at the beginning of a frame. The counter then begins with the number which was loaded in, say it was 5, and counts 6, 7, . . . 24, 0, 1 . . . 4 at the rate of one count every 10 microseconds. At the end of the subframe, the counter begins again at 5 and repeats the pattern so that each vehicle receives two bits in a 500 microsecond subframe. At this point, the first counter delivers another four-digit word, the LSB is changed from a 1 to a 0 so that the next frame begins with an even number; and the process repeats itself. A storage network (STG in Figure 4.1.1-3) remembers the counter loading so that the pattern is repeated twice, and a multiplexer unit drives the format sequencer so that the proper TDMA range word and the proper data bit are strobed.

The data for each vehicle may be retransmitted in other vehicle time slots provided the other time slots are not used - i.e., less than 25 vehicles are used. The number of times retransmission occurs is selected by the "modularity" of the vehicle. The format sequencer receives the current time slot number and vehicle modularity and requests the proper vehicle data channel. Each frame a new vehicle data bit is presented for transmission and is used as often as the modularity requires during the frame. The modularity of each vehicle is adjustable depending upon the number of unused time slots available. When all 25 vehicles are used, each has a modularity of one. At the other extreme, two vehicles may have a modularity of 12 each, using a total of 24 time slots. The format sequencer receives the current time slot number and enables the proper vehicle data channel as determined by the selected vehicle modularity.

Additional modularity may be obtained by reducing the control system data rate to each vehicle in submultiples of 2 kHz. In that case, each bit is retransmitted for two or more frames. Vehicle data rates of 1 kHz, 2/3 kHz, and 2/4 kHz result in vehicle modularities of 2, 3, and 4 respectively. This option does not modify the ground or vehicle modem, but only the command data rate and hence the vehicle decommutation rate.

A nominal IF output frequency of 100 MHz has been selected for the command modulator, primarily because the surface wave devices used to generate the chirped signals can most conveniently be built with bandwidths of between 25 and 35 percent of center frequency. Since the required bandwidth is 25.6 MHz, 100 MHz is quite suitable. Also, the IF amplifiers needed at the outputs of the devices must have bandwidths of at least 30 MHz to avoid degrading modem performance due to amplitude and phase ripple. For this bandwidth, 100 MHz is also a very suitable center frequency.

For simplicity, the block diagrams show that the delay lines are driven directly by the logic which determines the timing for the ramp. In fact, a driver circuit must be included which takes the logic command and generates a pulse of approximately 100 milliwatts peak to drive the delay line. The line output is then amplified by 60 dB to provide a nominal modulator output level of 1 milliwatt.

117

4.1.2　Command Demodulator

The command demodulator, located in the remote vehicle, receives the spread command signals at IF, despreads them, establishes bit timing, and demodulates the command circuitry. In addition, the PN sequence used for the despreading goes to the vehicle status modulator for retransmission to the ground master and slave stations for ranging.

The spread energy into the demodulator is collapsed by using surface-wave dispersive delay lines identical to those in the command modulator. However, this alone does not "despread" the signal. A pulse from one of the delay lines can be in any one of 128 different time slots within a bit time, so that the signal is still, in effect, time-hopped. True despreading occurs only when the receiver knows exactly when the pulse will arrive and opens a gate at just that time, closing it for all the other slots to shut out interference. The demodulator knows when to open its gate; because it contains the same PN sequence that the modulator contains, and uses it in the same way to derive a pulse time. However, the demodulator sequence must be in time synchronism with the modulator sequence so that the gate does indeed open at the proper time.

The command demodulator must, therefore, contain the dispersive delay lines to compress the "chirped" energy, a PN sequence which matches that in the modulator so that it can know at what time the pulse will come out of the delay lines, and a timing loop to keep its PN sequence exactly synchronized with that in the modulator. Figure 4.1.2-1 is a simplified block diagram of the demodulator timing loop, which will be helpful in beginning the explanation of the hardware implementation.

The pulse from the dispersive delay line enters the timing loop at the left of the figure. Since this pulse is sin x/x in shape, its exact arrival time is ambiguous; and so a "pulse arrival time" determining block is needed to exactly locate the pulse in time. The output of this network is a short pulse which tells the actual pulse arrival time. This pulse enters a comparison circuit whose other input is the demodulator's estimate of the pulse arrival time. This estimate is made by generating the pseudo-random number from the PN generator output exactly the same way that the modulator originally did this. The comparison circuit determines the amount of time error between the demodulator arrival time estimate and the true arrival time, and sends this error signal, through an appropriate loop filter, to the demodulator clock to correct its timing. Although the actual implementation of the loop will seem rather unusual when we get into the details, Figure 4.1.2-1 shows that the loop, in fact, is like any other timing loop in its basic operation.

Figure 4.1.2-2 shows some of the demodulator functions in greater detail. The input signal, at a nominal 100 MHz center frequency, is amplified in a gain-controlled amplifier. The signal then passes through a switch which turns off the alternate bits into the demodulator - for example, an odd-numbered vehicle ignores all the even-numbered data bits - as explained in Paragraph 4.1.1. After further amplification, the signal is applied to the two dispersive delay lines in parallel. Only one of the lines responds to the input signal, depending on whether the data received was an "up-chirp" or a "down-chirp" (i.e., a "1" or a "0"). The output of one of the lines will thus be a pulse of energy about 20/128 microseconds wide at its base; while the
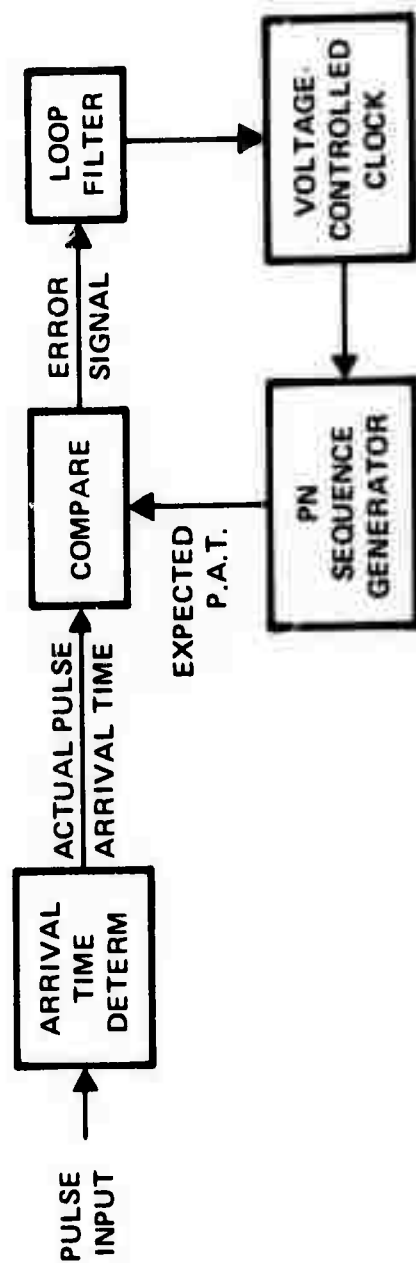
118

Figure 4.1.2-1.   The Command Demodulator Timing Loop
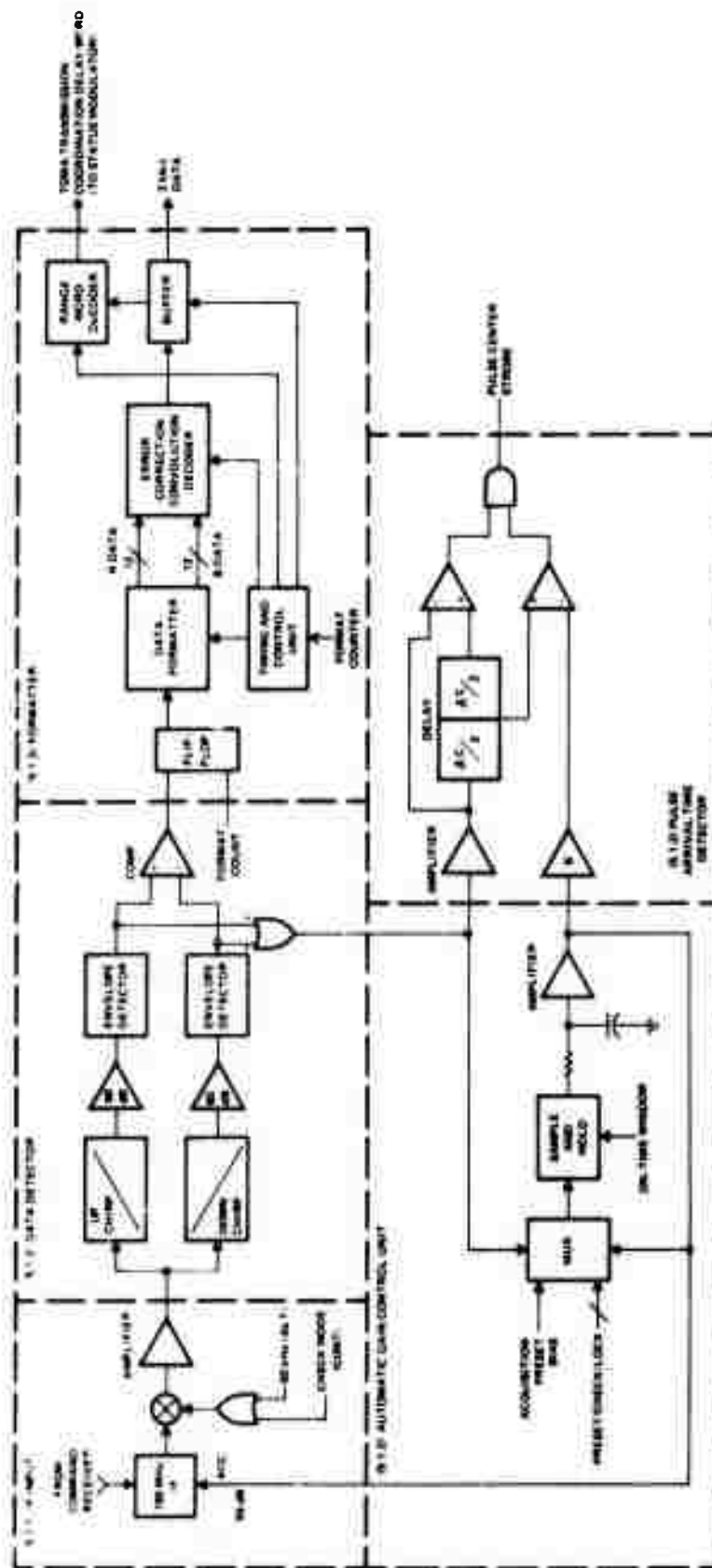
86482-38

119

Figure 4.1.2-2. A Closer Look at Some Command Demodulator Functions

other line puts out only noise. After envelope detection, the baseband energy is applied to a comparator which determines which line contains the high-energy pulse, and, therefore, decides whether a "1" or a "0" was sent.

The envelope detector outputs also go to a summing network so that the summer output always carries a pulse for each data bit, regardless of whether a "1" or a "0" was sent. This pulse is applied to the pulse arrival time detector, or centroid detector, which works as follows. The pulse is split into two paths, one delayed and one not delayed. The delay consists of a pair of delays, each one-half chip width, or 5/128 microseconds long. (Note that the pulse is 20/128 microsecond long at its base.) Figure 4.1.2-3 shows this operation in better detail.

Refer to Diagram A on the figure. This describes the pulse 2τ or 20/128 microsecond wide, as it arrives undelayed at the comparator. Diagram B shows the delayed version at the other input to the comparator. The comparator takes the difference, B-A, in the next diagram, and switches from negative to positive when this value crosses zero. The comparator output is shown in Diagram C, switching at 1.5τ. Diagram D shows the half-time delayed input pulse, and we can see that the peak of this pulse occurs exactly at the point where the comparator output switches. Thus, we have at points D and C, respectively, a received pulse (delayed by 5/128 microsecond), and a logic switching function which occurs at exactly the peak of the delayed pulse.

Next, refer back to Figure 4.1.2-2. The delayed pulse goes to another comparator where it is compared against a threshold level derived from the demodulator automatic gain control (agc). The comparator determines whether, in fact, a data bit has arrived and enables the output gate of the centroid detector. The reason for this is that, when no data pulses are present, or when the side lobes of the data pulse are present in the delay/comparator network, the centroid detector will be generating spurious pulses at its output. Therefore, a circuit is needed which will determine whether the data bit main lobe is present, by comparing the centroid detector input against a threshold. If the input pulse exceeds the threshold, the network decides that the detector is indeed making a valid decision, and enables the centroid detector output.

The agc is also derived from the summed envelope detector outputs. A sample/hold circuit timed to sample only at the pulse arrival times provides the signal into the agc amplifier. This technique effectively gives the agc system the same antijam protection that the signal itself has. The system is also capable of being preset for a nominal signal level during the initial, controlled phase of acquisition; and is also capable of being held for a time when loss of lock is sensed (check mode), and "opened up" for maximum receiver gain during an operational reacquisition when loss of lock is extensive.

The agc range required for vehicle ranges of 1 to 250 nautical miles is 48 dB. A 55 dB control capability is built into the IF amplifier to allow for incidental variations in received signal strengths. In addition to the agc capability, the IF amplifier will also employ soft limiting and have a logarithmic response near saturation, so that imprecise agc during search, high peak level jamming, or sudden signal level shifts will not result in serious information loss due to long amplifier recovery time.

121
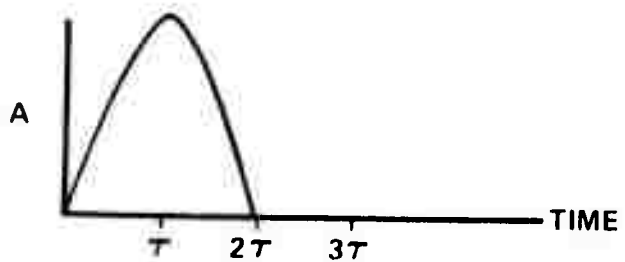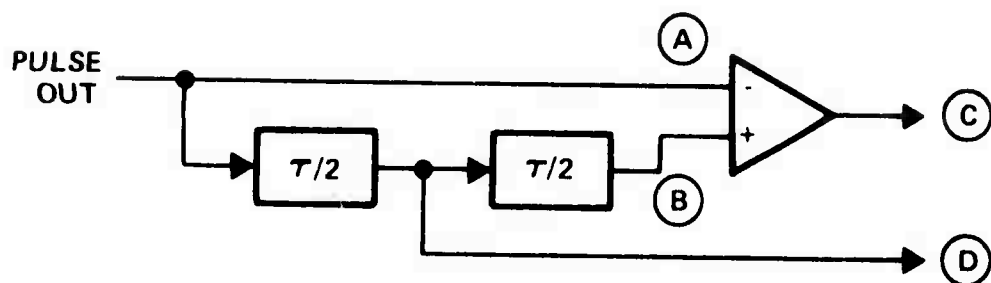
$\tau = \frac{10}{128} \ \mu SEC$
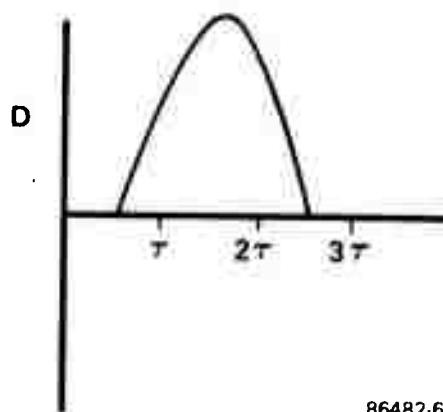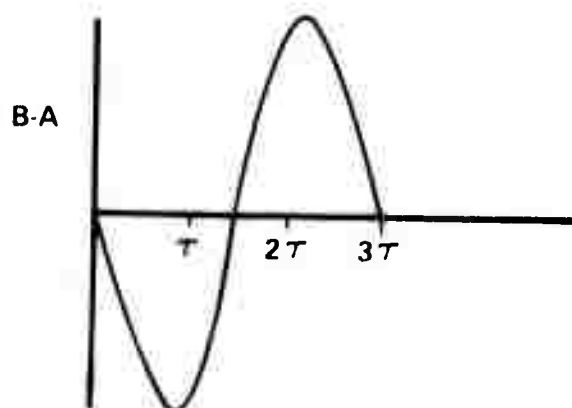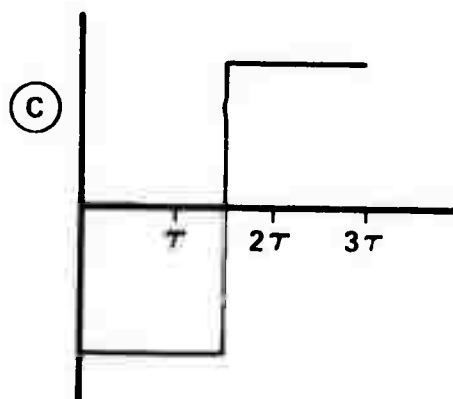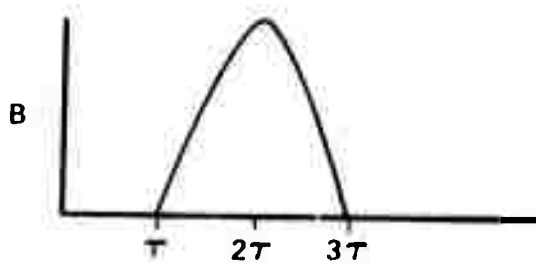
Figure 4.1.2-3.   Centroid Detector Operation

86482-6

The data from the data comparator is clocked by the synchronized demodulator "on-time" signal into the data formatter. The incoming data is detected, formatted, error-corrected, and outputted as a serial bit stream at 2.0 kb/s. Each data bit in the frame is examined with the vehicle number and modularity by the formatter for selecting and storing it in Register A or B. At the end of each frame time, the A and B data words are transferred to a 24-bit input register, which is the error correction input register.

Thus, the modularity is controllable in increments which are divisors of 24, i.e., 1, 2, 3, 4, 6, 8, 12. If 25 vehicles are in use, the modularity is 1, and the formatter duplicates the input bit so that 12 identical A and B bits are transferred. If the modularity is 4, then four bits are sent for each vehicle, and each A and B bit is transferred three times to fill up the register. If only one vehicle is in use (modularity 24), 24 bits are different; and each bit has only one location in the register.

The error correction processor accepts the 24-bit word and converts it to a single bit before routing it to the output buffer. Thus, if the modularity is 1, the processor has only one A and B bit to process through; but if the modularity is, say, 4, then the processor has four independent samples of the data bit and can do additional error correction to increase the processing gain.

The operation of error correction processor, a maximum-likelihood decoder, is typical of others previously built, so it will not be discussed extensively here. However, recall that in the command modulator, every input command data bit resulted in a pair of bits, A and B, at the output of the coder (in fact, the A and B bits do not both describe the same input bit, but rather a linear combination of the input bit and the two previous bits). The decoder, in processing these, can correct some of the errors in the decision process to improve both the communication efficiency of the system and its resistance to jamming.

We have so far discussed the circuitry for detecting the arrival time of the pulse, as well as that for data detection and error correction. Next, we will discuss the comparison circuit, which compares the actual pulse arrival time with that estimated by the vehicle demodulator, and the loop filter which determines the dynamic tracking performance of the loop. These functions are combined in the delay lock loop corrector shown in Figure 4.1.2-4.

The pulse center strobe shown in the center of the figure is the output of the centroid detector discussed previously. This signal is AND'ed with the adaptive window, which, when the demodulator is locked, is a narrow pulse whose time of arrival is the vehicle demodulator estimate of when the received pulse should arrive. The output of the AND gate is then a narrow pulse which is a 0 if the vehicle timing is early, and a 1 if it is late relative to the true arrival time. (Recall that the pulse center strobe from the centroid detector is a signal whose value is 0 until the pulse arrives, at which time it switches to a 1.) This signal becomes the clock for the up/down counter.

The up/down input to the counter is the vehicle estimate of the pulse arrival time. The counter, which counts from 0 to 255, is preset to 128. If the vehicle's pulse arrival time estimate is early, the count signal arrives when the clock has value 0, and the counter will

Figure 4.1.2-4. Delay Lock Loop Corrector

count down by 1. If late, the clock pulse is a 1 and the counter will count up. Suppose that the vehicle timing is lagging. Then, the counter will count up at each pulse until it reaches 255. At this point, it sends a signal to the vehicle clock, causing it to lag in phase by 5 nanoseconds (the operation of the clock will be explained later). At the same time, the counter sends itself a signal to reset to 128, at which time the process repeats. If the demodulator timing now leads the input signal, the counter will count down to 0, direct the demodulator clock to lag in phase by 5 nanoseconds, and reset to 128.

We have just described a first-order loop in which the demodulator clock phase is controlled by an error signal through a time delay - effectively an integrator. However, for tracking when Doppler frequency offsets exist, a second-order loop which also controls clock frequency is highly desirable. This is implemented by the second counter which counts up one increment whenever the phase counter hits maximum, and down one when the phase counter hits minimum. If the demodulator clock frequency is too low, for example, the demodulator phase will consistently lag, and the phase counter will keep hitting its maximum. Each time this happens, the least significant bit increments in the frequency counter. The frequency counter output is a 6-digit word which controls the frequency of the demodulator clock. After 8 successive increments in the LSB's, the MSB increments and causes the clock frequency to change.

We have just described a two-level control: control of clock phase by the error signal through a time delay (integration), and control of clock frequency through another time delay. This forms a second order loop which is capable of tracking Doppler frequency shifts. Note that the frequency counter cannot reset, but must stop when its count reaches either all 1's or all 0's. This sets the tracking range of the loop, and must be designed to cover the full Doppler swing expected. The number of LSB's which must be counted but do not appear in the counter output determines the delay and hence the loop bandwidth. This must be wide enough to track the expected rate of change of Doppler, but narrow enough to provide adequate smoothing (i.e., a low noise bandwidth). The remaining logic elements on the figure determine the width of the adaptive "on-time" window which is explained below.

After the delay lock loop corrector (or comparison network), the next element in the timing loop is the voltage-controlled clock. The clock is implemented by using a synthesizer whose phase and frequency are controlled by the logic signals from the corrector. This synthesizer is shown in Figure 4.1.2-5.

The standard for the synthesizer is a 102.4002 MHz crystal oscillator from which all necessary frequencies are derived. In the normal mode of operation, the oscillator is followed by a divide-by-8 circuit which supplies a 12.800025 MHz signal. Under the direction of the lead/lag signal from the corrector, a pulse swallower can delete or add one sixteenth of a clock period or 4.9 nanoseconds. This is the clock phase control.

The clock frequency control works as follows. The 102.4002 MHz clock is divided by 8 to produce a 12.800025 MHz signal, 25 Hz above the nominal 12.8 MHz clock. The clock is also divided by 2^{19} to produce a (very nearly) 200 Hz signal. This signal goes to the rate multiplier which, when M is 0, deletes no pulses, resulting in the maximum clock frequency of 12.80025. However, when M is 32, 1/8 of the 200 Hz or 25 Hz is deleted, resulting in a 12.8 MHz clock. When M is 64, 50 Hz is deleted, resulting in a clock frequency 25 Hz
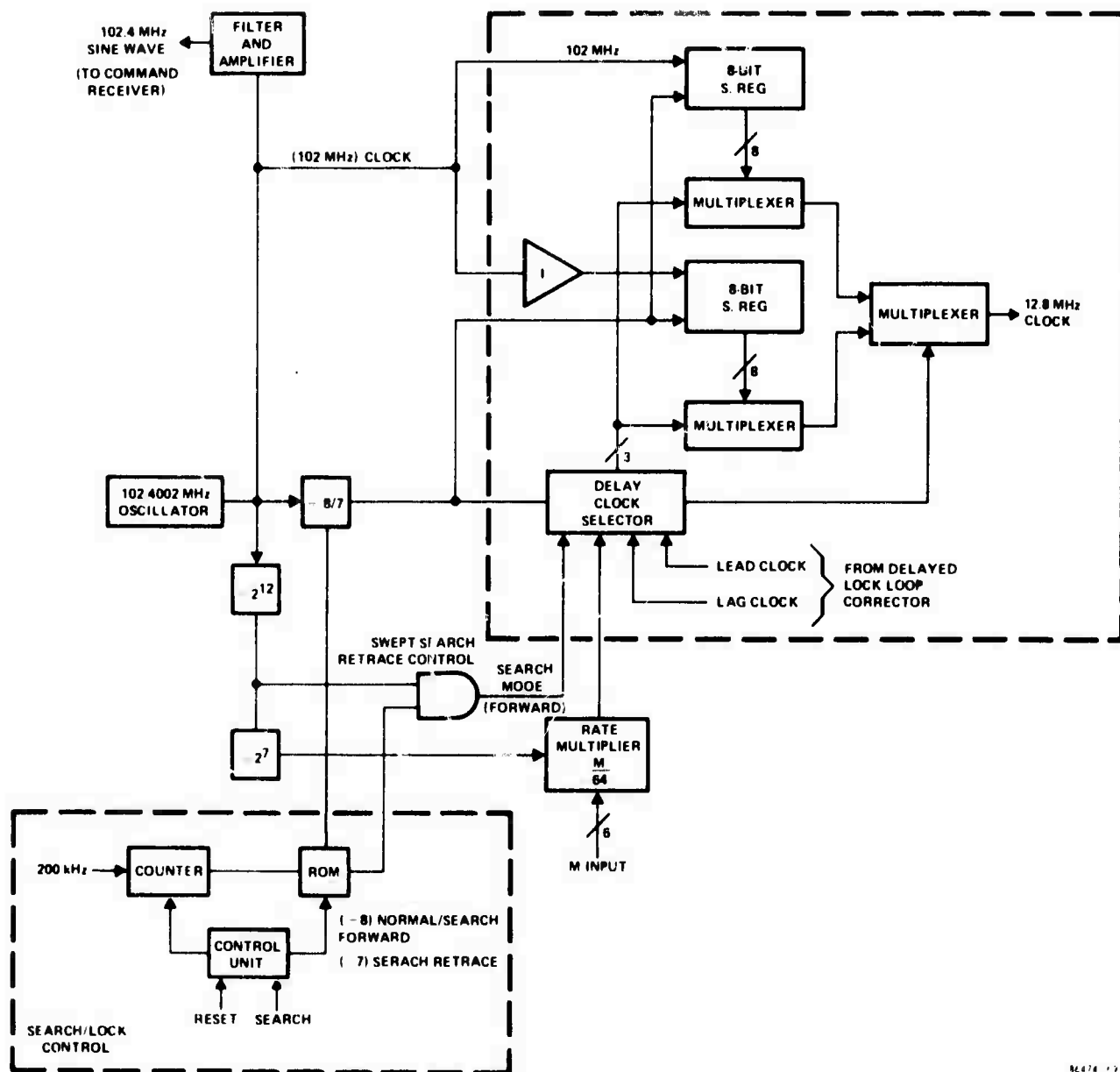
125

Figure 4.1.2-5. Frequency Synthesizer and Search/Lock Control

126

below the nominal 12.8 MHz. Of course, the control is proportional so that each increment of M results in a change of about 25/32 Hz.

The shift registers and multiplexers serve to distribute the deletions uniformly, so that the output frequency is constant when M is constant, rather than having bursts of pulses with empty spaces where deletion occurs. It is now apparent that the basic clock must run higher than the nominal frequency; because the circuitry can only delete pulses, not add them. The clock used in the modulator also runs at 102.4002 MHz, with M set always at 32, and no lead/lag control. This permits using the same design for both systems.

When the demodulator senses that lock has been lost for a long enough time that a frequency sweep is necessary, the search/lock control goes into action. When the control unit senses that search has been initiated, the read-only memory (ROM) begins to control the synthesizer frequency. First, the pulse swallower is made to operate 2^7 times faster by reducing the division ratio from 2^{19} to 2^{12} (the M input from the corrector is ignored). This controls the forward, or search sweep. In the retrace mode, the divide-by-8 circuit is changed to divide-by-7 to provide very fast retrace. The ROM then causes the synthesizer to sweep and retrace in a widening cone of frequencies until acquisition is detected. At that point, the control unit receives a "reset" signal, and clock frequency control is turned back over to the delay lock loop corrector.

Why is this apparently complex approach taken to obtain a voltage-controlled clock when a voltage-controlled crystal oscillator (VCXO) could also be used? The reason is that VCXO's are significantly more expensive than fixed-tuned oscillators having comparable stability; while the synthesizer, which costs more to design initially, can be reproduced at a relatively small cost; because it uses inexpensive logic elements. Also, the capacitors and operational amplifiers needed for the loop filter and amplifier would be bulky because long time constants are needed, are more expensive than digital logic, and are prone to drifting with time and temperature. VCXO's drift also, and their tuning slopes can vary from unit to unit, so that loop gains must be adjusted individually. The net result is more time required for alignment, more frequent alignment, more weight, and higher power consumption. Therefore, the digital synthesizer, while initially a more expensive design, has significant advantages both technically and on a recurring cost basis over the analog filter and VCXO approach.

At this point, it is well to pause and study how the demodulator senses that it is in lock, and what happens when loss of lock is detected. To do this, refer to Figure 4.1.2-6, the phase error detector. The basic criterion for lock is that the demodulator's estimate of the time of arrival of the data pulse, its adaptive window, coincides with the true arrival time, the pulse center strobe from the centroid detector. These two signals are AND'ed in the circuit at the left center of the figure. When they coincide, a "count up" pulse goes to the long-term confidence counter, which saturates after 2^{16} counts. To prevent overflow, a short-term confidence counter sets the counter to 63,000 if the short-term counter detects 2^7 bits in a row received on time.

The four most significant bits from the long-term counter go to the decoder/select gate. If the adaptive window (at its narrowest width at present) begins missing data bits, the short-term counter releases its hold on the confidence counter, which begins counting down at

127
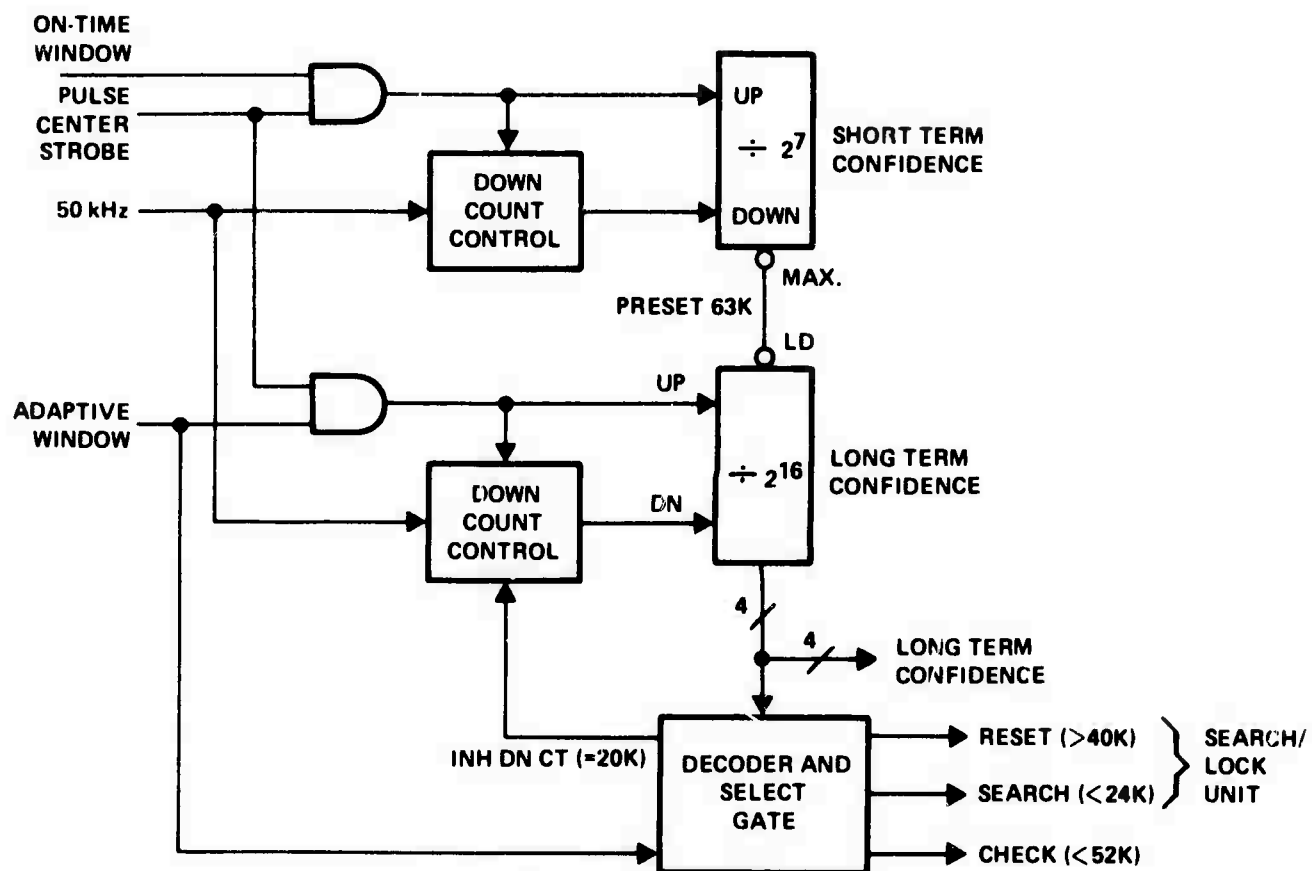
Figure 4.1.2-6. Demodulator Phase Error Detector

128

the 50 kHz clock rate (once for each missed bit). As the confidence falls, the adaptive window starts to increase in width by the ratio $2N+1$, where N is 0 when the confidence is 63,000 and increases by 1 for every 2^{12} or 4096 misses. Finally, when N reaches 5, after 32,758 misses, the adaptive window reaches its maximum width of 1260 nanoseconds. If the misses continue so that the confidence count drops below 24,000, then the search mode is initiated to sweep the frequency synthesizer.

Since the width of the adaptive window should always be kept at the minimum possible so that the maximum jamming protection is realized, it is desirable to collapse the window quickly once acquisition has been accomplished. If we allow the counter to count up normally, it could take over a second at the 50 kilobit rate to collapse the window completely. This problem is circumvented by using the short-term confidence counter, which is counted up by coincidence of the pulse center strobe with the narrow (not adaptive) on-time window. When, as would normally occur, the demodulator locks up such that the timing is nearly exact, the resulting up-counts fill the counter in 128 bits or 2.56 milliseconds. This counter then jams the long-term counter to its maximum 63,000 count to immediately collapse the adaptive window.

The last item of importance in the demodulator loop is the PN generator/format circuit which, clocked by the demodulator clock, generates the various timing functions. This unit is virtually identical to that used in the modulator to generate the gating pulses and the vehicle selection. Figure 4.1.2-7 is a block diagram of the demodulator format counter and decoder.

Consider first the vehicle selection. The PN generator inserts its sequence into the first modulo 25 counter which counts up each 1 at its "D" input. On a signal from the format counter, the second counter is loaded with the number in the first counter, after which the first counter is cleared to begin again. The second counter now counts down at a 100 kHz rate, outputting its count to a comparator (the least significant bit is ignored), which creates a pulse when its two inputs are equal. The other input to the comparator is the actual number of the vehicle, plus other vehicle numbers if the modularity is greater than one. The least significant bit is not sent to the comparator, but rather to an EXCLUSIVE-OR circuit such that the final AND gate is enabled only on every other pulse from the comparator.

As an example, consider that our vehicle number is 4. The comparator output rises whenever a 4 or a 5 comes from the second counter. However, the AND gate output is disabled for the 5 count because the LSB is wrong, and only the 4 count initiates the data strobe. The data strobe, in turn, clocks a flip-flop which gates the data into the decoder shown in Figure 4.1.2-2.

The demodulator window timing is derived just as it is in the modulator. The sequence generator pattern is read into the 8-bit shift register to produce a 7-bit number which identifies the time slot for each data bit. This number, the PN select bit, goes to the delay lock loop corrector shown in Figure 4.1.2-4, where it is used to generate the on-time pulse and the adaptive window. Thus, while only the data for its own number is actually read into the vehicle command decoder, the vehicle loop knows where the data bit for every other vehicle will appear, and uses the data bits for all the even-numbered vehicles (when the demodulator is

129

Figure 4.1.2-7. Demodulator Format Counter and Decoder

130

in an even-numbered vehicle) or vice versa to keep its timing loop in synchronization with the command modulator.

Now we can understand why a delay was required in the vehicle selection in the modulator. After vehicle selection is made, the data pulse must pass through the modulator and then the demodulator delay lines. Then, when the sequence is put into sync in the demodulator, the composite delay is such that the data pulses, which have been delayed, no longer line up properly with the vehicle numbers which have not been delayed. That is, the vehicle number was assigned to a bit before it passes through the delay lines, and is extracted by the demodulator after the delay lines. Therefore, a delay is required in the modulator so that the vehicle number is artificially delayed before it is assigned, and the data bits align correctly with the vehicle numbers after demodulation.

131

4.2   Status Link

The status link is composed of the status modulator in the vehicle and the status demodulator in the master ground station. This link carries the 2-kilobit/second status data from each of up to 25 vehicles in a time-division-multiplex format controlled by the ranging system and the command transmitter. Another demodulator in the slave ground station also receives the PN ranging signal being carried on the status downlink, so that the two independent range readings can be combined for accurate position location. The slave station does not demodulate the status data.
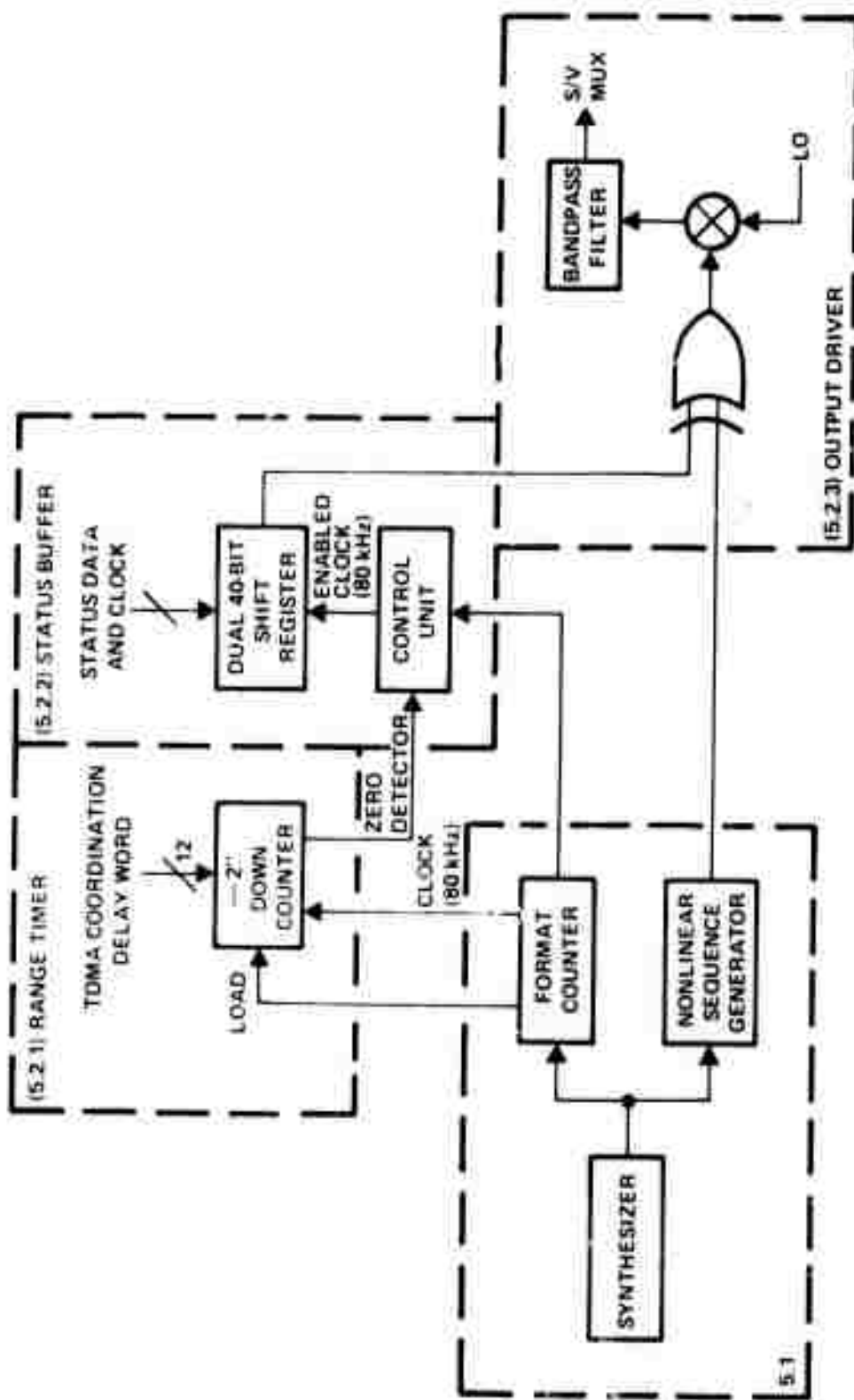
4.2.1   Status Modulator

The status modulator, located in the remote vehicle, receives the vehicle status data, buffers it, and sends it in bursts within the proper time slots as directed by the range word which it receives from the command system. The status data is spread by the same PN sequence which is used in the command demodulator. This spreading provides antijam protection and provides the medium for closing the two-way ranging loop.

Figure 4.2.1 is a simplified block diagram of the status modulator. The 12-bit TDMA coordination word is loaded at the start of a frame into the down-counter, after which it begins counting down at an 80 kHz rate. When the zero count is reached, the status data clock is enabled and the vehicle status data is clocked out in an 80-kilobit/second burst. The status word thus controls the time of transmission relative to the start of the frame, because the size of the status number determines how long it will take the counter to count down to zero. The range word is updated every 20 milliseconds, and the maximum time for the counter to count down (for a range of 250 miles) is 7.5 milliseconds.

When the time slot for the status buffer is enabled by the range timer, the status data signal is formatted into a 44-bit shift register and transferred to the output driver at a burst rate of 80 kilobits/second. The burst is formatted into approximately a 175-microsecond preamble, a 500-microsecond data message, and a 125-microsecond guard time.

In order to spread the output spectrum and provide the necessary range resolution, the status data is combined with the 12.8 MHz PN sequence from the command demodulator in an EXCLUSIVE-OR gate. This gate simply performs a modulo-two addition of the data and the sequence, resulting in a direct-spread 12.8-megabit/second signal. The data and spreading signals are differentially encoded to permit noncoherent detection at the demodulator. The composite data/spreading signal is then biphase modulated on to the 384 MHz carrier, and filtered to prevent interference with the video transmission and command reception.

Note that the synthesizer and sequence generator in Figure 4.2.1 are, in fact, the units used in the command demodulator timing loop. The spreading sequence on the status link is, therefore, time-locked to the PN sequence which controls the format in the command modulator. This time coherence, we will see in the next section, permits accurate ranging.

132

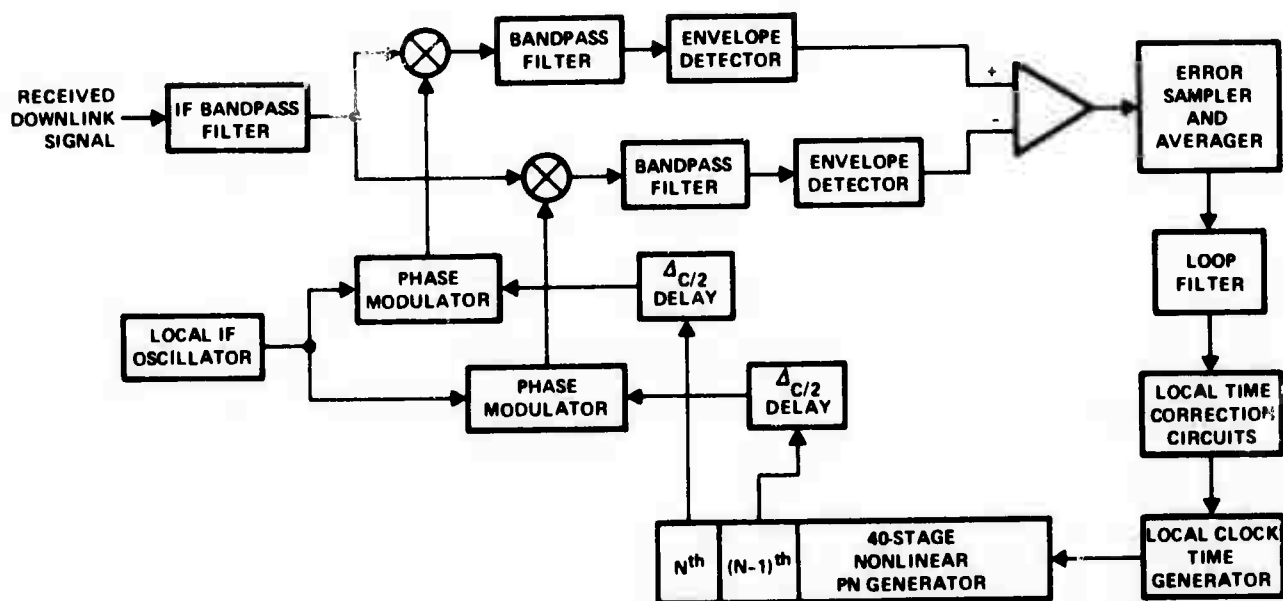Figure 4.2.1. The Status Modulator

133

4.2.2   Status Demodulator

The status demodulator in the ground terminal receives the IF signal modulated and spread by the status modulator, despreads and demodulates, decommutates the TDM-formatted bursts from each vehicle, and provides a 2-kilobit/second status output line for each vehicle. Since the vehicle data bursts are time multiplexed, the master ground station has only to demodulate one data burst at a time; therefore, only one status demodulator is required. However, because all of the spreading sequences will, in general, be far out of alignment with each other because of the large differences in time delays, a separate sequence generator is needed for each vehicle in use. The status demodulator must therefore take the form of a sampled data delay-lock loop (SDDLL), in which up to 25 separate loops are kept locked based on a sampled burst of only 1/25 of the total reception time for each loop.

Figure 4.2.2-1 is a simplified block diagram of the status demodulator timing loop, showing the operation of a single loop. The IF, which has been converted to 76.8 MHz in the status/video demultiplexer, is filtered, amplified, and applied to a pair of balanced mixers used in a dual role as downconverting mixers and biphase demodulators. The local oscillator (LO) signal into these mixers comes from a 51.4 MHz oscillator which has been biphase modulated by the locally generated PN sequence which is identical to that used to spread the signal in the status modulator. The two signals are modulated with a time delay equal to one chip length (where a "chip" is one bit of the 12.8 MHz spreading sequence) between them. The result of the mixing process is a 25.4 MHz second IF, which has had the PN spreading sequence "stripped off" by the identical sequence modulated on to the LO.

If the despreading sequence matches in time to within one chip of the spreading sequence, the spread energy is collapsed and concentrated in the bandpass filters which follow the mixers. The amount of energy is proportional to the closeness of the timing, the energy peaking when the local sequence is exactly aligned with the transmitted sequence. Envelope detectors provide signals proportional to this energy. The envelope detector outputs are applied to a differential amplifier whose output is proportional to the difference in energy between the two channels. Since the amplifier output is zero when the two energies are equal, and since the two channels differ in time by one chip width, for the energies to be equal one channel must be 1/2 chip "early" and the other 1/2 chip "late" relative to the transmitted sequence.

If the timing changes, an error signal whose sign indicates whether the local signal is "early" or "late" appears at the output of the differential amplifier. This error signal is converted to a digital signal to control a synthesizer which works in just the same way as that described in Paragraph 4.1.2 for the command demodulator. The loop thus acts to keep equal energy in the early and late channels, so that they each have a built-in timing error of 1/2 chip. If we now take a third sample of the PN sequence which lies exactly between the other two in time, it will be exactly aligned with the transmitted sequence. We can now use this signal to modulate a third branch of the 51.4 MHz LO (not shown on this figure) and mix that with a third branch of the incoming IF signal (also not shown), to obtain a despread signal having the maximum possible energy.

134

86474-65

Figure 4.2.2-1.   Status Demodulator Timing Loop

135

This is, in fact, what is done; as we can see by referring to Figure 4.2.2-2, which shows one channel of the complete status demodulator. The delay lock loop occupying the central portion of the figure consists of the phase-error detector (the two-channel IF), the sample/hold, MUX, and a/d circuits which provide the digital error signal and permit switching of the control through the twenty-five channels in the proper sequence, the synthesizer and PN generator (of which there are up to twenty-five in the demodulator), and the multiplexers which again select which one of the twenty-five will be programmed into the loop at the proper time.

The top of Figure 4.2.2-2 shows the data demodulator. The data demodulation is done in a noncoherent manner to obviate having to lock a coherent loop each time a new signal is received. The mixer at the top of the figure is driven by the LO which is modulated by the center or "on-time" sample from the PN generator to produce the despread IF signal at the differential phase-shift keyed (DPSK) detector. The DPSK detection can be done in any of several well-known ways, such as by filter/delay/phase detect, or matched filter/detect. The performance of the various approaches is essentially the same, and the method used will be dictated primarily by implementation considerations such as recurring cost, size, weight, and reliability. The data signals are decommutated and supplied as an output using timing generated by the format counters.

Since the efficiency of DPSK detection depends on the frequency accuracy of the IF input signal, and because the vehicles, going at various velocities, will, in general, produce differing IF frequencies into the demodulator, an automatic frequency control loop is desirable for optimum detection efficiency. The loop must operate at sufficient speed to correct almost immediately when a new signal enters the demodulator, but yet the loop bandwidth must be narrow enough that noise does not disturb its operation and, hence, degrade the demodulator performance. This is done by employing a loop which, although having a narrow noise bandwidth, can switch instantaneously to near the proper frequency for each vehicle. This is implemented by employing a digital loop which "remembers" the previous frequency from each vehicle and switches to that frequency at the proper time.

After the data channel is despread, a sample of this IF is taken and doubled, using a full-wave rectifier. The doubled signal has all of the data modulation removed, since the 180-degree phase shifts become 360 degrees, that is, zero, after doubling. This signal goes to a discriminator which is tuned to twice 25.4, or 50.8 MHz. The error signal from the discriminator is converted to a digital signal and stored. Suppose that we have just sampled the signal from vehicle number 1. The next time the signal from vehicle number 1 enters the demodulator, this stored value is recalled and sent to control the frequency of a vco which is, in fact, the 51.4 MHz local oscillator. The resulting IF is now at the proper frequency for optimum demodulation, plus or minus a slight error due to changes in vehicle velocity between samples. Since the vehicle dynamics are limited, the change will not be sufficient to cause significant degradation.

Each of the frequency offsets for up to twenty-five vehicles is stored in this manner, and called up by the proper signal from the format counter. As each vehicle is received, the actual IF is measured by the discriminator, and the value stored in memory is updated. Thus, the AFC loop always runs one sample or 20 microseconds (when all twenty-five vehicles are used)

136

Figure 4.2.2-2. Block Diagram of Status Demodulator

137

behind the actual frequency, but the vehicle velocity and hence the received frequency changes very little in this short interval.

An automatic gain control (agc) is also necessary; because the varying distances and attitudes of the vehicles causes a wide range of received signal levels in the demodulator, leading to saturation of sensitive circuits on high level signals and loss of data on subsequent low-level signals. Rapid level changes are experienced in switching between vehicles, which requires that the agc system work the same way as the AFC system by digitizing, storing, and recalling the proper IF amplifier gain for each vehicle.

During the 40-bit word for a particular vehicle, each bit provides a correction to the particular vehicle agc value. The output of the data detector is sampled and held each bit time, while the summation adder takes 1/16 of the new value and 15/16 of the stored value, converts the new total to a digital number, and stores this corrected value in the scratch pad memory. Each frame, as a particular vehicle is addressed, the agc value is taken from memory, and converted to an an analog agc voltage to use during the 800 microsecond burst window. A preset agc value can be inserted during initial acquisition to set approximately the correct IF gain for the expected signal level.

The sweep mode, acquisition detection, and confidence counters for indicating lock and initiating reacquisition all work in a manner similar to that described in Paragraph 4.1.2, The Command Demodulator.

The PN sequence used to despread the status signal is locked to the sequence generated in the status modulator, which, in turn, comes from the command demodulator and is, therefore, locked to the same sequence which is generated in the command modulator. There exists, therefore, in the ground station, a locally generated sequence in the command modulator and another in the demodulator time-locked to the first through the delays in the various transmitters and receivers and through the link. When the hardware delays have been calibrated out, the two-way range can be determined by measuring the residual delay between the two sequences. The command up-link and down-link thus carry the ranging information as an inherent part of the spectrum spreading.

138

4.3   Video Link

The video link consists of a quadriphase (QPSK) modulator in the vehicle and a coherent QPSK demodulator in the master ground station. Spectrum spreading has not been recommended for the baseline 20 Mb/s link because of the bandwidth limitations; however, a means of obtaining significant processing gains at lower video data rates is outlined.

4.3.1   Video Modulator

A block diagram of the modulator is shown in Figure 4.3.1-1. The input data stream at 20 Mb/s is processed in what amounts to a two-channel time division demultiplexer. The output is two 10-megabit data streams containing the same information as the single 20-megabit data stream. Each data stream is differentially encoded and applied to modulator drivers which convert the standard TTL logic levels to bipolar signals suitable for driving the modulators. The 140.8 MHz carrier input is buffered and split into two orthogonal carriers by means of a 90-degree hybrid.

The modulators are balanced mixers which biphase modulate each of the 140.8 MHz carriers. This results in the phase relationships shown in Figure 4.3.1-2 (a) and (b) (i.e., Carrier A is either at 0 degree for one on Channel A or at 180 degrees for a zero. Similarly, Channel B is at +90° for a one and +270° for a zero). The two biphase carriers are linearly summed resulting in a single quadriphase modulated carrier as shown in Figure 4.3.1-2 (c).

This signal is amplified and supplied to the status/video MUX for up-conversion. A carrier on-off relay allows the carrier to be shut off when no video is being transmitted. This prevents unnecessary interference and intermodulation with other video channels.

Since the QPSK modulator, at any instant, is in one of four possible states, it must be modulated with data having one of four possible states at any instant. This means that two binary data streams are required. The single 20-megabit data stream is converted to two 10-megabit streams by the signal processor shown in Figure 4.3.1-3a. Typical input and output waveshapes are shown in Figure 4.3.1-4a. The processor is simply a time-division multiplexer. Every other input bit is clocked into Channel A and held until the next A clock pulse. Channel B is derived from an identical processor on the alternate bits.

Channels A and B could be passed through a QPSK modem and remultiplexed into a single 20-megabit data channel. The multiplexing circuitry required is shown in Figure 4.3.1-4b. Note that if the channels are switched (Channel X's data on Channel Y and vice versa) the output data is still correct but delayed one bit. This is also true if the clock is inverted.

Unfortunately, the QPSK demodulator arbitrarily references to any of the four possible phases of the QPSK modulated input signal. This means that the data on Channels X and Y may be switched as shown in Figure 4.3.1-4b, or that the data on either or both channels may be inverted.

139

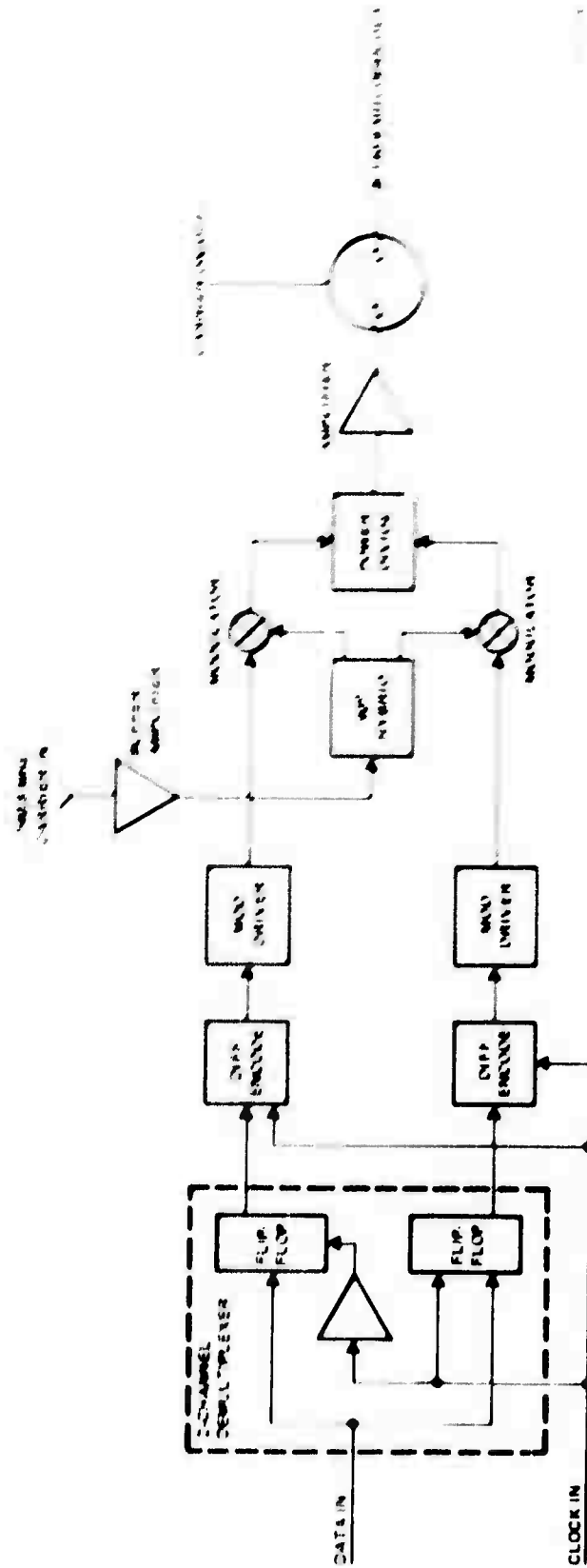Figure 4.3.1-1. Block Diagram of OPSK Modulator

(a) CARRIER A (b) CARRIER B (c) CARRIER A + CARRIER B
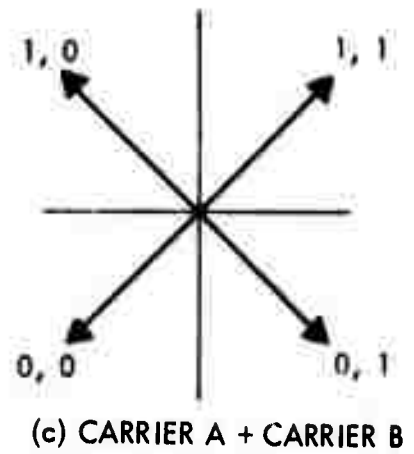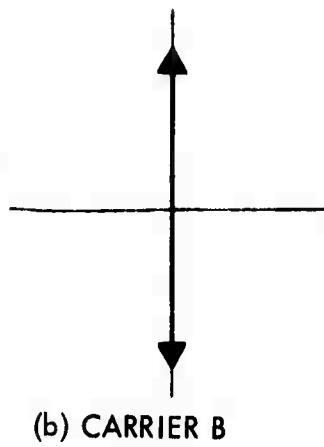
Figure 4.3.1-2. QPSK Phase Relationships

FLIP-FLOP

CHANNEL A

DATA IN

A. MODULATOR
   PROCESSOR

CLOCK IN

CHANNEL B

FLIP-FLOP

CHANNEL X

B. DEMODULATOR
   PROCESSOR

DATA OUT

CHANNEL Y

CLOCK IN
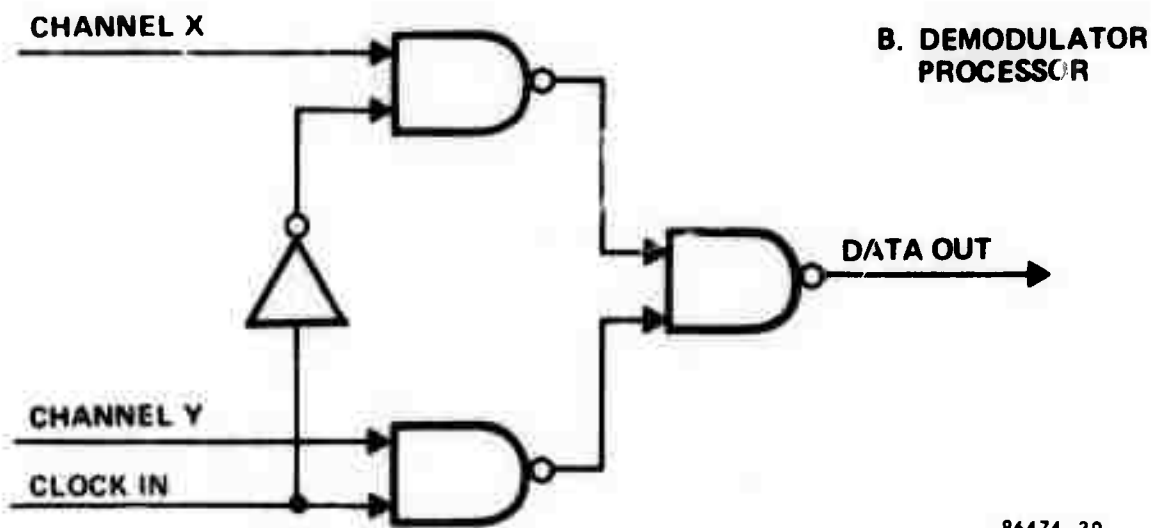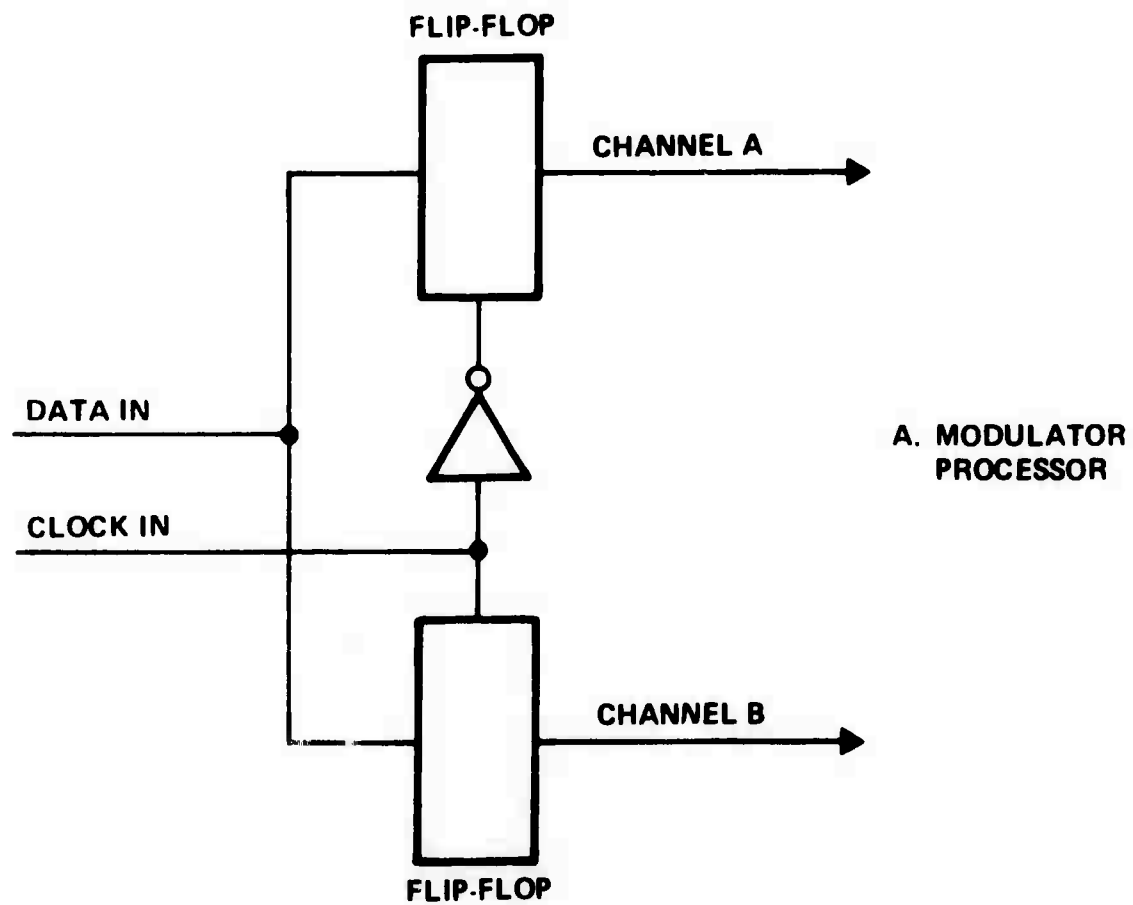
86474-39

Figure 4.3.1-3.   Signal Processors

142
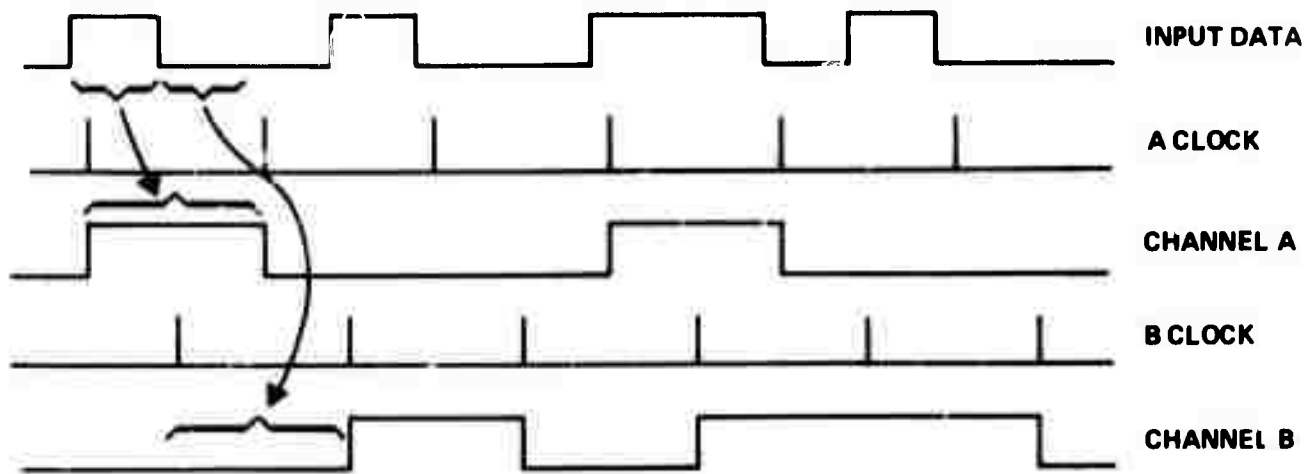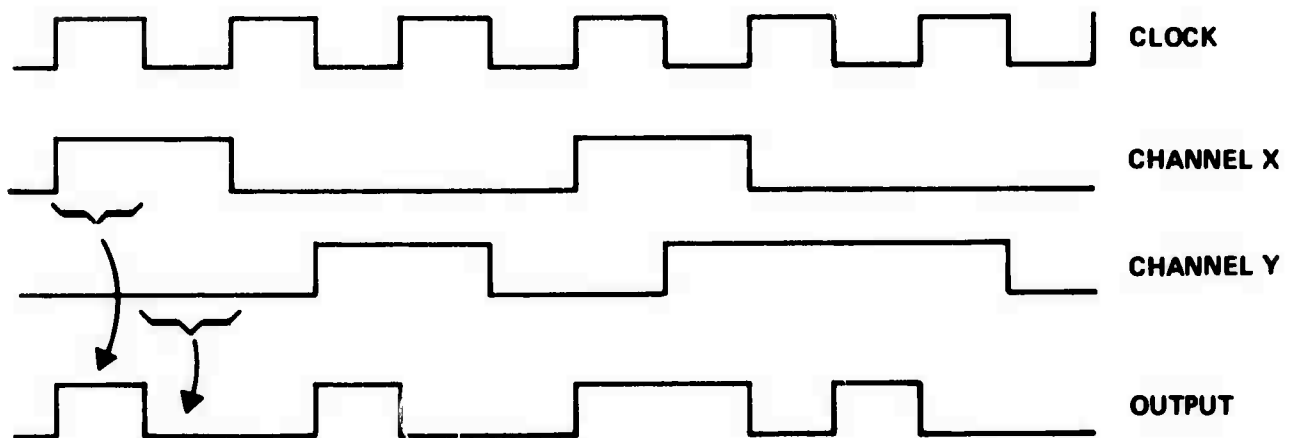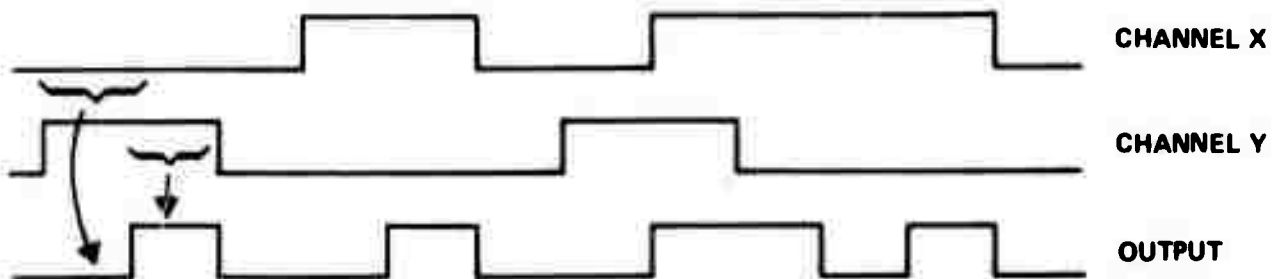
Figure 4.3.1-4. Data Waveshapes

143

The case for switched, but not inverted, data was shown in Figure 4.3.1-4 (c) to cause only a 1-bit delay in the data. However, if either or both channels are inverted, the output data is incorrect. To prevent inversion of data, both channels are differentially encoded prior to modulation and differentially decoded after modulation as shown in Figure 4.3.1-5. This completely resolves the ambiguity resulting in an output signal identical to the input signal.

4.3.2   Video Demodulator

The video demodulator separates, by means of a bandpass filter, the QPSK spectrum centered at 76.8 MHz from the other QPSK spectra; applies agc to provide a constant output over 48 dB variation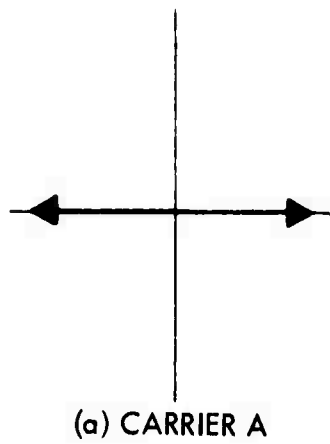 in signal level; demodulates the QPSK signal outputting two data streams; synchronizes a clock to the bit transitions; optimally filters the data streams with matched filters; differentially decodes the data streams; and multiplexes the two 10 Mb/s data streams into a single 20 Mb/s data stream which, along with modulator encoding, resolves the demodulator phase ambiguity resulting in a single 20 Mb/s output with the same polarity as the input data.

A functional block diagram of the demodulator is shown in Figure 4.3.2. The 76.8 MHz quadriphase modulated input signal is amplified to establish the noise figure at less than 10 dB and provides buffering for the bandpass filter. The predetection filter is a 4-pole .1 dB ripple Chebychev with bandwidth of 20 MHz. Its purpose is to separate the desired 76.8 MHz spectrum from other QPSK modulated video channels.

A PIN diode variable attenuator provides 48 dB of variable attenuation (i.e., the input level varies between 0 dBm and -48 dBm while the output remains at approximately -50 dBm). An amplifier following the VGA provides 50 dB of gain, increasing the signal to a level compatible with the agc detector. The detector and loop amplifier provide a control signal to the VGA.

The agc'd signal is applied through a power divider to a frequency multiplier (X4). This removes the modulation, outputting an unmodulated signal at 307.2 MHz which is coherent with the input. The 4 MHz bandpass filter removes unwanted harmonics and improves the signal-to-noise ratio into the carrier-tracking phase-lock loop.

The 307.2 MHz signal is applied to the phase detector of a phase-locked loop consisting of the phase detector itself, loop filter, vco operating at 76.8 MHz, and a frequency multiplier (identical to that in the signal path). The output of the frequency multiplier at 307.2 MHz is locked to the 307.2 MHz input causing the vco output at 76.8 MHz to be coherent with the 76.8 MHz quadriphase input.

The 307.2 MHz signal and the 307.2 MHz quadrupled vco output are applied to a coherent amplitude detector. A phase adjust network permits the phase between the two signals to be set to 0 degree. The resulting output (dc proportional to signal level plus noise) is filtered to remove the noise and applied to a threshold detector. When the loop is in lock, the dc level exceeds the threshold and drives an indicator.

144
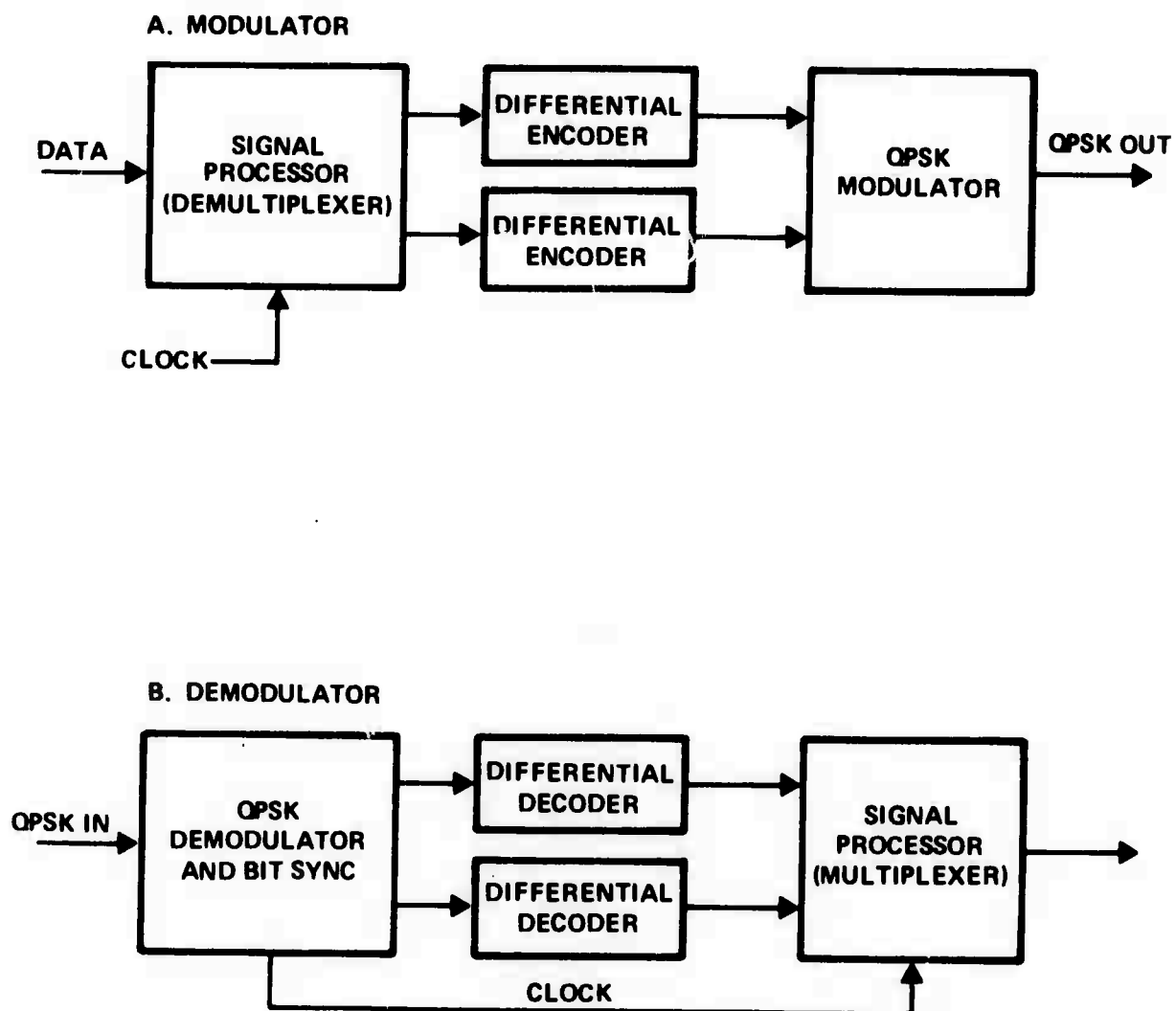
Figure 4.3.1-5. QPSK Modem with Ambiguity Resolution

Figure 4.3.2. Block Diagram of QPSK Demodulator

i46

The vco output at 76.8 MHz is coherent with the input signal. It is applied through a phase adjust network to a 90-degree hybrid where it is split into two signals in quadrature. These signals are applied to the reference ports of the data detectors (balanced modulators). The quadriphase modulated signal is applied through a power divider to both reference ports of the data detectors. The data detector outputs (10 megabits data and noise) are amplified and applied to the bit sync and matched filter circuitry.

The data outputs are applied to zero crossing detectors which convert the bipolar data to logic levels. The two outputs are exclusive OR'ed providing an output which has a transition when either input has a transition. This doubles the number of transitions available to the bit synchronizer.

A digital phase detector is used to generate an error signal which is amplified, filtered and applied to a VCXO, with the center frequency of 20 MHz. The 20 MHz VCXO output is applied to the phase detector as a reference completing the loop. The loop locks to the bit transitions generating a square-wave clock synchronous with the data. The 20 MHz is also frequency divided by two and applied to a clock to the output multiplexer, and the matched filters, which are conventional integrate-and-dump circuits. Both matched filter outputs are differentially decoded and multiplexed to provide a single 20 megabit data stream identical (except for errors due to noise) to that applied to the modulator.

4.3.3   Spread Spectrum Option

This option would, without altering the capability to transmit and receive 20-megabit QPSK, add the capability of reducing the data rate (say to 1 megabit) and QPSK-spread the spectrum to 20 megabits. The demodulator would be capable of despreading the spectrum and demodulating the 1-megabit QPSK data. This option has the advantage of adding a minimum of equipment to the modulator in the vehicle (a PN generator and two EXCLUSIVE-OR circuits). However, the complexity of the ground receiver is increased in order to provide the improved performance at the lower data rate. A block diagram of the proposed system is shown in Figure 4.3.3.

A 20-megabit PN sequence is generated and separated into two 10-megabit PN sequences which are EXCLUSIVE-OR'ed with the data. This spreads the 1-megabit input data with 20 megabits QPSK. The signal processing circuitry, differential encoders, and QPSK modulator remain unchanged. A spreader on-off switch would feed a "1" logic level to both exclusive OR's in the spreader-off mode. The 20-megabit QPSK demodulator and bit sync would remain unchanged except for replacing the 3-way power divider following the agc circuitry with a 4-way divider.

The agc'd spread spectrum QPSK signal tapped off the power divider is fed to a delay lock receiver where it is despread and downconverted to a 20 MHz carrier. The delay lock receiver provides an error signal to a vco which, in turn, clocks a PN generator identical to the modulator PN generator. The PN generator feeds the delay lock receiver with the PN code required for despreading the spectrum. The output is a 20 MHz carrier modulated with

147
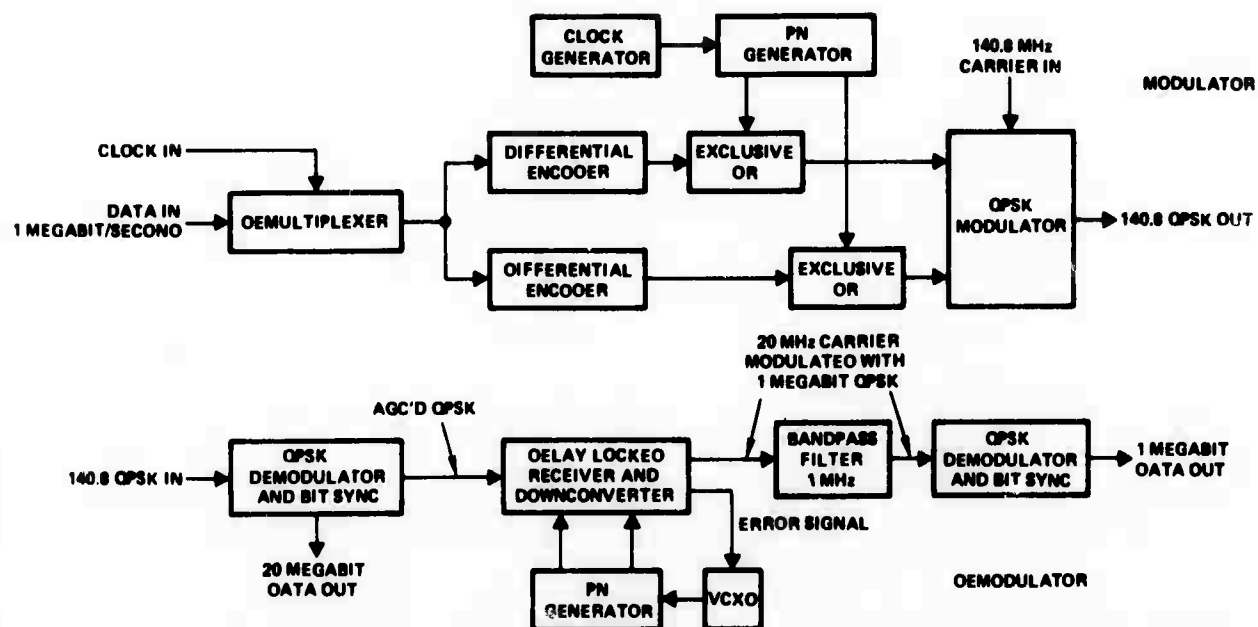
Figure 4.3.3. Video Modem with Spread Spectrum

148

1 megabit QPSK data with noise and/or jamming signals spread over a 20 MHz bandwidth. This signal is passed through a 1 MHz filter to remove noise and jamming. The filtered signal is demodulated with a QPSK demodulator and bit sync. The functional block diagram of the demodulator and bit sync is identical to that of the 20 megabit demodulator with the agc circuitry excluded.

SECTION 5.0

RF CONFIGURATION

150

5.0   RF CONFIGURATION

This section identifies a design approach to implement the baseline design at C-band. The RF circuits for the RPV and ground station are blocked out and specifications for the individual blocks are identified. In addition, a block diagram description of the circuit and the mechanical characteristics of the hardware are provided.

Figure 5.0 depicts the RF frequency assignments in C-band for the Wideband Modem command, status and video signals.

The frequency plan chosen is derived from several factors.

● Implementation within a 500 MHz bandwidth

● Waveform bandwidth requirements dictated by system design analysis

● Practical considerations related to design economy

5.1   RPV RF Design

The RPV RF circuitry consists of six basic modules which are identified in the simplified block diagram of Figure 5.1-1. This division of modules is made on the basis of the functions performed and practical integration of the associated RF hardware components. Each module is described in the following discussion and specifications identified to define the module performance requirements.

Diplexer Module

The Diplexer Module functions to isolate the transmit and receive channels to enable simultaneous operation and to discriminate against undesired signals, noise and spectral spillover resulting from the transmitter saturated power amplifier. It also limits the receiver local oscillator reradiation level and suppresses the transmitter harmonics consistent with the EMI requirement of MIL-STD-461.

The Diplexer Module is fabricated in a waveguide structure to achieve the high Q required for low loss in the filters. The module is essentially a 6-pole bandpass filter in the receive path and a 9-pole bandpass filter with a low-pass section in the transmit path. The design parameters for the Diplexer Module are summarized in Table 5.1-1.

151

COMMAND

4917.6 MHz

87037-8

64 MHz

STATUS

4684.8 MHz

FREQUENCY IN MHz

25.6 MHz

4620.8 MHz

VIDEO CHANNEL 5

VIDEO CHANNEL 4

VIDEO CHANNEL 3

4518.4 MHz

VIDEO CHANNEL 2

VIDEO CHANNEL 1
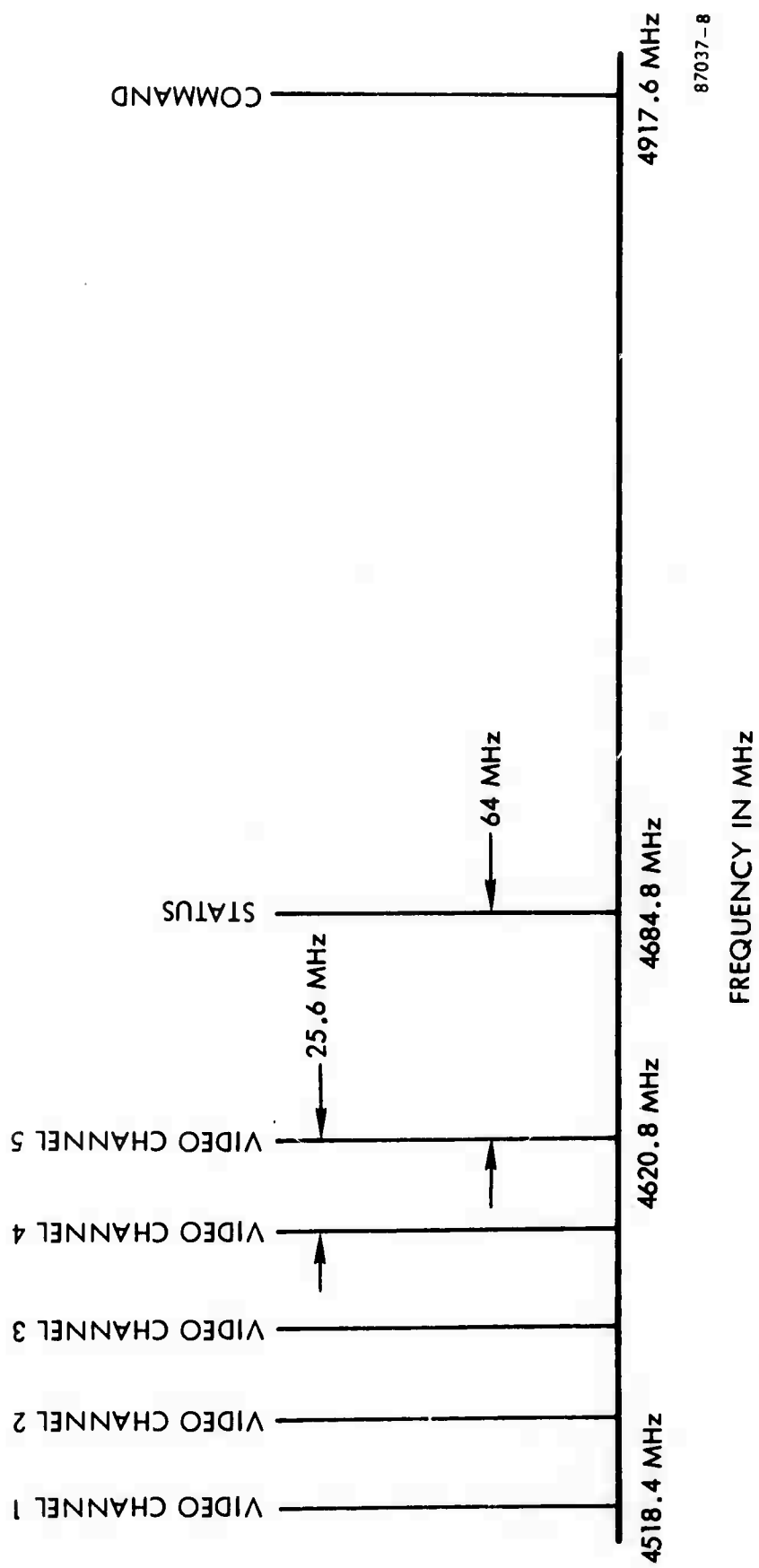
Figure 5.0.   Wideband Modem C-Band Frequency Plan

152
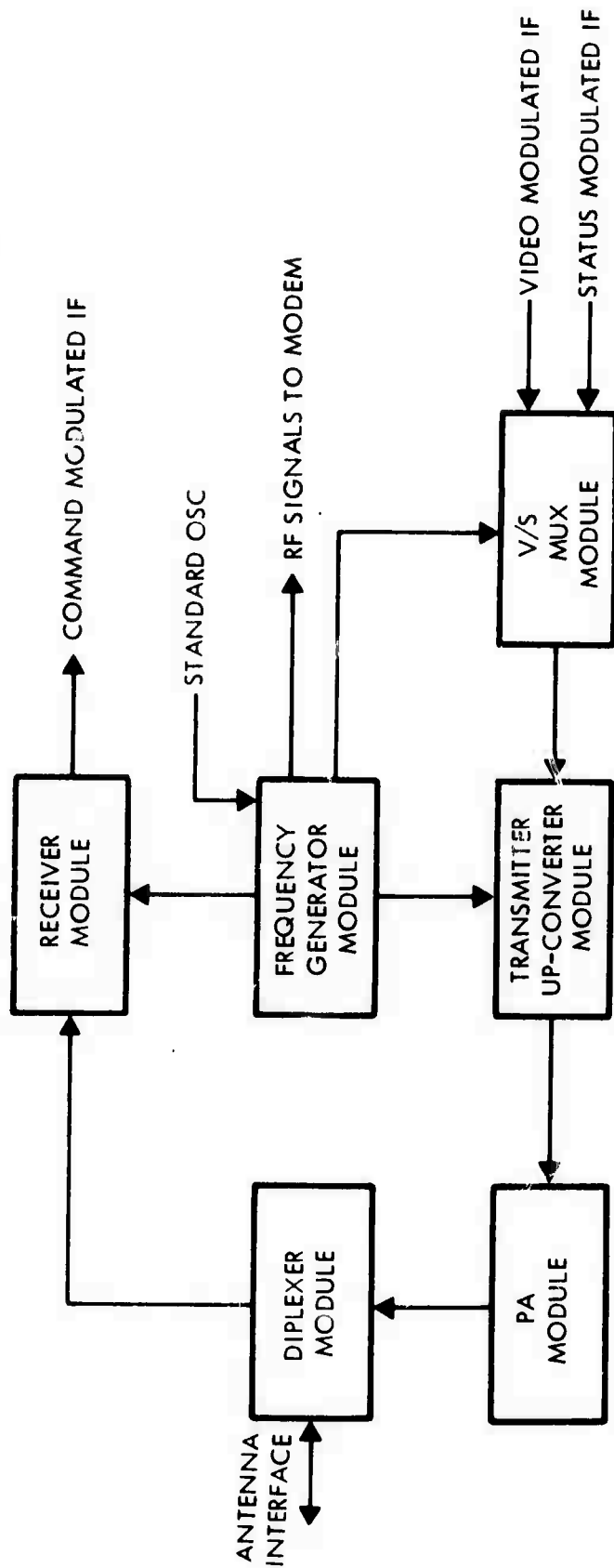
Figure 5.1-1. Simplified Block Diagram of RPV RF Circuitry

153

Table 5.1-1.   Diplexer Design Parameters

Receive Bandwidth	4867.6-4967.6 MHz
Transmit Bandwidth:	4492.8-4723.2 MHz
Insertion Loss	
Antenna to Receive:	1 dB maximum
Transmitter to Antenna:	1 dB maximum
VSWR (50 ohm system):	1.4:1 maximum
Transmitter Power:	+13 dBw maximum
Rejection	
Receiver Local Oscillator:	>75 dB
Receiver Image Frequency:	>75 dB
Transmitter Harmonics:	>42 dB
Spectral Spillover:	90 dB
Transmit/Receive Isolation:	80 dB
Amplitude Response:	±0.5 dB
Phase Linearity	< ±10° over any 50 MHz bandwidth

154

Receiver Module

The Receiver Module circuitry is blocked out in the RPV block diagram shown in Figure 5.1-?. This module established the RPV receiver noise figure and functions to downconvert the receiver TDMA/Chirp command signals from RF to IF frequencies in two conversions. The modules also contain the X5 multiplier required to generate the first converter local oscillator frequency.

The time-division multiplexed chirp command link signal is received at 4917.6 MHz and directed to the Receiver Module via the Diplexer. The signal is downconverted to a first IF of 458.4 MHz and amplified by 15 dB in the IF preamplifier. At this point, the signals are filtered in a 5-pole 0.1 dB Chebychev filter which discriminates against the undesired signals resulting from the conversion and further suppresses the undesirable transmitter signal products. The command signal is then further amplified and downconverted to an IF frequency of 100 MHz prior to coupling to the Command Demodulator. The receiver gain is set to provide a signal to the Command Demodulator 20 dB above the thermal noise level of the demodulator. It is further between the two amplifiers in the Receiver Module consistent with design economy. The first amplifier gain establishes the RPV receiver noise figure and is optimized for its noise performance; the second is optimized for its dynamic range performance. The receiver requires no AGC and will handle input signals up to -30 dBm. The specifications for the Receiver Module are identified in Table 5.1-2.

Table 5.1-2.   Receiver Module Specifications

Input RF Bandwidth:	4867.6-4967.6 MHz
Output IF Bandwidth:	50-150 MHz
Gain (RF to IF):	20 dB
Noise Figure:	8.5 dB
VSWR (50-ohm system):	1.3:1 (RF in) 1.5:1 (IF out)
Maximum Input Level:	-30 dBm
Transmitter Rejection: (4518.4-4684.8 MHz):	> 50 dB
Phase Linearity:	$< \pm 10^\circ$
Amplitude Response:	± 0.5 dB

155

Figure 5.1-2. Detailed Block Diagram of RPV RF Modules

Status/Video Multiplexer

Figure 5.1-2 shows the block diagram of the S/V MUX. The unit interfaces between the Status and Video Modulators and the Transmitter's up-converter. It frequency division multiplexes the status and video signals which are transmitted from a common power amplifier when the RPV is transmitting video data. When no video data is commanded, the status signal is routed through the unit in exactly the same manner. The status and video data are always modulated at independent fixed frequency IF carriers to simplify the modulator. The video modulated IF signal is converted to one of five remotely programmable video channels and combined with the status modulated IF signal into a single output from the S/V MUX unit.

The frequency assignment for the status and video signals results from system requirements and hardware implementation considerations. System analysis of cochannel interference identified the requirements for 25 MHz video channel separation and 60 MHz status/video channel separation. Hardware implementation, considering design economy, simplicity, RF and modem interfaces, resulted in the frequency allocations shown previously in Figure 2.5-4 for the status and video signals. This assignment is consistent with the RF translation strategy for converting to C-band operation as required.

Referring to Figure 5.1-2, the status modulated 384 MHz signal from the Status Modulator is fed directly to a signal combiner through a variable attenuator. The attenuator functions as a level adjustment for proper signal leveling at the power amplifier output. The attenuator is a "tee" configuration employing pin diodes and adjustable over a 30 dB range. In operation, the status signal will nominally be attenuated below the video by 12 dB to maintain the desired power sharing.

The video modulated 140.8 MHz signal from the Video Modulator unit is directed to a balanced mixer via a variable attenuator identical to that in the status channel. This attenuator will control the power level of the video transmission and provide an additional degree of freedom to minimize effects of power amplifier nonlinearity, if desired. When the RPV is commanded to transmit video, a video channel will also be assigned by the ground station. This command is used to select one of five comb-line frequencies for the local oscillator signal to the mixer which up-converts the 140.8 MHz video modulated signal to the desired video channel. The filtered output is then connected to the signal combiner which provides the desired FDM output.

The comb-line generator operates from a 25.6 MHz source derived from the RPV's stable clock. The amplifier provides 27 dB gain and drives a Step Recovery Diode (SRD) to generate the 25.6 MHz comb lines. The third through seventh lines (76.8 MHz, 102.4 MHz, 128.0 MHz, 153.6 MHz and 179.2 MHz) are used to translate the 140.8 MHz video signal to the five video channels. The following filter bank consists of five filters, one of which is selected by the video channel command, to couple the desired comb line to the mixer and provide 60 dB rejection to the undesired comb lines. The bandpass filter following the mixer is required to suppress the undesired mixer products.

157

An alternate approach, using an indirect digital synthesizer, was considered. However, the comb-line generator approach was selected as the most cost-effective method to generate the one of five frequencies required for the video channels.

Table 5.1-3 identifies the S/V MUX module characteristics.

Table 5.1-3.   S/V MUX Module Characteristics

Input

Bandwidth	Status: 384 MHz ±50 MHz
	Video: 140.8 MHz ±25 MHz
Level	-10 dBm
Impedance	50 ohms 1.5:1 VSWR

Output

Bandwidth	192-434 MHz
Level	Status: -30 dBm
	Video: -42 dBm
Impedance	50 ohm 1.5:1 VSWR
Spurious Level	60 dB below signal

Transmitter Up-Converter Module

The Transmitter Up-Converter Module translates the frequency division multiplexed status and video modulated IF signals to RF frequencies at C-band. The translation is accomplished in two conversions to simplify the filtering and amplification processes.

Referring to the block diagram of Figure 5.1-2, the status and video IF signals are fed to the Transmitter Up-Converter Module from the Status/Video MUX Module at 217.6-384 MHz. The signals are amplified by 20 dB and coupled to the first up-converter. The gain distribution philosophy is to provide as much gain at the lowest frequency consistent with the mixer intermod performance.

In the first up-converter, the Status and Video signals are translated to an intermediate frequency in the 1267.2 to 1497.6 MHz bandwidth. The signals are then filtered in the 5-pole, 0.1 dB Chebychev filter to reject the unwanted image and local oscillator signal by 70 dB and then amplified prior to the second conversion. The second converter translates these signals to the desired C-band frequencies in the 4492.8 to 4723.2 MHz range. After filtering

158

in the 4-pole, 0.1 dB Chebychev filter, the signals are then coupled to the Transmitter Power Amplifier Module. All spurious signals are 60 dB below the desired output. Attenuator pads between the mixers and bandpass filters are added to provide a broadband termination at the mixer ports for improved mixer intermod and spur performance. The transmitter up-converter specifications are summarized in Table 5.1-4.

Table 5.1-4.   Transmitter Up-Converter Specification

Input Bandwidth:	217.6-384 MHz
Input Level:	-30 dBm maximum
Gain (IF to RF):	10 dB minimum
C/N_0	-95 dBm/Hz
Output Bandwidth:	4518.4-4684.8 MHz
Spurious Level:	>60 dB below signal
VSWR (50-ohm system)	
Input IF:	1.5:1
Output RF:	1.3:1
Amplitude Response:	±0.5 dB
Phase Linearity:	$< \pm 10^\circ$

Transmit Power Amplifier Assembly

For continuous wave wide bandwidth microwave communications transmit requirements, the silicon planar N-P-N Bipolar Transistor and the IMPATT Diode are the active solid-state power sources available for serious consideration at this time. CW power output, efficiency, cost and the requirement to amplify wide bandwidth communications signals limits the list of available active solid-state devices to the two listed above. These devices have been significantly improved over the last few years and with the future improvements, as predicted by S. Kakihana,[1] aerospace communications transmitters giving 10 watts linear output through 12 GHz can be expected in the near future. Further in the future, the GaAs and silicon MESFET technology now developing is expected to have a profound effect on microwave power generation, overshadowing the silicon bipolar and the silicon and GaAs IMPATT diodes in the microwave range.

---

[1] Microwave Transistors, Bipolar and Filed Effect - Today and Tomorrow, S. Kakihana, 1972 PGMTT Conference

159

For the RPV 10-watt linear transmit requirement, based on the current technology growth rate, it is assumed that silicon bipolar transistor chips with 2.5 watts linear power output at 4 dB gain (1 dB compressed) will be available in production quantities when required. Using this power device and other high quality lower power devices, two amplifier block diagrams have been configured to meet the RPV transmit requirements. A two module cascade assembly is envisioned for the transmit power amplifier: 1) a Low Power Module will provide 45 dB of linear gain with less than 1.0 dB of gain compression at +25 dBm output power, 2) a High Power Module will deliver the required +40 dBm output power with 15 dB gain. Figure 5.1-3A is a block diagram of the Low Power Module configured with 5 stages using presently available high performance microwave transistors. The indicated power levels are for the +40 dBm transmit case. This module will dissipate approximately 2 watts of supply power.

Figure 5.1-3B is a suggested configuration, for the companion High Power Module, using 6 transistor chips in a hybrid coupled circuit driven by a single gain stage. This configuration is approximately one to two years ahead of the state-of-the-art for 10-watt linear output power at 4.5 GHz. A 60-watt dc power input for 15 dB gain and +40 dBm output is estimated. A power output of between 2 to 3 watts could be expected using currently available state-of-the-art devices in this configuration. Linear output at 10 watts may be presently obtainable using a much larger quantity of transistors in a more complicated power combining configuration.

A High Power Module using three IMPATT diode amplifiers is configured in Figure 5.1-3C. While this amplifier has one-half the efficiency of its transistor equivalent at 4.5 GHz, it will be the selected approach in the near future at the higher microwave frequencies because of the rapid degradation of the silicon bipolar transistor with increasing frequency.

The following specifications (Table 5.1-5) are for the overall transmit power amplifier assembly consisting of the Low Power Module and the High Power Module.

Frequency Generator Module

The Frequency Generator Module functions to generate the required IF and RF signals in the RPV. The frequency plan chosen enables all the required signals to be synthesized from a single stable oscillator in the vehicle. This reference oscillator operates at 102.4002 MHz. This frequency was selected to satisfy the clock requirements for the digital portion of the modem. The module block diagram is shown in Figure 5.1-2.

The 102.4 MHz reference is first divided to obtain outputs at 51.2 MHz, 25.6 MHz and 12.8 MHz. The 51.2 MHz output is then multiplied by 7 to obtain 358.4 MHz. A 3 dB hybrid splits this signal, providing a +10 dBm signal for the receiver second converter local oscillator. The other output from the hybrid is coupled to a times three multiplier to obtain the 1075.2 MHz signal source required for the local oscillator drive to the first converter in the transmitter up-converter module and the input to the times three and times five multipliers in the Transmitter Up-Converter and Receiver Modules for generation of the respective local oscillator signals. The 1075.2 MHz signals are isolated by the three-way power divider in the Transmitter Up-Converter Module.
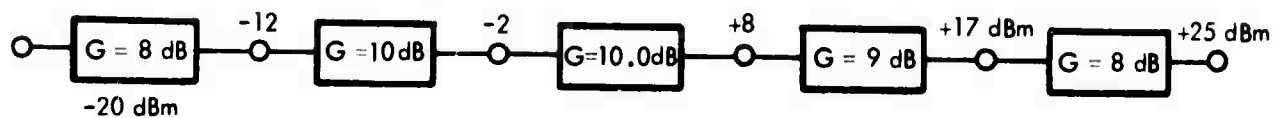
160

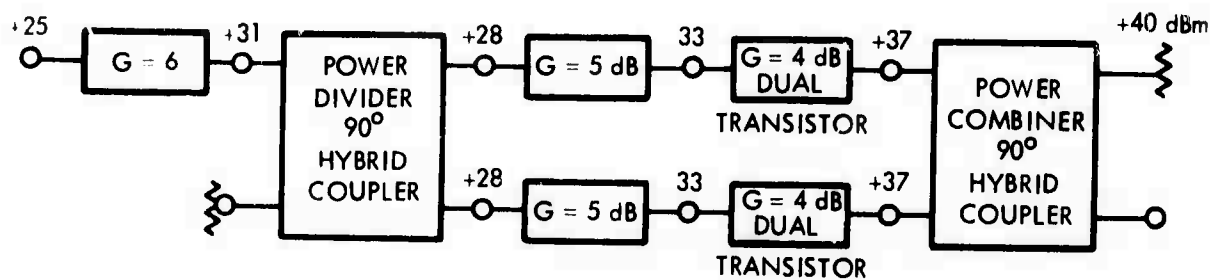Figure 5.1-3A. Low Power Module Using Present Available Hardware

Figure 5.1-3B. Low Power Module for 1975-1980 Time Frame
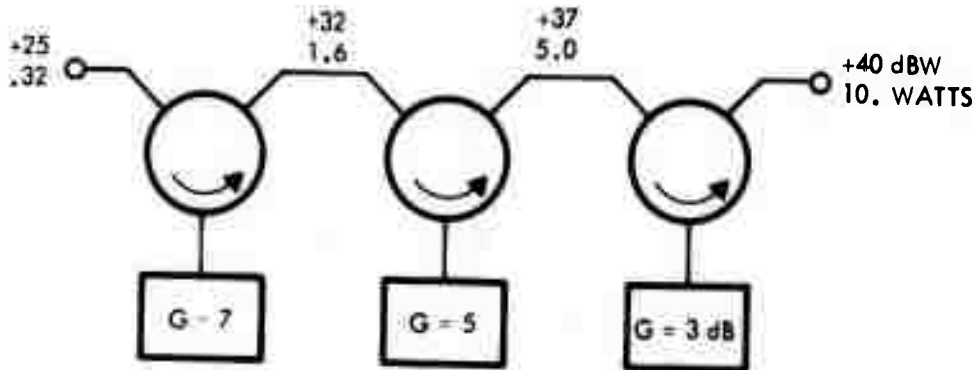
87037-5

Figure 5.1-3C. High Power Module

161

Table 5.1-5. Power Amplifier Specifications

Power Output:	+40 dBm minimum (saturated)
Frequency Range:	4500 MHz-4700 MHz
Gain (small signal):	66 dB maximum
Gain (+40 dBm output):	60 dB minimum
Gain Compression Characteristics:	Smooth decreasing function up to +40 dBm output
Gain Flatness:	±0.5 dB
Phase Linearity:	±5° (each band) maximum
Input VSWR:	1.3:1
Output VSWR:	1.3:1
Input Power DC (maximum):	70 watts
Heat Transfer Surface:	70° C maximum/-20° C minimum

The 25.6 MHz output is multiplied by fifteen by the cascaded times three and times five multipliers to obtain the 384 MHz IF carrier for the status modulator. A 25.6 MHz output is also coupled to the comb-line generator in the Status Video Multiplex Module. The 12.8 MHz signal is multiplied by eleven to obtain the 140.8 MHz IF carrier for the video modulator. The specifications for this module are indicated in Table 5.1-6.

Mechanical Characteristics

The RPV RF circuitry with the exception of the Diplexer Module can be designed using Hybrid and Microwave integrated circuits to minimize size and weight. The module design, as indicated by the heavy dashed outlines in the block diagram of Figure 5.1-2, represents a practical grouping of the circuits from a packaging viewpoint.

162

Table 5.1-6.   Frequency Generator Module Specifications

Input Frequency:	102.4002 MHz
Level:	T^2L Compatible
Frequency Stability:	$\pm 1 \times 10^{-7}$
Frequency Accuracy:	$\pm 1 \times 10^{-7}$
Short-Term Stability:	$\pm 1 \times 10^{-9}$
VSWR	1.5:1
Outputs:	
Frequency 1	25.6 MHz
Level	0 dBm
Frequency 2	140.8 MHz
Level	0 dBm
Frequency 3	358.4 MHz
Level	+10 dBm
Frequency 4	384 MHz
Level	0 dBm
Frequency 5	1075.2 MHz
Level	+15 dBm
VSWR:	1.5:1

Ground Modem RF Design

The RF portion of the Ground Modem consists of seven basic modules which are identified in the simplified block diagram of Figure 5.2-1. The following discussion describes each module and identifies the specifications which defines the module performance.

Diplexer Module

The diplexer module in the ground modem performs the same functions os the RPV diplexer. The primary difference is the higher transmitter power in the ground station. Since receiver noise performance is of much more importance at the ground station considerable care must be taken ta suppress the broadband transmitter noise. Also since a paramp is required caution must be taken to limit the transmitter leakage to avoid overload and unwanted transmitter spur products in the first dawnconverter. The transmitter section is therefore a 9 pole filter with a low pass section to suppress harmonics. This filter will limit the transmitter broadband noise to -188 dBm/Hz and keep the transmitter harmonics within the EMI requirements. The receiver path requires a 13-pole filter to limit the transmitter leakage into the paramp to a practical level. The Diplexer module is fabricated in a waveguide structure to achieve the high Q required for low loss and to improve the thermal problem, since the unit will dissipate 150-200 watts. The design parameters for the module are summarized in Table 5.2-1.

Table 5.2-1. Diplexer Design Parameters

Receiver Bandwidth:	4492.8-4723.2 MHz
Transmit Bandwidth:	4867.6-4967.6 MHz
Insertion Loss	
Antenna to Receiver:	1 dB Maximum
Transmitter to Antenna:	0.1 dB Maximum
VSWR (50 Ohm System):	1.4:1 Maximum
Transmitter Power:	+33 dBw CW
Amplitude Response:	±0.5 dB
Phase Linearity:	$<\pm10^{\circ}$ Over Any 50 MHz Bandwidth

Table 5.2-1.   Diplexer Design Parameters (Continued)

Rejection Characteristics

Receiver Local Oscillator:	>75 dB
Receiver Image Frequency:	>75 dB
Transmitter Harmonics:	>65 dB
Transmit/Receive Isolation:	>130 dB

## Receiver System

The receiving system is required to simultaneous receive the five FDM video signals and the DPSK-TDMA status signal from the 25 RPV's. The wide bandwidth and desired link noise performance requires an uncooled paramp to achieve this performance. The Paramp Design Parameters are outlined in Table 5.2-2.

Table 5.2-2.   Paramp Performance Requirements

1 dB Bandwidth:	4492.8-4723.2 MHz
VSWR (50 Ohm System):	1.5:1
Gain:	20 dB
1 dB Compression:	-30 dBm
Amplitude Response:	±0.5 dB
Phase Linearity:	$<±5°$ Over Any 50 MHz Bandwidth
Noise Figure:	2.5 dB

The performance specification for the downconverter in the receiver system is listed in Table 5.2-3. Referring to the block diagram for the Receiving System in Figure 5.2-2 the received signals are coupled from the Diplexer to the Paramp where they are amplified by 20 dB. The signals are then downconverted to IF in the 1267.2-1497.6 MHz bandwidth. After filtering to suppress the image and undesired transmitter leakage signals, the desired signals are amplified and fed to the second converter. The second converted down-converts to frequencies in the 192 to 422.4 MHz bandwidth and routes the signals to the S/N

165
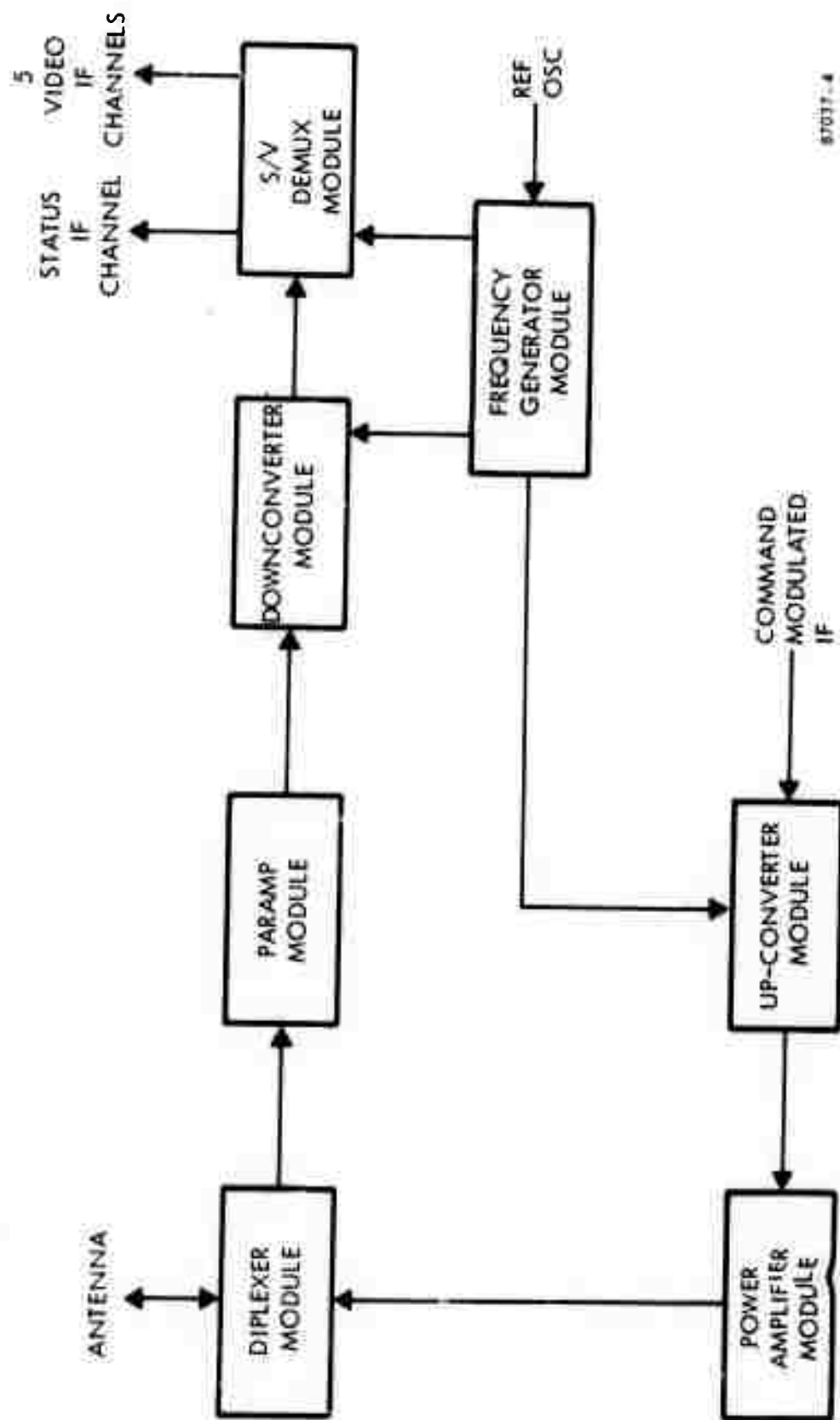
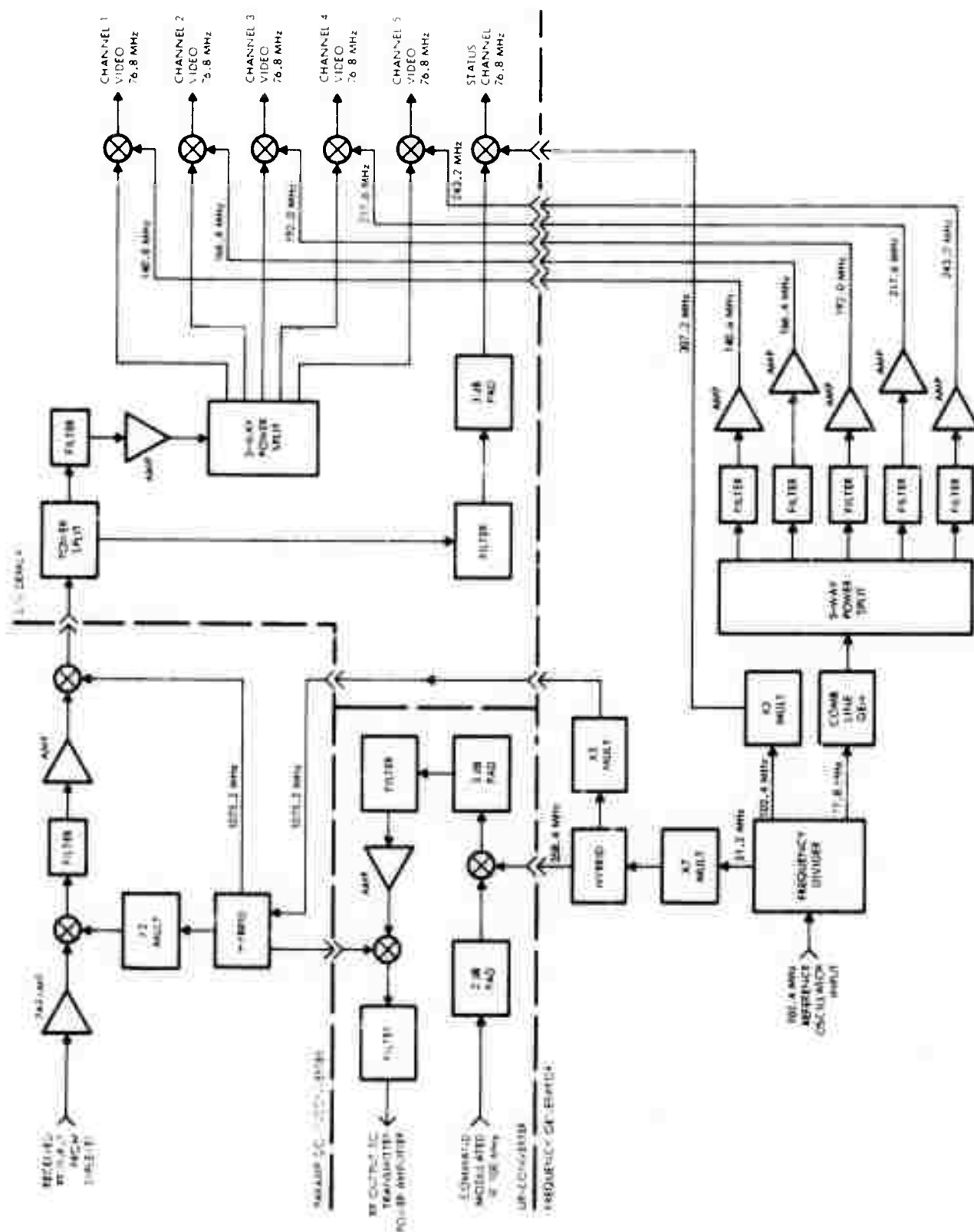Figure 5.2-1. Simplified Block Diagram of Ground Modem RF

Figure 5.2-2. Detailed Block Diagram of Ground Modem

167

DEMUX. The Receiving system does not require agc and has a dynamic range capability of 70 dB in the status channel and 50 dB in the video channels.

Table 5.2-3. Downconverter Specification

RF Bandwidth:	4492.8-4723.2 MHz
Input Level:	-20 dBm
Gain (RF to IF):	36 dB
VSWR:	1.3:1
IF Output Bandwidth:	192-422.4 MHz
Spurious Level:	>60 dB Below Signal
VSWR:	1.5:1
Amplitude Response:	±0.5 dB
Phase Linearity:	<±10°

Status/Video Demultiplexer

The S/V DEMUX in the ground receiver functions to separate the FDM'ed status and video signal into six IF channels (five video and one status). The unit interfaces with the RF Receiver's Downconverter and the Status and Video Demodulators. The frequency assignment enables back-to-back operation between the RPV modem and the ground modem. This feature provides flexibility in evaluating the modem design independent of the RF link.

The design is predicated on providing a minimum output signal level 20 dB above the thermal noise level of the modem. Thus, a 60 dB dynamic range is easily achievable with no agc in the S/V DEMUX.

Figure 5.2-2 identifies the block diagram of the S/V DEMUX. The multiplexed TDMA status signal and the five video signals are coupled from the Receiver Downconverter in the 192-4224 MHz band to a 3 dB power divider. The bandpass filter (4-pole 0.1 dB Chebychev) in the status channel following the divider passes the 384 MHz status signals and provides a nominal 30 dB rejection to the video signals. The status signal is then downconverted to a 76.8 MHz IF and fed to the Status Demodulator.

168

In a similar manner the video signals pass through a 5-pole 0.1 dB Chebychev band-pass filter in the video channel (which attenuates the undesired status signal by 30 dB) to an amplifier. This amplifier is required to equalize the loss and level difference between the status and video channels. These amplified signals are then coupled to five balanced mixers via a power divider where they are downconverted to the five 76.8 MHz channels for the Video Demodulator. Each mixer downconverts all video signals, however, only the desired channel is translated to the proper 76.8 MHz IF center frequency and is accepted by the filter in the proper Video Channel Demodulator.

The S/V DEMUX characteristics are summarized in Table 5.2-4.

Table 5.2-4. S/V DEMUX Characteristics

Input

Bandwidth:	192-434 MHz
Level:	-4 dBm Maximum
Impedance:	50 Ohm 1.5:1 VSWR

Frequency

Video Channel 1:	217.6 MHz
Video Channel 2:	243.2 MHz
Video Channel 3:	268.8 MHz
Video Channel 4:	294.4 MHz
Video Channel 5:	320.0 MHz
Status Channel:	384 MHz

Output

Frequency (6 Channels):	76.8 MHz
Loss (RF to IF):	12 dB Maximum
VSWR (50 Ohms):	1.5:1

169

Table 5.2-4.   S/V DEMUX Characteristics (Continued)

Dynamic Range	50 dB Minimum
Amplitude Response	±0.5 dB
Phase Linearity	$<\pm5^{\circ}$

Up-Converter

The up-converter required to translate the time-division multiplexed chirp command signal from the 100 MHz IF to 4917.6 MHz is shown in Figure 5.2-2. The translation is made in two conversions to simplify the filtering and amplification processes. Referring to the block diagram, the command signal is coupled from the modulator to the first converter at a -10 dBm level. The output, 5 pole 0.1 dB Chebychev, filter selects the upper sideband at 458.4 MHz and rejects the image by 60 dB. The signal is then amplified and coupled to the second converter at a 10 dBm level. The lower sideband is filtered by the 4 pole 0.1 dB Chebychev filter which provides greater than 70 dB rejection at the local oscillator and image frequencies. The up-converted signal is then routed to the Transmitter Power Amplifier Module. The module specifications are identified in Table 5.2-5.

Table 5.2-5.   Up-Converter Specifications

Input Bandwidth:	50-150 MHz
Input Level:	-10 dBm Maximum
Loss (IF to RF):	10 dB Maximum
C/No	-95 dBm/Hz
Output Bandwidth:	4867.6-4967.6 MHz
Spurious Level:	60 dB Below Signal
VSWR (50 Ohm)	
Input IF:	1.5:1
Output RF:	1.5:1
Amplitude Response:	±0.5 dB
Phase Linearity:	$<\pm5^{\circ}$

170

Transmitter Power Amplifier

To achieve the one kilowatt CW output power level to cascaded traveling wave tube amplifiers will be required. The output TWT is rated at 1 KW and has 25 dB gain. It is driven from a 10 watt TWT operating in the linear range with 55 dB gain. Forced cooling will be required to cool the units. The performance requirements are listed in Table 5.2-6.

Table 5.2-6. TWT Performance Requirements

Bandwidth:	4867.6 - 4767.6 MHz
Power Out:	+30 dBw minimum
Gain:	80 dB minimum
VSWR: 50 ohm	1.5:1
Amplitude Response:	±0.5 dB
Phase Linearity:	$< \pm 10^\circ$
Noise	40 dB maximum

Frequency Generator Module

Generation of the required IF and RF signals for the Ground Modem's up- and downconverters and the S/V DEMUX mixers is accomplished as indicated in the block diagram of Figure 5.2-2. The approach taken is similar to that used in the RPV design. A reference oscillator at 102.4 MHz is the basic source from which all the signals are synthesized. Referring to the block diagram the reference signal is divided down to obtain outputs at 51.2 MHz and 12.8 MHz. It is also fed directly to a times three multiplier to provide the local oscillator signal at 307.2 MHz for the Status Channel DEMUX

The 51.2 MHz output is used to generate the four local oscillator signals required in the receiver downconverter and transmitter up-converter. It is first multiplied by seven to obtain the 358.4 MHz signal. A 3 dB hybrid splits this signal providing a +10 dBm signal for the up-converter first mixer. The other output is multiplied by three to yield the 1075.2 MHz signal source required as the local oscillator drive to the second converter in the Receiver and the input to the times three and times five multipliers in the Receiver downconverter and transmitter up-converter.

The 12.8 MHz signal is used to generate the five local oscillator signals required for the five video channels in the S/V DEMUX. The signal is amplified and used to drive an

171

harmonic generator. The input for each channel is taken from the power divider output. One of the odd harmonics between eleven and nineteen is used for each channel. The desired harmonic is filtered and amplified to obtain a +10 dBm signal with all undesired harmonics down 80 dB.

5.3   Slave Station RF Configuration

The Slave Station Receiving system for the Wideband Command and Control Modem is shown in Figure 5.3. Its primary function is to recover ranging information from the RPV TDMA status transmissions. The Slave Station receiver is optimized for noise performance since the antenna design must be consistent with a mobile station.

The received signals are coupled from the antenna to a 5-pole 0.1 dB Chebychev preselector filter. The filter provides 75 dB rejection to the Ground Transmitted signals in addition to providing image rejection and limiting the local oscillator reradiation. The video transmissions will also be discriminated by this filter in varying degrees demanding their separation from the status signal. The closest video channel is attenuated by 6 dB all the others are reduced by greater than 24 dB.

After preselection the TDMA status signal is amplified and downconverted to a 76.8 MHz IF in two conversions. The first conversion is to 384 MHz. The receiver requires no AGC. The required local oscillator RF and IF signals are derived from the 102.4 MHz reference oscillator available from the modem. Table 5.3 summarizes the Receiver RF performance. The Receiver can be packaged to mount with the associated antenna system.

Table 5.3.   Receiver RF Performance

RF Bandwidth	4635 - 4735 MHz
Noise Figure	3.5 dB
Grain (RF to IF)	27 dB
1 dB Compression	-35 dBm
VSWR (50 ohm)	1.4:1
Amplitude Response	±1.0
Phase Linearity	$< \pm 10^{\circ}$
Image Rejection	< 75 dB

172

Table 5.3.   Receiver RF Performance (Continued)

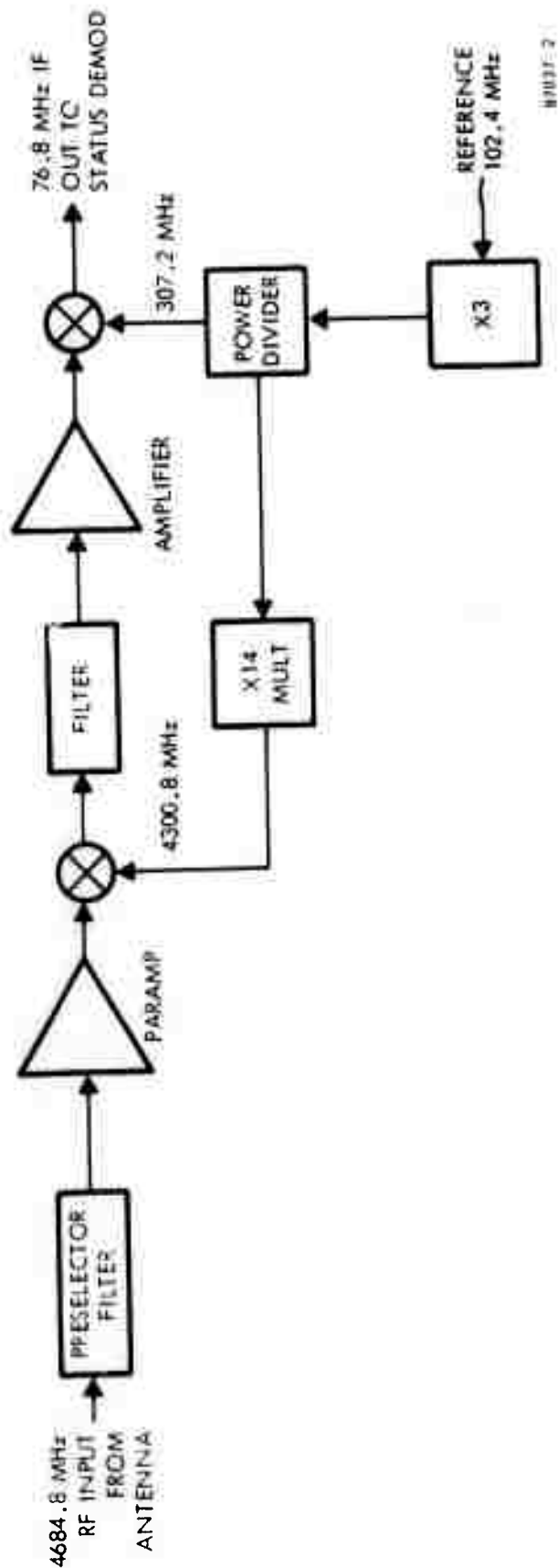|	
Local Oscillator Reradiation	<-74 dBm
IF Frequency	76.8 MHz
Output VSWR (50 ohm)	1.5:1

173

Figure 5.3. Block Diagram of Slave Station RF Configuration

174

SECTION 6.0

SAMPLE SYSTEM CONFIGURATION

175

6.0   SAMPLE SYSTEM CONFIGURATION

The Wideband Command and Control Modem study included system design considerations to ensure a flexible modem design which would be compatible with various ranging baselines and RF equipment implementations. This paragraph will define a typical overall system to illustrate typical system parameter values, position location and man-machine interface considerations.

6.1   System Configuration

Figure 6.1 shows the overall system configuration which provides command and control of RPV's, status and video data reception from RPV's, and position location of RPV's. Three ground stations are shown, two slaves and one master. The primary function of each slave station is to provide independent range measurements, therefore, actual system implementation may use only one slave station with the third range measurement provided by altitude information from the RPV. The master stations provide overall network coordination and data control.

The master ground station consists of a master/slave interface subsystem, RF subsystem, modem subsystem and data subsystem. A master/slave interface subsystem is provided to establish a link between the master and slave ground stations. This subsystem may have both a microwave link and cable interface with the exact microwave link interfaces being dependent on system considerations such as baseline length and slave/master data rates. The RF Subsystem establishes the link between the RPV and the Modem Subsystem. It interfaces at IF with the modem and at RF with the air link. The Modem Subsystem formats/deformats, modulates/demodulates the status, video, command and ranging data. The Data Subsystem provides data storage, display, computation and man-machine interfaces necessary for proper system generation.

The following paragraphs will provide additional definition of the system in terms of the Master Ground Station and Slave Ground Station. Topics covered will include functional block diagram descriptions, trade-off considerations and major system parameters.

6.1.1   Master Ground Station

The master ground station provides network control, display and computation capabilities. An overall functional block diagram of this station identifying subsystems is shown in Figure 6.1.1-1 with each subsystem described in the following paragraphs.

Master/Slave Interface Subsystem

The Master-Slave Interface Subsystem consists of buffers to format the data plus RF equipment to establish a microwave link between the master and slave stations. Depending on the baseline length and implementation approach, there may also be cables between the master and slave to carry reference signals and housekeeping data. The microwave link design provides
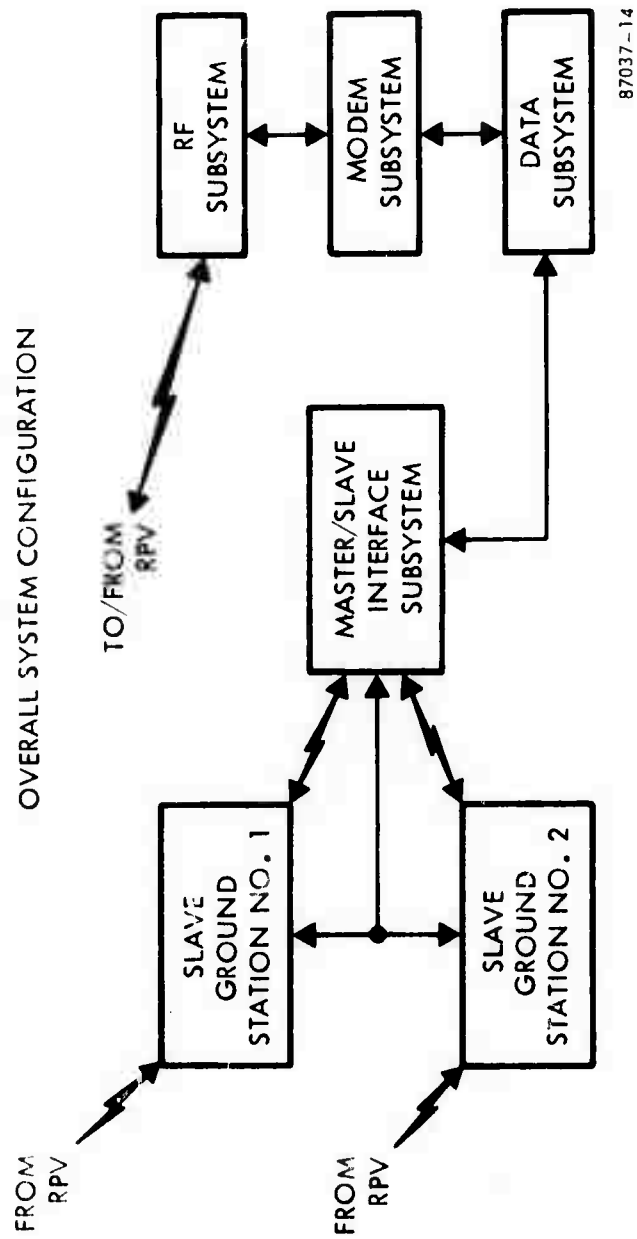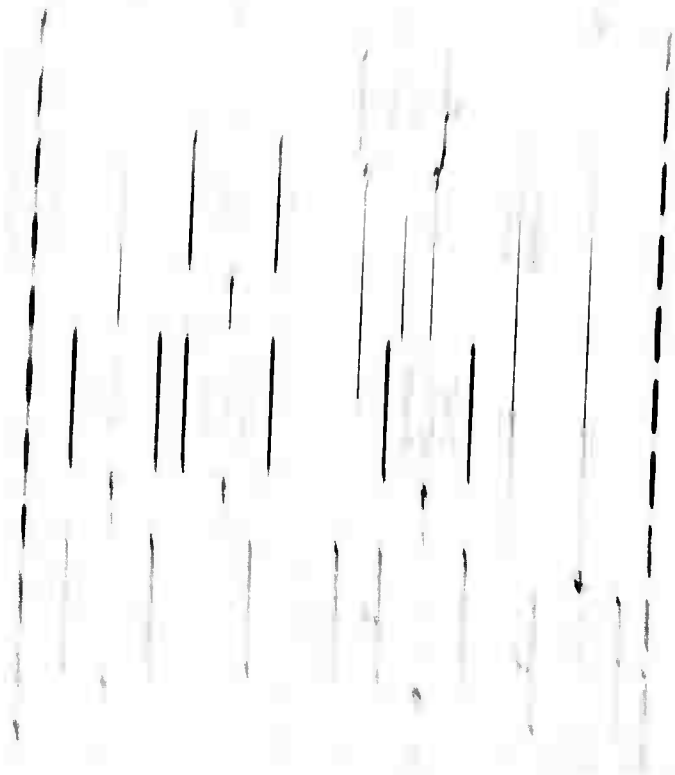
176

OVERALL SYSTEM CONFIGURATION

Figure 6.1

Figure 4.1.1-1

several system trade-off considerations. One major consideration is to design for disturbances in the microwave link which could seriously degrade the range data.

Disturbances in a microwave system include thermal noise, waveform distortion, and intersymbol interference. Of these three types of disturbances, thermal noise is the largest contributing factor in a well-designed system which suffers from signal fading at the receiver. Line-of-sight microwave paths are subject to fading, which at times, can cause the received signal on a path to drop appreciably below the normal signal level. Microwave routes which are engineered properly provide adequate fade margin to satisfy reliability objectives set for the system. The magnitude of this fade margin is dependent upon both equipment and radio path consiaerations.

Two basic types of fading have been identified as being significant; namely, path attenuation and frequency selective. Path attenuation fading is usually related to precipitation or some other phenomenon resulting in excess path attenuation. In most cases, adequate path clearance and fade margins can be used to combat fading caused by path attenuation. Frequency-selective fading, on the other hand, is usually caused by changes in the atmospheric refraction index and is a complex phenomenon whose mechanism is not completely understood. This type of fading is usually fast and always involves multiple paths. Large fade margins are useful in combating these effects, although the deepest fading of this type cannot be completely overcome by fade margin alone. Other means might be the application of diversity operation at the receiver end. In both instances, fading tends to be a function of the path length; i.e., very long paths are more subject to fading than very short paths.

It is generally agreed that, with adequate path clearance and in the absence of a single specular reflection on a path, the very deep fading is due to multipath propagation through the atmosphere, which, over a single section, gives rise to a Rayleigh distribution of the received signal amplitude against time. Rayleigh fading depth depends primarily upon the phase differences and the amplitude ratio of the components contributing to the received field. In radio hops where the first Fresnel Zone is clear of obstruction, the ground reflection component is usually small compared with the direct path component. When reflecting on the surface of water or an very smooth land surfaces, for example, on snow, the direct component and the reflected component may be of approximately equal strength. As the length of the microwave path is increased, the number of possible indirect paths by which the signal may be received increases rapidly. The signals from these various indirect paths, when added to the direct signal, cause field strength variations around the mean signal value. In most cases, the variation will be completely random resulting in the Rayleigh fading.

Multipath fading is usually plotted as the fraction of the total time that the received signal will be above or below a given mean level. (Although this level is actually the rms value of the variation, it is usually permissible to associate it with the normal received carrier level.) It is handled in this manner because a Rayleigh distributed signal represents the random addition of a large number of equal vectors. Although in multipath fading, the actual number of fades per unit of time increases directly with the frequency of operation, total outage time is not related to operating frequency so long as the fading is strictly the multipath type.

179

Experience to date has shown that nominal path lengths of 10 miles may be considered as prospects for Rayleigh fading without regard to the frequency of operation. The Rayleigh distribution is characterized by a 10 dB per decade slope for fading depths greater than 10 dB. Furthermore, the multipath type of fading has been found to occur for just a portion of the month, with less severe fading occurring during the rest of the month. One hour of Rayleigh type fading is considered as a worst-hour condition. Hops with adequate path clearance (ray path is not obstructed even under the most extreme conditions of atmospheric refraction) have a long-term mean received carrier level equal to the free space (no fading) value. The short-term mean received carrier level, however, is generally depressed below the free-space value during hours of fading. This is generally explained by a defocusing effect due to a nonlinear gradient of atmospheric refractive index. This mean depression has been found to be proportional to path length.

Some paths, independent of length, exhibit a more severe amount of mean depression than others. These paths are usually in coastal areas, and the signal can suffer 30 dB attenuation or more for periods of a few hours. Unfortunately, these fadeouts are difficult to predict, and there is usually no practical method of overcoming them, other than increasing fade margin and/or shortening path lengths.

The microwave link can be envisioned as either of the two models shown in Figure 6.1.1-2. In the double hop model, a passive relay is assumed, therefore, no power facilities are required; only a tower, antenna and microwave component.

To implement either link, existing microwave equipment would be used, thereby permitting a cost-effective approach to the master-slave link. Typical parameters of existing microwave equipment and assumed link parameters are provided in Table 6.1.1-1.

Table 6.1.1-1. Microwave Link Parameters

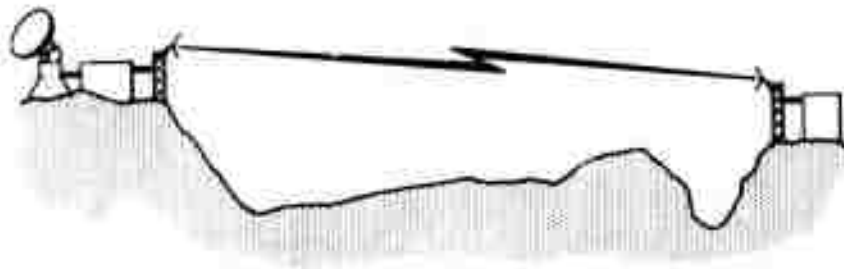|	
Operating Frequency (Typical)	8 GHz
Transmitter Output Power (Typical)	+27 dBm
Receiver Noise Figure (Typical)	10 dB
Antenna Diameter (One Hop Link) (Assumed)	2 feet
Antenna Diameter (Double Hop Link) (Assumed)	5 feet
Fixed Losses (Single Hop) (Typical)	2 dB
Fixed Losses (Double Hop) (Typical)	3 dB
Path Length (Single Hop) (Assumed)	20 miles
Path Length (Each Leg, Double Hop) (Assumed)	10 miles

180

Table 6.1.1-1. Microwave Link Parameters (Continued)
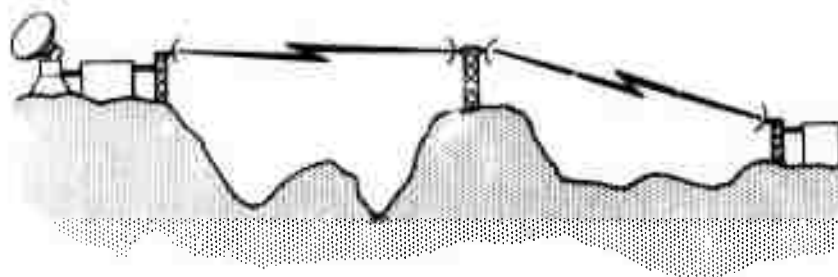
IF Bandwidth (3 dB Points) (Typical)　　　　25 MHz

Path Clearance (Assumed)　　　　Line-of-sight path exists with at least 0.6 Fresnel Zone Radius clearance over all obstacles, based on true earth profile.

A) SINGLE HOP MODEL

B) DOUBLE HOP MODEL

86432-103

Figure 6.1.1-2. Microwave Link Models

　　　　The link reliability which is a function of fade margin is of primary importance. As a result, two power budgets have been compiled to estimate a typical link fade margin. The power budget in Table 6.1.1-2 is for the single hop model and the power budget in Table 6.1.1-3 is for the double hop model. Each budget was computed for three different data loop bandwidths. These bandwidths are compatible with a slave station implementation which either acts as a relay or demodulator of received range data. For relay operation, a nominal data bandwidth of 2 kHz to 10 kHz

181

	Link Loss Budget		
	Link 1	Link 2	Link 3
Trans Power (dBm)	142.0	142.0	142.0
Trans Loss (dB)	2.0	2.0	2.0
Antenna Gain (dB)	63.0	63.0	63.0
Space Path Loss (dB)	81.0	81.0	81.0
Received Power (dBm)	27.0	27.0	27.0
Noise Received Carrier (dBm)	54.0	-54.0	-54.0
kT (dBm/Hz)	174.0	-174.0	-174.0
Noise Figure (dB)	10.0	10.0	10.0
Noise B/W (Bandwidth) (dB)	42.0	40.0	33.0
Total Noise (dBm)	115.0	-124.0	-131.0
Noise Carrier/Noise (dB)	-61.0	-70.0	-77.0
Reference Threshold C/N (dB)	13.0	13.0	13.0
Fade Margin (dB)	+48.0	+57.0	+64.0

Table 6.1.1-3. Link Power Budget (Double Hop Model)

	Data Loop Bandwidth		
	80 kHz	10 kHz	2 kHz
Free Space Loss (dB)	272.0	272.0	272.0
Fixed Losses (dB)	3.0	3.0	3.0
Antenna Gain (dB)	158.0	158.0	158.0
Total Path Loss (dB)	117.0	117.0	117.0
Transmit Power (dBm)	27.0	27.0	27.0
Mean Received Carrier (dBm)	-90.0	-90.0	-90.0
Total Noise (dBm) (From Table 6.1.1-2)	-115.0	-124.0	-131.0
Mean Carrier/Noise (dB)	25.0	34.0	41.0
Reference Threshold (dB)	13.0	13.0	13.0
Fade Margin (dB)	12.0	21.0	28.0

183

Table 6.1.1-1. Microwave Link Parameters (Continued)

IF Bandwidth (3 dB Points) (Typical)   25 MHz

Path Clearance (Assumed)   Line-of-sight path exists with at least 0.6 Fresnel Zone Radius clearance over all obstacles, based on true earth profile.

A) SINGLE HOP MODEL

B) DOUBLE HOP MODEL

86432-103

Figure 6.1.1-2. Microwave Link Models

The link reliability which is a function of fade margin is of primary importance. As a result, two power budgets have been compiled to estimate a typical link fade margin. The power budget in Table 6.1.1-2 is for the single hop model and the power budget in Table 6.1.1-3 is for the double hop model. Each budget was computed for three different data loop bandwidths. These bandwidths are compatible with a slave station implementation which either acts as a relay or demodulator of received range data. For relay operation, a nominal data bandwidth of 2 kHz to 10 kHz

181

Table 6.1.1-2. Link Power Budget (Single Hop Model)

	Data Loop Bandwidth		
	80 kHz	10 kHz	2 kHz
Free Space Loss (dB)	142.0	142.0	142.0
Fixed Losses (dB)	2.0	2.0	2.0
Antenna Gain (dB)	63.0	63.0	63.0
Total Path Loss (dB)	81.0	81.0	81.0
Transmit Power (dBm)	27.0	27.0	27.0
Mean Received Carrier (dBm)	-54.0	-54.0	-54.0
KT (dBm/Hz)	-174.0	-174.0	-174.0
Noise Figure (dB)	10.0	10.0	10.0
Noise BW (Baseband)(dB)	49.0	40.0	33.0
Total Noise (dBm)	-115.0	-124.0	-131.0
Mean Carrier/Noise (dB)	-61.0	-70.0	-77.0
Reference Threshold C/N (dB)	13.0	13.0	13.0
Fade Margin (dB)	+48.0	+57.0	+64.0

Table 6.1.1-3. Link Power Budget (Double Hop Model)

	Data Loop Bandwidth		
	80 kHz	10 kHz	2 kHz
Free Space Loss (dB)	272.0	272.0	272.0
Fixed Losses (dB)	3.0	3.0	3.0
Antenna Gain (dB)	158.0	158.0	158.0
Total Path Loss (dB)	117.0	117.0	117.0
Transmit Power (dBm)	27.0	27.0	27.0
Mean Received Carrier (dBm)	-90.0	-90.0	-90.0
Total Noise (dBm) (From Table 6.1.1-2)	-115.0	-124.0	-131.0
Mean Carrier/Noise (dB)	25.0	34.0	41.0
Reference Threshold (dB)	13.0	13.0	13.0
Fade Margin (dB)	12.0	21.0	28.0

may be used depending on the range loop smoothing required. The microwave link spectrum required is approximately 25 MHz in order to pass the ±12.6 MHz range code. For demodulation operation, a nominal data bandwidth of 10 kHz to 80 kHz may be used. This bandwidth range assumes a complete range word per RPV which is transmitted over the microwave link once per second. An additional forty-nine messages per RPV are sent each second with information which denotes change of range from the previous message.

For a link which fades in a Rayleigh manner, the fade margin to percentage time below the reference threshold [13 dB] is shown in Table 6.1.1-4 for the fade margins in Tables 6.1.1-2 and -3. Since this level of performance is predicted using standard commercial microwave practices, the link itself should not be a significant problem or design risk.

The selected microwave link approach will be dependent on the earth profile between slave and master ground stations. In the sample system configuration, the single loop microwave link is assumed. The single hop link uses small antennas and towers and should represent an easy installation. Assuming a slave relay results in the following overall system carrier-to-noise density ratio:

$$\left(\frac{C}{N}\right)_{System} = \frac{1}{\left(\frac{1}{\frac{C}{N}}\right)_{Slave} + \left(\frac{1}{\frac{C}{N}}\right)_{Relay}}$$

where:

$\left(\frac{C}{N}\right)_{Slave}$ is the carrier-to-noise ratio established by the RPV-to-slave station link

$\left(\frac{C}{N}\right)_{Relay}$ is the carrier-to-noise ratio established by the microwave link

During a large percentage of time $(C/N)_{slave}$ will be much less than $(C/N)_{relay}$. For the small percentage of time when this is not true, the additional degradation of range S/N due to the master-to-slave link will be dependent on the fading depth and link signal margin. As shown in Table 6.1.1-4, a fade margin of 57 dB [which represents the 10 kHz data bandwidth case in Table 6.1.1-2] corresponds to the master-to-slave link signal being less than 13 dB only 0.00012 percent of the time.

184

Table 6.1.1-4. Microwave Link Performance

Fade Margin	% of Below Reference Threshold
64 dB	0.000024
57 dB	0.00012
48 dB	0.001
28 dB	0.1
21 dB	0.5
12 dB	4

RF Subsystem

The RF Subsystem establishes the link between the master ground station and RPV's. This subsystem interfaces at IF with the Modem Subsystem and at RF with the air link. The major design element in this subsystem is the antenna since various divergent approaches are available to implement the antenna. Several key considerations which will impact the antenna selection are:

- What is the best way to recover data from 25 spatially separated RPV's?

- Are electronic beam-steering techniques applicable?

- Are multiantennas the best solution?

- Is a combination simultaneous lobing and sequential lobing feasible?

- Should the receive and/or transmit function be integrated into the array aperture rather than having separate receive/transmit functions?

A set of link parameters are now defined to establish transmitter and receiver requirements. An RF frequency value of 5 GHz (C-band) will be assumed in computing the link parameters.

The two major parameters which define the RF Subsystem are G/T, which is the antenna gain to system noise temperature ratio, and EIRP, which is effective radiated power. Link budgets will be defined for the uplink (command data) in order to identify the EIRP requirement plus downlink (status and video data) in order to identify the G/T requirement. System parameters which are assumed for the sample system calculations are shown in Table 6.1.1-5.

Table 6.1.1-5. Assumed RPV-to-Ground Link Parameters

Drone Antenna Gain	=	0	dB
Drone Power Amplifier Output	=	40	dBm
Drone Status Output Power	=	21.3	dBm
Drone Video Output Power	=	38.8	dBm
RF Frequency	=	5	GHz
Range	=	250	nmi

· 186

The uplink budget is itemized in Table 6.1.1-6 where the EIRP requirement is shown to be 67.6 dBm. The downlink (status and video) budgets are itemized in Tables 6.1.1-7 and 6.1.1-8, respectively. An RPV transmit video/status power ratio of 17.5 dB is assumed which approximately accounts for the difference in data rates and E_b/N_o requirements for the two types of data. The required RF Subsystem G/T requirement to support both video and status data channels is 13.4 dB/° K

Table 6.1.1-6.   Uplink Budget (Command)

*Required C/kT	=	70.4 dB Hz
kT (1200° K System Temperature)	=	-167.8 dBm/Hz
Required Receiver Power	=	-97.4 dBm
RPV Antenna Gain	=	0.0 dB
Miscellaneous Losses	=	2.0 dB
Free Space Loss	=	160.0 dB
Required Ground EIRP	=	64.6 dBm

*C/kT Budget

Theoretical E_b/N_o (10^{-5} BER – Assumes Coding)	=	12.4 dB
Bandwidth Factor	=	47.0 dB
Theoretical C/kT	=	59.4 dB Hz
Implementation Loss	=	1.0 dB
Margin	=	10.0 dB
Required C/kT	=	70.4 dB Hz

Table 6.1.1-7. Downlink Budget (Status)

Transmit EIRP (RPV)	=	21.3 dBm
Free Space Loss	=	160.0 dB
Miscellaneous Losses	=	2.0 dB
Received Signal (C)	=	-140.7 dBm
Boltzmann Constant (k)	=	-198.6 dBm/Hz-$^{\circ}$ K
C/k	=	57.9 dB/Hz-$^{\circ}$ K
*Required C/kT	=	71.3 dB/Hz
Required Ground G/T	=	13.4 dB/$^{\circ}$ K

*C/kT Budget

Theoretical E_b/N_o (10^{-5} BER)	=	10.3 dB
Bandwidth Factor	=	49.0 dB
Theoretical C/kT	=	59.3 dB/Hz
Implementation Loss	=	2.0 dB
Margin	=	10.0 dB
Required C/kT	=	71.3 dB/Hz

Table 6.1.1-8. Downlink Budget (Video)

Transmit EIRP (RPV)	=	38.8 dBm
Free Space Loss	=	160.0 dB
Miscellaneous Losses	=	2.0 dB
Received Signal (C)	=	-123.2 dBm
Boltzmann Constant (k)	=	-198.6 dBm/Hz-$^\circ$ K
C/k	=	75.4 dB/Hz-$^\circ$ K
*Required C/kT	=	88.8 dB/Hz
Required Ground G/T	=	13.4 dB/$^\circ$ K

*C/kT Budget

Theoretical E_b/N_o (10^{-3} BER)	=	6.8 dB
Bandwidth Factor	=	70.0 dB
Theoretical C/kT	=	76.8 dB/Hz
Implementation Loss	=	2.0 dB
Margin	=	10.0 dB
Required C/kT	=	88.8 dB/Hz

If the antenna size is based on the G/T requirement, an approximate antenna diameter of 6 to 9 feet is needed depending on the type of low-noise amplifier. The lower diameters correspond to an uncooled parametric amplifier of the type readily available. With such a unit, a 300° K system temperature is easily achievable. The larger sizes correspond to tunnel-diode amplifiers, also commonly available. With these units, system temperatures of 650° K or less are achievable.

For the sample system configuration, an EIRP of 68 dBm and a G/T of 14 dB/° K are assumed. The range of ground antenna sizes is 6 to 9 feet which permits application of noncooled paramps to tunnel-diode preamplifiers. The ground transmitter is approximately 10 watts assuming a 6- to 9-foot antenna. The transmitter power may be much larger if an antenna system design is selected which uses a sequentially switched, narrow beam receive antenna and a broad-beam transmit antenna. For this case a 4 dB transmit antenna gain would require a 2.5 KW power amplifier which is still a realistic ground requirement. The intent of the above numbers is to show a flexible system design exists since various system parameter tradeoffs are possible to achieve the desired cost ratio between ground and RPV equipments.

Modem Subsystem

The Modem Subsystem is discussed in detail in the first four sections of this report. Section 1.0 defined the Command and Control requirements for RPV's. Section 2.0 developed the waveform trade-off considerations. Section 3.0 provided a description of the baseline modem in terms of a command link, a status link, and a ranging link. Section 4.0 provided a description of the baseline modem implementation. A summary of major characteristics of the Modem Subsystem are:

|	
Ground Receive IF:	217.6 to 384 MHz
Ground Transmit IF:	100 MHz
Airborne Receive IF:	100 MHz
Airborne Transmit IF:	217.6 to 384 MHz
Output Data	
Video:	20 Mb/s (total of 5)
Status:	80 kb/s data bursts
Range:	Ranging to 25 RPV's
Input Data	
Command:	2 kb/s (total of 25)

190

Data Subsystem

The Data Subsystem provides the man-machine interface plus interfacing with the Modem Subsystem. It consists of computation units, display units, data storage plus allowing real-time control for the RPV's. Man-machine interfaces are provided for five RPV's in the target area and twenty RPV's enroute to the target area. The various system range measurements are used by the Data Subsystem to compute the position of each RPV.

Command data, for up to twenty-five users, will be obtained from a computer or an operator. This data is formatted and sent to the modulator in the Modem Subsystem. Video and status data are received by the Data Subsystem from the Modem Subsystem. A maximum of 100 Mb/s of video data from five users must be processed by the Data Subsystem and then fed to station displays and/or storage. Status data from up to twenty-five users must be deformatted from a time-division multiplex format. This data will be displayed or stored by the Data Subsystem. Ranging data will be obtained by the Data Subsystem from both master and slave stations. This data will then be used to compute the location of a given airborne user. The resulting information may be used to update the airborne user flight path by sending command data or the data may be displayed and stored.

The master control console and display interfaces shown in Figure 6.1.1-1 must be capable of working with up to twenty-five RPV's. RPV's which are over their designated target areas will probably require more operator control than drones which are enroute. A conceptual central console layout for controlling RPV's in the target area is shown in Figure 6.1.1-3. Since five RPV's are assumed in the target area at a given time, five consoles per master ground station are required. Depending on the planned mission activity, either one or two operators per console may be needed. The console layout provides target related display and control on one side and flight path display and control on the second side. The video data from the RPV is displayed with controls being provided to aid the RPV sensor in locating its designated target. These control commands are sent to the airborne user over the command link. The planned flight path together with the actual flight path is displayed on the left side of the console. The actual flight path data is provided by the computer which is determining RPV position from the system range measurements. Controls to correct the RPV flight path are provided. Also shown are displays of various pages of data which can be called up from storage by making keyboard entries.

The total number of operators required at the master ground station will be dependent on the type of mission plus the degree of real-time control required when a man is in the loop interpolating data. In a system operating at the full twenty-five vehicle capacity, a total of seven or eight men may be required at the master ground station - one man per console for each drone over the target area (5) plus two men at the master control console plus one man for overall responsibility.

191

CONCEPTUAL CONSOLE LAYOUT
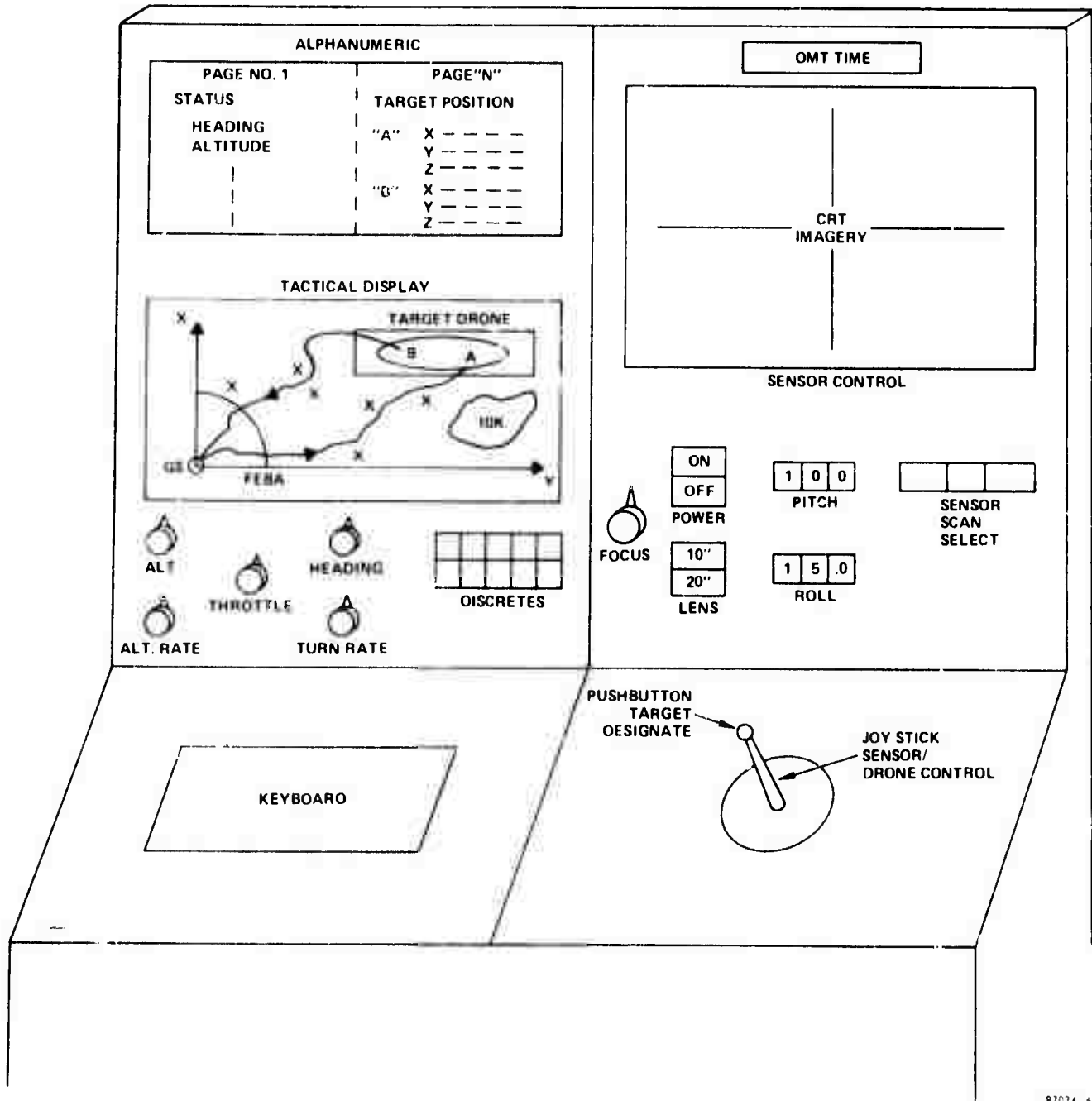
Figure 6.1.1-3. Conceptual Console Layout

6.1.2   Slave Ground Station

The purpose of a slave ground station is to provide a range measurement which is independent of the master ground station range measurement. Since these range measurements must be time correlated it is necessary to know the baseline length between slave and master as well as providing time and frequency references. Depending on the system implementation, these references may be required at either the slave station, or master station. As described earlier, various microwave links can be used as a means of providing a link between master and slave stations.

The two slave station configurations which will be discussed are a relay and a demodulator. The relay configuration will frequency translate range data at the slave station onto a microwave link with range data demodulation occurring at the master ground station. The demodulation configuration will demodulate range data at the slave station and then send the range measurement as digital information over the microwave link.

Figure 6.1.2-1 is a functional block diagram showing the relay slave station configuration. The incoming time division multiplexed data which consists of status data spread by the pseudonoise ranging code will be mixed to an intermediate frequency. Slave station status data will then be frequency multiplexed with the received status/range signal within a standard microwave link bandwidth. The resulting signal spectrum will then be frequency translated to the microwave link carrier frequency and transmitted to the master ground station. Timing and frequency reference signals are not needed at the slave station. What is critical is the RF link from the slave station to the master station. Changes in path length of this link due to propagation anomalies can cause errors in the range measurement. To overcome this potential problem, a set of frequency tones can be sent from the master to the slave station, turned around at the slave station and sent back to the master station. Effectively, these frequency tones would calibrate the master to slave baseline. The master station would monitor the frequency tones and any phase changes could be used to correct the range data in the computer. Another advantage of this configuration is eliminating a secure PN generator at a slave station which could be close to enemy lines, thereby simplifying operational procedures.

The second slave station configuration is the demodulator approach shown in Figure 6.1.2-2. In this approach, the master-to-RPV-to-slave range must be measured at the slave. Consequently, a reference range word plus the PN sequence must be sent from the master to the slave station over the microwave link. Again, the RF path length between master and slave stations is important since path changes will advance or retard the reference timing resulting in a ranging error. As in the first configuration, range tones could be used to keep this link calibrated. The time-division multiplexed status/range data will be demodulated in an identical approach as used at the master station. The resulting range data would be time tagged and formatted into a digital data stream which would be sent to the master station over the microwave link. A given range measurement is made every 0.02 second resulting in fifty range measurements per second. The complete range probably only needs to be sent to the master station once a second. The remaining forty-nine range words sent to the master station each second would be range

193
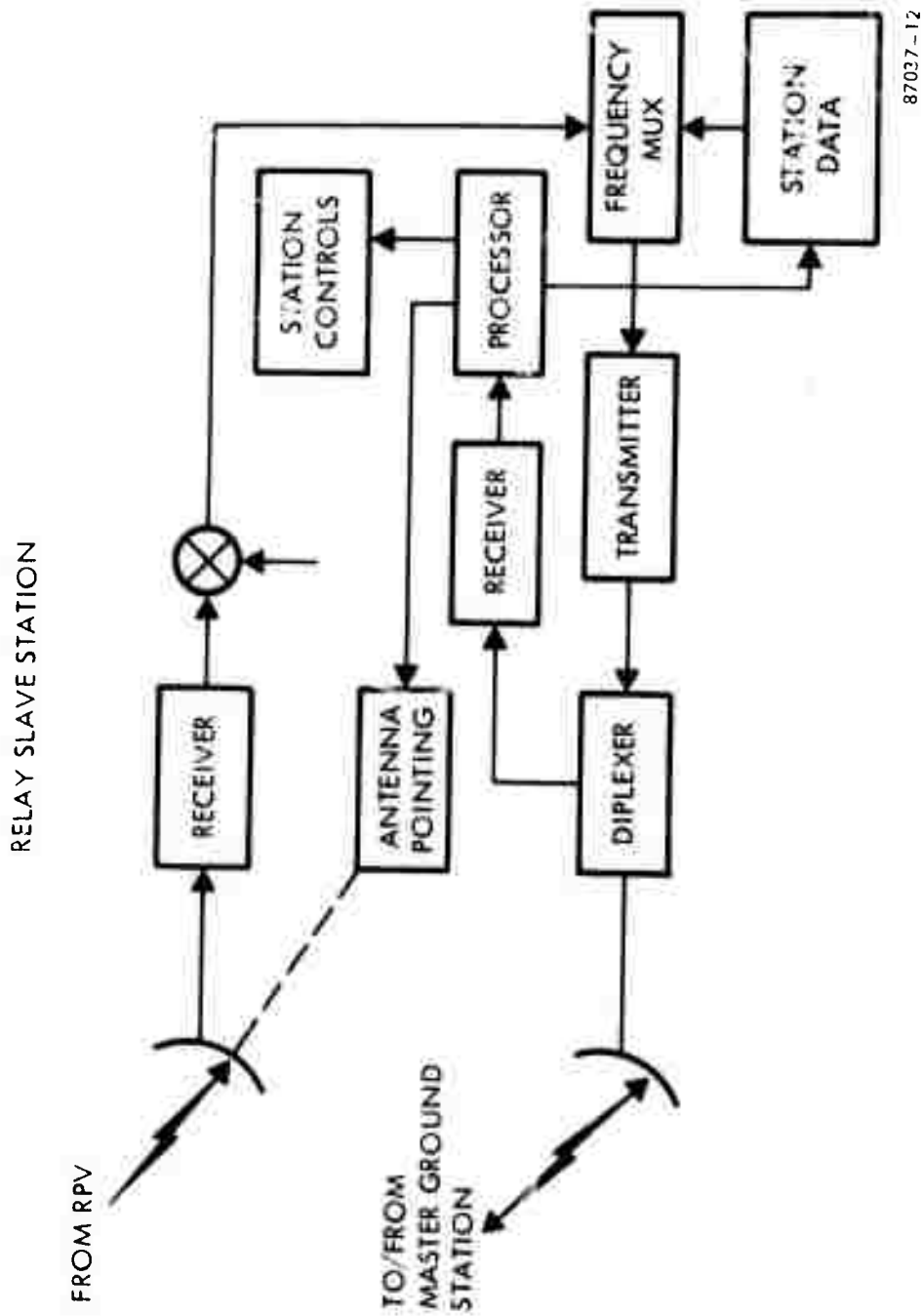
RELAY SLAVE STATION

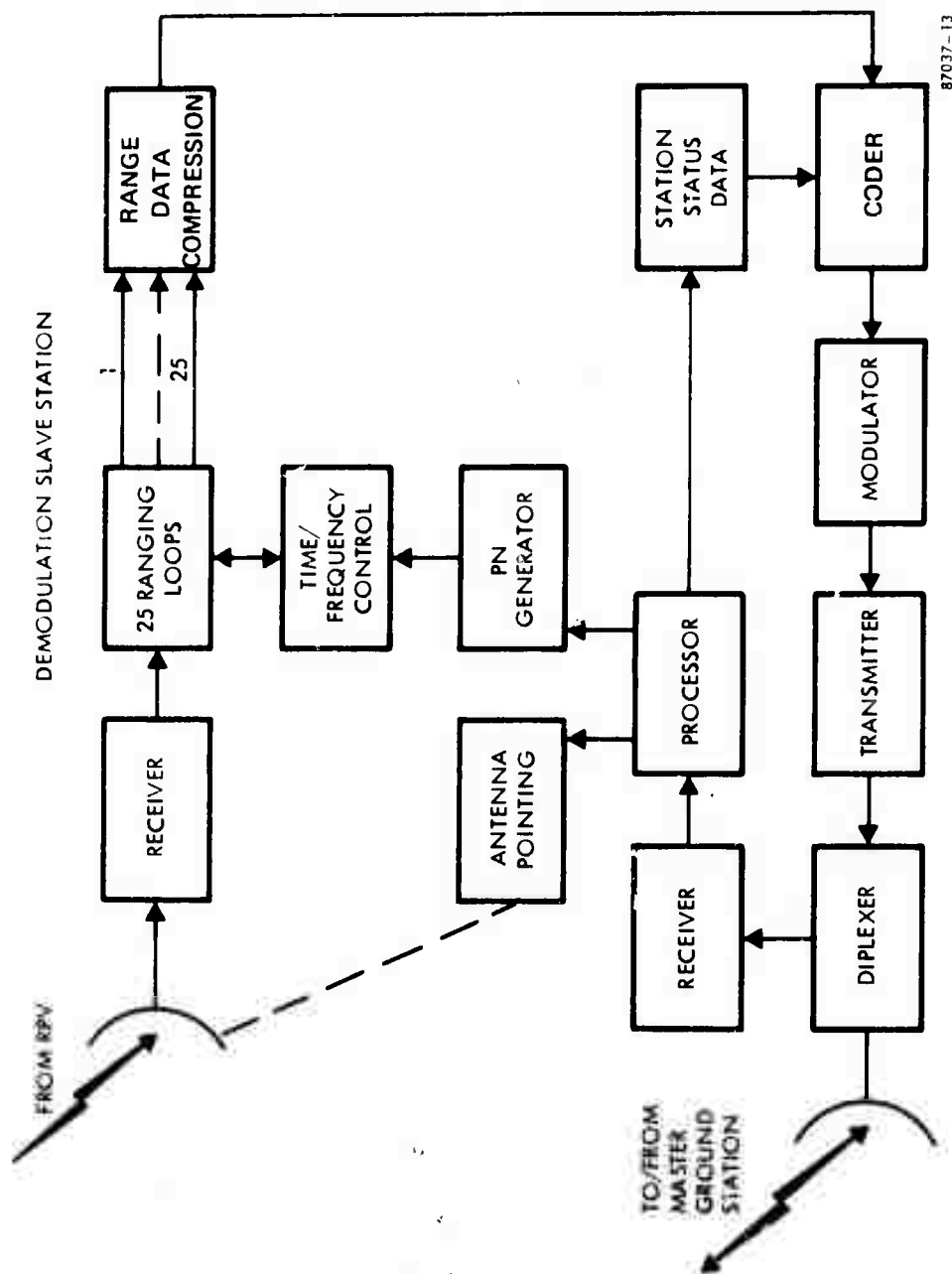Figure 6.1.2-1. Relay Slave Station

87037-12

194

Figure 6. 1.2-2. Demodulator Slave Station

195

differences between consecutive range measurements. Error correction coding can also be used to ensure valid range data detection at the master station.

The relay implementation approach is selected for the sample system implementation. This configuration permits a simple, flexible slave ground station design with the design complexities being kept at the master ground station.

The G/T requirement for the drone-to-ground link will nominally be 13.4 dB/K as itemized in Table 6.1.1-7 for the status link. This will give a signal-to-noise ratio of approximately 13 dB in an 80 kHz bandwidth. The range loop will provide additional narrow banding to further improve the range data signal-to-noise ratio. As stated earlier, depending on the station noise temperature, the slave C-band antenna diameter may be between six to nine feet.

6.2   Position Location

An RPV position location system can be supplied which will meet position location accuracy requirements while requiring only two ranging ground stations, one of which may be the master command station. This minimization of ground station requirements has obvious tactical and economic significance and is made possible by optimal processing of the received signals and by reasonable operational constraints of vehicle locations.

The RPV position location system can be presented as the concatenation of ranging and position estimation processes as shown in Figure 6.2.

6.2.1   Range Finding

The range finding process functions as follows. The range signal is transmitted to the appropriate RPV. Upon decoding of this signal, the RPV will transmit a range response signal which is interpreted by each ground station. The times T_1, ranging time up to the RPV and back down to the master station, and T_2, ranging time up to the RPV and back down to the slave station, are then supplied to the position estimation process in order to compute the estimate of RPV position.

Main ranging variabilities arise from range signal decoding jitter at the RPV and at the ground stations. Other variabilities such as propagation, medium inhomogeneities, etc., are not specifically described although they could be incorporated into the model.

In order to illustrate the optimality of the position estimation process to be implemented, it is necessary to formalize the ranging process through the use of mathematics. The ranging times, T_1 and T_2, may be expressed as

$$T_1 = 2R_1 + \epsilon_1 + \epsilon_2 \tag{1}$$

$$T_2 = R_1 + R_2 + \epsilon_1 + \epsilon_3 \tag{2}$$

where

a. The times T_1 and T_2 are measured in terms of feet traveled rather than units of time.

b. R_1 is the distance from the master ground station to the RPV.

c. R_2 is the distance from the RPV to the slave ground station.

d. ϵ_1 is the range signal decoding error of the RPV.

e. ϵ_2 is the range signal decoding error of the master ground station.

f. ϵ_3 is the range signal decoding error of the slave ground station.

197

The true RPV position (x, y) is related to the ranges R_1 and R_2 through the non-linear equations

$$R_1 = \sqrt{x^2 + y^2} \tag{3}$$

$$R_2 = \sqrt{x^2 + (s - y)^2} \tag{4}$$

where s is the master-slave ground station distance. About a point $(\widetilde{x}, \widetilde{y})$ in space, Equations (3) and (4) can be simplified to

$$(R_1 - \widetilde{R}_2) = \cos\theta\,(x - \widetilde{x}) + \sin\theta\,(y - \widetilde{y}) \tag{5}$$

$$(R_2 - \widetilde{R}_2) = -\cos\phi\,(x - \widetilde{x}) + \sin\phi\,(y - \widetilde{y}) \tag{6}$$

where the angles θ and ϕ are related to the spatial geometry as illustrated in Figure 6.2.1-1.

Using Equations (1), (2), (5), and (6), the ranging configuration is that of Figure 6.2.1-2 where the signals are given by

$$x = \begin{bmatrix} x \\ y \end{bmatrix}, \quad R = \begin{bmatrix} R_1 \\ R_2 \end{bmatrix}, \quad T = \begin{bmatrix} T_1 \\ T_2 \end{bmatrix}, \quad \epsilon = \begin{bmatrix} \epsilon_1 \\ \epsilon_2 \\ \epsilon_3 \end{bmatrix}, \quad v = \begin{bmatrix} v_1 \\ v_2 \end{bmatrix}.$$

$$\Delta x = x - \widetilde{x}, \quad \Delta R = R - \widetilde{R}, \quad \Delta T = T - \Delta T$$

and the transforms are given by

$$A = \begin{bmatrix} \cos\theta\,\sin\theta \\ -\cos\phi\,\sin\phi \end{bmatrix}, \quad B = \begin{bmatrix} 2 & 0 \\ 1 & 1 \end{bmatrix}, \quad C = \begin{bmatrix} 1 & 1 & 0 \\ 1 & 0 & 1 \end{bmatrix}$$

and for simplicity let
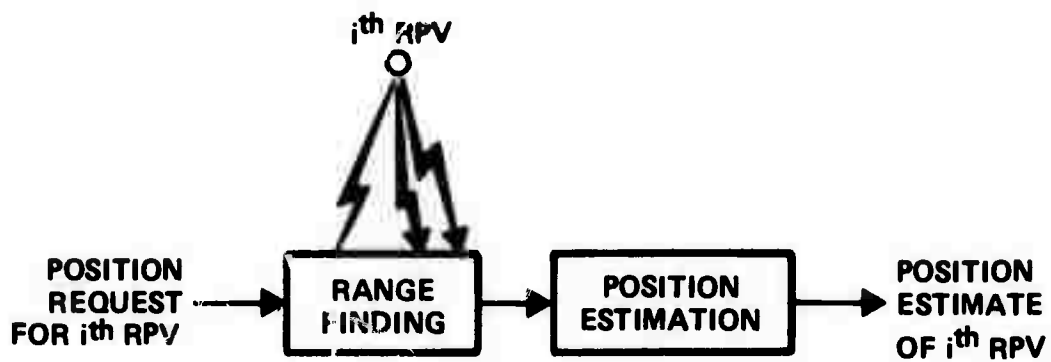
$$H = BA$$
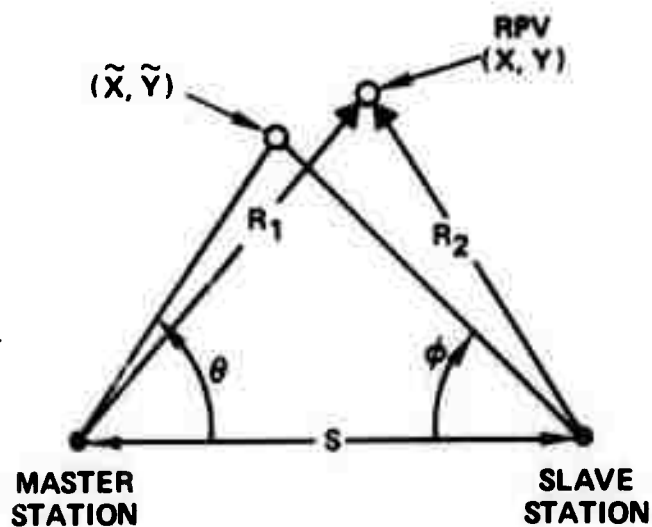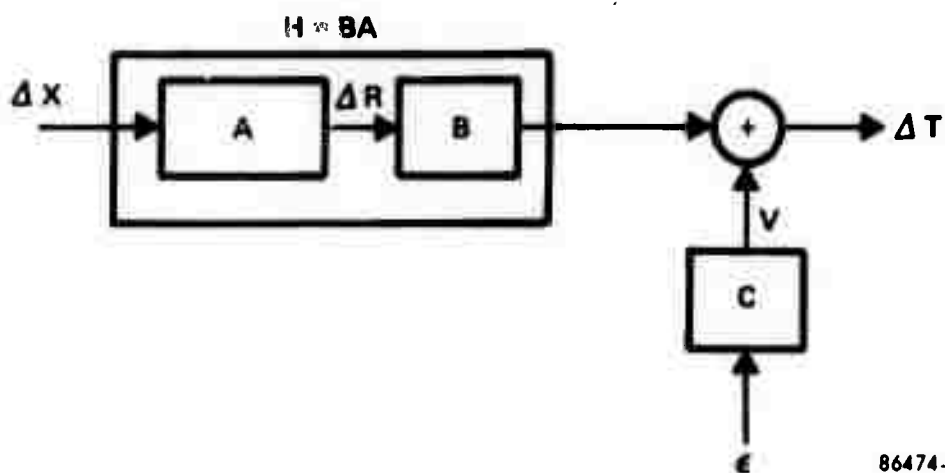
198

Figure 6.2.   Ranging

Figure 6.2.1-1.   Geometry

86474-60

Figure 6.2.1-2.   The Ranging Process

199

Under the reasonable assumption that all uncertainties are Gaussian random variables and that decoding biases are appropriately subtracted out, the measurement noise may be specified by

$$E(\epsilon) = 0, \qquad \text{cov}(\epsilon) = \begin{bmatrix} \sigma_1^2 & 0 & 0 \\ 0 & \sigma_2^2 & 0 \\ 0 & 0 & \sigma_3^2 \end{bmatrix}$$

and the a priori statistics of the RPV may be specified as

$$E(x) = \mu_x \qquad \text{cov}(x) = M$$

This completes the specification of the ranging process in a statistical sense.

6.2.2 Position Estimation

The position estimation process functions by taking the range measurements of an RPV and generating its position estimate. The approach to be proposed here is essentially optimal in that it finds the most likely position $\hat{x}$ for the RPV in space given the range measurement uncertainty. To show this, the structure of the position estimation process will be directly derived from the statement of optimality,

$$\hat{x} = \text{Arg}\left(\max_{\hat{x}} (p(x|T))\right)$$

As $\qquad p(x|T) = p(\Lambda x|\Lambda T)$

then $\qquad \Lambda\hat{x} = \text{Arg}\left(\max_{\hat{x}} (p(\Delta x|\Delta T))\right)$

Maximization of $p(\Lambda x|\Delta T)$ can most easily be accomplished through manipulation,

$$p(\Lambda x|\Lambda T) = \frac{p(\Delta x, \Delta T)}{p(\Delta T)}$$

$$= \frac{p(\Delta x, v)\,|J|^{\frac{1}{2}}}{p(\Delta T)}$$

but J, the Jacobian of the transform from ΔT to v, is the identity matrix.

$$p(\Delta x \mid T) = \frac{p(\Delta x, v)}{p(\Delta T)}$$

and upon substitution of $v = t - H\Delta x$

$$p(\Delta x \mid \Delta T) = \frac{p(\Delta x)\, p(\Delta T - H\Delta x)}{p(\Delta T)} \tag{7}$$

Observe that all probabilities in Equation (7) are Gaussian, i.e.,

$$p(\Delta x) = \frac{1}{2\pi |M|^{1/2}} \exp\left\{-\frac{1}{2}(\Delta x - \mu_{\Delta x})^T M^{-1} (\Delta x - \mu_{\Delta x})\right\}$$

$$p(\Delta T - H\Delta x) = \frac{1}{2\pi |CRC^T|^{1/2}} \exp\left\{-\frac{1}{2}(\Delta T - H\Delta x)^T (CRC^T)^{-1} (\Delta T - H\Delta x)\right\}$$

$$p(\Delta T) = \frac{1}{2\pi |HMH^T + CRC^T|^{1/2}} \exp\left\{-\frac{1}{2}(\Delta T - H\mu_{\Delta x})^T (HMH^T + CRC^T)^{-1}\right.$$
$$\left. \cdot\, (\Delta T - H\mu_{\Delta x})\right\} \tag{8}$$

Substituting Equation (8) into Equation (7)

$$p(\Delta x \mid \Delta T) = \frac{\left|HMH^T + CRC^T\right|^{1/2}}{2\pi |M|^{1/2}\, |CRC^T|^{1/2}} \exp\left\{-\frac{1}{2}\right.$$

$$\cdot \left[(\Delta x - \mu_{\Delta x})^T \left(M^{-1} + H^T (CRC^T) H\right)(\Delta x - \mu_{\Delta x})\right.$$

$$+ \Delta T^T \left((CRC^T)^{-1} - (HMH^T \quad CRC^T)^{-1}\right)\Delta T$$

$$\left.\left. -\, \Delta T^T (CRC^T)^{-1} H (\Delta x - \mu_{\Delta x}) - (\Delta x - \mu_{\Delta x}) H^T (CRC^T)^{-1} \Delta T\right]\right\} \tag{9}$$

Upon completing the square in the exponent of Equation (9)

$$p \, (\Delta x \, \Delta T) = \frac{|HMH^T + CRC^T|^{1/2}}{2\pi |M|^{1/2} |CRC^T|^{1/2}}$$

$$\cdot \exp \left\{ -\frac{1}{2} (\Delta x - \Delta \hat{x}) \, p^{-1} (\Delta x - \Delta \hat{x}) \right\}$$

where

$$\Delta \hat{x} = \mu_{\Delta x} + PH^T (CRC^T)^{-1} (\Delta T - H\mu_{\Delta x}) \qquad (10)$$

and

$$P = (M^{-1} + H^T (CRC^T)^{-1} H)^{-1} \qquad (11)$$

or equivalently by the matrix inversion lemma

$$P = M - MH^T (MHM^T + CRC^T)^{-1} HM \qquad (12)$$

It is obvious that $\Delta \hat{x}$ maximizes $p \, (\Delta x \mid \Delta T)$ and thus $\hat{x} = \Delta \hat{x} + \tilde{x}$ is the optimal position estimate in the sense that it is the most likely RPV position.

Discussion of Errors

Any position estimation process working on uncertain data such as provided by the ranging signals T_1 and T_2 will unavoidably make estimation errors. In the last section it was shown that an optimal estimation process can be formulated to find the most likely RPV position under ranging uncertainties. In order to show adherence to accuracy requirements, it is necessary to investigate the position errors as a function of ranging uncertainties.

Observe that P, of Equation (11), is the covariance matrix of the Gaussian error about the optimal position estimate. Then, the square roots of the eigenvalues λ_1, λ_2 of P define the major and minor axis of the 39 percent likelihood ellipse about the optimal position estimate. Thus, the maximum distance error will be less than $D_e = \max (\sqrt{\lambda_1}, \sqrt{\lambda_2})$ with 39 percent likelihood. The maximum position error will be less than $2 D_e$ with 87 percent likelihood, $3 D_e$ with 99 percent likelihood, etc.

Selecting the worst-case (occurring immediately upon initial or reacquisition of ranging signals where the flight statistics of the RPV are unknown), we find M^{-1} to be zero valued. Thus,

$$P = (H^T (CRC^T)^{-1} H)^{-1}$$

Assuming equal noise variances, σ^2, at the RPV, master ground station, and slave ground station, D_e has been calculated for various ranges and angles from the master ground station. The results of this most unfavorable case are displayed in Figure 6.2.2. Using the estimate of 10 feet as the value of each ranging error σ achievable with the ranging equipment proposed, it is seen that the
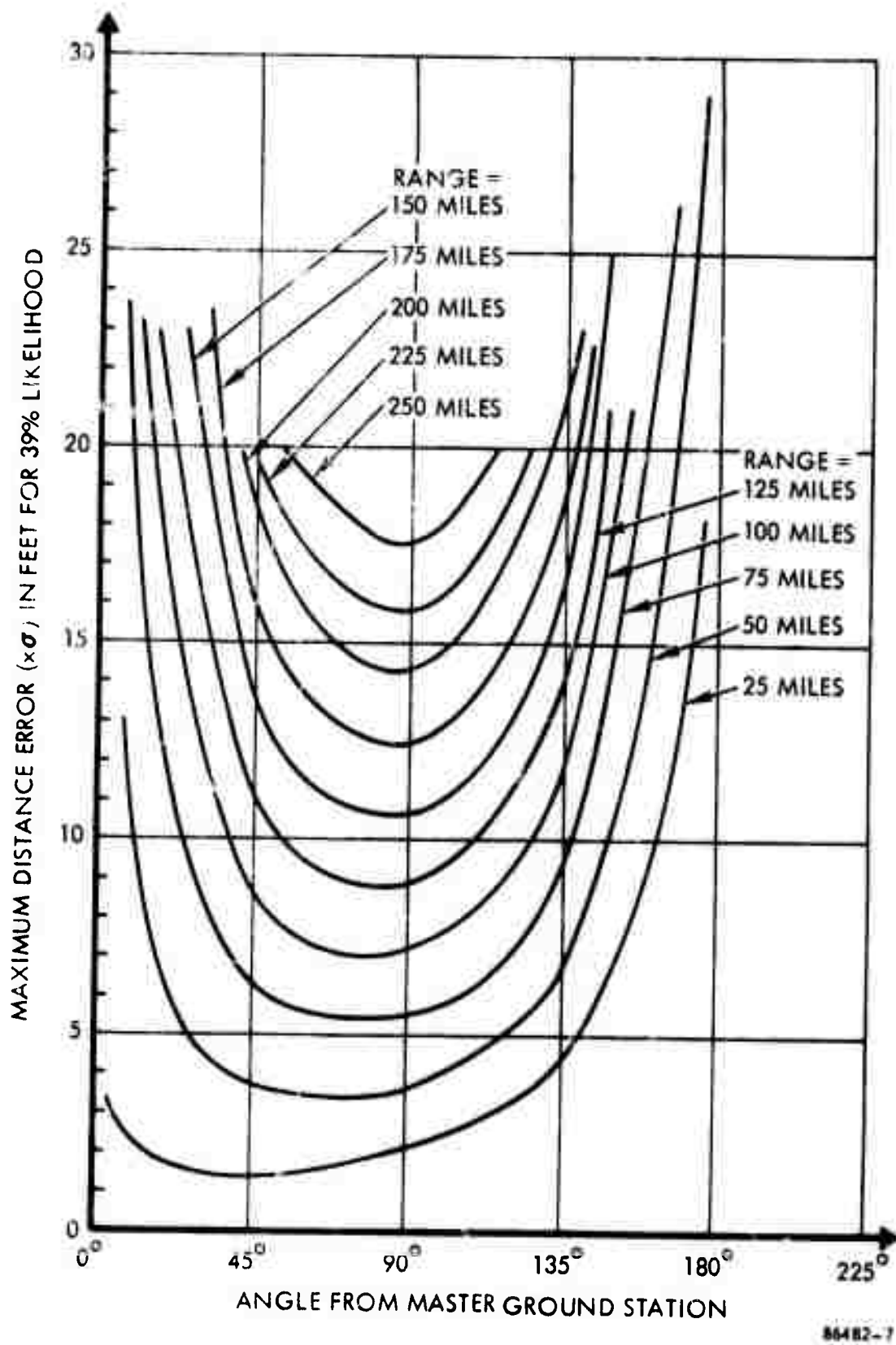
202

Figure 6.2.2.   Error Characteristics of the Two-Station Position Location System

203

RPV maximum position estimation error is less than 64 feet with 39 percent likelihood and less than 128 feet with 87 percent likelihood over a 90-degree sector at 50 miles range. For narrower sectors the error is correspondingly lessened – dropping to a low of 65 feet with 87 percent likelihood at 50 miles range. As this represents the initial most unfavorable error upon acquisition, a further reduction of error can be expected as the flight history of the RPV is built up.

Although the optimal incorporation of flight statistics has been developed for implementation, the resulting reduction in error has not yet been calculated. An upper bound can be quickly established, however. The equation of motion of the RPV is, in one dimension,

$$x = x_o + v_o t + 1/2 a t^2$$

Assuming a maximum RPV velocity of 1000 feet/second and a maximum acceleration of 20 g, and the proposed range sampling rate of 50 samples per second, then over 2 samples

$$x = x_o$$

within a 10.128-foot error, if v_o is taken to be 500 ft./sec. If two successive position estimates are averaged, this 10.128-foot maximum error, due to velocity and acceleration effects, will be reduced to 5.065 feet. More importantly, however, since the two position estimates are statistically independent, the error covariance P_{AVE} for the averaged position estimates becomes

$$P_{AVE} = \frac{1}{2} P$$

resulting in a $(D_e)_{AVE}$ of $\frac{1}{\sqrt{2}} D_e$. Now, with 87 percent likelihood at ranges over 50 miles and a sector of over 90 degrees the maximum position error is less than $\frac{128}{\sqrt{2}} + 5$ feet or 95 feet.

This upper bound establishes that the approach considered satisfies the basic accuracy requirement. Moreover, as the optimal process to be implemented fully utilizes the statistical information present in the ranging signals and the past flight history, it will meet the basic accuracy requirements over ranges considerably greater than 50 miles and sectors considerably greater than 90 degrees. Specific error characteristics as a function of acquisition time, range and angle will be furnished with the implementation.

Implementation of the Position Estimation Process

Considering that relative position errors must be held to less than .01 percent, the position estimation process can best be implemented on a digital basis through use of a minicomputer. The implementation will take the nature of a computer program which solves the equations

$$P = (M^{-1} + H^T (CRC^T)^{-1} H)^{-1} \tag{13}$$

$$\hat{x} = \mu_x + P H^T (CRC^T)^{-1} (\Delta T - H\mu_{\Delta x}) \tag{14}$$

for $\hat{x}$ about some linearization point $\tilde{x}$ where $\tilde{x}$ may be taken as

$$\tilde{x} = \begin{bmatrix} \frac{1}{2} T_1 \\ \\ T_2 - \frac{1}{2} T_1 \end{bmatrix}$$

upon initialization of the process, or as the last $\hat{x}$ upon continued execution.

Based upon a priori knowledge of the flight statistics, optimal values can be assigned to M^{-1} and μ_x. Initially, M^{-1} may be taken to be zero valued and μ_x may be taken as the initial $\tilde{x}$.

Solution of Equations (13) and (14) are not particularly formidable. In a higher level programming language such as FORTRAN, solution for P would require at most four statements while solution for $\hat{x}$ would require at most two statements. In the interest of maximum execution speed, however, these solutions will be accomplished directly in assembly language with an attendant increase of coding complexity. The following is a functional outline of the required program:

Position Estimation Program

A. <u>Input Range Timings</u>

Read in T. Time – 10 µs.

B. <u>Reinitialization Required?</u>

If the ranging signal is newly acquired, set

$$\tilde{R} = \begin{bmatrix} \frac{1}{2} T_1 \\ \\ T_2 - \frac{1}{2} T_1 \end{bmatrix}$$

Note – This is a simplification of the actual process to be used.

Time – 120 µs on a nonreoccurring basis.

C. <u>Compute the Linearized Position $\tilde{x}$ Based on the Range $\tilde{R}$</u>

$$\tilde{R}_1^{\ 2} = (\tilde{R}_1)^2$$

205

$$\widetilde{x} = \begin{bmatrix} (\widetilde{R}_1^{\,2} - (\widetilde{R}_2)^2 + C_1)/C_2 \\ \sqrt{(\widetilde{R}_1^{\,2} - (\widetilde{x}_2)^2)} \end{bmatrix}$$

Time – 127 µs for 4 scalar additions, 1 scalar subtraction, 4 scalar multiplications, 1 scalar division and 1 square-root operation.

Note – $C_1 = S^2$, $C_2 = 2S$. Both are precalculated.

D. <u>Compute A</u>

The linearized array A can be computed as

$$A = \begin{bmatrix} \widetilde{x}_1/\widetilde{R}_1 & \widetilde{x}_2/\widetilde{R}_1 \\ -\widetilde{x}_1/\widetilde{R}_2 & \widetilde{x}_2/\widetilde{R}_2 \end{bmatrix}$$

Time = 40 µs for 1 complementation and 4 divisions.

E. <u>Compute $\mu_{\Delta x}$</u>

$$\mu_{\Delta x} = \mu_{\Delta x} - \widetilde{x}$$

Time – 8 µs for two subtractions.

F. <u>Compute ΔT</u>

$$\Delta T = T - B A \mu_{\Delta x}$$

Note – B is precalculated.

Time – 64 µs for 2 matrix multiplications and 1 matrix subtraction or equivalently 2 scalar additions, 2 scalar subtractions and 8 scalar multiplications.

G. <u>Compute P^{-1}</u>

$$P^{-1} = M^{-1} + A^T (B^T (CRC^T)^{-1} B^T) A$$

Note – $B^T (CRC^T)^{-1} B^T$ is precalculated and stored as a matrix of four numbers.

Time – 136 µs for 2 matrix multiplications and 1 matrix addition or equivalently 10 scalar additions and 16 scalar multiplications.

H. Compute P

$$d = 1 / \left(P_{11}^{-1} P_{22}^{-1} - P_{12}^{-1} P_{21}^{-1} \right)$$

$$P_{11} = d P_{22}^{-1}$$

$$P_{12} = -d P_{12}^{-1}$$

$$P_{21} = -d P_{21}^{-1}$$

$$P_{22} = d P_{11}^{-1}$$

Time – 48 μs for 3 subtractions, and six multiplications.

I. Compute $\hat{x}$

$$\hat{x} = \mu_x - P A^T (B^T (CRC^T)^{-1}) (\Delta T - H \mu_{\Delta x})$$

Note – $B^T (CRC^T)^{-1}$ will be precalculated.

Time – 144 μs for 4 matrix multiplications, and two matrix subtractions or equivalently 8 scalar additions, 4 scalar subtractions, and 16 scalar multiplications.

J. Compute μ_x

For the next position estimate μ_x may be set to the present value of x or by using more sophisticated programming, flight statistics may be introduced to better predict the μ_x.

Time – 10 – 380 μs.

K. Compute M^{-1}

A preset value of M^{-1} can be used throughout the program or an improved estimate of M^{-1} based upon the flight history of the RPV can be calculated. The latter approach will be taken in implementation.

Time – 0 – 200 μs.

L. Return With x, the Updated Position Estimate

Time – 10 μs.

207

Based upon the functional breakdown of the program given above, each position estimate can be calculated in .6-1.2 milliseconds - well within the real-time requirement of 1 estimation per 20 milliseconds. In a multitask environment, a typical minicomputer such as the PDP-11/45 would be forced to devote less than 3-6 percent of its execution time and less than 1-2K words to the position estimation task.

APPENDIX A

APPENDIX A

This appendix develops performance characteristics of the command, status and video channels. The subsequent paragraphs present the pertinent details for analyzing the signal and noise for each channel.

A.1 Command Link

The command link signal consists of time-division multiplexed chirp signals whose starting frequency has been pseudo-randomly selected. At the receiver, the appropriate chirp signal is gated to a matched filter long enough to accept all starting frequencies. Bits are determined by transmission of either an up or a down chirp.

In the following paragraphs the signal and white noise response of the receiver will be developed and the theoretically realizable bit error rates determined. The effects of receiver imperfections, IF filtering, side lobes, and frequency offsets on this bit error rate will be determined.

A.1.1 Signal Response of Filter

For all analyses, a linearly swept signal of the form

$$s(t) = A \cos\left(\omega_s t + \frac{r}{2} t^2\right) \qquad 0 < t < T_s$$
$$= 0 \qquad\qquad\qquad \text{otherwise}$$

will be assumed.

ω_s is the initial frequency of the chirp

r is the chirp rate $= \dfrac{2\pi\Delta f_s}{T_s}$

Δf_s is the range of the sweep

T_s is the time duration of the sweep

A is the peak amplitude of the signal $= \sqrt{2S}$

The receiver filter to be matched to this waveform will be assumed to have an impulse response of

$$m(t) = b(t) \cos\left[\omega_m t - \frac{r}{2} t^2 + \phi_e(t)\right]$$

where ω_m is the initial frequency of the impulse response

$\phi_e(t)$ is the phase error form ideal matching

T_m is the duration of the impulse response

and $b(t)$ is the envelope function of time and is only nonzero $0 < t < T_m$.

The output of the matched filter to a signal input can be written as

$$i(T) = \int_{-\infty}^{\infty} s(T-t)\, m(t)\, dt$$

$$= \int_{0,\ T-T_s}^{T_m,\ T} A\, b(t) \cos\left[\omega_s(T-t) + \frac{r}{2}(T-t)^2\right] \cos\left[\omega_m(t) - \frac{r}{2} t^2 + \phi_e(t)\right] dt$$

where the greater of the lower limits and the lesser of the upper limits is chosen. Taking the product of cosines

$$i(T) = \frac{A}{2} \int_{0,\ T-T_s}^{T_m,\ T} b(t) \left[\cos\left[\omega_s(T-t) + \omega_m t + \frac{r}{2}(T-t)^2 - \frac{r}{2} t^2 + \phi_e(t)\right]\right.$$

$$\left. + \cos\left[\omega_s(T-t) - \omega_m t + \frac{r}{2}(T-t)^2 + \frac{r}{2} t^2 - \phi_e(t)\right]\right] dt$$

Because of the large values of ω_s and ω_m, the second term will approach zero after integration. Rewriting the first term gives

$$i(T) = \frac{A}{2} \int_{0,\ T-T_s}^{T_m,\ T} b(t) \cos\left[(\omega_m - \omega_s - rT)t + \phi_e(t) + \left(\omega_s T + \frac{r}{2} T^2\right)\right] dt$$

Initially, assume $\phi_e(t)$ is zero and $b(t)$ is 1 so the matched filtering is perfect. Then

$$i(T) = \frac{A}{2}\, \frac{\sin\left[(\omega_m - \omega_s - rT) L_u + \left(\omega_s T + \frac{r}{2} T^2\right)\right] - \sin\left[(\omega_m - \omega_s - rT) L_L + \left(\omega_s T + \frac{r}{2} T^2\right)\right]}{\omega_m - \omega_s - rT}$$

where L_u is least of T_m, T and L_L is greater of $0, T - T_s$.

211

$$r(\tau) = A \cos\left[(\omega_m - \omega_s - r\tau)(L_U + L_L)/2 + \left(\omega_s \tau + \frac{r}{2}\tau^2\right)\right] \frac{\sin\left[(\omega_m - \omega_s - r\tau)(L_U - L_L)/2\right]}{\omega_m - \omega_s - r\tau}$$

This approaches a peak value at $\tau = (\omega_m - \omega_s)/r$ of

$$\frac{A}{2}(L_U - L_L) \cos\left(\omega_s \tau + \frac{r}{2}\tau^2\right)$$

For

$$T_s < \tau < T_m$$

$$L_U - L_L = T_s$$

and the envelope value is

$$\frac{A \sin\left[(\omega_m - \omega_s - r\tau) T_s/2\right]}{\omega_m - \omega_s - r\tau}$$

which has power $\dfrac{A^2 T_s^2}{8} = \dfrac{S T_s^2}{4}$

at peak. The effect of small $\phi_e(t)$ on the envelope of the peak of the time response is developed next.

The chirp response equation can be written as

$$r(\tau) = \frac{A}{2}\left[\cos\left(\omega_s \tau + \frac{r\tau^2}{2}\right)\right] \int_{\tau - T_s}^{\tau} \cos\left[(\omega_m - \omega_s - r\tau)t + \phi_e(t)\right] dt$$

$$- \sin\left(\omega_s \tau + \frac{r\tau^2}{2}\right) \int_{\tau - T_s}^{\tau} \sin\left[(\omega_m - \omega_s - r\tau)t + \phi_e(t)\right] dt$$

for

$$T_s < \tau < T_m$$

The envelope squared can be written as

$$|r(\tau)|^2 = \frac{A^2}{4}\left[\left(\int_{\tau - T_s}^{\tau} \cos(\omega_o t + \phi_e(t))\, dt\right)^2 + \left(\int_{\tau - T_s}^{\tau} \sin(\omega_o t + \phi_e(t))\, dt\right)^2\right]$$

212

where $\qquad \omega_o = \omega_m - \omega_s - r\tau$

It can be shown that for $\phi_e(t) = 0$, the peak occurs at $\omega_o = 0$. Assuming that it still occurs near this value and that $\phi_e(t)$ is small, the sin and cos functions can be replaced by their small signal values and near $\tau = (\omega_m - \omega_s)/r$.

$$|r(\tau)|^2 = \frac{A^2}{4}\left[\left(\int_{\tau-T_s}^{\tau} 1 - \frac{(\omega_o t + \phi_e(t))^2}{2}\, dt\right)^2 + \left(\int_{\tau-T_s}^{\tau}(\omega_o t + \phi_e(t))\, dt\right)^2\right]$$

$$= \frac{A^2}{4}\left[\left(T_s - \frac{\omega_o^2 \tau^3}{6} + \frac{\omega_o^2(\tau-T_s)^3}{6} - \int_{\tau-T_s}^{\tau}\omega_o t\, \phi_e(t)\, dt - \int_{\tau-T_s}^{\tau}\frac{\phi_e^2(t)}{2}\, dt\right)^2\right.$$

$$\left. + \left(\frac{\omega_o \tau^2}{2} - \frac{\omega_o(\tau-T_s)^2}{2} + \int_{\tau-T_s}^{\tau}\phi_e(t)\, dt\right)^2\right]$$

Because of the small values of ω_o and ϕ_e only terms multiplying T_s in the first square of the last expression need be considered.

$$|r(\tau)|^2 = \frac{A^2}{4}\left[T_s^2 - \frac{T_s}{3}\omega_o^2(3\tau^2 T_s - 3\tau T_s^2 + T_s^3) - 2T_s\omega_o\int_{\tau-T_s}^{\tau}t\,\phi_e(t)\, dt\right.$$

$$- T_s\int_{\tau-T_s}^{\tau}\phi_e^2(t)\, dt + \left(\omega_o\tau T_s - \frac{\omega_o T_s^2}{2}\right)^2$$

$$\left. + 2\left(\omega_o\tau T_s - \frac{\omega_o T_s^2}{2}\right)\int_{\tau-T_s}^{\tau}\phi_e(t)\, dt + \left(\int_{\tau-T_s}^{\tau}\phi_e(t)\, dt\right)^2\right]$$

and rewriting this becomes,

$$= \frac{(AT_s)^2}{4}\left[1 - \frac{(\omega_o T_s)^2}{12} + \left(\frac{1}{T_s}\int_{\tau-T_s}^{\tau}\phi_e(t)\, dt\right)^2 - \frac{1}{T_s}\int_{\tau-T_s}^{\tau}\phi_e^2(t)\, dt\right.$$

213

$$+ \frac{2\omega_o T_s}{T_s} \int_{\tau - T_s}^{\tau} \left(\frac{\tau - t}{T_s} - \frac{1}{2} \right) \phi_e(t)\, dt \Bigg]$$

The envelope is a peak when

$$\frac{d|r|^2}{d\omega_o} = \frac{(A T_s)^2}{4} \left(- \frac{\omega_o T_s^2}{6} + 2 \int_{\tau - T_s}^{\tau} \left(\frac{\tau - t}{T_s} - \frac{1}{2} \right) \phi_e(t)\, dt \right) = 0$$

which requires that,

$$\omega_o = \frac{12}{T_s^2} \int_{\tau - T_s}^{\tau} \left(\frac{\tau - t}{T_s} - \frac{1}{2} \right) \phi_e(t)\, dt$$

The timing error is

$$\Delta \tau = \omega_o / r = \frac{12}{r T_s^2} \int_{\tau - T_s}^{\tau} \left(\frac{\tau - t}{T_s} - \frac{1}{2} \right) \phi_e(t)\, dt$$

This value of ω_o yields an envelope

$$|r(\tau)|^2 = \left(\frac{A T_s}{2} \right)^2 \left(1 + 12 \left(\frac{1}{T_s} \int_{\tau - T_s}^{\tau} \left(\frac{\tau - t}{T_s} - \frac{1}{2} \right) \phi_e(t)\, dt \right)^2 \right.$$

$$\left. + \left(\frac{1}{T_s} \int_{\tau - T_s}^{\tau} \phi_e(t)\, dt \right)^2 - \frac{1}{T_s} \int_{\tau - T_s}^{\tau} \phi_e^2(t)\, dt \right.$$

Noting that,

$$\left(\frac{A T_s}{2} \right)^2 \qquad \text{is the value for zero error}$$

$$\frac{1}{T_s} \int_{\tau - T_s}^{\tau} \phi_e(t)\, dt \quad \text{is the average error } \overline{\phi_e}$$

214

$$\frac{1}{T_s} \int_{\tau-T_s}^{\tau} \phi_e^2(t) \, dt \quad \text{is the variance } \overline{\phi_e^2}$$

The loss can be written as,

$$L = 1 + \frac{(r \, T_s \, \Delta\tau)^2}{12} - \overline{\phi_e^2(t)} + \overline{\phi_e(t)}^2$$

where $\overline{(-)}$ denotes the average between $\tau - T_s$ and τ. The effect of slope mismatch can be determined using these relationships. If the actual slope is r_m

$$\phi_e(t) = \frac{(r - r_m) t^2}{2}$$

$$\Delta\tau = -\frac{12}{r \, T_s^3} \int_{\tau-T_s}^{\tau} \left(\tau - \frac{T_s}{2} - t\right) \frac{(r - r_m)}{2} t^2 \, dt$$

$$= \left(1 - \frac{r_m}{r}\right)\left(\tau - \frac{T_s}{2}\right)$$

The loss from the previous equations is

$$L = 1 + \frac{\left[\left(1 - \frac{r_m}{r}\right)\left(\tau - \frac{T_s}{2}\right) r \, T_s\right]^2}{12} - \frac{1}{T_s} \int_{\tau-T_s}^{\tau} \frac{(r - r_m)^2 t^4}{4} \, dt + \left(\frac{1}{T_s} \int_{\tau-T_s}^{\tau} \frac{r - r_m}{2} t^2 \, dt\right)^2$$

$$= 1 - \frac{(r - r_m)^2 T_s^4}{720}$$

and is independent of τ.

Noting that $r = \frac{2\pi\Delta f}{T_s}$, then

$$L = 1 - \frac{\left(1 - \frac{r_m}{r}\right)^2 \left(\Delta f_s T_s\right)^2}{18.2}$$

215

This loss is plotted in Figure A-1 along with the loss calculated without the small error approximation. It can be seen that a close agreement exists in the region of interest.

Effect of Amplitude Ripple on Peak

Assume $\phi_e(t)$ is zero and writing $r(\tau)$ in exponential notation gives

$$r(\tau) = r_e\left[\frac{A}{2}\int_{0,\,\tau-T_s}^{T_m,\tau} b(t)\,e^{i\left(\omega_0 t + \omega_s\tau + \frac{r}{2}\tau^2\right)}\right]dt$$

where $\qquad \omega_0 = (\omega_m - \omega_s - r\tau)$

The envelope of $r(\tau)$ is given by

$$|r(\tau)| = \frac{A}{2}\left|\int_{0,\,\tau-T_s}^{T_m,\tau} b(t)\,e^{i\omega_0 t}\,dt\right|$$

$$= \frac{A}{2}\,|B(\omega_0)|$$

where $|B(\omega_0)|$ is the magnitude of the Fourier transform of $b(t)$ over the time of the signal. For $b(t)$ flat the sin x/x curve previously derived is obtained.
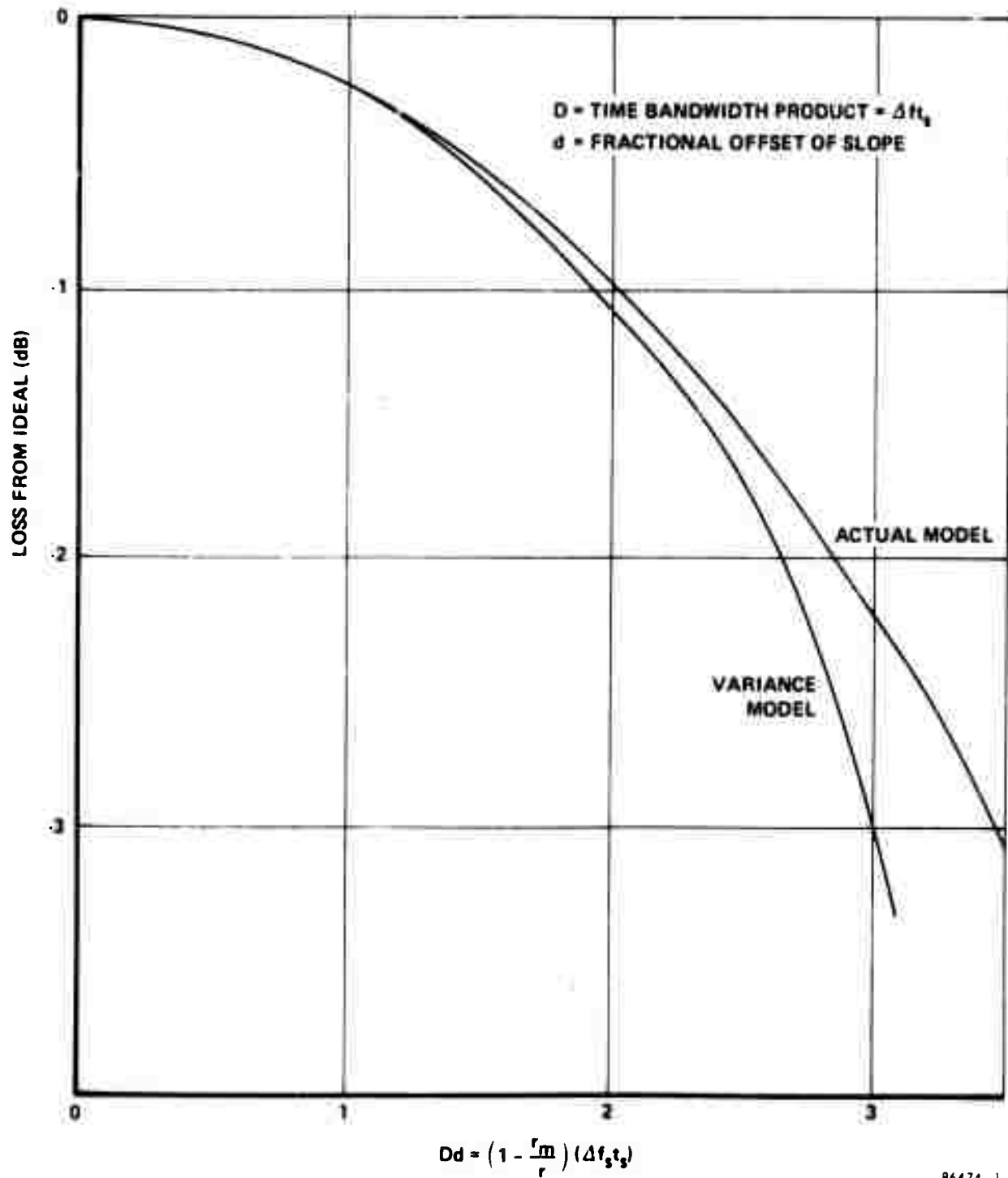
For no phase error and exponential amplitude rolloff of the matched filter, the envelope of the response can be written as

$$|r(\tau)| = \frac{A}{2}\left|\int_{\tau-T_s}^{\tau} e^{(-\alpha + j\omega_0)t}\,dt\right|$$

$$= \frac{A}{2}\left|\frac{e^{(-\alpha + j\omega_0)\tau} - e^{(-\alpha + j\omega_0)(\tau - T_s)}}{-\alpha + j\omega_0}\right|$$

where $\qquad \alpha = $ rolloff in nepers/second

$$\omega_0 = \omega_m - \omega_s - r\tau$$

and $\qquad T_s < \tau < T_m$

216

Figure A-1. Main Lobe Loss From Slope Offset

217

Performing the magnitude

$$|r(\tau)| = \frac{A}{2(\alpha^2 + \omega_o^2)}\left[\left[-\alpha\left(e^{-\alpha\tau}\cos\omega_o\tau - e^{-\alpha(\tau - T_s)}\cos\omega_o(\tau - T_s)\right)\right.\right.$$

$$+ \omega_o\left(e^{-\alpha\tau}\sin\omega_o\tau - e^{-\alpha(\tau - T_s)}\sin\omega_o(\tau - T_s)\right)\Big]^2$$

$$\left[-\alpha\left(e^{-\alpha\tau}\sin\omega_o\tau - e^{-\alpha(\tau - T_s)}\sin\omega_o(\tau - T_s)\right)\right.$$

$$\left.\left.- \omega_o\left(e^{-\alpha\tau}\cos\omega_o\tau - e^{-\alpha(\tau - T_s)}\cos\omega_o(\tau - T_s)\right)\right]^2\right]^{\frac{1}{2}}$$

Noting the similarities between lines 1 and 4 and between 2 and 3

$$|r(\tau)|^2 = \frac{A(\omega_o^2 + \alpha^2)^{\frac{1}{2}}}{2(\omega_o^2 + \alpha^2)}\left[\left(e^{-\alpha\tau}\cos\omega_o\tau - e^{-\alpha(\tau - T_s)}\cos\omega_o(\tau - T_s)\right)^2\right.$$

$$\left.+ \left(e^{-\alpha\tau}\sin\omega_o\tau - e^{-\alpha(\tau - T_s)}\sin\omega_o(\tau - T_s)\right)^2\right]^{\frac{1}{2}}$$

$$= \frac{A}{2(\omega_o^2 + \alpha^2)^{1/2}}\left[e^{-2\alpha\tau} + e^{-2\alpha(\tau - T_s)} - 2e^{-\alpha(2\tau - T_s)}\right.$$

$$\left.\left(\cos\omega_o\tau\cos\omega_o(\tau - T_s) + \sin\omega_o\tau\sin\omega_o(\tau - T_s)\right)\right]^{\frac{1}{2}}$$

$$= \frac{A}{2(\omega_o^2 + \alpha^2)^{1/2}}\left[e^{-2\alpha\tau} + e^{-2\alpha(\tau - T_s)} - 2e^{-\alpha(2\tau - T_s)}\cos\omega_o T_s\right]^{\frac{1}{2}}$$

Differentiating the envelope with respect to ω_o to determine the peak gives a peak at $\omega_o = 0$ and

$$|r(\tau)|_{max} = \frac{A}{2\alpha}\left(e^{-\alpha(\tau - T_s)} - e^{-\alpha\tau}\right)$$

$$r(\tau_m) = \frac{A}{2\alpha}e^{-\alpha\tau_m}\left(e^{\alpha T_s} - 1\right)$$

218

With τ_m being the time of the peak

$$\tau_m = \frac{\omega_m - \omega_s}{r_s} = \frac{(f_m - f_s) T_s}{\Delta f_s}$$

A.1.2   Effect of Noise on Matched Filter Output

In order to minimize the effects of noise on the chirp matched filter, the filter input is gated on only during the time a signal is present. The total filter is thus a function of time and a time domain analysis will be used.

Consider the noise of one-sided spectral density N_o and bandwidth B, larger than the highest signal frequency of concern. The noise into the chirp filter is $n_i(t)$ for $0 < t < T_s$ and zero otherwise. The output noise $N_o(\tau)$ can be written as

$$N_o(\tau) = \int_{0,\,\tau-T_s}^{T_m,\,\tau} n_i(\tau - t)\, b(t) \cos\left(\omega_m t - \frac{r}{2} t^2 + \phi_e(t)\right) dt$$

The mean square value is assuming $T_s < t < T_m$

$$\overline{N_o^2(\tau)} = \overline{\left(\int_{\tau - T_s}^{\tau} n_i(\tau - t)\, b(t) \cos\left(\omega_m t - \frac{r}{2} t^2 + \phi_e(t)\right) dt\right)^2}$$

$$= \int_{\tau - T_s}^{\tau} \int_{\tau - T_s}^{\tau} \overline{n_i(\tau - t)\, n_i(\tau - x)}\, b(t)\, b(x) \cos\left(\omega_m t - \frac{r}{2} t^2 + \phi_e(t)\right)$$

$$\cos\left(\omega_m x - \frac{r}{2} x^2 + \phi_e(x)\right) dx\, dt$$

letting $x = t + y$

$$\overline{N_o^2(\tau)} = \int_{\tau - T_s}^{\tau} \int_{\tau - T_s - t}^{\tau - t} \overline{n_i(\tau - t)\, n_i(\tau - t - y)}\, b(t)\, b(t + y)$$

$$\cos\left(\omega_m t - \frac{r}{2} t^2 + \phi_e(t)\right) \cos\left(\omega_m(t + y) + \frac{r}{2}(t + y)^2 + \phi_e(t + y)\right) dy\, dt$$

219

The noise term is simply the autocorrelation function $R_{nn}(y)$. For wideband noise, this will fall to zero for y significantly different from 0 so the expression can be written as

$$\overline{N_o^2(\tau)} = \int_{-\infty}^{\infty} R_{nn}(y)\,dy \int_{\tau-T_s}^{T} b^2(t)\cos^2\left(\omega_m t - \frac{r}{2}t^2 + \phi_e(t)\right) dt$$

but

$$\int_{-\infty}^{\infty} R_{nn}(y)\,dy = N_o/2$$

That is, the two-sided power spectral density of the noise at zero frequency.

$$N_o^2(\tau) = \frac{N_o}{2}\int_{\tau-T_s}^{T} b^2(t)\; \frac{1 + \cos\left(2\omega_m t - r\,t^2 + 2\phi_e(t)\right)}{2}\, dt$$

For $\omega_m T_s \gg 1$ the cosine term disappears and

$$\overline{N_o^2(\tau)} = \frac{N_o}{4}\int_{\tau-T_s}^{T} b^2(t)\,dt$$

for a flat matched filter $b^2(t) = 1$

$$\overline{N_o^2(\tau)} = \overline{N_o^2} = \frac{N_o T_s}{4}$$

for an exponentially decaying filter $b^2(t) = e^{-2\alpha t}$

$$\overline{N_o^2(\tau)} = \frac{N_o}{8\alpha}\left(e^{-2\alpha(\tau - T_s)} - e^{-2\alpha\tau}\right)$$

$$= \frac{N_o}{8\alpha}\, e^{-2\alpha\tau}\left(e^{2\alpha T_s} - 1\right)$$

The signal-to-noise ratio at the output peak is for the ideal case

$$S/N = \frac{S T_s^2}{4} \Big/ \frac{N_o T_s}{4} = \frac{S T_s}{N_o}$$

220

For the exponential rolloff in amplitude case

$$S/N = \frac{S e^{-2\alpha T_m}}{4\alpha^2} \left(e^{\alpha T_s} - 1\right)^2 \Big/ \frac{N_o}{8\alpha} e^{-2\alpha T_m} \left(e^{2\alpha T_s} - 1\right)$$

$$= \frac{2}{\alpha} \frac{S}{N_o} \frac{e^{\alpha T_s} - 1}{e^{\alpha T_s} + 1}$$

The degradation because of an exponential decaying filter is

$$L = \frac{2}{\alpha T_s} \frac{e^{\alpha T_s} - 1}{e^{\alpha T_s} + 1}$$

$e^{\alpha T_s}$ is the voltage decay across a time interval T_s or d dB

$$\alpha T_s = \frac{d}{20} \text{ in } 10 = .115 \, d$$

The loss is plotted versus d in Figure A-2.

It can be seen that reasonable attenuation with time in the matched filter has virtually no degrading effect on the signal.

A.1.3   **Effect of Doppler and Frequency Offset on Chirp**

The time of the peak of an ideal chirp through the ideal filter has been shown to be

$$\tau = \frac{\omega_m - \omega_s}{r} = \frac{(f_m - f_s) T_s}{\Delta f}$$

The error in τ from an error in ω_s is

$$\Delta \tau = \frac{d\tau}{d\omega_s} \Delta \omega_s = -\frac{\Delta \omega_s}{r}$$

The loss from this is assuming sampling at $t = 0$ is

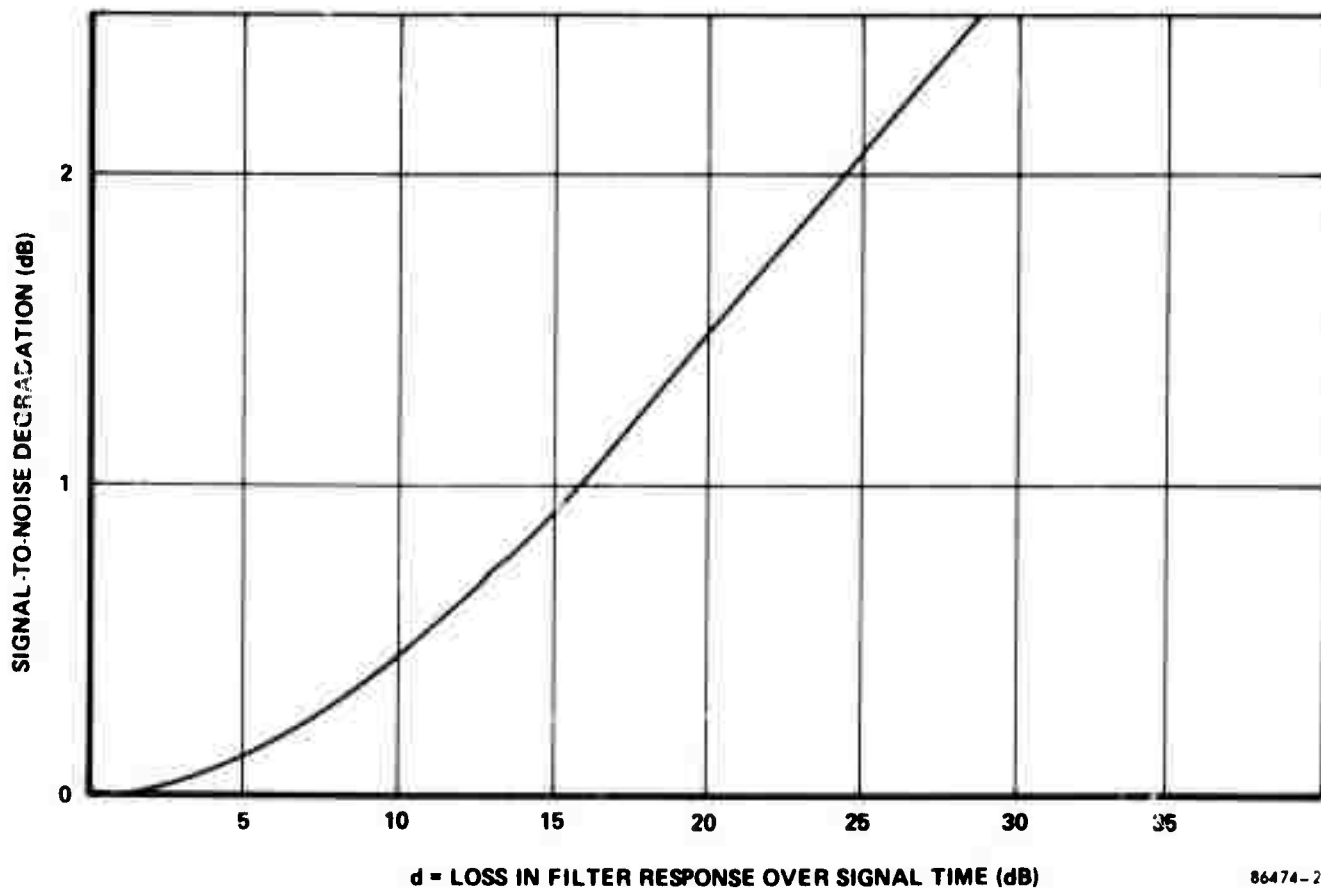$$L = \frac{Sin^2 \pi \Delta f_s T_s}{(\pi \Delta f_s T_s)^2}$$

221

Figure A-2.   Degradation Due to Matched Filter Decay

222

The loss is plotted versus frequency offset in Figure A-3.

Note that sampling will still occur at $T = 0$ since bits with chirps in opposite directions will have opposite sense ΔF's and the averaged ΔT will be zero.

A 15 GHz carrier with accuracy of 10^{-7} and doppler shift of 10^{-6} will have a frequency offset of 16.5 kHz corresponding to a loss of .39 dB.

Note that doppler will also provide a slope mismatch. It will only be on the order of .0001 percent, however, and will have virtually no effect on the loss.

A.1.4   Spectral Response of Chirp Matched Filter

The response of the filter plus IF gating to a complex sine wave can be written as

$$R(\omega,\tau) = \frac{1}{2} \int_{0,\,\tau-T_s}^{T_m,\,\tau} e^{i\omega(\tau-T)} b(t) \left[e^{i(\omega_m t - \frac{r}{2} t^2 + \emptyset_e(t))} \right.$$

$$\left. + e^{-i(\omega_m t - \frac{r}{2} t^2 + \emptyset_e(t))} \right] dt$$

For positive ω

$$\simeq \frac{1}{2} \int_{0,\,\tau-T_s}^{T_m,\,\tau} b(t)\, e^{i\left[(\omega_m - \omega)t - \frac{r}{2} t^2 + \emptyset_e(t) + \omega\tau\right]} dt$$

for an ideal filter $b(t) = 1$, $\emptyset_e(t) = 0$

$$R(\omega,\tau) = \frac{1}{2} \int_{0,\,\tau-T_s}^{T_m,\,\tau} e^{i\left[\frac{-(\omega_m - \omega)^2}{2r} - (\omega-\omega_m)t - \frac{r}{2} t^2 + \frac{(\omega-\omega_m)^2}{2r} + \omega\tau\right]} dt$$

$$= \frac{e}{2}^{i\left(\frac{(\omega-\omega_m)^2}{2r} + \omega\tau\right)} \int_{0,\,\tau-T_s}^{T_m,\,\tau} e^{-i\left(\frac{\omega-\omega_m}{\sqrt{2r}} + \sqrt{\frac{r}{2}} t\right)^2} dt$$

223
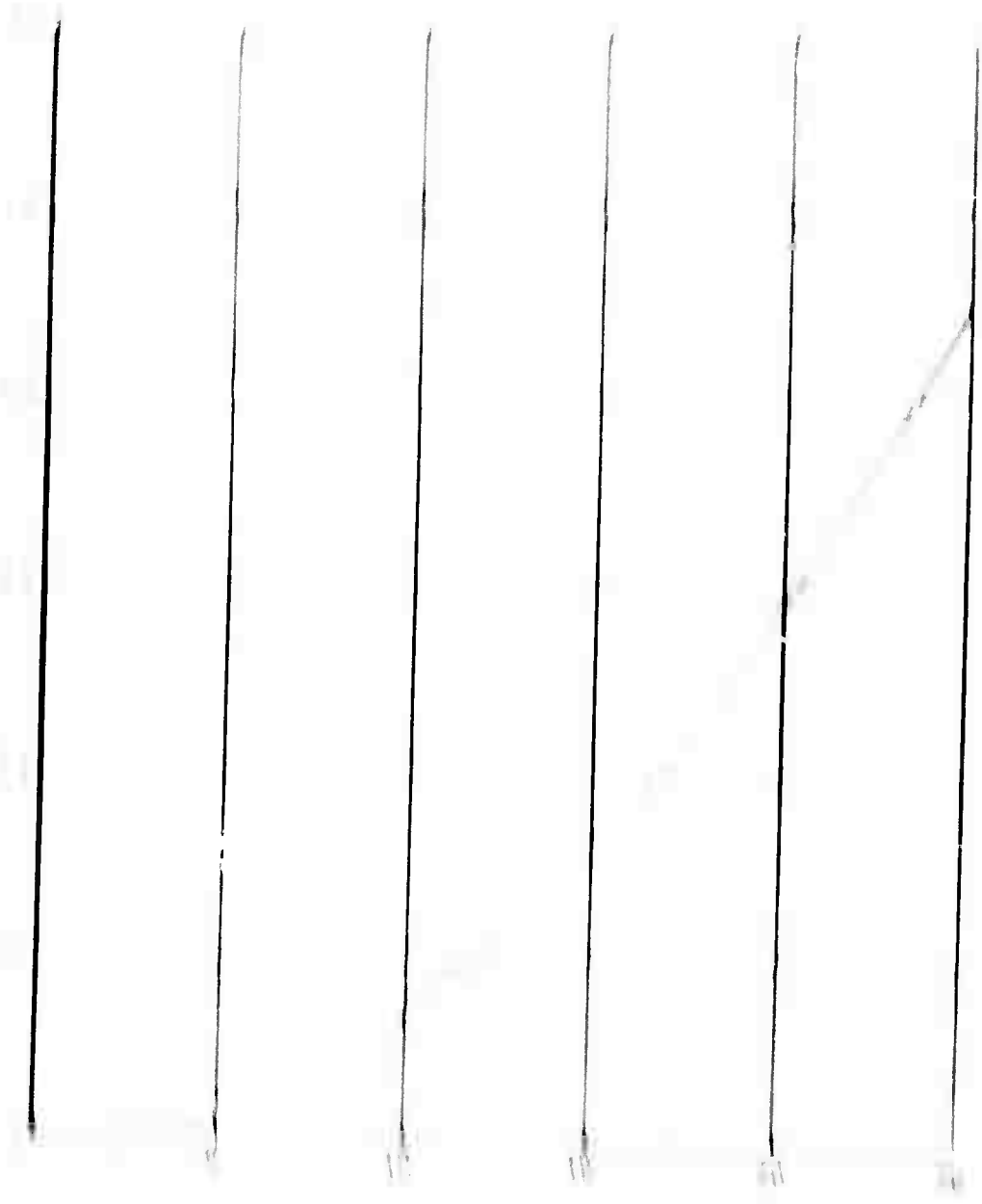
letting $x = \sqrt{\dfrac{r}{\pi}} \left(\dfrac{\omega - \omega_m}{r} + t \right)$

and writing the integral in trigonometric notation

$$R(\omega, \tau) = \frac{e}{2} i \left(\frac{(\omega - \omega_m)^2}{2r} + \omega\tau \right) \sqrt{\frac{\pi}{r}} \int_{L_1}^{L_2} \left(\cos \frac{\pi}{2} X^2 - i \sin \frac{\pi}{2} X^2 \right) dX$$

where L_1 is the greater of $\dfrac{\omega - \omega_m}{\sqrt{\pi r}}$ or $\sqrt{\dfrac{r}{\pi}} \left(\dfrac{\omega - \omega_m}{r} + \tau - T_s \right)$

and L_2 is the lesser of $\sqrt{\dfrac{r}{\pi}} \left(\dfrac{\omega - \omega_m}{r} + T_m \right)$ or $\sqrt{\dfrac{r}{\pi}} \left(\dfrac{\omega - \omega_m}{r} + \tau \right)$

substituting system parameters

$$L_1 = (2\Delta f T_s)^{\frac{1}{2}} \frac{f - f_m}{\Delta f}, \quad (2\Delta f T_s)^{\frac{1}{2}} \left[\frac{f - f_m}{\Delta f} + \frac{\tau}{T_s} - 1 \right]$$

$$L_2 = (2\Delta f T_s)^{\frac{1}{2}} \left(\frac{f - f_m}{\Delta f} + \frac{T_m}{T_s} \right), \quad (2\Delta f T_s)^{\frac{1}{2}} \left[\frac{f - f_m}{\Delta f} + \frac{\tau}{T_s} \right]$$

Noting that $\displaystyle\int_0^A \cos \frac{\pi}{2} X^2 \, dX = C(A)$

and $\displaystyle\int_0^A \sin \frac{\pi}{2} X^2 \, dX = S(A)$

are Fresnel integrals, the spectral response can be written as

$$R(\omega, \tau) = \frac{1}{2} \sqrt{\frac{\pi}{r}} \, e^{\, i \frac{(\omega - \omega_m)^2}{2r} + \omega\tau} \left[C(L_2) - C(L_1) - i \, S(L_2) + i \, S(L_1) \right]$$

225

The amplitude of the response is given by

$$\left| R(\omega,\tau) \right| = \frac{1}{2} \sqrt{\frac{\pi}{r}} \left[\left(C(L_2) - C(L_1) \right)^2 + \left(S(L_2) - S(L_1) \right)^2 \right]^{\frac{1}{2}}$$

and the phase by

$$\emptyset(\omega,\tau) = \frac{(\omega - \omega_m)^2}{2r} + \omega\tau - \tan^{-1} \frac{S(L_2) - S(L_1)}{C(L_2) - C(L_1)}$$

For $\qquad A \gg 1 \qquad C(A) \simeq S(A) \simeq .5$

for $\qquad A \ll -1 \qquad C(A) \simeq S(A) \simeq -.5$

For L_2 and L_1 that satisfy this relationship

$$\left| R(F,\tau) \right| = \frac{1}{2} \sqrt{\frac{2\pi}{r}} = \frac{1}{2} \sqrt{\frac{T_s}{\Delta f}}$$

$$\emptyset(F,\tau) = 2\pi \left(\frac{(f - f_m)^2}{2\Delta f} T_s + f\tau - \frac{1}{8} \right)$$

which indicates a constant amplitude and a quadradic phase response at a given delay time

Figure A-4 plots the degradation in R from $\frac{1}{2} \sqrt{T_s/\Delta f}$ and the difference in $\emptyset$ from quadric versus $f_0 \pm f$ for $\Delta f T_s = 128$ and $\Delta f = 12.8$. Where $f_0 = f_m - \left(\frac{\tau}{T_s} - \frac{1}{2} \right) \Delta f = f_c$ $+19.2 - 12.8 \frac{\tau}{T_s}$ and where f_c is the matched filter center frequency.

A.1.5 Signal Spectrum

Since the filter is matched to the signal it will have the same amplitude response and the inverse phase response for each sample provided τ in the matched filter response is chosen to correspond to $\frac{\omega_m - \omega_s}{r}$ making
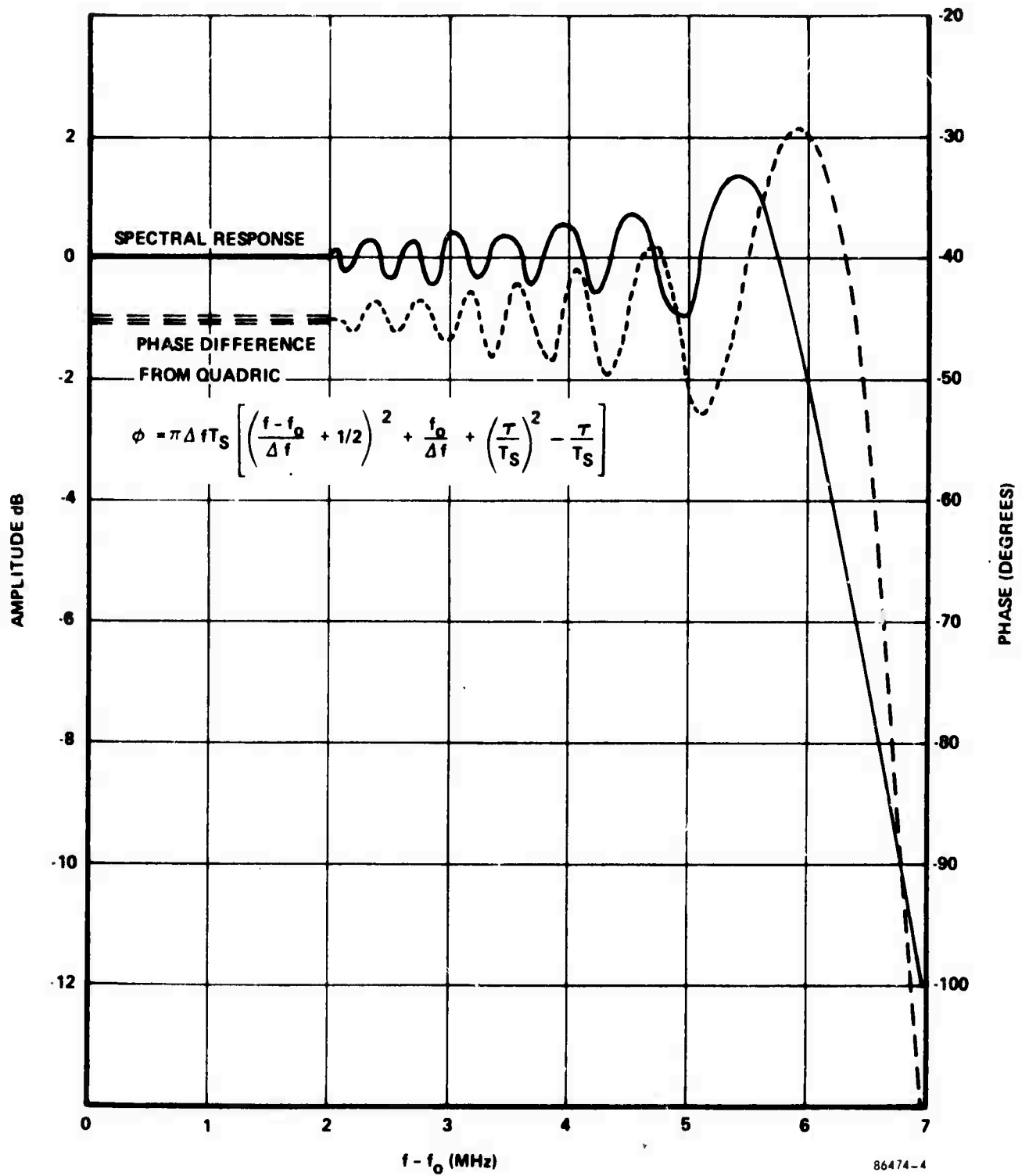
$$f_0 (\text{signal}) = f_s + \frac{\Delta f}{2}$$

226

$$\phi = \pi \Delta f T_S \left[\left(\frac{f - f_o}{\Delta f} + 1/2 \right)^2 + \frac{f_o}{\Delta f} + \left(\frac{T}{T_S} \right)^2 - \frac{T}{T_S} \right]$$

Figure A-4.   Frequency Characteristics of Chirp

227

Note from Figure A-4 the fast rolloff of power outside the band of interest greatly improving the problem of the chirp signal interfering with adjacent channels.

A.1.6   Power Rolloff With Frequency

Figure A-4 is reproduced in Figure A-5 with emphasis on the power beyond the chirp frequency range. Superimposed on this is the spectrum of a pn code with equivalent processing gain. It can be seen that the chirp spectrum is more than 25 dB below the peaks of the pn spectrum. This provides 25 dB more isolation from channel crosstalk than exists in the pn case.

A.1.7   Effect of IF Filtering

Let the spectral response of the signal be $AS(\omega)$. A matched filter then has spectral response $S(-\omega)$. Assume an IF filter with spectral response $H(\omega)$. Then

$$r(t) = \frac{A}{2\pi} \int_{-\infty}^{\infty} S(\omega)\, S(-\omega)\, H(\omega)\, e^{j\omega t}\, d\omega$$

$$= \frac{A}{2\pi} \int_{-\infty}^{\infty} |S(\omega)|^2\, H(\omega)\, e^{j\omega t}\, d\omega$$

It has been shown that the degradation due to amplitude variations of the input is minimal so only the phase shift of $H(\omega)$ will be investigated, and

$$r(t) = \frac{A}{2\pi} \int_{-\infty}^{\infty} |S(\omega)|^2\, e^{i(\phi_h(\omega) + \omega t)}\, d\omega$$

$$= \frac{A}{2\pi} \int_{0}^{\infty} |S(\omega)|^2 \left(e^{i(\phi_h(\omega) + \omega t)} + e^{i(\phi_h(-\omega) - \omega t)} \right) d\omega$$

$|S(\omega)|^2$ has been shown to be essentially flat from ω_s to $\omega_s + \Delta\omega$ with value

$$|S(\omega)|^2 \simeq \frac{2\pi}{4}\, \frac{T_s}{\Delta\omega} \qquad\qquad \omega_s < \omega < \omega_s + \Delta\omega$$
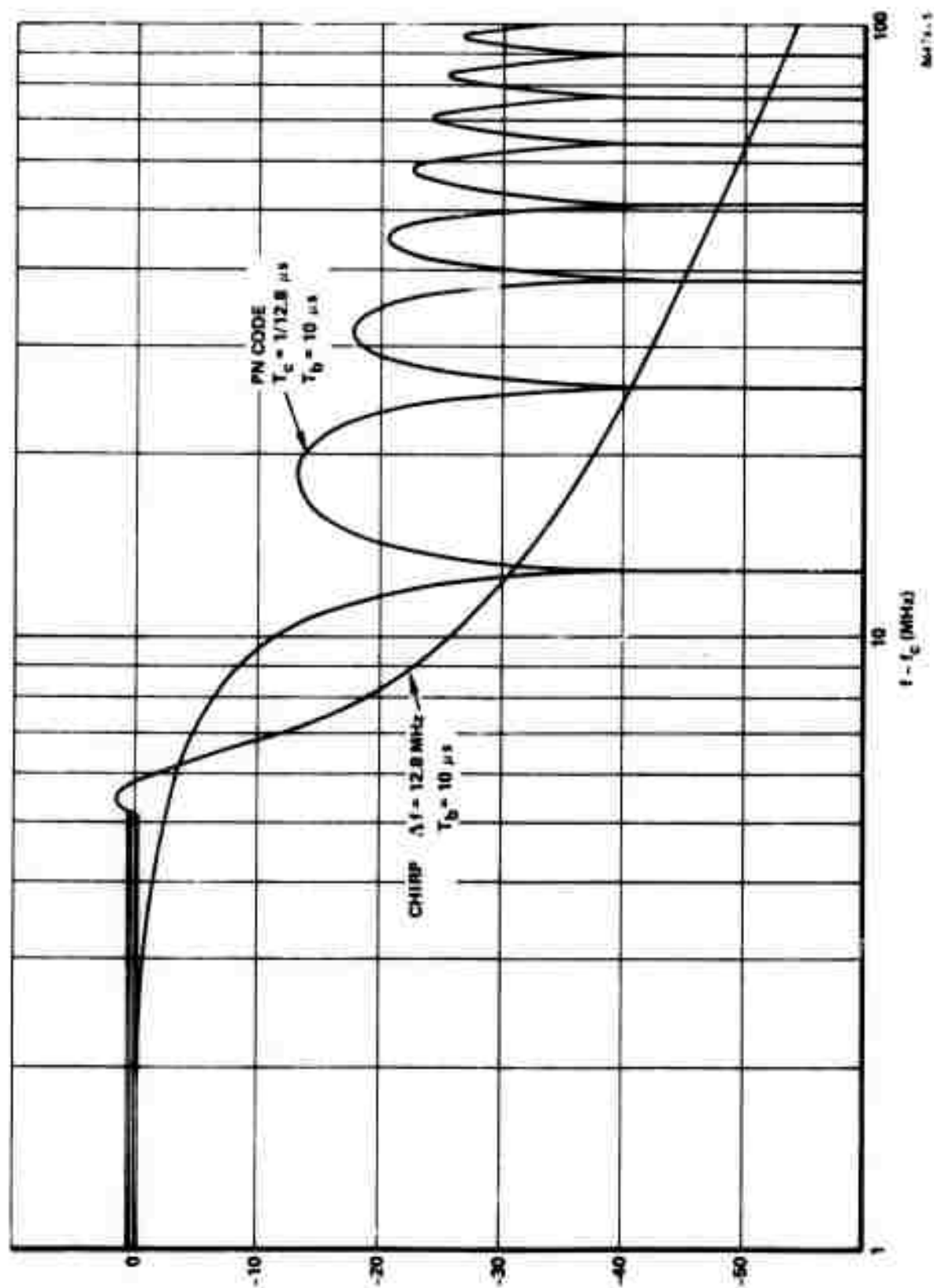
228

Figure A-5. Spectrum of Chirp and PN

229

and zero elsewhere. For physically realizable filters

$$\emptyset(-\omega) = -\emptyset(\omega)$$

$$r(t) \simeq \frac{AT_s}{4\Delta\omega} \int_{\omega_s}^{\omega_s + \Delta\omega} 2 \cos(\emptyset_h(\omega) + \omega t) \, d\omega$$

Since W is around the carrier frequency very small changes in f can give arbitrary phase and essentially any phase may be chosen and the equation related to the filter center frequency.

$$r(t) = \frac{AT_s}{2\Delta\omega} \int_{\omega_s - \omega_c}^{\omega_s + \Delta f - \omega_c} \cos(\phi_h(\omega' + \omega_c) + \omega' t + \phi) \, d\omega'$$

where t and ϕ are chosen to maximize the result.

For ϕ maximized

$$r(t) = \frac{AT_s}{2\Delta\omega} \left[\left[\int_{\omega_s - \omega_c}^{\omega_s + \Delta\omega - \omega_6} \cos(\phi_h(\omega' + \omega_c) + \omega' t) \, d\omega' \right]^2 + \left[\int_{\omega_s - \omega_c}^{\omega_s + \Delta\omega + \omega_c} \sin(\phi_h(\omega' + \omega_c) + \omega' t) \, d\omega' \right]^2 \right]^{1/2}$$

The form of this equation is identical to the instantaneous phase error equation developed earlier in Paragraph A.1.1. From that treatment

$$t_d = \frac{12}{\Delta\omega^3} \int_{\omega_s - \omega_c}^{\omega_s + \Delta\omega - \omega_c} (\omega_s - \omega_c + \frac{\Delta\omega}{2} - \omega) \phi_h(\omega + \omega_c) \, d\omega$$

is the time delay from the no filter case.

And,

$$r^2(t_d) = \left(\frac{AT_s}{2} \right)^2 \left(1 + \frac{(\Delta\omega t_d)^2}{12} \quad \overline{\emptyset_h^2(\omega)} + \overline{\emptyset_h(\omega)}^2 \right)$$

The loss compared to no filter is

$$L = 1 + \frac{(\Delta\omega td)^2}{12} - \overline{\emptyset_h^2(\omega)} + \overline{\emptyset_h(\omega)}^2$$

230

which is identical to the loss determined because of matched filter errors except the average is over frequency instead of time.

Numerical calculations were made for .5 dB ripple Chebyshev filters centered at spectrum center. The filters were run for various numbers of poles and ratios of 3 dB bandwidth to Δf. The filter phase shifts were determined by integrating group delay from Chebyshev response curves. The results are shown in Figure A-6. The curves show that the frequency spread can be .5 to .6 times the bandwidth for Chebyshev filter. More phase linear filters would allow somewhat larger Δf's but would have slower rolloff characteristics.

Note that chirping will actually go on over $2\Delta f$ because of the random start frequency. The IF bandwidth will therefore have to be about $3\Delta f$ or for a Δf of 12.8 MHz the 3 dB bandwidth should be about 38.4 MHz.

A.1.8   Bit Error Rate

At the time of peak signal from either the up-chirp or down-chirp filter, a comparison of the outputs is made and the bit decision is made corresponding to the largest envelope. Letting s be the signal envelope and r the envelope of noise alone the envelope of signal plus noise is represented by a Ricean distribution.

$$P(r_1) = \frac{r_1}{N} e^{-\frac{r_1^2 + s^2}{2N}} I_0\left(\frac{r_1 s}{N}\right)$$

Where r_1 is the envelope

N is the mean square noise

and I_0 is the modified Bessel function of the first kind and zeroth order.

The probability density function of the envelope r_2 out of the filter without a signal is Rayleigh distributed.

$$P(r_1) = \frac{r_2}{N} e^{-\frac{r_2^2}{2N}}$$

An error occures if $r_2 > r_1$. Its probability can be written

$$P_e = \int_0^\infty P(r_1) \int_{r_1}^\infty P(r_1) \, dr_2 \, dr_1$$
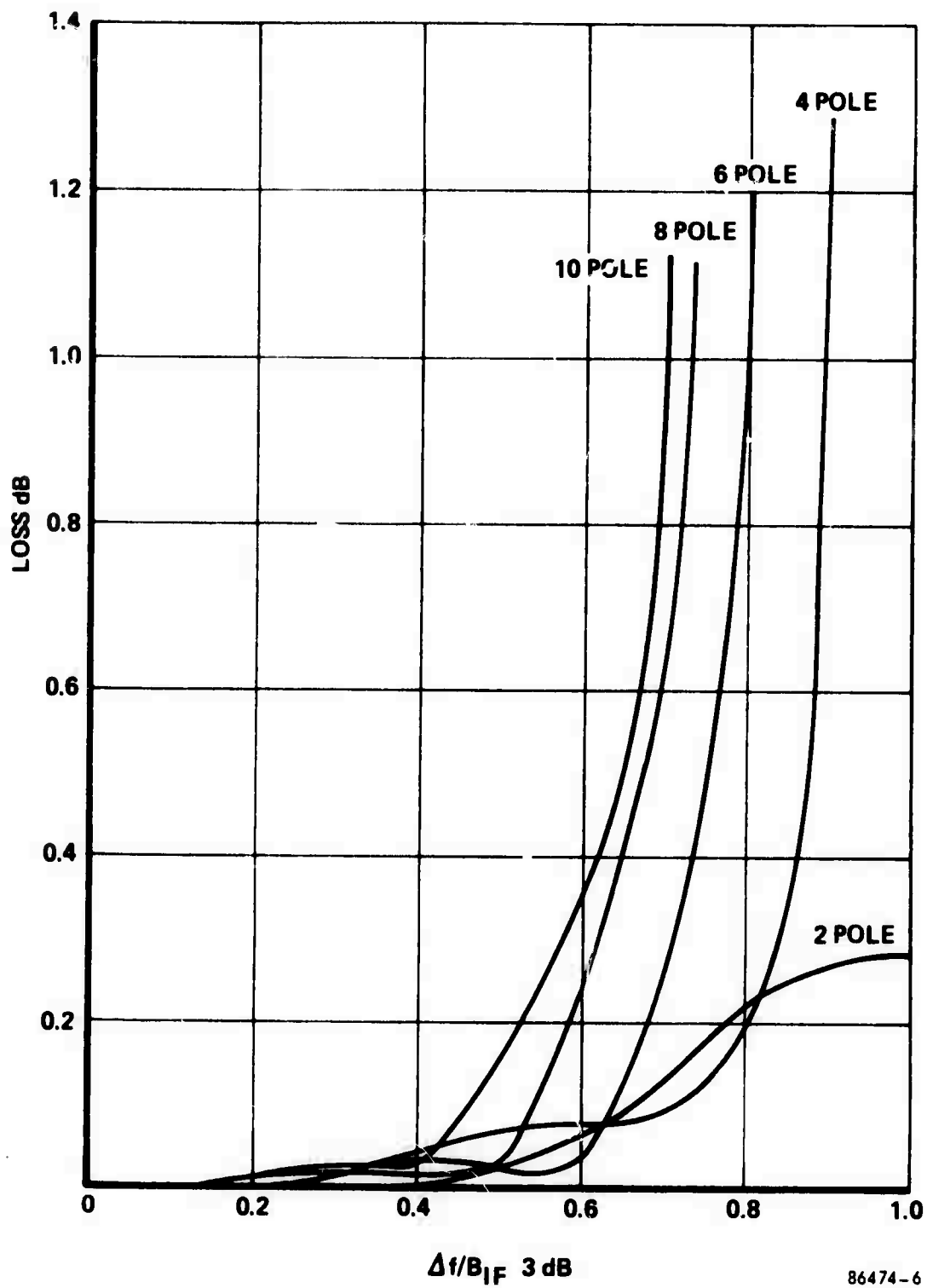
231

Figure A-6. Chebychev IF Effect on Chirp Gain .5 dB Ripple

232

$$= \int_0^\infty \frac{r_1}{N} e^{-\frac{r_1^2 + s^2}{2N}} I_0 \left(\frac{r_1 s}{N} \right) e^{-\frac{r_1}{2N}} dr_1$$

letting $\sqrt{2} r_1 = X$ and $\frac{s}{\sqrt{2}} = a$

$$P_e = \frac{1}{2} e^{-\frac{s^2}{4N}} \int_0^\infty \frac{X}{N} e^{-\frac{X^2 + a^2}{2N}} I_0 \left(\frac{aX}{N} \right) dX$$

The integral is the probability that an envelope from a signal with amplitude, a, plus noise of power N is greater than zero and is 1. Therefore,

$$P_e = \frac{1}{2} e^{-\frac{s^2}{4N}} = \frac{1}{2} e^{-\frac{1}{2} (S/N)}$$

A.2   BER Status Link

The downlink status data will consist of pulses of data time division multiplexed from each of the vehicles. The data will be PN code modulated DPSK data.

The data will be detected by regenerating the PN code, reproducing the DPSK and detecting it through matched filters. An appropriate model for the subsequent analysis consists of two matched filter devices of duration two bits. One of the devices is matched to a transition between bits and the other is not.

Three separate considerations will be made in determining bit error rate; the effect of frequency offset from the matched filter, the effect of timing jitter or offset and the effect of band limiting on the PN code. The band limiting will only degrade the level of the DPSK signal since any limitations will be much larger than the bit rate.

A.2.1   Effect of Frequency Offset

The outputs of the two matched filters will be compared at the appropriate time and the one with the largest envelope at the sampling time will determine the presence or absence of a transition. An error will occur if the output of the unmatched filter is larger than the output of the matched filter.

The matched filter model assumes the two filters have impulse responses of,

$$i_1 (t) = \text{Cos } \omega_0 t \qquad\qquad 0 < t < 2T_b$$

$$= 0 \qquad\qquad\qquad \text{otherwise}$$

233

$$i_2(t) = \text{Cos } \omega_o t \qquad\qquad 0 < t < T_b$$

$$\qquad\qquad = -\text{Cos } \omega_o t \qquad\qquad T_b < t < 2T_b$$

$$\qquad\qquad = 0 \qquad\qquad\qquad\qquad \text{otherwise}$$

It can be shown that for a signal matched to device 1 the output signal envelope at optimum time is

$$S_1 = AT_b \ \frac{\text{Sin} \Delta T_b}{\Delta T_b}$$

and from the unmatched device is

$$S_2 = AT_b \left(\frac{\text{Sin}^2 \Delta T_b/2}{(\Delta T_b/2)^2} - \frac{\text{Sin}^2 \Delta T_b}{(\Delta T_b)^2} \right)^{1/2}$$

where Δ is the frequency offset from ω_o in radians/second.

From a development identical to that of Paragraph A.1.2.

$$N = \frac{N_o}{2} \ T_b$$

If Δ is zero

$$S_1 = AT_b$$

$$S_2 = 0$$

$$S_{out} = \frac{A^2 T_b^2}{2} = P_s T_b^2$$

For this case, with no signal in the undesired device the output bit error rate can be expressed identically to the way it was for chirp since the envelope of signal plus noise is being compared to the envelope of noise alone.

$$BER = \frac{1}{2} \ e^{-(S/N) \ out/2} = \frac{1}{2} \ e^{-P_s T_b/N_o}$$

This bit error rate is plotted in Figure A-7.

As the frequency drifts from ω_o the signal out of the desired channel goes down and that in the undesired channel goes up. As long as the signal in the undesired channel is

234

Figure A-7

235
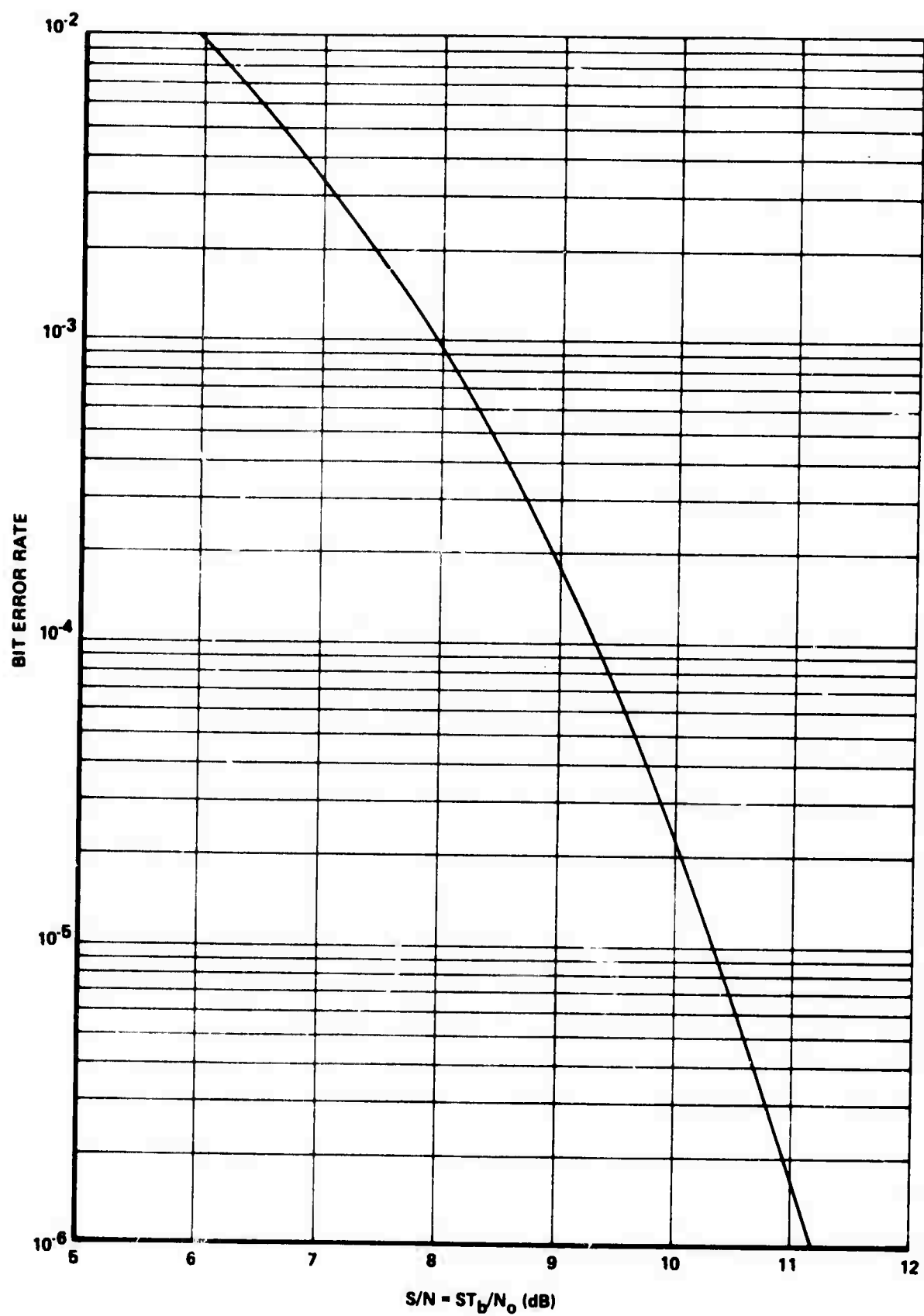
86474-27

much less than the noise only the reduction in power in the desired channel will contribute to errors and

$$BER = \frac{1}{2} e^{-\frac{P_s T_b}{N_o}} \frac{\sin^2 \Delta T_b}{(\Delta T_b)^2}$$

As the signal in the undesired channel increases the envelope in both channels tends to be Gaussian distributed about the signal with mean square value N and an error occurs if noise of power 2N is greater than the difference between S_1 and S_2. For this case

$$BER = \int_{S_1 - S_2}^{\infty} \frac{1}{\sqrt{4\pi N}} e^{-\frac{x^2}{4N}} dx$$

$$= \int_{\frac{S_1 - S_2}{\sqrt{2N}}}^{\infty} \frac{1}{\sqrt{2\pi}} e^{-\frac{y^2}{2}} dy$$

This integral is numerically solved in terms of the error function with the result that for 10^{-5} BER

$$\frac{S_1 - S_2}{\sqrt{2N}} = \sqrt{2\pi} \times 3.03$$

and

$$\frac{P_s T_b}{N_o} = \frac{3.03^2}{\left[\frac{\sin \Delta T_b}{\Delta T_b} - \left(\frac{\sin^2 \Delta T_b / 2}{(\Delta T_b / 2)^2} - \frac{\sin^2 \Delta T_b}{(\Delta T_b)^2} \right)^{1/2} \right]^2}$$

This curve along with the small signal in the undesired device curve for 10^{-5} BER are plotted in Figure A-8. The actual requirement will transition between the worst of these curves as shown by the dotted line. The curve shows considerable degradation with frequency offset primarily because of the nonorthogonality of the two inputs.
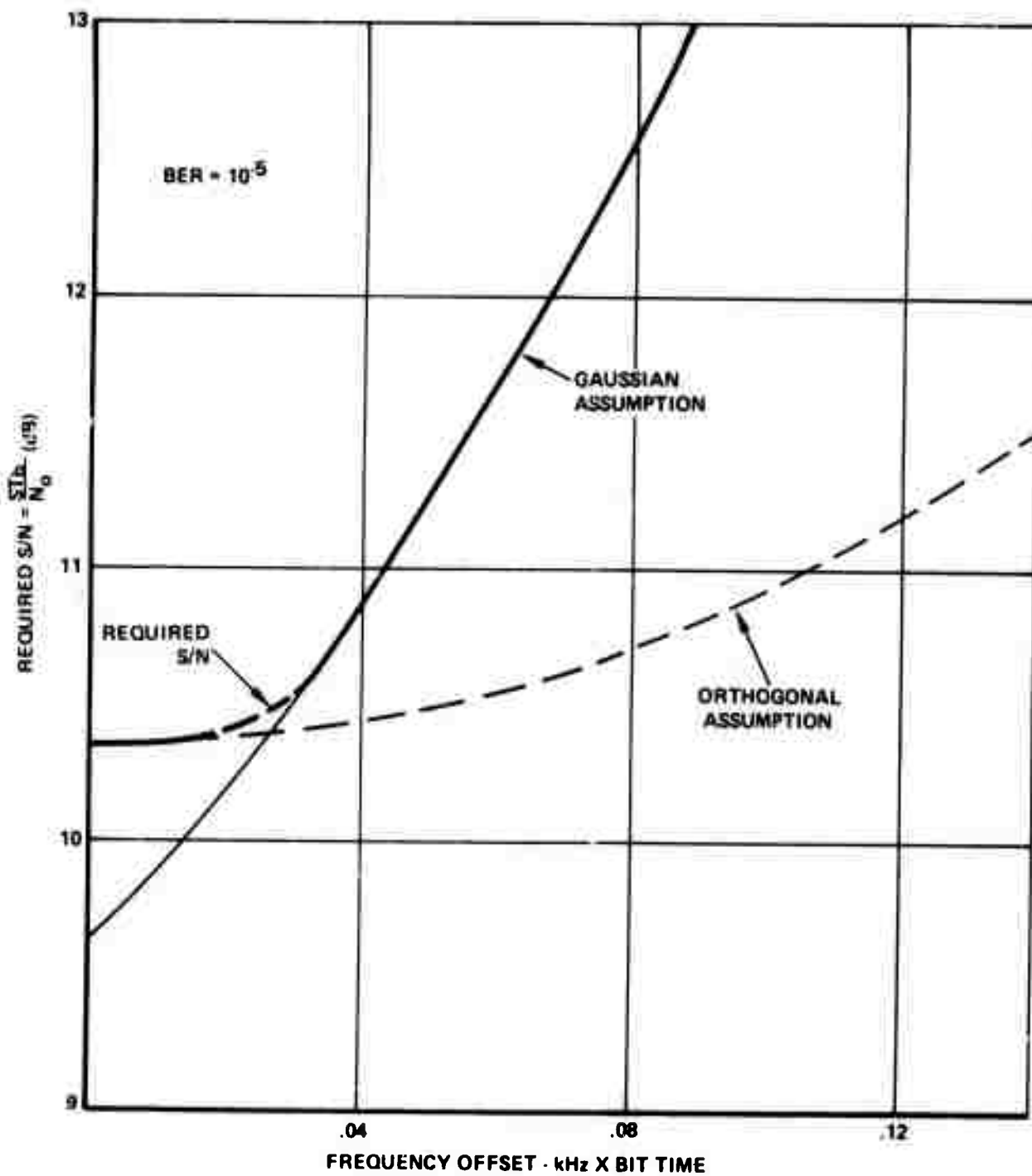
Figure A-8.   DPSK SN Requirement Versus Frequency Offset

237

A.2.2   Effect of Timing Jitter

The effect of timing jitter can be determined from the rolloff of the PN code correlation with timing error. The voltage gain is proportional to the time error so the loss for a constant offset is

$$L = \left(1 - \left|\frac{t}{T_c}\right|\right)^2$$

The loss is shown in Figure A-9. If a varying jitter from bit to bit is evident instead of a constant timing error, the 1 sigma value of the jitter can be used for reasonably close indication of the loss as it affects bit error rate.

A.2.3   Effect of Filtering

The effects of the IF filter on degrading the PN code can be ascertained by use of the following relation developed for PN detection

$$L = \frac{\left|\int_{-\infty}^{\infty} |H(\omega)| \, S_{xx}(\omega) \, \cos\left(\phi(\omega) - \Delta\omega\right) \, dw\right|^2}{2\pi \int_{-\infty}^{\infty} |H(\omega)|^2 \, S_{xx}(\omega) \, dw}$$

where:

$H(\omega)$ is the amplitude response of the IF filters

$\phi(\omega)$ is the phase response of the IF filters

$S_{xx}(\omega)$ is the power transfer function of the PN code

$$S_{xx}(\omega) = \frac{T_c}{2} \, \frac{\sin^2\left(\omega - \omega_c\right) T_c/2}{\left(\left(\omega - \omega_c\right) T_c/2\right)^2}$$

and Δ is a time delay adjustable for minimum loss.

This equation was solved using a digital computer to determine filter degradation for Chebychev IF filters centered at the IF frequency. Filters of 4, 6, 8, 10 and 12 poles and with .05 and .5 dB ripple were considered. The 3 dB IF bandwidth was left as a parameter.

Figures A-10 and A-11 show the results of these runs. They show that nominally 1.5 to 2 times the chip rate is required and a degradation of about one-half a dB can be expected. This degradation can be added to the S/N in the previous figures to get the requirements when filtering is considered.
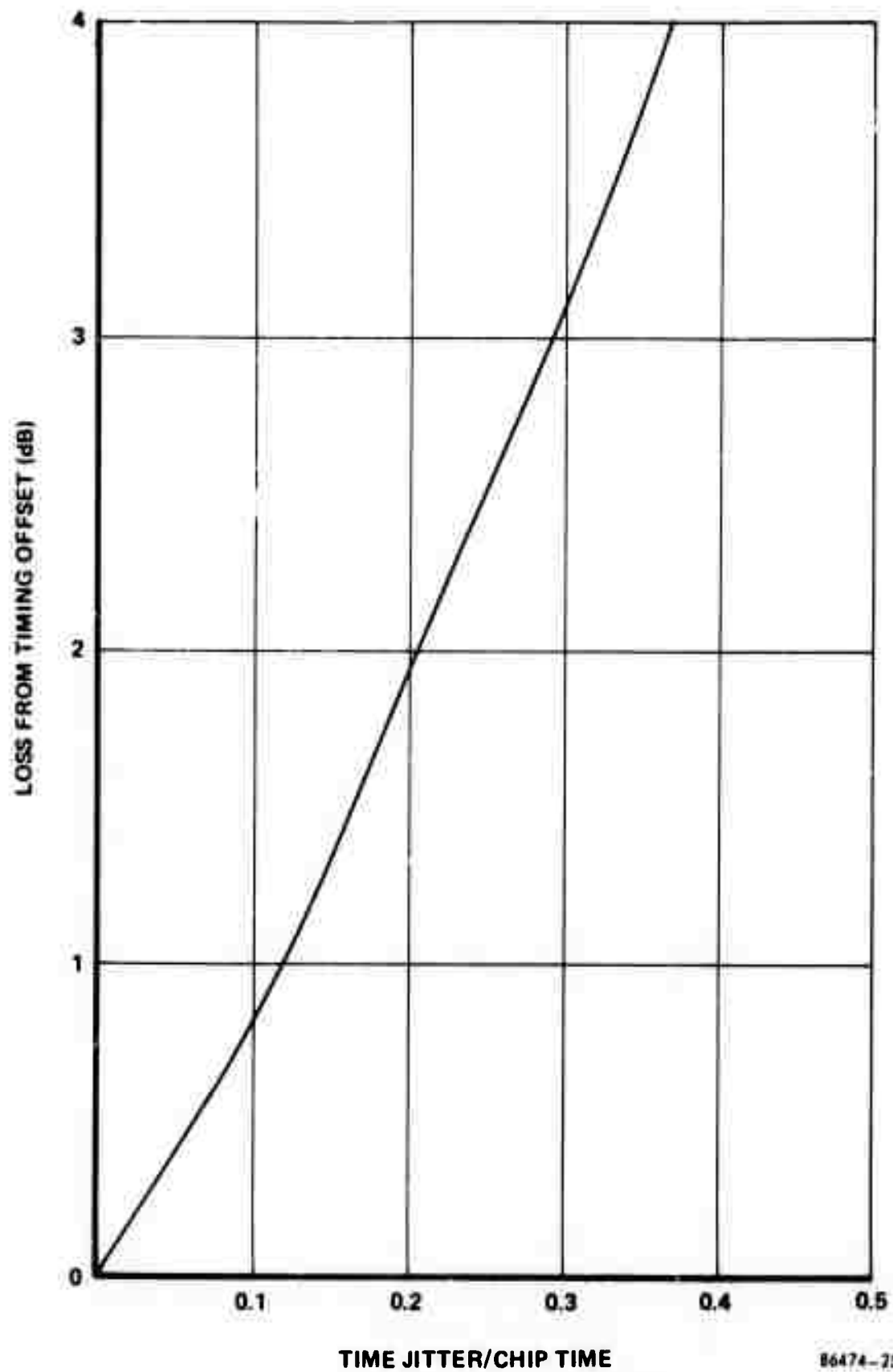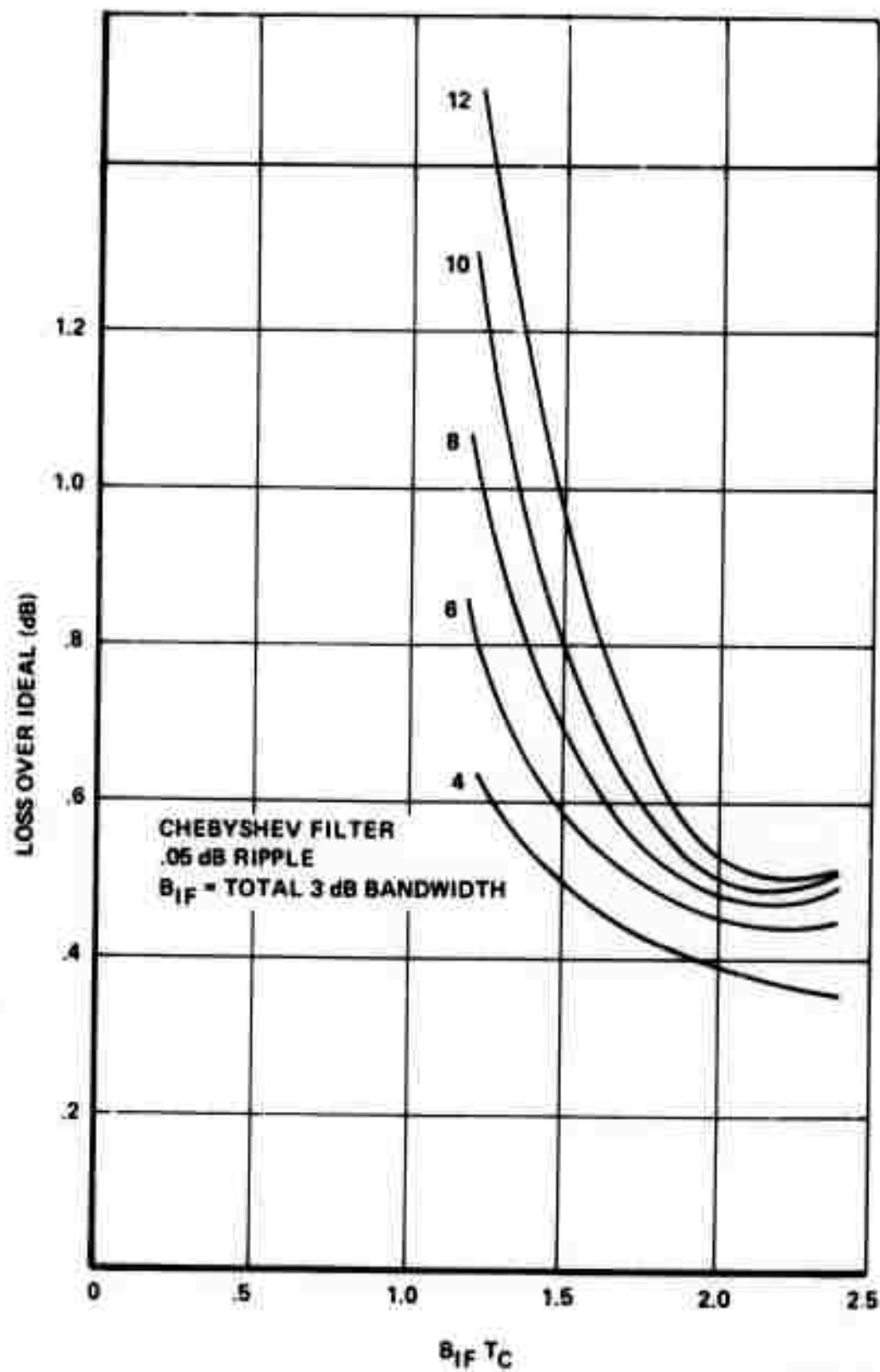
238

Figure A-9. Status Link Timing Offset Loss
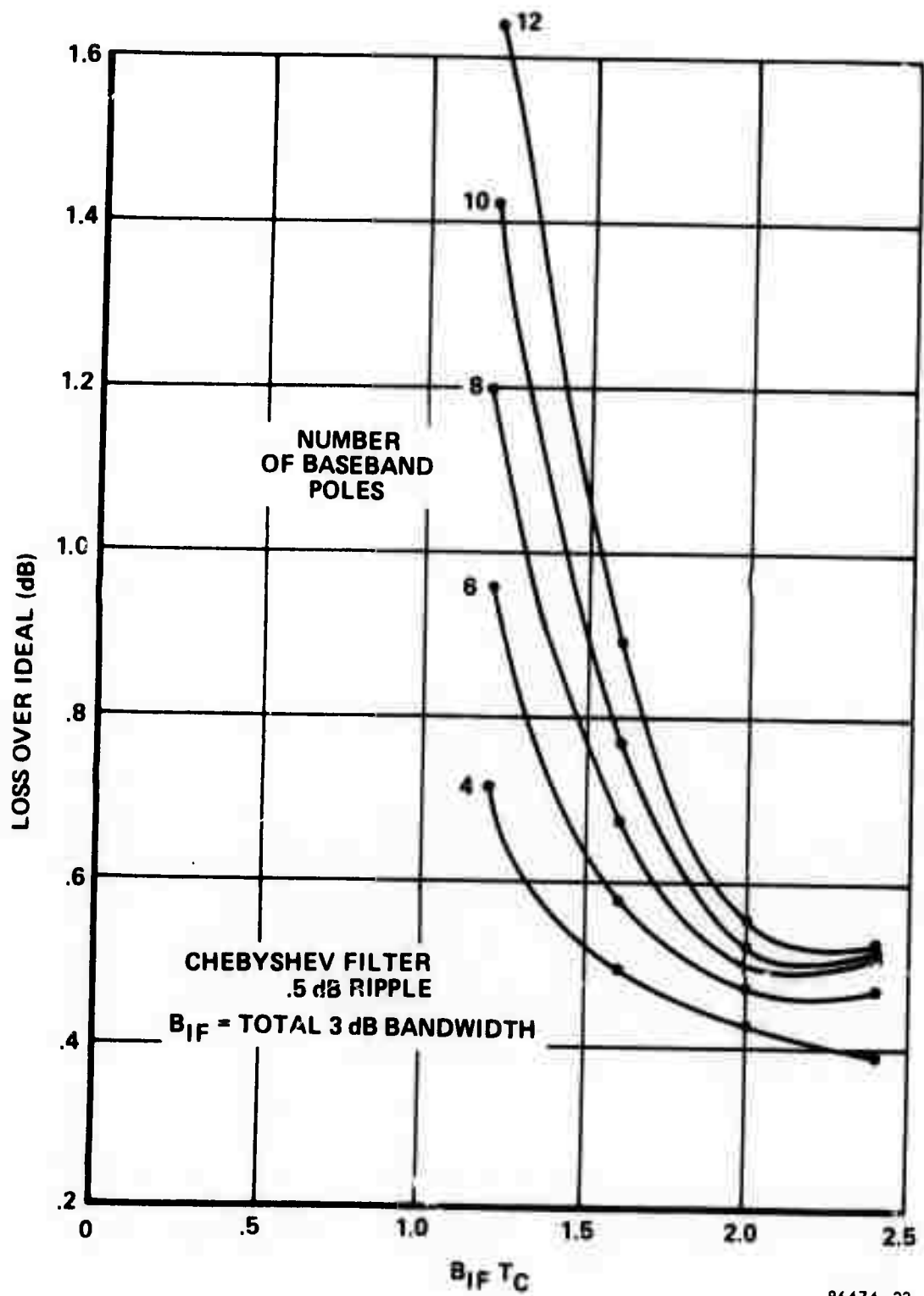
86474-25

Figure A-10

240

Figure A-11.   IF Filter Degradation To PN Detection

241

A.3   BER Video Link

The video link will consist of QPSK data that has orthogonal binary streams offset in time by the bit period. Using this technique allows phase transitions of only 90 degrees at a time and greatly reduces the amplitude modulation caused by band limiting the transmitted signal.

A.3.1   Ideal Bit Error Rate

Let the transmitted bit rate be R_b then each of the orthogonal channels has bit rate $R_c = R_{b/2}$ and shares half the power $P_c = P_{s/2}$.

Ideally each of the channels is orthogonal because their carriers are orthogonal and they can be treated separately. Each channel can be considered coherently detected biphase data for which the bit error rate is

$$BER = \frac{1}{2} \, erfc\left(\sqrt{E_b/N_o}\right)$$

Where erfc is the complementary error function and E_b/N_o is the energy constant ratio

$$E_b/N_o = \frac{P_c/R_c}{N_o} = \frac{P_s}{N_o R_b}$$

This bit error rate is plotted in Figure A-12 and is identical to the biphase error rate. It will be noted, however, that the required transmission bandwidth is only half that required for biphase since the data is being transmitted at half the bit rate over two orthogonal channels in the same band.
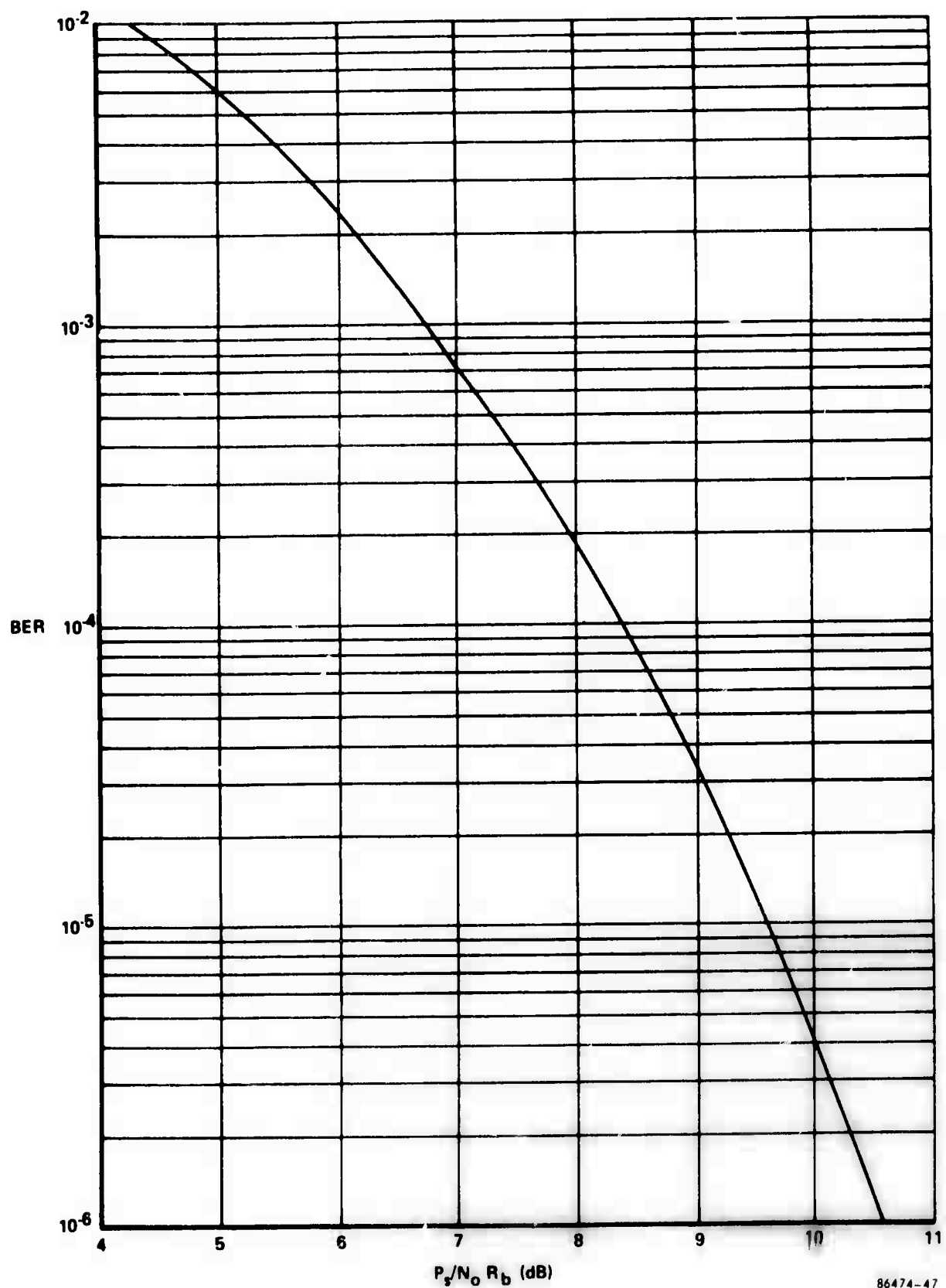
A.3.2   Timing Jitter Effect

For a nonband limited signal the level of the matched filter output will fall off on the average proportional to the timing error and the loss is treated identically to that of the status link.
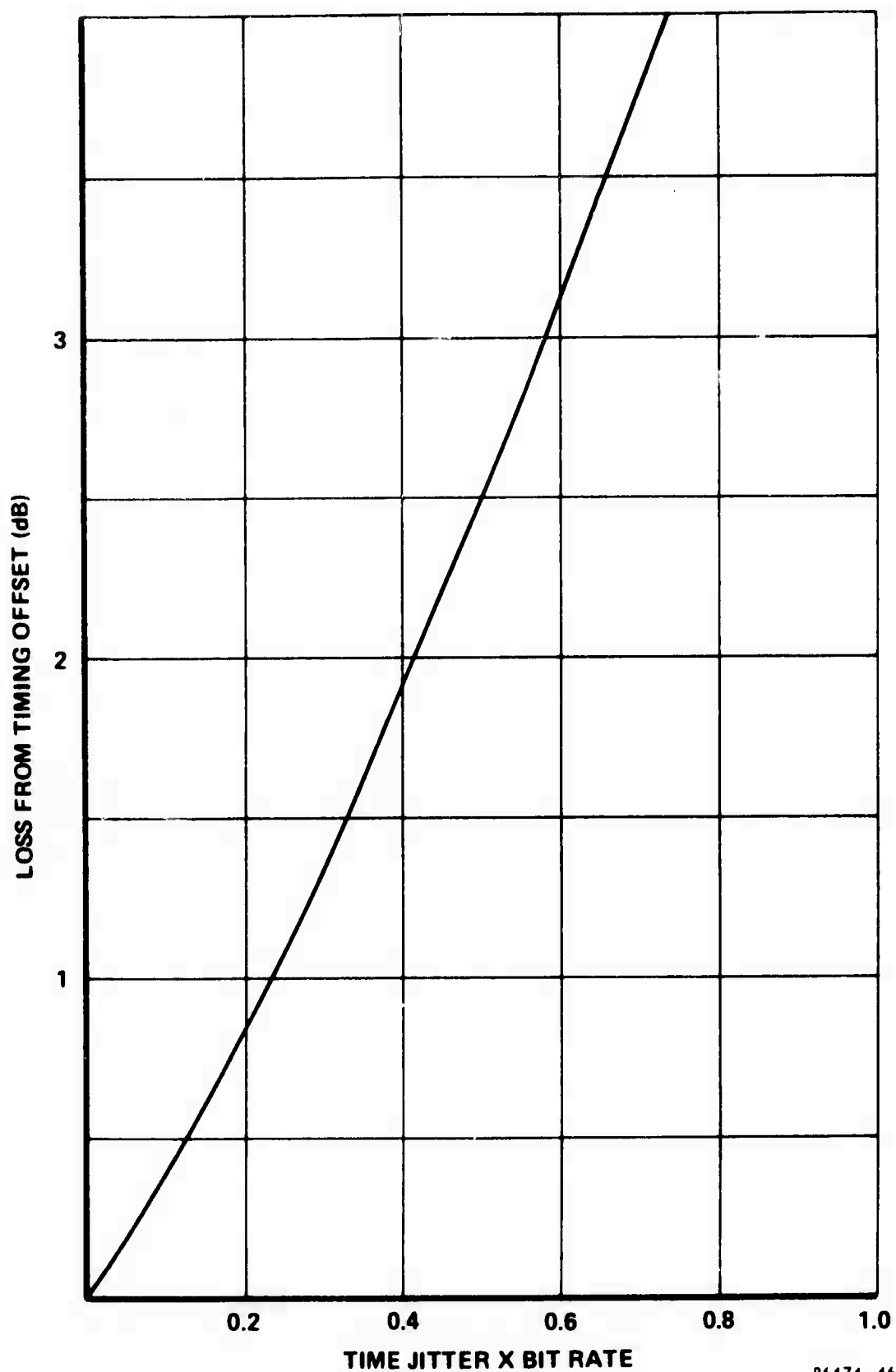
$$L = \left(1 - \left|\frac{t}{T_c}\right|\right)^2 = \left(1 - \left|t \, R_b/2\right|\right)^2$$

This loss is plotted in Figure A-13.

242

Figure A-12.   Video Link Bit Error Rate

243

Figure A-13. Video Link Timing Offset Loss

Since the actual data will be band limited, the power will fall off at a lesser rate because of noninstantaneous transitions and the loss is pessimistic.

A.3.3 Effect of IF Filtering

The effect of single receive or transmit and receive filters on QPSK data has been analyzed in the literature.*

It is shown that for Chebyshev IF filters with .1 dB ripple and a 3 dB bandwidth equal to twice the channel rate about 1 dB of loss can be expected for from three to eleven poles. Also, this same loss applies for biphase indicating no degrading interchannel interference. Since there is no interchannel interference, the proposed offset QPSK will have identical error properties; hence, 1 dB of degradation can be assigned to the effect of band limiting the transmitted and received signal.

"Filter Distortion and Intersymbol Interference Effects on PSK Signals" by J. Jay Jones, in the April 1971 IEEE Transactions on Communications Technology.

APPENDIX B

Four types of jamming will be investigated for the chirp signal: noise, CW, chirp replica, and time position chirp. All will be considered to be on continuously and the effect of pulsing to increase peak power will be investigated separately.

CW Jamming

In Appendix A it was determined that the amplitude response to CW was

$$R(\omega, \tau) = \frac{1}{2} \sqrt{\frac{\pi}{r}} \left[\left(C(L_2) - C(L_1) \right)^2 + \left(S(L_2) - S(L_1) \right)^2 \right]^{\frac{1}{2}}$$

where L_2 and L_1 are functions of frequency and time. The largest value the Fresnel integral expression can achieve is 1.896 which occurs only when $L_2 = 1.20$ and $L_1 = 1.20$ or only at one r for a given frequency. Nominally, it will be 1.414 and this will be taken as the output for a unit amplitude sine wave. The output envelope for a sine wave of amplitude B is in this case.

$$J_e = B \times .707 \left(\frac{T_s}{2\Delta f} \right)^{\frac{1}{2}}$$

The signal envelope has been shown to be

$$Se = \frac{AT_s}{2}$$

where A is the peak amplitude of the signal and T_s is the time duration of the sweep.

An error will occur if the envelope of signal plus jammer at a random phase $\emptyset$ is less than the jammer alone

$$BER = Pr \left((S_e + J_e \cos \emptyset)^2 + (J_e \sin \emptyset)^2 < J_e^2 \right)$$

$$= Pr \left(S_e^2 + 2 S_e J_e \cos \emptyset < 0 \right)$$

$$= Pr \left(-\cos \emptyset > \frac{S_e}{2 J_e} \right)$$

$$= \frac{2 \cos^{-1} \frac{S_e}{2 J_e}}{2\pi}$$

$$= \frac{1}{\pi} \cos^{-1} \left(\frac{P_s \, M \, \Delta f \, T_s}{P_J \quad 4} \right)^{\frac{1}{2}}$$

247

where M is the number of channels sharing the average power and P_s is the average power per channel.

Noise Jamming

White noise will produce a bit error rate derived in Appendix A to be

$$BER = \frac{1}{2} e^{-\frac{1}{2}(S/N)} out = \frac{1}{2} e^{-\frac{1}{2}\frac{S T_s}{N_o}}$$

If N_o is made from a power limited jammer the power must be spread over $2\Delta f$ so

$$N_o = \frac{P_J}{2\Delta f}$$

also note

$$S = M P_s$$

and

$$BER = \frac{1}{2} e^{-\frac{P_s}{P_J} M \Delta f T_s}$$

Chirp Replica Jamming

Consider a jammer that sends a constant train of chirp signals with the proper slope, each lasting for time T_J. Each of these will from the considerations of Appendix A produce a time waveform out of the matched filter with envelope

$$r_J = A_e \frac{\sin \tau \pi^1 T_J 2}{\tau \tau^1}$$

where τ^1 is the delay from output peak.

This will cause an error if the wrong up or down chirp filter is excited during a bit sample time and its amplitude is greater than the signal amplitude. This latter requirement is met if

$$\tau^1 > \frac{A_1 T_s}{2}$$

248

Let t be the time from $\tau' = 0$ over which this is true then the following constraint equation can be written

$$\frac{A\,T_s}{2} = J_e \frac{\sin rt\,T_s/2}{rt}$$

The jammer can produce a false indication for 2t out of every T_i which it will do with .5 probability so the bit error rate can be written as

$$\alpha = BER = .5 \times \frac{2t}{T_J} = \frac{t}{T_J}$$

$$t = \alpha\,T_J$$

and

$$\frac{A\,T_s}{2} = J_e \frac{\sin r\alpha T_J^2/2}{r\alpha T_J}$$

Assume the jammer can adjust T_i for maximum bit error rate. This occurs when

$$\frac{d\alpha}{dT_J} = 0$$

Differentiating the constraint equation with respect to T_J

$$0 = \frac{J_e}{r}\left[\left(-\frac{1}{\alpha\,T_J^2} - \frac{1}{\alpha^2\,T_J} \cdot \frac{d\alpha}{dT_J}\right)\sin r\alpha\,T_J^2/2 + \left(r\alpha T_J + \frac{rT_J^2}{2}\frac{d\alpha}{dT_J}\right)\right.$$

$$\left.\frac{\cos r\alpha T_J^2/2}{r\alpha T_J}\right]$$

$$= \frac{J_e}{2}\left[\frac{\sin r\alpha T_J^2/2}{r\alpha T_J^2/2}\left(-1\frac{T_J}{\alpha}\frac{d\alpha}{dT_J}\right) + \cos r\alpha T_J^2/2\left(2+\frac{T_J}{\alpha}\frac{d\alpha}{dT_J}\right)\right]$$

from which the derivative can be equal to zero only if

$$\frac{\sin r\alpha T_J^2/2}{r\alpha T_J^2/2} = 2\cos r\alpha T_J^2/2$$

The first point at which this occurs is when

$$r\alpha T_J^2/2 = 1.16557 \text{ rad} = 66.7822 \text{ deg}$$

Substituting back into the constraint equation gives

$$\frac{AT_s}{2} = \frac{J_e T_J}{2} \times .788467$$

or

$$T_J = \frac{A}{T_c} \frac{T_s}{.788467}$$

is the optimum jammer sweep time for a given jammer to signal ratio.

The worst case bit error can now be established from

$$\alpha = \frac{2 \times 1.16557}{rT_J^2} = \frac{2 \times 1.16557}{\frac{2\pi\Delta f}{T_s} \times \left(\frac{AT_s}{J_c .788417}\right)^2}$$

and noting that

$$\left(\frac{J_e}{A}\right)^2 = \frac{P_J}{MP_s}$$

$$BER = \alpha = \frac{.231}{M\Delta fT_s}\frac{P_J}{P_s}$$

250

Time Position Chirp Jamming

A jammer can conceivably determine bit timing and simultaneously send chirps during this time to jam several of the time slots. The jammer would require power equal to the signal power for each of the time slots to be jammed. If the appropriate time slot were jammed, an error would occur with probably .5. The total power required would be that needed for each time slot jammed.

$$BER = \frac{.5}{M\Delta f T_S} \quad \frac{P_J}{P_S}$$

This is believed to be the worst-case system in that the jammer is using just enough power to produce a given error rate.

This limit will be approached if the CW or noise jammer is pulsed since the average jammer power will remain constant but when it is on the bit error probability will approach .5.